



HAL
open science

Identification and characterization of known and novel gene defects involved in inherited retinal degenerations

Vasily Smirnov

► **To cite this version:**

Vasily Smirnov. Identification and characterization of known and novel gene defects involved in inherited retinal degenerations. Genetics. Sorbonne Université, 2022. English. NNT : 2022SORUS490 . tel-04348745

HAL Id: tel-04348745

<https://theses.hal.science/tel-04348745>

Submitted on 17 Dec 2023

HAL is a multi-disciplinary open access archive for the deposit and dissemination of scientific research documents, whether they are published or not. The documents may come from teaching and research institutions in France or abroad, or from public or private research centers.

L'archive ouverte pluridisciplinaire **HAL**, est destinée au dépôt et à la diffusion de documents scientifiques de niveau recherche, publiés ou non, émanant des établissements d'enseignement et de recherche français ou étrangers, des laboratoires publics ou privés.

Identification and characterization of known and novel gene defects involved in stationary and progressive inherited retinal diseases

Par Vasily SMIRNOV

Thèse de doctorat de Génétique

Dirigée par Isabelle AUDO et Christina ZEITZ

Présentée et soutenue publiquement le 16 Décembre 2022

Devant un jury composé de :

Pr. Eric LE GUERN, Professeur, Président du jury

Pr. Katarina STINGL, Professeure, Rapportrice

Pr. Bart LEROY, Professeur, Rapporteur

Dr. Jasmina CEHAJIC-KAPETANOVIC, Honorary Clinician Scientist, Examinatrice

Dr. Anne-Françoise ROUX, Praticien Hospitalier, PharmD, PhD, HDR, Examinatrice

Pr. Isabelle AUDO, Professeure, Co-directrice de thèse

Dr. Christina ZEITZ, DR2, Co-directrice de thèse

Acknowledgements – Remerciements

First of all, I would like to thank the members of the jury for accepting to review my work and for accepting to come to Paris to attend my defense. I'm grateful to Dr Kinga Bujakowska and Pr Laurent Mesnard who followed my PhD studies and made sure that my thesis run smoothly.

Isabelle et Christina, permettez-moi de vous exprimer toute ma reconnaissance et une immense gratitude pour m'avoir permis d'accéder au monde merveilleux de biologie moléculaire et pour m'avoir guidé et accompagné avec tant de patience et bienveillance. Avec vous, j'ai fait mes premiers pas dans le monde de la recherche, publications, présentations dans les congrès. Sans vous, ma formation en ophtalmogénétique serait très incomplète et ma carrière caduque!

Merci à tous les gens merveilleux que j'ai rencontré dans l'Institut de la Vision, et notamment à Christel Condroyer qui m'a parrainé, materné, tout appris en matière de séquençage et m'a toujours aidé; à Christelle, Camille, Aline, Emma, toujours présentes et de bon conseil. A Géraldine qui a partagé mes joies et mes peines autour d'un café ou un repas.

Marco, Tasnim et deux Juliettes, j'étais heureux de faire votre connaissance et travailler avec vous ! Merci pour toute entraide, conseils, foux rires, nos voyages communs...Cécile, merci de m'avoir laissé le terrain si travaillé ! J'ai continué dans ton sillage. Cyntia, Luiza, Helen, Leila qui ont débloqué mon anglais oral et qui m'ont tellement appris sur leur pays nataux. Merci à l'imperturbable Baptiste qui m'a montré et appris beaucoup de choses. Julien, sans toi je ne pourrais pas pénétrer dans les mystères de bioinformatique !

J'exprime ma reconnaissance sans bornes à Sabine Defoort, qui m'a donné le gout pour l'ophtalmogénétique et qui a fait tout son possible pour que je puisse l'exercer. Partie clinique, j'ai tout appris auprès de vous. D'autre part, je remercie toute l'équipe d'EVNO qui m'a poussé et soutenu dans ce projet périlleux, qui a assuré la continuité du travail clinique lors de mes absences prolongées et répétitives. Merci d'être une équipe de travail mais également une équipe de soutien de tous les jours. Merci à Claire-Marie Dhaenens, avec qui on a bien collaboré pour les publications et dans mon activité clinique de tous les jours. A mes maîtres, Pr Rouland et Pr Labalette, qui m'ont accompagné dans mon parcours avec de la bienveillance.

Enfin, je souhaiterais remercier ma famille française, Antoine, Véronique, Paul qui m'ont tant soutenu pendant ces années de travail intense sans broncher quand j'étais absent ou peu disponible. Mon père et ma sœur pour leur politique de non-empêchement et leur soutien moral lors de passages à vide. Mes fidèles amis Asel, Christelle, Elena et Maxime.

Merci à tous !

Table of contents

Acknowledgements – Remerciements	3
Table of contents.....	4
List of abbreviation.....	7
List of figures.....	10
Introduction	12
1. The eye and the retina.....	12
1.1. The structure of the eye.....	12
1.2. The structure of the retina.....	12
1.2.1. Fundoscopic and microscopic retinal structure.....	12
1.2.2. Cell types in the retina.....	13
1.3. Visual signal transduction and transmission and their correlation with genes involved in pathologic conditions.....	16
1.3.1. Phototransduction in rods.....	16
1.3.2. Phototransduction in cones.....	19
1.3.3. Signal transmission from photoreceptor to bipolar cells.....	21
1.3.4. Further signal transmission and modulation.....	23
1.4. Metabolism and supply of the retina incorporating genes involved in pathologic conditions.....	23
1.4.1. Retinal pigment epithelium.....	23
1.4.2. Visual cycle.....	24
1.4.3. Phagocytosis of photoreceptor outer segments.....	26
2. Inherited retinal diseases: clinical retinal investigations, general considerations, taxonomy, phenotypes.....	26
2.1. Clinical retinal investigations.....	26
2.1.1. Functional retinal evaluation.....	26
2.1.2. Morphologic retinal evaluation.....	28
2.2. General considerations on inherited retinal disorders.....	30
2.3. Stationary retinal diseases.....	30
2.3.1. Cone dysfunctions.....	30

2.3.2. Congenital stationary night blindness	31
2.4. Progressive inherited retinal degenerations.....	32
2.4.1. Rod-cone dystrophies	32
2.4.2. Cone/cone-rod dystrophies	33
2.4.3. Inherited macular dystrophies or maculopathies.....	34
2.5. Vitreoretinopathies	34
2.6. Isolated and syndromic inherited retinal disorders.....	34
2.7. Genetics of inherited retinal disorders.....	35
3. Strategies for gene identification in inherited retinal disorders.....	36
3.1. Linkage studies.....	37
3.2. High throughput sequencing.....	37
3.3. Types of variants.....	38
3.4. Functional studies of candidate genes	39
3.5. Purpose of my work.....	40
Materials and Methods	41
1. Inherited retinal disorders cohort followed at the XV-XX hospital.....	41
2. Phenotyping.....	41
3. Genotyping workup.....	41
3.1. Next generation sequencing.....	42
3.2. Whole Exome Sequencing.....	52
3.3. Retinal expression databases.....	53
3.4. Confirmation and segregation of variants.....	54
4. Expression analysis of candidate genes.....	55
4.1. RNA in situ hybridization.....	55
4.2. Immunohisto fluorescence.....	55
4.3. Western blot	56
Results	56
1. Epidemiological picture of REFERET inherited retinal disorder cohort analyzed by targeted NGS.....	56
1.1. Phenotypes.....	56

1.2. Genotypes.....	57
1.3. Post hoc analysis: changes in assumed inheritance pattern; critical review of initial clinical diagnosis.....	59
1.4. Unsolved cases.....	59
2. Gene defect identification by Whole Exome Sequencing.....	59
2.1. Whole Exome Sequencing identified a known pathogenic variant in F163.....	59
2.2. Whole Exome Sequencing identified a known hypomorphic variant leading to isolated IRD in F510.....	60
2.3. Whole Exome Sequencing identified a known hypomorphic variant leading to isolated IRD in F2799.....	60
3. Specific and unusual genotype-phenotype associations identified by next generation sequencing technologies	60
3.1. Isolated retinal degeneration linked to <i>CLN3</i> variants.....	60
3.2. High dose vitamin A improves retinal function in <i>RBP4</i> -related fundus albipunctatus.....	78
3.3. Retinal degeneration in French patients harboring variants in <i>CLRNI</i>	88
3.4. <i>TTL5</i> collaborative work.....	100
3.5. Novel phenotype of congenital stationary night blindness associated with missense variants in <i>VSX2</i>	117
4. Novel gene defect identification and characterization in F4752 with North Carolina Macular Dystrophy.....	129
Discussion and perspectives.....	134
1. Deep phenotyping, phenotype-genotype correlations and natural history studies.....	134
2. Identification of gene defects in inherited retinal disorders.....	134
3. Candidate genes and novel mechanisms in inherited retinal disorder field.....	136
4. Novel strategies in inherited retinal disorders gene defect identification.....	137
References.....	140

List of abbreviations

5'-GMP: guanosine 5'-monophosphate
ABCA4: ATP-binding cassette subfamily A member 4 protein
ACMG: American College of Medical Genetics
ad/AD: autosomal dominant
AMPA: α -amino-3-hydroxy-5-methyl-4-isoxazolepropionic acid
ar/AR: autosomal recessive
BBS: Bardet-Biedl syndrome
BC: bipolar cell
BEST1: bestrophin 1
Ca: calcium
cAMP: cyclic adenosine monophosphate
CC2D2A: coiled-coil and C2 domain containing 2A
cd.s.m-2: candela second per meter square
COD/CORD: cone/cone-rod dystrophy
CGH: comparative genomic hybridization
cGMP: cyclic guanosine 3',5'-monophosphate
Cl: chloride
CLN3: lysosomal/endosomal transmembrane protein, battenin
CLRN1: clarin 1
CNG: Cyclic-nucleotide-gated
CNGA1/CNGA1: cyclic nucleotide gate channel subunit a 1
CNGA3/CNGA3: cyclic nucleotide gated channel subunit a 3
CNGB1/CNGB1: cyclic nucleotide gate channel subunit b 1
CNGB3: cyclic nucleotide gated channel subunit b 3
CNV: Copy number variations
CSNB: congenital stationary night blindness
DA: dark-adapted
DAPI: 4',6-diamidino-2-phenylindole
DHDDS: dehydrodolichyl diphosphate synthase subunit
DNA: deoxyribonucleic acid
Dys: dyschromatopsia
eQTL: expression of quantitative trait loci
ERG: electroretinogram
GBN1/GNB1: G protein subunit b transducin 1
GCL: ganglion cell layer
GDP: guanosine diphosphate
GDP: guanosine diphosphate
GNAT1/GNAT1: G protein subunit/ transducin 1
GNAT2/GNAT2: G protein subunit/transducin 2
GNB3/GNB3: G protein subunit b transducin 3
GNB5: G protein subunit 5
GNGT1/GNGT1: G protein subunit g transducin 1
GNGT2/GNGT2: G protein subunit g transducin 2
GRK1/GRK1: G protein-coupled receptor kinase 1
GRK7: G protein-coupled receptor kinase 7
GRM6/mGluR6: glutamate metabotropic receptor 6 gene
GTP: guanosine triphosphate

GUCA1A: guanylate cyclase activator 1A
GUCA1B: guanylate cyclase activator 1B
GUCY2D: guanylate cyclase 2D, retinal
h: hour
HSPB11: heat shock protein family B (small) member 11
IFT: intraflagellar transport
IFT: intraflagellar transport genes
InDel: insertion/deletion
INL: inner nuclear layer
IPL: inner plexiform layer
IRD: inherited retinal dystrophies
IS: inner segment
JS: Joubert syndrome
K: potassium
KIF3A: kinesin family member 3A
LA: light-adapted
LCA: Leber congenital amaurosis
LRAT: lecithin retinol acyltransferase
MAF: minor allele frequency
MERTK: receptor tyrosine kinase c-mer
min: minutes
MKS: Meckel-Grüber syndrome
MLPA: multiplex ligation dependent probe amplification
MRI: magnetic resonance imaging
mRNA: messenger ribonucleic acid
ms: milliseconds
Na: sodium
Na⁺/K⁺-ATPase: sodium/potassium adenosine triphosphatase
NEK2: never in mitosis gene A-related kinase 2
NGS: next generation sequencing
NMD: nonsense-mRNA mediated decay
N-methyl-D-aspartate (NMDA)
NPHP: nephronophthisis
NRL: neural retina leucine zipper
OMIM: Online Mendelian Inheritance in Man
ONL: outer nuclear layer
OPL: outer plexiform layer
OPN1LW/OPN1LW: opsin 1, long wave sensitive
OPN1MW/OPN1WM: opsin 1, medium wave sensitive
OPN1SW/OPN1SW: opsin 1, short wave sensitive
OS: outer segments
PBS: phosphate-buffered saline
PCARE/C2orf71: photoreceptor cilium actin regulator
PCR: polymerase chain reaction
PDE6: cGMP phosphodiesterase 6
PDE6A/PDE6A: phosphodiesterase 6A
PDE6B/PDE6B: phosphodiesterase 6B
PDE6G/PDE6G: phosphodiesterase 6G

PRDM13: positive regulatory domain-containing 13
PRPF31: pre-mRNA processing factor 31
Q-PCR: quantitative-PCR
RBP1: Retinol binding protein 1
RBP3: retinol binding protein 3
RBP4: retinol binding protein 4
RCD: rod-cone dystrophy
rd1: mouse model with *Pde6b* variants
RD3: retinal generation 3, GUCY2D regulator
RDH11: retinal dehydrogenase 11
RDH12: retinol dehydrogenase 12
RDH5: retinal dehydrogenase 5
RDH8: retinol dehydrogenase 8
REEP6: receptor accessory protein 6
RGS9/RGS9: regulator of G protein signaling protein 9
RGS9BP: regulator of G protein signaling 9 binding protein
RHO/Rho: rhodopsin
RLBP1: retinaldehyde binding protein 1
RPE: retinal pigment epithelium (RPE)
RPE65/RPE65: retinoid isomerohydrolase RPE65
RT: room temperature
SAG/SAG: S-antigen or visual arrestin
SD-OCT: spectral domain optical coherence tomography
s: seconds
SLC24A1/SLC24A1: solute carrier family 24 member 1
SLC24A2/SLC24A2: solute carrier family 24 member 2
SLS: Senior-Løken syndrome
SNP: single nucleotide polymorphism
SNVs: single nucleotide variants
TRPM1: transient receptor potential cation channel subfamily M member 1
TTLL5: tubulin tyrosine ligase-like 5
USH: Usher syndrome
UTR: untranslated regions
VSX2: visual system homeobox 2
WDR19/WDR19: WD repeat domain 19
WES: Whole Exome Sequencing
WGS: Whole Genome Sequencing
XL: X-linked

List of figures

Figure 1. Eye and retina normal anatomy.....	13
Figure 2. Schematic structure of primate photoreceptors.....	14
Figure 3. Caliceal processes.....	14
Figure 4. Cone and rod densities along the horizontal meridian of the human retina.....	15
Figure 5. Maximum of spectral absorption for different types of photoreceptors.....	15
Figure 6. Initial steps of phototransduction.....	17
Figure 7. Phototransduction inactivation in rod photoreceptor.	18
Figure 8. Schematic drawing of photoreceptor-ON bipolar cell synapse.....	21
Figure 9. ON- and OFF - pathways in the retina.....	22
Figure 10. The role of ABCA4 in all-trans-retinol clearance from discs.....	24
Figure 11. Visual cycle and RPE retinoid supply.....	25
Figure 12. Kinetic (left) and static (right) visual field map of right eye.....	27
Figure 13. Full field ERG recordings and equipment.....	28
Figure 14. Techniques of retinal imaging.....	30
Figure 15. Schematic representation of the main differences between common IRD.....	33
Figure 16. Mendelian patterns of inheritance and symbols used in medical genetic pedigrees....	36
Figure 17. Maternal inheritance linked with mitochondrial DNA variants.....	36
Figure 18. Workflow.....	55
Figure 19. Presumed diagnostic distribution in the cohort of 768 IRD patients: 87.2% of assessed cases had RCD.....	57
Figure 20. Gene defects in RCD (n=670) cases (all patterns of inheritance confounded).....	57
Figure 21. Gene defects found in solved autosomal recessive rod-cone dystrophy cases.....	58
Figure 22. Gene defects in solved autosomal dominant cases.....	58
Figure 23. Post-hoc analysis of inheritance pattern.....	59
Figure 24. Pedigrees and variant segregation in families solved by WES.....	60
Figure 25. Pedigree of F4752 with North Carolina Macular Dystrophy.....	129
Figure 26. qPCR on chosen 3 of 12 genes inside and 2 chosen genes outside the duplication...	130
Figure 27. Predictions for retinal expression of AZDINE7.....	130
Figure 28. In situ RNA hybridization with <i>AZdine7</i> exon 9_10 probes.....	131

Figure 29. Immuno-histo-fluorescence on mouse retina. Co-staining with anti-AZdine7 and anti-glutamine-synthetase.....	132
Figure 30. Immuno-histo-fluorescence on mouse retina. Staining with anti-AZdine7 and anti-Sox9.....	132
Figure 31. Immuno-histo-fluorescence on human retina. Anti-AZdine 7 staining.....	133
Figure 32. Annual rate of gene identification in IRD since 1980.....	138

Introduction

1. The eye and the retina

1.1. The structure of the eye

The eye is the evolutionary acquired complex sensory structure. The collective function of the eye components is to bring a focused clear image of the outside world at the retina (Fig.1 A). The retina, located at the back of the eye, translates light into an electrochemical signal that is transmitted through the retinal layers until it reaches the optic nerve and then the entire visual pathway until it reaches the brain resulting in a meaningful visual scene[1,2].

1.2. The structure of the retina

1.2.1. Fundoscopic and microscopic retinal structure

The vertebrate retina (*rete=net*) is a layered structure with a large diversity of cells that conform distinct circuits that work in parallel and in combination to produce a complex visual output. Its function is to capture, integrate and process the light signal. The retina includes two structures derived from the optic vesicle: the neural layer (*pars optica retinae*, inner part of the optic vesicle) and the retinal pigment epithelium (photoreceptor renewal, recycling of retinoids, absorption of scattered light, transport of nutrients and metabolites selectively through the extraretinal blood barrier and formation of extracellular matrix).

The neural retina is a layered white semitransparent tissue. The layers are (Fig. 1B): the photoreceptor layer with the subcellular structures composed of outer segments (OS) and inner segments (IS) of the photoreceptors, the outer nuclear layer (ONL) formed by the photoreceptor cell bodies with nuclei; the outer plexiform layer (OPL) is a connection layer corresponding to the synapses between photoreceptor, bipolar and horizontal cells; the inner nuclear layer (INL) composed of bipolar, horizontal and amacrine cell bodies; the inner plexiform layer (IPL) is a connection layer corresponding to synapses between bipolar, amacrine and ganglion cells; finally, a ganglion cell layer (GCL), composed of ganglion cell bodies and their axons (retinal nerve fiber layer – RNFL) which will converge to form an optic nerve head (ONH), the beginning of the optic nerve and visible structure of the fundus.

The retina can be divided geographically in various sections with different histological and functional characteristics (Fig.1C). The macula and fovea are central parts of the retina with high cone density and specific structure (extrusion of the innermost layers in the form of foveal pit), responsible for the discrimination of fine details and colors of the visual scene. Peripheral retina has a lesser density of photoreceptors which are mostly rods and scattered cones. Vision of shapes and movements – an overall function of visual alert -is performed by peripheral retina[3].

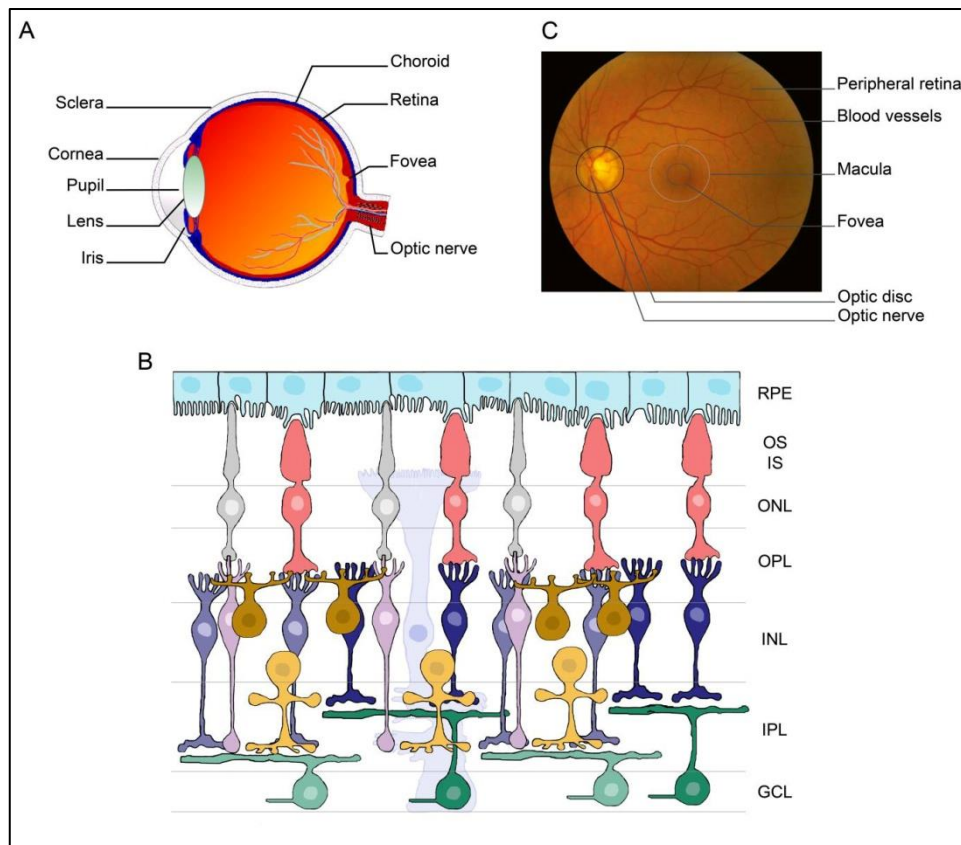


Figure 1. Eye and retina normal anatomy. A. Schematic section of the eye (adapted from Webvision, Helga Kolb, <https://webvision.med.utah.edu>). (B) Retinal layer structure. Retinal pigment epithelium (RPE) and neuroretina. OS and IS: outer and inner segments, respectively; ONL: outer nuclear layer; OPL: outer plexiform layer; INL: inner nuclear layer; IPL: inner plexiform layer; GCL: ganglion cell layer. Rod photoreceptors are in grey, cones in red; rod bipolar cells in pale pink, ON- and OFF- cone bipolar cells are in pale purple and dark purple, respectively; horizontal cells are in brown, amacrine cells in yellow; ON- and OFF-ganglion cells are in light and dark green, respectively; Müller cells are depicted in pale blue. (C) Normal fundus.

1.2.2. Cell types in the retina.

Normal vertebrate retina includes different cell types. **Photoreceptors** (Fig.2) are light-sensitive cells which are crucial for phototransduction – an initial step of vision process - a conversion of light into electrochemical signal. There are two types of photoreceptors in mammalian retina: rods and cones. The structure of photoreceptors is highly compartmentalized. Both rods and cones contain an outer segment (OS), a connecting cilium (CC), an inner segment (IS), a cell body with a nucleus and a synaptic region. The OS is formed of a stack of discs of plasma membrane containing photopigments; their main role being photon capture.

The OS is connected with the IS by the connecting cilium, a highly organized structure allowing the trafficking of molecules from the cytoplasm/IS towards the OS and OS structure maintenance. *Photoreceptor cilium* is a primary sensory cilium. It is composed of different parts: a basal body formed from a centriole, at the limit between OS and IS from which the axoneme extends; a transition zone or ciliary gate where some proteins, interact with the plasma membrane and create a gate between the IS and OS; and the axoneme. The photoreceptor sensory cilium is a microtubular structure highly important for photoreceptor development, structure and protein transport[4]. Of note, the proper functioning of the primary cilium is critical not only for

photoreceptors, but also for other cells such as the epithelial cells in kidney, inner ear, glial neural cells. Variants in genes encoding proteins involved in ciliogenesis, ciliary structure, and transport, lead to a heterogeneous group of pathologies, known as ciliopathies[5].

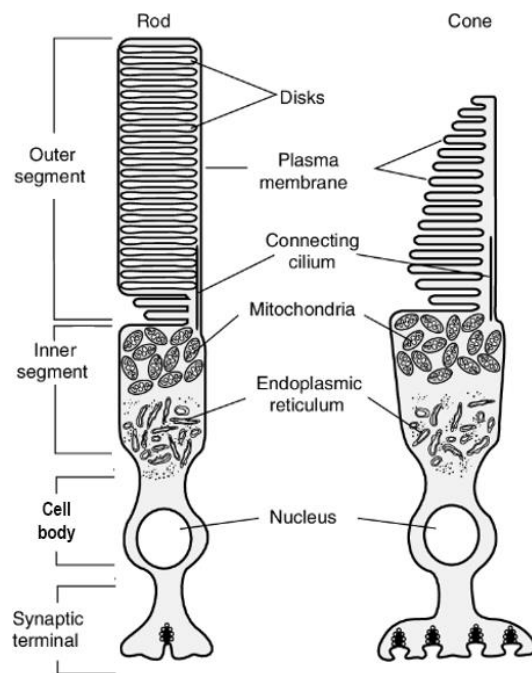


Figure 2 Schematic structure of primate photoreceptors. Adapted from [6]

The IS ensures the metabolic function of photoreceptors and contains mitochondria, Golgi apparatus, endoplasmic reticulum (ER) and lysosomes. IS are in continuity with cell bodies including the nucleus. Microvillus-like structures called *calyceal processes* emerge at the tip of the inner segment and surround the base of the OS (Fig.3). They are specialized membrane processes (F-actin microvilli) generally 8 to 16 in number, organized in a ring pattern, and forming a calyx around the outer segment. Their structure is different in species and they are absent from mouse photoreceptors, for instance[7]. Opposite to the OS is a synaptic region (spherule for rods and pedicle for cones) for transmission of the visual signal from photoreceptors to bipolar cells[3,8,9].

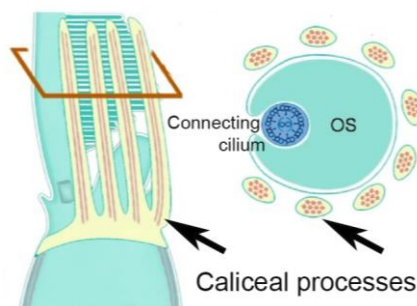


Figure 3 Calyceal processes. Microvilli-like structures filled with F-actin, forming a scaffold around the outer segment. OS – outer segment. Adapted from[10].

Spatial distribution of photoreceptors is not uniform at the surface of the retina (Fig.4). Rods are more numerous (120 millions/eye in humans), their surface density is highest in the

midperipheral retina. Rods are absent from fovea. Cones (6 millions/eye in humans) are present with highest density in the fovea and are scattered in the peripheral retina[11,12]. Cones and rods are organized in non-random mosaics[13].

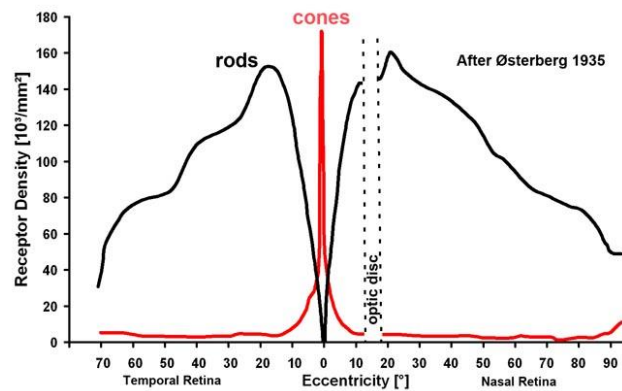


Figure 4. Cone and rod densities along the horizontal meridian of the human retina. Cone density is maximal in the foveal, where rods are absent. Rod density is maximum in the midperiphery of the retina. There are no photoreceptors in the optic disc (“blind spot” in the monocular visual field). Adapted from [11].

Rods are photoreceptors functioning in dimly lighted (scotopic) conditions. There are highly sensitive to light, at least 100-1000 times more sensitive than cones[14]. The rods can capture one photon and generate a response to it, but their time of recovery after bleaching is long. Therefore, their function is saturated in bright (photopic) conditions. The visual pigment of rods is rhodopsin with peak of absorbance at 510 nm.

Cones are less sensitive to light but their photo recovery is at least 10 times more rapid than in rods. This fact explains the possibility of adaptation to a large panel of luminance which is important for the perception of moving objects[15]. Cones have differential sensitivity to chromatic content of the daylight (Fig.5), dependent on the pic light absorbance of their chromophore, cone opsin. Three types of cones could be subdivided: red (long-wavelength sensitive, expressing OPN1LW opsin), green (middle-wavelength sensitive, expressing OPN1MW opsin) and blue (short-wavelength sensitive, expressing OPN1SW opsin) cones.

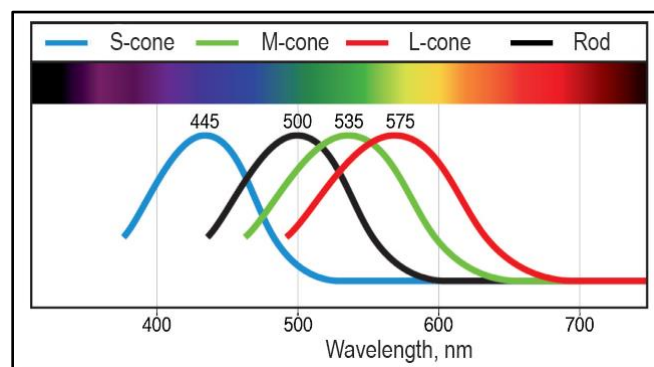


Figure 5 Maximum of spectral absorption for different types of photoreceptors. Adapted from [16].

The synaptic terminals of photoreceptors are called pedicles in cones and spherules in rods. They are highly specialized structures with complex biochemical equipment responsible for vertical and horizontal signal transmission from photoreceptors.

Bipolar cells are second order neurons which transmit signals from photoreceptors to ganglion cells. Their nuclei are in the inner nuclear layer, the dendrites extend into outer plexiform layer to make contact with photoreceptor synaptic terminals and axons extending into inner plexiform layer to form contact with ganglion cells. There is a high anatomical multiplicity of bipolar cells and the subtypes are still to be discovered[17]. Nevertheless, functionally all bipolar cells could be classified into ON-bipolar cells (depolarizing to light stimulation) and OFF-bipolar cells (hyperpolarizing to light stimulation)[18,19], dependent on their different glutamate receptor equipment [20].

Amacrine and horizontal cells are mostly responsible for lateral inhibition in retinal circuits. Horizontal cell dendrites are laterally present at the spherule of rods and pedicles of cones, surrounding bipolar cell dendrites. Amacrine cells synapse with rod bipolar cells, cone ON- and OFF-bipolar cells. Rod-bipolar cells have only synapses with a specific subset of amacrine cells – AII - which then transfer the signal to ON- and OFF-ganglion cells [8].

Ganglion cells are the first neuronal cells able to produce action potential. Their cell bodies form the ganglion cell layer. The axons of ganglion cells are travelling at the inner surface of the retina to finally fuse altogether at the optic disc and form the optic nerve.

Müller cells are retinal glial cells, serving as structural and metabolic support of the overall retinal architecture. They control the extracellular environment homeostasis, take part in the metabolism of the different retinal cell types and provide a cone visual cycle. They can also play a role of light guidance as an “optic fibers”[21].

The **Retinal pigment epithelium** (RPE) is a pigmented epithelial cellular monolayer of multiple functions: a blood-retinal barrier, a nutrient supply, a regulation of subretinal ion homeostasis, secretion of neurotrophic factors, light and heat absorption, the rod visual cycle and photoreceptor OS phagocytosis[22].

1.3. Visual signal transduction and transmission and their correlation with genes involved in pathologic conditions

The phototransduction is a first step in vision which takes place in photoreceptor OS. The phototransduction is a complex photochemical process which allows the incident light to be converted into an electrochemical signal. It is highly dependent upon the overall photoreceptor structure and protein equipment. The phototransduction cascade share some similarities but is clearly distinct in rods and cones.

1.3.1. Phototransduction in rods

Rhodopsin (encoded by *RHO*) is the rod-specific photosensitive protein. It is a transmembrane protein, localized in the disc plasma membrane, belonging to the family of G

protein-coupled receptors. It contains a chromophore molecule, the 11-*cis*-retinal[23]. The phototransduction starts by photon capture which results in photoisomerization of 11-*cis*-retinal in all-*trans*-retinal in less than 200 femtoseconds[24], than metarhodopsin formation in few ms[25]. Spatial conformation changes in metarhodopsin allows the molecule to recognize, bind and activate rod transducin. Rod transducin is a heterotrimeric G protein, composed of the α subunit (GNAT1), the β (GNB1) and the γ (GNGT1) subunits. Activation of transducing by metarhodopsin produce the replacement of GDP by GTP in the α subunit, that changes conformation and dissociates from β and γ subunits. Metarhodopsin dissociates from the complex also and can subsequently activate up to 1300 molecules of transducin/s[26]. The next step of phototransduction is the activation of rod-specific phosphodiesterase 6 composed of two catalytic subunits, α (PDE6A) and β (PDE6B), and two inhibitory subunits, γ (PDE6G) which form a heterotrimeric protein at the resting state. GNAT1-GTP activates PDE6: the two γ inhibitory subunits PDE6 are displaced from the catalytic subunits PDE6A and PDE6B which hydrolyze cGMP into 5'-GMP. The hydrolase activity of PDE6 is extremely high (6000 – 8000 cGMP molecules/s)[27]. This results in a sudden drop in cGMP intradiscal concentration and the closure of cyclic-nucleotide-gated channels present at the rod plasma membrane, composed of three α (CNGA1) and one β (CNGB1) subunits. In the resting state these channels are maintained opened by cGMP and allowing Ca^{2+} and Na^+ entry, balanced by the $\text{Na}^+/\text{Ca}^{2+}$, K^+ exchangers of solute carrier family 24 member 1, encoded by *SLC24A1*, which represent a voltage-dependent channel which exchanges one Ca^{2+} and one K^+ to four Na^+ . When CNG channels are closed, *SLC24A1* continues to pump Ca^{2+} from the cell and causes a sudden drop in intracellular Ca^{2+} concentration. This will produce an overall rod hyperpolarization and the decrease in glutamate release from the synaptic terminals[9]. The steps of phototransduction are summarized in the Fig.6

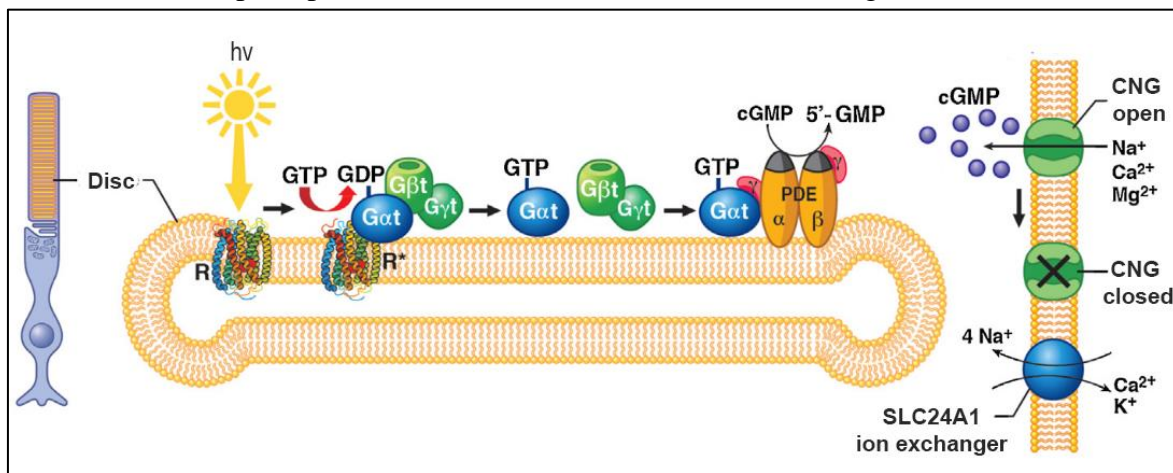


Figure 6 Initial steps of phototransduction. Adapted from [16]

Inactivation of phototransduction in rods takes about 250-500 ms, dependent on light intensity[15]. The crucial steps are inactivation of RHO and PDE6 followed by resynthesis of cGMP and restauration of Ca^{2+} concentration (Fig.7). The sudden drop in Ca^{2+} concentration activates recoverin (encoded by *RCVRN* or *RCVI*) by the burial of myristoylated tail of this latter inside the molecule and the dissociation of recoverin from plasma membrane. Recoverin imbedded in the plasma membrane acts as a rhodopsin kinase (RK, encoded by *GRK1*) inhibitor. Activated RK will phosphorylate RHO. Phosphorylated RHO is recognized by arrestin (aka S-antigen visual arrestin, encoded by *SAG*) quenching the link between RHO and transducin. GNAT1 subunit of

transducin has its own GTPase activity, but this process is slow. The GNAT1-GTP hydrolysis is accelerated by a GTPase-activating protein complex composed of the regulator of G protein signaling 9 (RGS9), the long form of the G protein subunit β 5 (GNB5) and a membrane-anchored protein, regulator of G protein signaling 9 binding protein (RGS9BP)[28]. GNAT1 is thus dissociated from PDE6: the GNAT1-GDP reforms the heterotrimeric complex with subunits GNB1 and GNGT1 and binds back to rhodopsin while the inactivated heterotrimeric complex PDE6 reassembles. In parallel, the low Ca^{2+} concentration leads to the activation of the guanylate-cyclase-activating proteins, GUCA1A (guanylate cyclase activator 1A) and GUCA1B (guanylate cyclase activator 1B), which activates the guanylate cyclase, GUCY2D (guanylate cyclase 2D, retinal): the intracellular cGMP concentration is restored at the resting state[9].

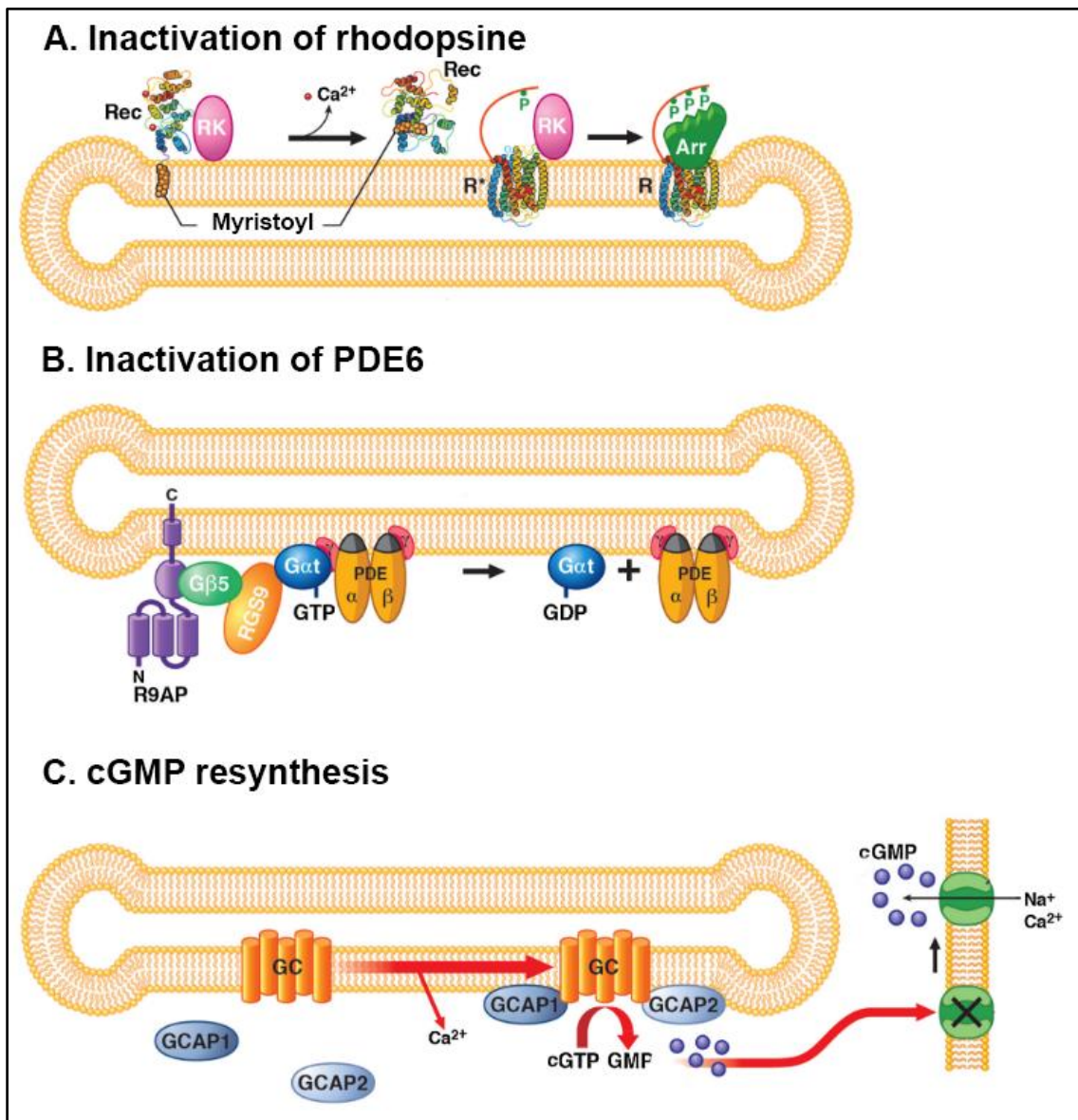


Figure 7 Phototransduction inactivation in rod photoreceptor. Adapted from [16].

Defects in nearly all the proteins of phototransduction cascade are associated with retinal pathology (Tab.1), both inherited and acquired (e.g. autoimmune and paraneoplastic retinopathies).

Table 1. Rod phototransduction cascade genes/proteins and known human retinal pathology.

Gene	Protein	Associated disease (OMIM reference) phenotype	OMIM reference gene
Phototransduction cascade			
<i>RHO</i>	rhodopsin	ad /ar RP (613731), ad Riggs CSNB (610445)	180380
<i>GNAT1</i>	α subunit of rod transducin	ad /ar Riggs CSNB (610444) ar RP[29]	139330
<i>PDE6A</i>	α subunit of rod phosphodiesterase	ar RP (613810)	180071
<i>PDE6B</i>	β subunit of rod phosphodiesterase	ar RP (613801) ad Riggs CSNB (163500)	180072
<i>PDE6G</i>	γ subunit of rod phosphodiesterase	ar RP (613582)	180073
<i>CNGA1</i>	α subunit of cyclic nucleotid gated ion channel	ar RP (613756)	123825
<i>CNGB1</i>	β subunit of cyclic nucleotid gated ion channel	ar RP (613767) ar Riggs CSNB[30]	600724
<i>SLC24A1</i>	Solute carrier family 24 (sodium/potassium/calcium exchanger) member 1	ar RP[31] ar Riggs CSNB (613830)	603617
Inactivation cascade			
<i>RCVRN</i> or <i>RCVI</i>	recoverin	Cancer-associated retinopathy[32,33] Autoimmune retinopathy[34,35]	179618
<i>GRK1</i>	G protein-coupled receptor kinase 1	Oguchi disease-2 (613411)	180381
<i>SAG</i>	Rod arrestin, S-antigen	Oguchi disease-1 (258100) ar RP47 (613758)	181031
<i>RGS9</i>	Regulator of g protein signaling 9	Bradyopsia (608415)	604067
<i>RGS9BP</i>	Regulator of G protein signaling 9-binding/anchoring protein; RGS9AP	Bradyopsia (608415)	607814
<i>GUCA1A</i>	Guanylate cyclase activator 1a, GCAP1	ad COD/CORD (602093)	600364
<i>GUCA1B</i>	Guanylate cyclase activator 1b, GCAP2	ad RP (613827)	602275
<i>GUCY2D</i>	Guanylate cyclase 2d	ad /ar COD/CORD (601777) ar LCA (204000)	600179

1.3.2. Phototransduction in cones

The phototransduction cascade in cones roughly reproduces the steps of rod phototransduction, but the protein equipment (isoforms) is different and the kinetics of the cascade is much faster. Cones express 3 types of light sensitive cone opsins (iodopsins, photopsins): S-cones express the short wavelength-sensitive cone opsin OPN1SW; M-cones express the medium wavelength-sensitive cone opsin OPN1MW and L-cones express the long wavelength-sensitive cone opsin OPN1LW. As rhodopsin, they are photosensitive G protein-coupled receptors, using

11-*cis*-retinal as chromophore. The lifetime of activated cone photopigment is about 3–5 ms. The lifetime of activated transducin/PDE is about 9–18 ms; turnover time for cytoplasmic Ca²⁺ concentration is about 3 ms and the turnover time for cytoplasmic cGMP is as short as 4–6 ms[36].

It is not entirely understood why cones are so rapid in their response. It is most probably due to their higher rate of recovery. For the rapid quenching of the cone opsin activation, the cone opsin kinase (GRK7, G protein-coupled receptor kinase 7) and the cone arrestin (ARR3) must act extremely rapidly. The more rapid quenching of cone transducin/PDE interaction is a result of the higher concentration of RGS9 and RGS9BP, which accelerate the GTPase activity[37]. The more rapid variations of cytoplasmic Ca²⁺ concentration presumably result from the more important plasma membrane surface, since the cone OS is not composed of staking of separate discs such as in rods, but from the direct folding of a continuous plasma membrane[36].

Phototransduction and quenching protein isoforms in cones are listed in the Tab.2

Table 2 Cone phototransduction cascade genes/proteins and known human retinal pathology.

Function	Gene	Protein	Associated disease (OMIM phenotype reference)	OMIM gene reference
Phototransduction cascade				
Photopigment	<i>OPN1LW</i> <i>OPN1MW</i> <i>OPN1SW</i>	Cone opsin L Cone opsin M Cone opsin S	xl color blindness, protan (303900) XI color blindness, deutan (303800) ad color blindness, tritan (190900)	300822 300821 613522
Transducin	<i>GNAT2</i>	α subunit	ar ACHM (613856)	139340
	<i>GNB3</i>	β subunit	ar CSNB (617024)	139130
	<i>GNGT2</i>	γ subunit	-	139391
Phosphodiesterase	<i>PDE6C</i>	α' subunit	ar COD ar ACHM(613093)	600827
	<i>PDE6H</i>	γ' subunit	ar ACHM(610024)	601190
CNG channels	<i>CNGA3</i>	α subunit	ar ACHM(216900)	600053
	<i>CNGB3</i>	β subunit	ar ACHM (262300)	605080
Na ⁺ /Ca ²⁺ ,K ⁺ exchangers	<i>SLC24A2</i>	solute carrier family 24 member 2	-	609838
Inactivation cascade				
Recoverin	<i>RCVN</i>	The same as in the rod		
Opsin kinase	<i>GRK7</i>	G protein-coupled receptor kinase 7	-	606987
Arrestin	<i>ARR3</i>		Probably linked with xl myopia, female-limited (301010)	301770
GTPase-activating protein complex	<i>RGS9</i>	The same as in the rod, but the concentration in cones is much higher[37]		
	<i>RGS9BP</i>			
	<i>GNB5</i>	Guanine nucleotide-binding protein, beta-5	ar intellectual developmental disorder with cardiac arrhythmia(617173) with Retinal signaling defect[38]	604447
Guanylate cyclase activator	<i>GUCA1A</i>	Guanylate cyclase activator 1a, GCAP1	ad COD/CORD (602093)	600364

	<i>GUCA1B</i>	Guanylate cyclase activator 1b, GCAP2	ad RP (613827)	602275
Guanylate cyclase	<i>GUCY2D</i>	Guanylate cyclase 2d	ad /ar COD/CORD (601777) ar LCA (204000)	600179

1.3.3. Signal transmission from photoreceptor to bipolar cells

Under dark adapted conditions, photoreceptors are partially depolarized (or more properly – less hyperpolarized – as the membrane potential is about -40 mV) and release glutamate in the synaptic cleft between photoreceptor and bipolar cells. The underlying mechanism is known as *dark current*: a steady ionic current flows inward through the plasma membrane of the rod outer segments. It is balanced by equal outward current distributed along the remainder of each rod. Rods and S-cones make synapse with ON-bipolar cells while L- and M-cones make synapse with both cone ON- and OFF-bipolar cells. The axons of OFF- and ON-cone bipolar cells terminate at different levels in the IPL: OFF- in the outer half and ON- in the inner half. ON- and OFF-bipolar cells are characterized by distinct glutamate receptors at their dendritic tips. The metabotropic glutamate receptors (mGluRs), mainly mGluR6 (encoded by *GRM6*), is present at the dendritic tips of ON-bipolar cells and is activated by glutamate released from photoreceptors in scotopic conditions. Metabotropic glutamate receptors also belong to the G protein-coupled receptor family and their activation triggers the activation of this G protein and a transduction cascade, which results in the closing of the transient receptor potential cation channel subfamily M member 1 (encoded by *TRPM1*) and ON-bipolar cell hyperpolarization. GPR179, LRIT3 and NYX are partners in this cascade (Fig.8).

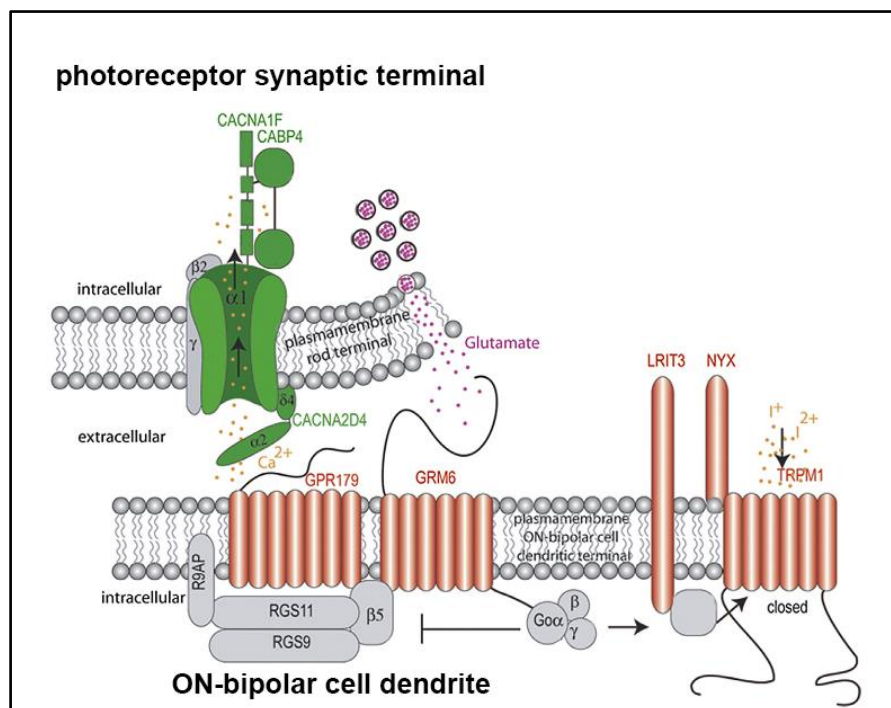


Figure 8 Schematic drawing of photoreceptor-ON bipolar cell synapse. Simplified from [39].

Ionotropic glutamate receptors (iGluRs) are localized at the dendritic tips of OFF-bipolar cells. Based on their pharmacological and electrophysiological properties, iGluRs can be classified

into NMDA (encoded by *GluN_x* genes) and non-NMDA receptors, which are further divided into AMPA (encoded by *GluA_x*) and kainite (encoded by *GluK_x* genes) receptors. They are themselves channels which open status can directly be modulated by glutamate concentration within the synaptic space[40].

Upon light stimulation, photoreceptors become more hyperpolarized (membrane potential is about -70mV) the release of glutamate at the synaptic cleft drops. mGluRs are then inactivated which results in the opening of TRPM1 and in ON-bipolar cell depolarization (so called sign-inverting signal transmission). Depolarizing rod ON-bipolar cells synapse with amacrine AII cells. Depolarized cone ON-bipolar cells synapse directly with ON-ganglion cells (Fig.9). In contrast, under light condition, iGluRs are closed and lead to cone OFF-bipolar cell hyperpolarization (so called sign-conserving transmission). Cone OFF-bipolar cells synapse directly to OFF-ganglion cells[20].

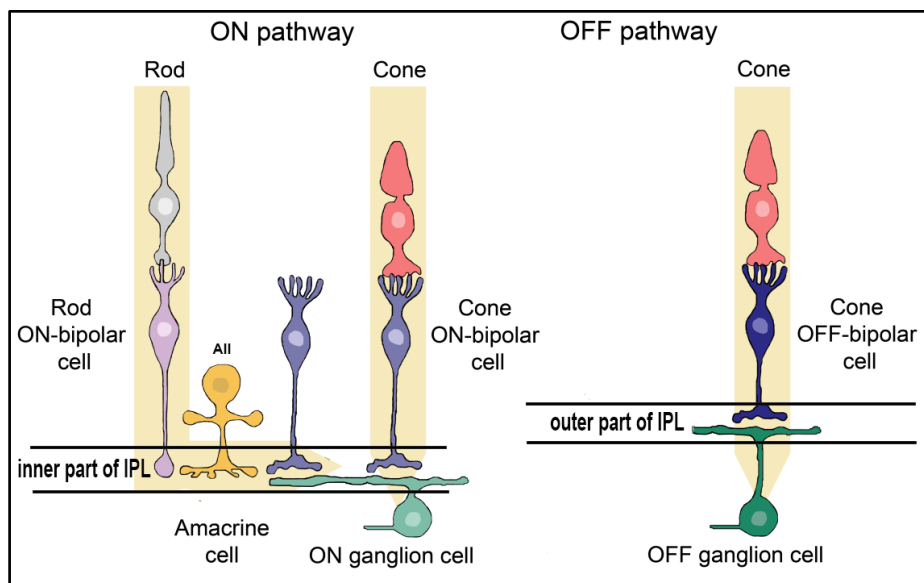


Figure 9. ON- and OFF - pathways in the retina. Adapted from [20]

Many of the genes/proteins involved in signal transduction from photoreceptor to bipolar cells (mainly ON-BC) are associated with human retinal disease (Tab.3). So far, IRD associated with isolated OFF-bipolar cell defects (e.g. iGluR dysfunctions) has not been described.

Table 3. Main proteins involved in photoreceptor to bipolar cell signal transmission and associated human diseases

Gene	Protein	Associated disease (OMIM phenotype reference)	OMIM gene reference
Photoreceptor synaptic terminals			
<i>CACNA1F</i>	Calcium channel, voltage-dependent, alpha-1 subunit	xl CSNB, incomplete (300071) xl CORD (300476) Aland eye disease(300600)	300110
<i>CABP4</i>	Calcium-binding protein 4	ar Cone-rod synaptic disorder, congenital nonprogressive (610427)	608965
<i>CACNA2D4</i>	Calcium channel, voltage-dependent, alpha-2/delta subunit 4	ar retinal cone dystrophy (610478) ar retinal dysfunction [41,42]	608171
<i>RIMS2</i>	Protein regulating synaptic membrane exocytosis 2	Cone-rod synaptic disorder syndrome, congenital nonprogressive (618970)	606630
ON-bipolar cells			
<i>GRM6</i>	Glutamate receptor, metabotropic, 6	ar CSNB, complete (257270)	604096
<i>GPR179</i>	G protein-coupled receptor 179	ar CSNB, complete (614565)	614515
<i>LRIT3</i>	Leucine-rich repeat, immunoglobulin-like, and transmembrane domains-containing protein 3	ar CSNB, complete (615058)	615004
<i>TRPM1</i>	Transient receptor potential cation channel, subfamily m	ar CSNB, complete (613216)	603576
<i>NYX</i>	Nyctalopin	xl CSNB, complete (310500)	300278
<i>GNB3</i>	Guanine nucleotide-binding protein, beta-3	ar retinal signaling defect (617024)	139130
<i>GNB5</i>	Guanine nucleotide-binding protein, beta-5	ar intellectual developmental disorder with cardiac arrhythmia (617173) with retinal signaling defect[38]	604447

1.3.4. Further signal transmission and modulation

Amacrine and horizontal cells could be seen as interneurons with a role of modulation and lateral inhibition of intraretinal signal transmission. Dendritic tips of horizontal cells make contact with both rod spherules and cone pedicles laterally to dendrites of bipolar cells. Amacrine cells make synapses with both photoreceptors and bipolar cells. The rod pathway is finally wired to cone signal transmission pathway through amacrine AII cell (Fig.9). At last, bipolar cell axons make synapse with ganglion cells, the first cell which could give rise to action potentials, then transmitted through the optic nerve to the brain[3].

1.4. Metabolism and supply of the retina incorporating genes involved in pathologic conditions

A metabolic supply of the retina is mostly provided by the RPE and the Muller cells.

1.4.1. Retinal pigment epithelium

RPE is a monolayer of hexagonal cells between Bruch's membrane and photoreceptor OSs. RPE cells contain melanosomes which contain melanin, a pigment absorbing most of visible light and thus giving a dark appearance to RPE cells[3].

RPE has multiple functions in the eye. First, it acts as the outer blood-retinal barrier, separating neural retinal layers from direct contact with choriocapillaris. Lateral RPE cell membranes present multiple tight junctions, limiting molecule diffusion between the choriocapillaris and photoreceptors[22]. Second, RPE maintain ion (K^+ , Na^+ , Ca^{2+} and Cl^-) and water homeostasis in the virtual subretinal space (between photoreceptors and RPE). It is important as the phototransduction cascade is dependent upon small ion concentration. Hydric surcharge in the subretinal space could lead to exudative retinal detachment. Third, the RPE provides light absorption, protecting the neural retina against light scattering and thermal/energetic damage. Melanin (product of tyrosine metabolism) and lipofuscin (fluorescent byproduct of lipid and retinoid metabolism) are two main pigments of the RPE. Forth, RPE produces retinal neurotrophic factors, as pigment epithelium-derived factor (PEDF), a potent inhibitor of angiogenesis and neuroprotector[43]. Fifth, RPE performs chromophore synthesis and reactivation, known as visual cycle.

1.4.2. Visual cycle

After photon activation of a rhodopsin molecule, its visual chromophore, 11-*cis*-retinal is isomerized into all-*trans*-retinal, which is dissociating from opsin molecule in few ms. All-*trans*-retinal is regenerated in 11-*cis*-retinal through multiple transfer and enzymatic isomerization steps, both in photoreceptors and in RPE cells.

At the recovery step, all-*trans*-retinal is released in the disc lumen of rods, where it links with phosphoethanolamine which could dimerize in potentially toxic bisretinoid A2E. The all-*trans*-retinal is transferred from lumen to the outer disc membrane through the flippase activity of the ATP binding cassette subfamily A member 4 (ABCA4) protein (Fig.10), which facilitates the removal of potentially toxic retinoid compounds from photoreceptors[44].

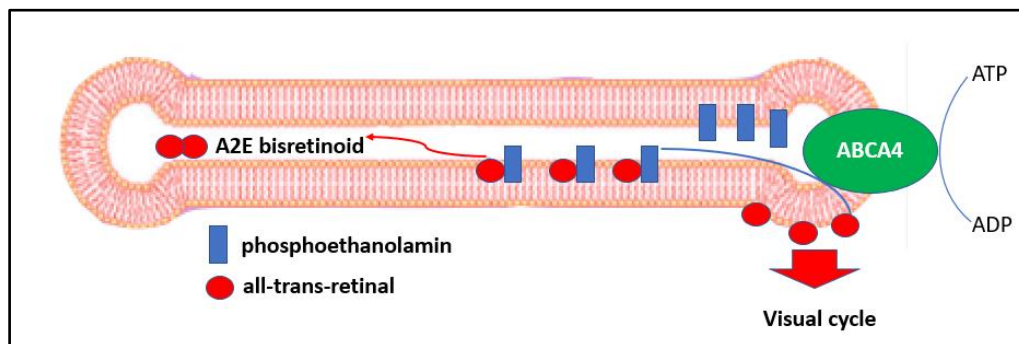


Figure 10. The role of ABCA4 in all-*trans*-retinol clearance from discs

In rod OS, the all-*trans*-retinal is reduced into all-*trans*-retinol by the retinol dehydrogenase 8 (RDH8) and possibly the retinol dehydrogenase 12 (RDH12)[45]. The all-*trans*-retinol is thus bound to the retinol binding protein 3 (RBP3) which transfers the chromophore to the RPE[46,47]. The retinol binding protein 1 (RBP1) interacts with the chromophore and transports it into ER, where the visual cycle occurs. Inside the organelle, the esterification of the all-*trans*-retinal into palmitate or stearate retinyl esters is catalyzed by the lecithin retinol acyltransferase (LRAT). The retinoid isomerohydrolase RPE65 hydrolyzes and isomerizes these retinyl esters in 11-*cis*-retinol[48]. The retinaldehyde binding protein 1 (RLBP1) interacts with 11-*cis*-retinol, which can affect its isomerohydrolysis, to help retinal dehydrogenase 5 (RDH5) and 11 (RDH11) to oxydate

it into 11-*cis*-retinal. RBP1 binds the 11-*cis*-retinal and translocates it into RPE cytosol, where RBP3 transports back the recycled chromophore into the rod OSs. The recycled chromophore will form a novel functional rhodopsin (Fig.11).

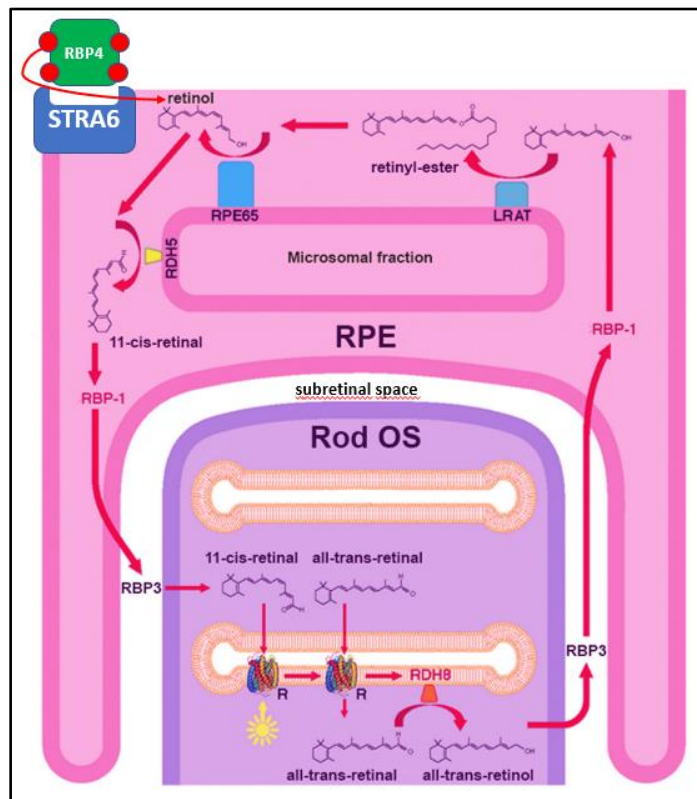


Figure 11 Visual cycle and RPE retinoid supply. Adapted from[16]

The RPE is highly dependent upon retinol supply. Retinol-binding protein 4 (RBP4) is the major plasma carrier of retinol and retinoids. It forms a heterohexameric complex with transthyretin in the blood, a characteristic which protects small molecules of RBP4 (21k Da) from glomerular filtration[49]. There are two different pathways for retinoids to reach RPE. The main pathway depends upon RBP4, which is complexed to retinol (holo-RBP4) and then recognized and bound to a membrane retinoid receptor STRA6, located at the basal side of the RPE. STRA6 allows the internalization of retinol[50]. The minor pathway is under the control of the scavenger class B type I receptor (Sr-BI) which enables the absorption of the protein-free fraction of retinoids transported within circulating lipoprotein complexes and chylomicrons[51]. RPE genes and proteins involved in visual cycle and frequently associated with IRD are listed in the Tab.4.

Table 4. Main genes coding for proteins involved in the visual cycle and retinoid supply associated with human diseases.

Gene	Protein	Associated disease (OMIM phenotype reference)	OMIM gene reference
------	---------	---	---------------------

<i>ABCA4</i>	ATP-binding cassette, subfamily A, member 4	Stargardt disease (248200) Cone-rod dystrophy (604116) Fundus flavimaculatus (248200)	601691
<i>RDH5</i>	Retinol dehydrogenase 5	Fundus albipunctatus (136880)	601617
<i>RDH12</i>	Retinol dehydrogenase 12	Leber congenital amaurosis (612712)	608830
<i>RBP3</i>	Retinol-binding protein 3	Retinitis pigmentosa (615233)	180290
<i>RBP4</i>	Retinol-binding protein 4	Retinal dystrophy, iris coloboma, and comedogenic acne syndrome (615147)	180250
<i>STRA6</i>	Stimulated by retinoic acid 6	Microphthalmia, isolated, with coloboma (601186)	610745
<i>RLBP1</i>	Retinaldehyde-binding protein 1	Retinitis punctata albescens (136880) Bothnia retinal dystrophy (607475) Newfoundland rod-cone dystrophy (607476) Fundus albipunctatus (136880)	180090
<i>RPE65</i>		Leber congenital amaurosis (204100) Retinitis pigmentosa (613794)	180069
<i>LRAT</i>	Lecithin retinol acyltransferase	Leber congenital amaurosis and Retinal dystrophy, early-onset severe (613341)	604863

1.4.3. Phagocytosis of photoreceptor outer segments

Photoreceptor OSs are continuously renewed through a turnover process including disc phagocytosis by RPE. Proteins expressed in the OS membrane are recognized by receptors at the apical surface of RPE cells, which activate RPE cell reorganization and internalization of photoreceptor OS. In this process, the receptor tyrosine kinase *c-mer* (MERTK) is particularly important. After phagocytosis, photoreceptor OS are enzymatically digested. The final byproduct of this digestion, which is incomplete, is lipofuscin, a fluorescent pigment which – if not properly eliminated – could be toxic for RPE[52].

2. Inherited retinal diseases: clinical retinal investigations, general considerations, taxonomy, phenotypes

2.1. Clinical retinal investigations

Evaluation of the retinal structure and function is essential to establish a correct diagnosis, prognosis and management in patients suffering from IRD. The first step of examination in IRD clinic is a detailed questionnaire including patient's complaints (vision loss, light sensitivity, night blindness, poor color distinction), associated past medical history (in view of syndromic IRD diagnosis), current medication (in view of differential for drug retinal toxicity) and family history with the drawing of a family tree.

2.1.1. Functional retinal evaluation

Visual acuity is the ability to recognize small details with precision or a limit of spatial resolution of the visual system. It is directly connected to foveal cone function. It is usually

defined as *minimum separabile* (least separation at which two parallel lines are recognized by the eye as separated). It is clinically tested using optotypes (standardized drawings with known line separation) presented to a subject in a grouped view (so called visual charts) at a given distance under standardized light conditions. One of the highly standardized charts widely used by retinal specialists is an Early Treatment Diabetic Retinopathy Study (ETDRS) chart, giving the evaluation of the visual acuity in letter score, logMAR, decimal and Snellen equivalents[53].

Visual field is as the entire area that can be seen when an eye is fixing straight at a point. It was imaginatively described by Traquair as an “island of vision surrounded by a sea of blindness”[54]. Visual field-testing studies the retinal sensitivity through static or kinetic approaches. Briefly, the patient is placed in front of a concave dome presenting stimuli of various intensities at different location in a static (fixed) or kinetic (moving) way while the patient is asked to push a button when the stimulus is perceived. This generates a map of retinal sensitivity (Fig.12). Different strategies of stimulation could be used to separate a cone subtype (e.g. blue-yellow perimetry), rod (scotopic perimetry) or visual pathway (doubling frequency perimetry) sensitivity[55].

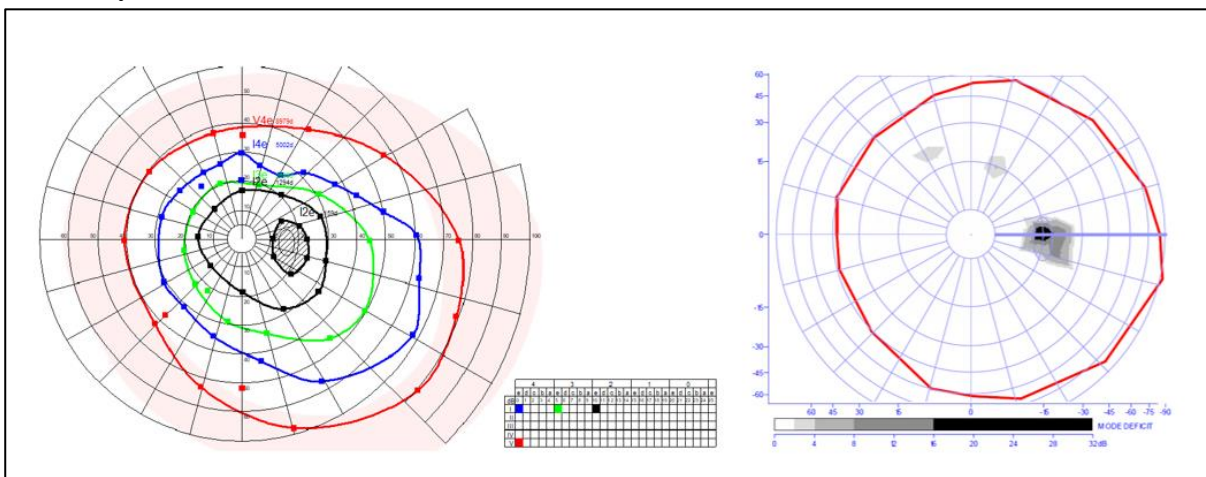


Figure 12 Kinetic (left) and static (right) visual field map of right eye. The points of retinal iso-sensitivity to a given moving stimulus are linked in circular isopters (left). A card of retinal sensitivity loss in dB comparing to a normal subject of the same age and sex (right). Metrovision MonCVOne visual field analyzer, candidate’s own collection.

The electroretinogram is the recording of an electrical potential generated in the retina in response to a change in illumination (Fig.13). A Full-field electroretinogram is the recording of an overall electrical activity of photoreceptors and bipolar cells. It is recorded noninvasively from the corneal surface, using ocular surface electrodes and a flash stimulator (usually a dome producing flashes of controlled duration, intensity, chromatic content and frequency or repetition). The protocol is standardized and regularly updated by the International Society of Clinical Visual Electrophysiology (ISCEV, <https://iscev.wildapricot.org/>)[56].

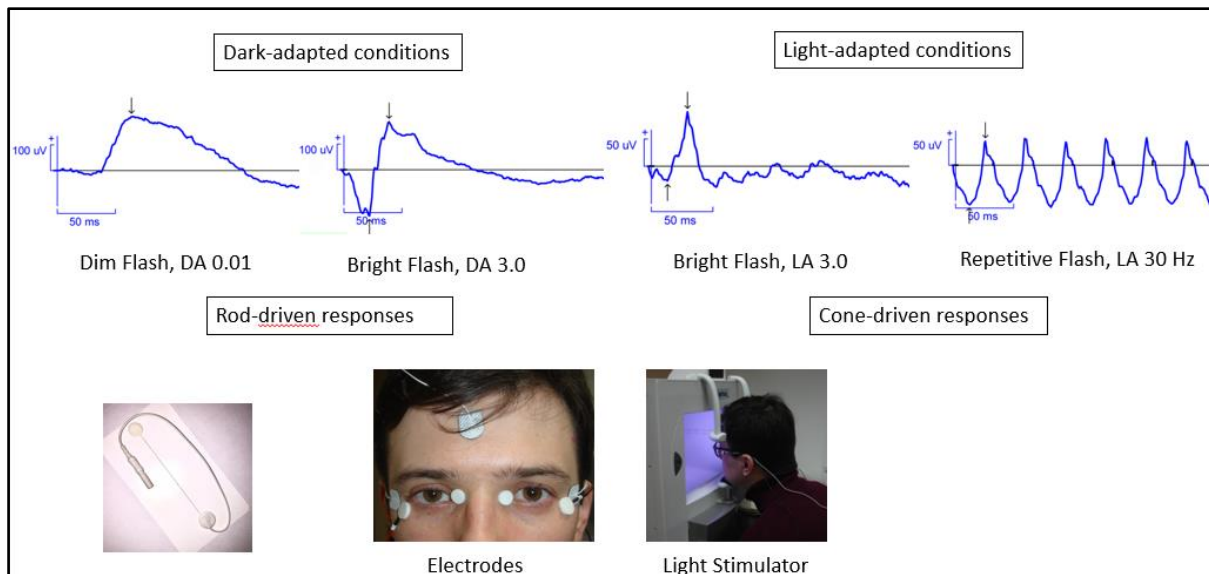


Figure 13 Full field ERG recordings and equipment. Candidate's own collection.

Under dark-adapted or scotopic conditions (DA), responses to a dim flash of 0.01 cd.s.m^{-2} generate a b-wave originating from rod ON-bipolar cell depolarization (Fig.12). Increased intensities of flashes (DA 3.0 and DA 10.0) ERG recordings show an a-wave corresponding to both rod and cone hyperpolarization in response to light stimulation (see §1.3 in Introduction), and a b-wave corresponding to ON-bipolar cell depolarization. Under light-adapted or photopic (LA) conditions, rod function is saturated and a 3.0 cd.s.m^{-2} flash elicits an a-wave, originating from cone photoreceptor and cone OFF-bipolar cell hyperpolarization, and a b-wave, originating from cone ON- (ascending limb) and OFF- (descending limb) bipolar cell responses[57].

2.1.2. Morphologic retinal evaluation

The observation of the retina using the ophthalmoscope or a magnifying lens at the slit lamp is a gold standard technique, but a photographic documentation of the fundus allows a more reliable follow-up.

Retinography (or fundus photography) enables to obtain a direct view of retina (Fig.14). It is a non-invasive ocular examination. Recent technical achievements enable to obtain an ultra-wide (up to 200°) fundus view without pupil dilation. Different wavelengths of visible light can be used while performing a retinography, allowing a better visualization of different retinal structures dependent upon their wavelength documenting a different depth of the retina. Fundus photographs in red light give a better view of the choroid, green or red-free snapshots highlight vascular structures and a photography in monochromatic blue light enables a better visualization of retinal nerve fiber layer and the vitreo-retinal interface.

Fundus autofluorescence is based on the fact that retinal pigments could absorb specific wavelengths (eliciting light) and emit a secondary light in another wavelength (fluorescence) (Fig14). Short-wavelength ("blue") fundus autofluorescence (SWAF) objective the lipofuscin accumulation (a peak excitation wavelength of 470 nm and emit yellow-green light with a peak wavelength of 600 nm) and thus dynamic interaction between photoreceptor outer segment and

RPE[58]. In a normal fundus without retinal pathology, blood vessels will appear dark (blood is intensely absorbing a blue light) as well as the optic nerve head (due to the absence of RPE or lipofuscin). With SWAF, the fovea will usually be visualized as a dark spot of hypoautofluorescence (due to the high concentration of blue-light-absorbing xanthophyll pigment).

Near-infrared fundus autofluorescence (NIRAF) objective melanin distribution in the RPE (Fig.14). For NIRAF excitation at 785 nm, there is a broad emission spectrum from melanin with maxima at 870 to 900 nm. The pic of NIRAF is formed by the fovea and the signal decreases progressively from the fovea to the retinal periphery. Retinal vasculature and optic nerve head appear dark[59].

Additionally, sub-retinal structures and pigment accumulation can be visualized on infrared reflectance imaging (IRR). The basis is a long excitation wavelength (~820 nm) that penetrates the optic media and enables visualizing the retina and choroid in detail. Changes in reflection and absorption of light through retinal tissues enhance the visualization of structures beneath the RPE[60].

Optical coherence tomography (OCT) is a major breakthrough in retinal imaging techniques. It is a non-invasive method providing a retinal scan and allowing the analyses of the retinal layers with near-histological resolution (Fig14). It is based on differential reflectance of retinal layers. A reconstruction of full-depth image objectives the retinal nerve fiber layer, GCL, IPL, INL, OPL, ONL, external limiting membrane, ellipsoid zone (corresponds to the interface between photoreceptors IS and OS), the interdigitation zone (corresponding to the invagination of the photoreceptors OS within the RPE), the RPE/Bruch's membrane complex and then choriocapillaris, choroid and sclera. Pathologic changes of the retinal layers could be easily detected by this technique.

The combination of multiple techniques of retinal imaging is known as **multimodal retinal imaging**. It is widely used to establish the diagnosis of IRD.

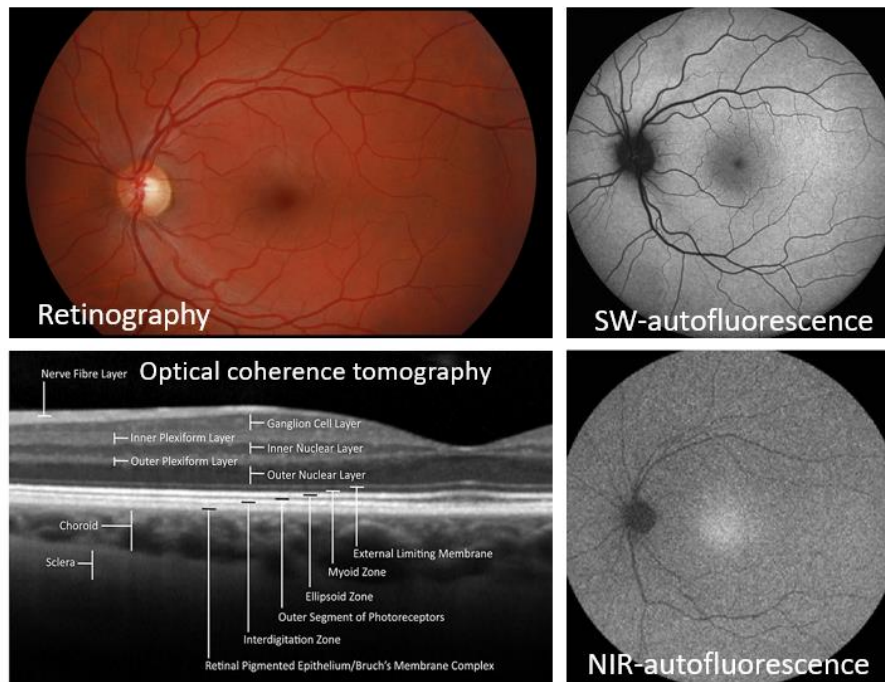


Figure 14 Techniques of retinal imaging. Normal retinal appearance at fundus photography, SWAF, NIRAF and OCT.

2.2. General considerations on inherited retinal disorders

Inherited retinal disorders (IRD) are a clinically and genetically heterogeneous group of retinal diseases. They occur at any age. These diseases affect approximately 4.5 million people worldwide. Their cumulative prevalence is about 1:2 000 persons in European countries with some local disparities[61–63]. There is a considerable phenotypic heterogeneity for individual clinical disorders. Despite this; IRD can be usefully divided clinically according to whether they i) are stationary or progressive, ii) exhibit predominantly rod, cone or inner retinal involvement. However, there is a substantial overlap in the clinical presentations and the molecular causes of IRD. Some of them could be accompanied by extraocular manifestations and thus called syndromic IRD; the remaining are retina-restricted, non-syndromic or isolated retinal degenerations. The latter are more frequent: 70-80%[64].

2.3. Stationary retinal diseases

In stationary IRD, there is usually no or few morphological retinal alterations with time. Alterations usually only affect the retinal function, that is why this group of disorders is also known as “stationary retinal dysfunctions”. Stationary IRD could be further subdivided in i) cone dysfunctions and ii) congenital stationary night blindness.

2.3.1. Cone dysfunctions

This group of IRD is characterized by reduced central vision and varying degrees of color vision abnormalities, nystagmus and photophobia[65]. Further clinical entities could be subdivided.

Achromatopsia (ACHM) is an autosomal recessive condition associated with a lack of cone function which affects about 1 in 30 000 people. It manifests in birth/early infancy with infantile/spasmus nutans-like nystagmus[66], poor visual acuity, a complete lack of color vision and marked photophobia[67]. Full-field ERG shows undetectable (in complete ACHM) or

severely reduced (in incomplete ACHM) cone-driven responses and normal rod-driven responses. Defects in five genes involved in the cone-specific phototransduction cascade have been reported in patients with ACHM. These are namely: *CNGA3* and *CNGB3* (encoding the α - and β -subunits of the cyclic nucleotide-gated channel 3 found in cone photoreceptor OS), *GNAT2* (encoding the α -subunit of the transducin) *PDE6C* and *PDE6H* (encoding the α - and γ -subunits of the cone photoreceptor-specific phosphodiesterase, respectively). More recently, *ATF6* has been identified as a sixth gene associated with ACHM. It encodes a transmembrane transcription factor ATF6 playing a role in ER homeostasis[67].

Blue cone monochromatism (BCM) clinical symptoms are close to ACHM, but the molecular basis is different. This X-linked condition is characterized by an absence of long (L)- (red) and middle (M)- (green) wavelength-sensitive opsins, both encoded on the X-chromosome. As the S-cones are present, patients retain a tritan (blue-yellow) color discrimination and ERG responses to short wavelength stimuli remain detectable[68].

Bradyopsia, oligocone trichromacy and Bornholm eye disease are far less frequent than ACHM and BCM. They reflect various degrees of cone-driven function impairment[65].

2.3.2. Congenital stationary night blindness

Congenital stationary night blindness with largely normal fundus appearance is a vast group of genetically and clinically heterogeneous congenital retinal disorders. The most common form manifests with infantile nystagmus, reduced visual acuity, variable degree of myopia, poor visual behavior in dim lighting. The diagnosis is ascertained by full-field electroretinogram, displaying characteristic waveform changes.

Most of the patients with CSNB have a distinct *Schubert-Bornschein type* electronegative waveform (b/a amplitude ratio < 1) under dark-adapted conditions[69], in relation with a signaling defect from photoreceptors to adjacent bipolar cells. Two subtypes of Schubert-Bornschein CSNB can be distinguished on the basis of additional ffERG features: the incomplete (icCSNB) and complete (cCSNB)[70]. In icCSNB, there is preserved but reduced and delayed b-wave to the DA0.01 ERG. Light-adapted responses are markedly reduced and delayed, reflecting a cone to cone ON- and OFF-bipolar cell transmission defect which can be documented using long duration stimulations. Patients have variable degrees of night blindness, strabismus, nystagmus, a wide range of refractive errors and a normal fundus, apart from myopic changes. Photophobia may be the main complaint for some patients who also experience difficulties in dimly lighted environment. Pathogenic variants in *CACNA1F* and *CABP4* lead to icCSNB. Proteins encoded by these genes are localized at the presynaptic membrane of both rods and cones. They play a role in glutamate release into the synaptic cleft. icCSNB represents thus a photoreceptor to ON- and OFF-bipolar cell transmission defect. In cCSNB, the b-wave is typically absent on the DA 0.01 ERG. The a-wave has typically a square shape with a sharply arising b-wave and a reduced b/a amplitude ratio at the LA 3.0 ERG, with absence of ON- responses but preserved OFF-responses to long duration stimulations. Patients with cCSNB consistently present with high myopia, nystagmus, night blindness and low visual acuity. Variants in *NYX*, *GRM6*, *TRPM1*, *GPR179* and *LRIT3* lead to cCSNB. Genes listed above code for proteins localized mainly at the dendritic tips of the ON-bipolar cells. They are important for glutamate-induced signaling. cCSNB represents thus a photoreceptor to ON-bipolar cell transmission defect[39].

Patients affected with the *Riggs-type of CSNB*[71] show a severe reduction of both the a- and b-waves at the DA 3.0 and 10.0 ERG in keeping with a generalized rod dysfunction. Photopic ERGs are preserved consistent with normal cone system function. Pathogenic variants in *GNAT1*, *RHO*, *PDE6B* and *SLC24A1* are linked to this form of CSNB[39].

2.4. Progressive inherited retinal degenerations

Progressive IRD are characterized by progressive retinal tissue degeneration responsible for RPE/photoreceptor loss. They are further subdivided by the age of onset and predominant cell type loss. Early-onset retinopathies are usually severe and include Leber Congenital Amaurosis (LCA) and early-onset severe retinal degeneration (EOSRD). Teenage- and adulthood-onset progressive IRD are more frequent. Late-onset IRD affects elderly populations.

2.4.1. Rod-cone dystrophies

Rod-cone dystrophies (RCD), also known as retinitis pigmentosa (RP), affect one person over 4,000 births worldwide[64,72]. Patients affected with RCD experience primary night blindness and loss of peripheral vision with a progressive visual field constriction, reaching tubular vision; total blindness, in more severe cases and at the end-stage disease. This phenotype is due to progressive rod photoreceptor dysfunction and death followed by cone degeneration. Fundus examination of RCD patients typically reveals pale optic disc, narrowed retinal vessels and in advanced cases, pigment migration at the retinal surface resembling bone spicules. FfERG recording confirms photoreceptor dysfunction, with reduction or total loss of the a- and b-wave under scotopic conditions in keeping with generalized rod photoreceptor dysfunction (Fig.15); photopic responses are less affected at the disease onset, but could also become undetectable due to a loss of cone function at the end-stage disease. Although the vast majority of RCD are isolated, some syndromic associations are frequent. Among them, Usher syndrome, including various degrees of hearing loss, vestibular dysfunction and RCD is the most common. Its prevalence is estimated between 3 to 6 for 100 000 and it is a leading cause of inherited blindness and deafness worldwide[73].

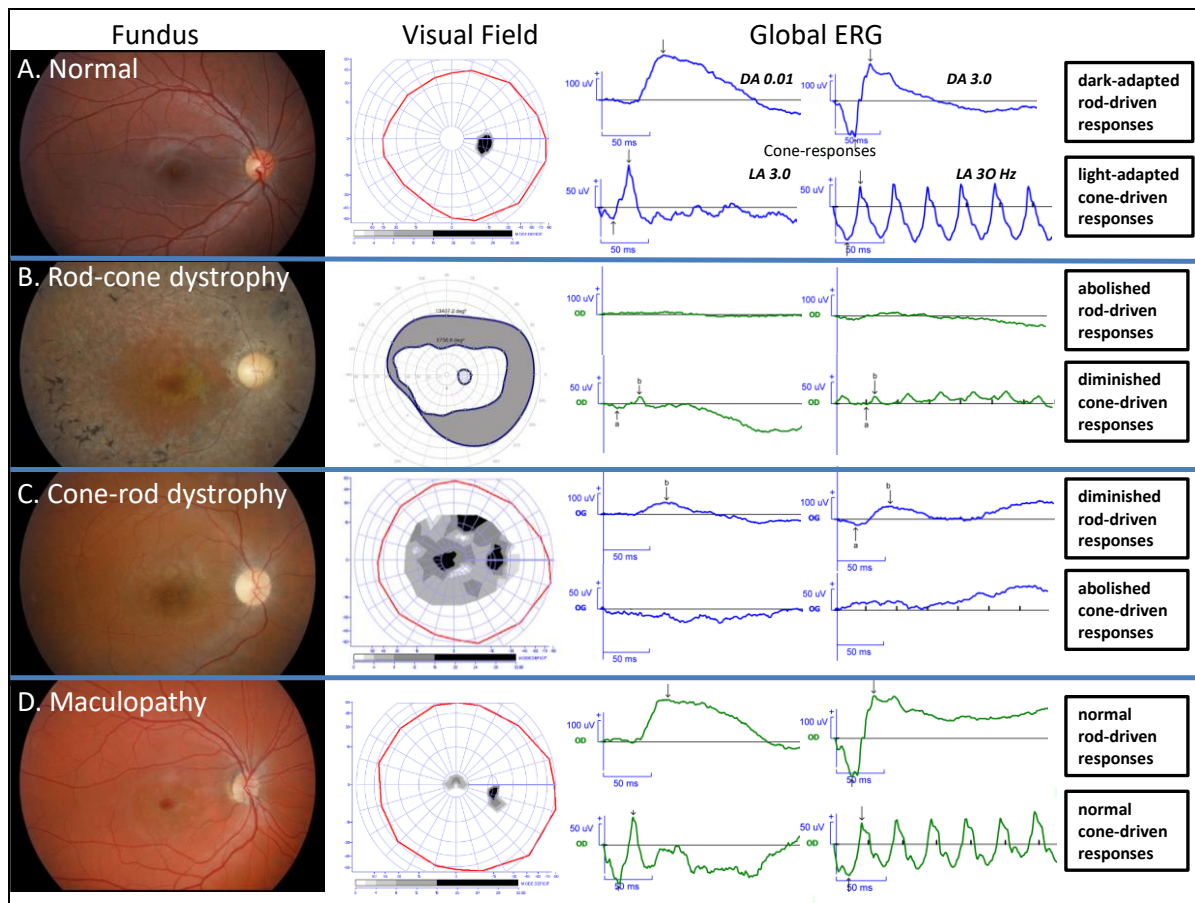


Figure 15. Schematic representation of the main differences between common IRD. A. Normally appearing fundus, visual field and ERG. B. Rod-cone dystrophy associated with biallelic variants in *EYS*. Optic disc pallor, retinal vasculature narrowing and bone spicules-like pigmentary changes are the classic ophthalmoscopic triad. Peripheral visual field loss (in grey) with spared central vision. ERG reveals undetectable rod-driven responses and diminished cone-driven responses. C. Cone-rod dystrophy associated with homozygous variant in *PROM1*. Prominent macular changes and relatively spared midperipheral retina. Visual field examination revealed an absolute central scotoma (black central dot) circled by a zone of hyposensitivity (in grey). ffERG is inverted compared to the previous one: rod-driven responses are diminished; cone-driven responses are undetectable. D. Maculopathy in Stargardt disease, associated with biallelic *ABCA4* pathogenic variants. Fundus changes are restricted to the macula. Visual field shows a small central scotoma. ERG is normal. Author's patients.

2.4.2. Cone/cone-rod dystrophies

Cone/cone-rod dystrophies (COD/CORD) are characterized by photophobia, color vision abnormalities and a primary loss of central vision[74,75], which can be followed by patchy losses of peripheral visual field[74]. Fundus examination reveals various degrees of macular changes. ERG recordings typically show abnormal responses under photopic conditions in keeping with generalized cone dysfunction and secondary alteration of the a- and b-waves under scotopic conditions when rod photoreceptors become affected (Fig.15). Cases of pure COD are very rare. Usually, there is a clinical continuum between COD and CORD. The course of CORD is more severe than that of COD, but both disorders progress to complete blindness in most cases.

The estimated prevalence for nonsyndromic COD and CORD is between one in 30,000 and one in 40,000, and all modes of Mendelian inheritance have been reported. They are highly

genetically heterogeneous, but as COD and CORD overlap strongly in their clinical characteristics, the genetic descriptions of both entities are generally merged. Ten genes involved in autosomal dominant forms of COD/CORD, twenty-three genes involved in recessive forms and two genes involved in X-linked forms have been reported in the Retnet database (<https://sph.uth.edu/retnet/sum-dis.htm#B-diseases>). However, 30–50% of recessive or simplex COD/CORD cases remain unsolved [76,77].

2.4.3. Inherited macular dystrophies or maculopathies

Inherited macular dystrophies (MD) or maculopathies primarily affect the central zone of the retina; there is usually no preference to the cell type loss (rods, cones and RPE). As for the CD/CORD the first symptoms are light aversion, visual acuity loss and color vision defects. Full-field ERG recordings are usually normal at the onset of MD (Fig.15). However, some MD could evolve in more widespread retinal disease (CORD) at the late stages so that various degrees of rod- and cone-dysfunction could be seen at this time point[78,79]. Age-related macular degeneration (AMD) is the most common cause of macular degeneration, a major health issue of ageing subset of population[80]. AMD is associated with some genetic susceptibility but the underlying pathogenic mechanisms are more complex and the disease does not follow a Mendelian pattern of inheritance[81] and thus is not studied here. Stargardt disease[82], Best vitelliform macular degeneration[78] and pattern-dystrophies[83] are the most frequent diseases in this group.

2.5. Vitreoretinopathies

Vitreoretinopathies (VRP) is a group of IRD characterized by an abnormal-appearing vitreous gel with associated retinal changes, leading to the instability of retinal attachment. The major risk in vitreoretinopathies is a retinal detachment. VRP could be further subdivided in exudative and degenerative. Exudative VRP are characterized by abnormal retinal vascular growth and distribution, leading to neovascular complications. The most common is familial exudative vitreoretinopathy (FEVR), which could be inherited in AR, AD or XL mode. Degenerative VRP is usually linked with abnormality of vitreous collagen structure and dominated by Stickler syndrome[84].

2.6. Isolated and syndromic inherited retinal disorders

Some of IRD are associated with extraocular manifestations and thus called syndromic IRD; the remaining are retina-restricted, non-syndromic retinal degenerations. The latter are more frequent: 70-80%[64,85].

The most common syndromic form is Usher syndrome (USH), characterized by RCD and hypoacusis/deafness[73,86]. Genes associated with Usher syndrome encode proteins involved in calyceal processes or in the primary cilium. Indeed, these genes are expressed in the retina and the ear. USH is a clinically heterogeneous group of eye-ear ciliopathies with three main reported subtypes associated with variable degrees of deafness, vestibular dysfunction and a RCD. Usher type 1 (USH1), the most severe form of USH, includes bilateral profound congenital sensorineural hearing loss, vestibular dysfunction and RP. Pathogenic variants in *MYO7A*, encoding myosin VIIA are the most common cause of USH1[87]. Usher type 2 (USH2) is characterized by various degrees (mild to severe) of congenital hearing loss without vestibular dysfunction and RCD[88]. Biallelic variants in *USH2A* are the most common cause of USH2 but responsible for non-syndromic autosomal recessive RCD as well[89,90]. Usher type 3 (USH3) is characterized by progressive postlingual hearing loss and variable vestibular dysfunction. Language development

is normal in most subjects[91,92]. Pathogenic variants in one gene have been associated with USH3: *CLRN1*, encoding clarin-1[93].

Ciliopathies could affect not only the retina and inner ear, but e.g. also the kidney, brain, bones. Bardet-Biedl syndrome is characterized by IRD (both RCD and CORD), obesity, polydactyly, hypogonadisms, renal and cognitive defects[94]. Senior-Loken syndrome is an IRD associated with renal failure due to nephronophthisis[95,96]. Jeune Asphyxiating thoracic dystrophy is a severe disease characterized by skeletal dysplasia (short limbs and ribs causing reduced thoracic capacity, narrow thorax, polydactyly, brachydactily) leading to respiratory insufficiency and a retinal degeneration[97].

Variants in genes associated with metabolic disorders are also frequently reported in patients with syndromic and isolated IRDs. Next Generation Sequencing technologies (NGS) enabled identification of variants in genes linked with lysosome (e.g. *CLN3*[98] and *MFSD8*[99]), peroxisome (e.g. *PEXI*[100] and *PEX26*[101]), Golgi apparatus, mitochondrial function and a molecule metabolism in patients with apparently non syndromic IRD. The ocular defects can occur before other features in these cases; gene identification is crucial for proper follow-up and prognosis, as the associated feature could appear later in life.

2.7. Genetics of inherited retinal disorders

IRD are genetically heterogeneous. All described patterns of inheritance could be seen. Most cases follow a classical Mendelian patterns: autosomal dominant (AD), autosomal recessive (AR) and X-linked (XL)(Fig. 16). In rare cases the transmission is mitochondrial; some exceptional cases have been also described in IRD field (digenic, uniparental isodisomy, complex rearrangements).

Autosomal dominant (AD) transmission is due to pathogenic variants in genes on autosomes (non-sexual chromosomes). One pathogenic allele is enough for developing a disease. Usually, affected members are seen in each generation on the pedigree. Father-to-son transmission is a hallmark in AD IRD. Theoretical risk of recurrency is 50% in offspring of affected individuals. Moreover, AD IRD are characterized by variable penetrance and expressivity. Incomplete penetrance is defined by the absence of clinical manifestations despite the carrier status of a pathogenic allele in a given individual. Variable expressivity encompasses differences in clinical picture (usually in terms of severity, more rare in terms of different disease manifestations) in individuals harboring the same pathogenic variant[102].

In autosomal recessive (AR) transmission, variants occur on autosomes at a homozygous state (two identical alleles) or at a compound heterozygous state (two different alleles). Each parent carries one of the variants in simple heterozygous state. The risk for the offspring of heterozygous parents to be affected is 25%. Usually, only one generation is affected on a pedigree. AR diseases are more frequent in consanguineous families and in inbred, usually isolated (geographically, behaviorally, etc.) populations. Some variants, called founder mutations, can be enriched (i.e. to have a higher frequency) in a specific population due to the absence of population mixing[102].

X-linked inheritance is associated with a pathogenic variant occurring on the X chromosome, females being carriers with a 50% risk of a having a girl as a carrier and an affected boy. Classically, only males are affected, since they have only one X chromosome. Disease manifestation in female carriers may be variable depending of the X chromosome inactivation bias (unequal, skewed lyonization), with potential development of disease if the X chromosome harboring pathogenic variant is predominantly expressed[102].

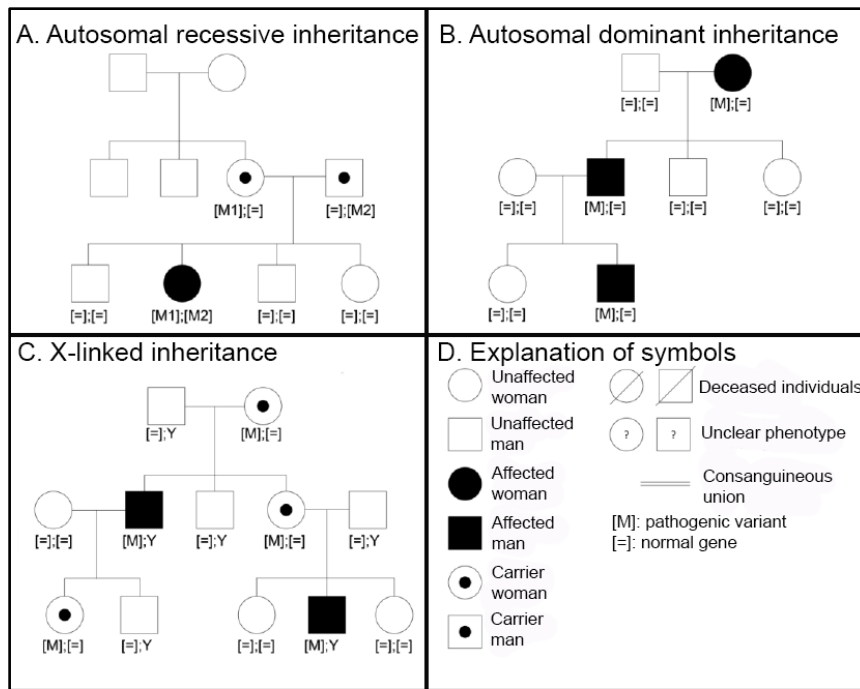


Figure 16. Mendelian patterns of inheritance and symbols used in medical genetic pedigrees.

Diseases linked with mitochondrial DNA defects are maternally inherited: the offspring of affected female (Fig.17) will harbor the pathogenic variant in homoplasmic (all copies of mitochondrial DNA are pathologic) or heteroplasmic (a proportion of mitochondrial DNA is pathologic, some copies are normal) state. Heteroplasmic variants tend to become homoplasmic with generations (“mitochondrial bottleneck”) if the disease is not lethal. Mitochondrial IRD are mostly syndromic with associated systemic (neurological, metabolic, endocrine, etc.) symptoms[103].

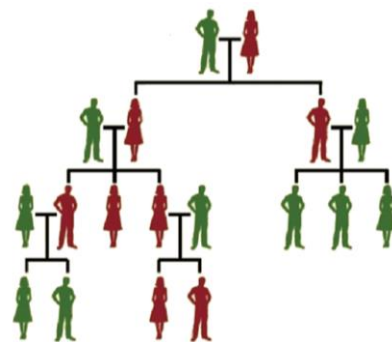


Figure 17. Maternal inheritance linked with mitochondrial DNA variants. Affected patients are in deep red.

In a lot of cases, only one family member is affected with IRD and the underlying inheritance mode is difficult to establish. These are sporadic (or simplex) cases. Most frequently they may represent recessive or X-linked cases but these cases can also show newly arisen (*de novo*) dominant variants.

3. Strategies for gene identification in inherited retinal disorders

3.1. Linkage studies

Linkage analysis is a genetic method that searches for chromosomal segments that cosegregate with the specific phenotype through families. Parametric linkage analysis is the traditional approach, when the probability that a gene is important for a given disease is linked to a genetic marker is studied using the LOD (logarithm of odds) score. LOD score assesses the probability that a given pedigree, where the disease and the genetic markers are cosegregating, is due to the existence of linkage or to chance[104].

Restriction enzymes were first used to cleave the DNA and calculate the linkage between the polymorphic “marker” and the disease-associated locus using the technique of restriction fragment length polymorphisms (RFLP). This method allowed to identify the “loci” in which the genes associated with the human disease could be. It was applicable only for multigenerational pedigrees with multiple affected members (mainly autosomal dominant disease) or for consanguineous families to know a homozygous region of their genome (homozygosity mapping).

In parallel, development of direct Sanger sequencing[105] and polymerase chain reaction to amplify the fragments of DNA[106], allowed to sequence the loci of interest and the genes linked with inherited retinal diseases[107]. Due to a large number of genes in the mapping locus, the precise detection of the gene linked with disorder can be difficult. Some erroneous results were also obtained. For example, disease linked with RP17 locus was first ascribed to the variants in *CA4* gene, but the final mechanism is a structural variant on this locus: duplication/inversion not involving *CA4*[108].

Another approach developed to discover IRD associated genes is a “candidate gene” approach proposed by Dryja[109]. Briefly, proteins and genes involved in the retinal physiology and morphology were directly sequenced in patients with IRD. This approach enabled to identify a large number of IRD genes but did not take in account genes expressed ubiquitously and still involved in the retinal disease (e.g. *PRFP31*, a major gene of adRP coding for a spliceosome component).

3.2. High throughput sequencing

A gene-by-gene approach to identify a gene defect in a given IRD pedigree is time-consuming and costly. That is why a *massive parallel sequencing* of a large number of known and candidate genes or loci has been developed and known under the name of Next Generation Sequencing (NGS). Targeted NGS panels are used to identify gene defects in a limited preset list of known-to-date genes associated with specific disease but could also be enriched in candidate genes[110]. When no variant in known genes have been identified, a Whole Exome Sequencing (WES) or Whole Genome Sequencing (WGS) could be performed in a limited number of pedigree members (usually in trio: affected patient and both parents) using a strategy of prioritizing (“filtering”) and comparison of variants to identify a gene linked with IRD[111,112]. Filtering methods differ depending on the lab but are based usually on the pattern of inheritance, the minor allele frequency (MAF). Pathogenic variants underlying IRD are rare or even absent from population allele frequency databases, (a cut-off of 0.005 is usually retained for an IRD and 0.001

for XL and ad), by type of variants and imbedded algorithms of pathogenicity prediction[113]. NGS could also be combined with classical linkage studies[114].

Data obtained from high throughput sequencing has limitations because of DNA quality and the sequencing coverage of the regions of interest: false-positive and false-negative results could be a feature. All the variants found through NGS studies should be validated by a gold standard technique: direct Sanger sequencing for small polymorphisms, qPCR and MLPA studies for structural variants. Due to the length of amplified fragments, large structural variants (copy number variations, inversions, translocations) are imperfectly solved by NGS and usually need some additional strategies for their identification[115,116].

3.3. Types of variants

A gene is composed of different parts: regulatory sequences, a promoter, 5' and 3' untranslated regions (UTR), coding (exons) and non-coding (introns) regions. Junctions between exon and intron are called canonical splice site regions. The sequence consensus of the donor site comprises the three last nucleotides of the exon and the following seven nucleotides in the intron; the sequence consensus of the acceptor site comprises 26 nucleotides in the intronic region before the intron/exon junction and the two first nucleotides in the exon[102].

There are different types of gene defects which could lead to a disease. **Single nucleotide variants (SNVs)** are single base pair substitutions. They are further subdivided in:

- Transition: interchange of one purine by the other (A>G) or of one pyrimidine by the other (C>T);
- Transversion: interchange of a purine and pyrimidine nucleic acid (A>C, G>T).

Single nucleotide polymorphisms in exons lead to a number of possible effects:

- *Synonymous variants* (coding for same amino acid) may have consequences at the mRNA level, especially if the change is located close to the canonical splice site;
- *Missense variants* will change the amino acid at the protein level; this change could be benign, not affecting protein function or pathogenic, responsible for disease;
- *Nonsense variants* introduce a premature stop codon in the sequence and may result in a shorter protein or degradation of mRNA by nonsense-mediated mRNA decay. There is a peculiar case when the premature stop codon is in the last exon or in the 50-55 nucleotides upstream of the last exon-exon junction. In this latter case nonsense-mediated mRNA decay does not occur[117].

SNVs in introns could affect:

- Canonical splice sites, causing exon skipping, exon augmentation, or altered splicing with pseudo-exons;
- Non-canonical splice sites, resulting in activation of non-canonical splice site(s) or the change of splicing regulatory elements;
- Or could be benign.

Small insertions and deletions, when not multiple of 3, will produce a frameshift and introduce a premature stop codon in the sequence, leading to the same consequences as nonsense variants.

Structural variants (SV) are variations that occur over a larger DNA sequence. This category of genetic variation includes both *copy number variations* (CNVs: deletions and

duplications of one exon and more) and *chromosomal rearrangement events* (e.g. inversions, translocations)[102].

3.4. Functional studies of candidate genes

The evidence for a gene defect to be responsible for a given IRD is corroborated by subsequent functional studies and by the screening of unsolved cohorts of patients for defects in this candidate gene.

Retinal transcription of candidate genes could be checked using organ, tissue or even cell-specific transcriptomic databases[118–121] and then be confirmed by expression studies through RNA *in situ* hybridization studies and RT-qPCR experiments using several tissues including retina or peripheral blood when appropriate. Protein expression could be established by immunostaining and western blot assays and sometimes by functional activity tests of the proteins (e.g. if they are enzymes).

Further identification of mechanisms of retinal degeneration underlying the gene defect involves animal modeling and *in vitro* modelling using patient-derived induced pluripotent cells (iPS) and retinal organoids[122]. Transcriptomic analysis of retinal/retinal-organoid derived cells harboring a specific gene defect can also indicate pathways and partner genes implicated in the IRD[123].

Particularly important are the inter-researcher group collaborations, which enables to put together cohorts of rare diseases and to screen them for specific candidate genes. European retinal disease consortium (ERDC, <https://www.ercd.info/>) and GeneMatcher (<https://genematcher.org/>) were conceived to this aim of information sharing.

Regularly updated list of genes and loci linked with IRD could be found at <https://sph.uth.edu/retnet/disease.htm>.

3.5 Purpose of my work

The goal of my PhD work was to identify known and novel gene defect(s) associated with IRD in a large cohort of patients the majority of whom were clinically investigated at the National Reference Center For Rare Ocular Diseases, REFERET, of the Centre Hospitalier National d'Ophtalmologie des Quinze-Vingts through targeted NGS, WES and WGS analyses, with subsequent functional studies to better understand the associated disease mechanism(s). Genotype-phenotype correlations in IRD patients were also studied.

Materials and Methods

1. Inherited retinal disorder cohort followed at the XV-XX hospital

A cohort of approximately 6.000 index IRD patients of various geographic origins is clinically examined and followed at the reference centre for rare diseases, REFERET, of the Centre Hospitalier National d'Ophthalmologie de Quinze-Vingts (Paris, France).

After clinical phenotyping, the data of patients are gathered into the clinical and genetic databases. A unique family number (Fxxx) and individual number (CICxxx) are attributed to each patient in order to de-identify them for further research purposes.

The study protocol adhered to the tenets of the Declaration of Helsinki and was approved by a National ethics committee (CPP Ile de France V, Project number 06693, N°EUDRACT 2006-A00347-44, 11 December 2006).

Blood samples from the index case and if possible from case's parents were collected for genetic research after informed consent. These DNA samples are stored and obtained from the NeuroSensCol DNA bank, for research in neuroscience (PI: JA Sahel, co-PI I Audo, partner with CHNO des Quinze-Vingts, Inserm and CNRS, certified NFS96-900).

During my PhD, I studied:

- a. A cohort of 768 IRD cases analyzed on a targeted NGS panel.
- b. A batch of 31 IRD families unsolved by targeted NGS and analyzed by WES.
- c. One family with North Carolina Macula Dystrophy analyzed by WGS.

2. Phenotyping

Briefly, best-corrected visual acuity (BCVA), refractive error, color vision, slit-lamp biomicroscopy, static and kinetic visual fields, full-field electroretinogram according to the standards of International Society for Clinical Electrophysiology of Vision [56](Espion, Diagnosys LLC, Lowell, MA), fundus photography, spectral domain optical coherence tomography (Spectralis OCT, Heidelberg Engineering, Inc., Heidelberg, Germany), near infrared and short-wavelength autofluorescence, infrared reflectance (Heidelberg Retinal Tomograph, Heidelberg Engineering, Inc.) were performed on all patients. Some ancillary tests (e.g. microperimetry, full stimulus threshold, visual electrophysiology as VEP, pattern ERG, multifocal ERG) was performed depending on their utility for clinical diagnosis or follow-up of progression or treatment. For further and specific description, cf. chapter 2 of Introduction and individual articles in the Results.

3. Genotyping workup

Blood samples from patients and family members were collected for genetic research and genomic DNA was extracted from peripheral leucocytes in blood samples by standard salting out procedures according to manufacturer recommendation (Autogen and Puregen Kit, Qiagen, Courtaboeuf, France) as previously reported[124].

RPGR-ORF15 was prescreened by Sanger sequencing on samples of any male cases with RCD/CORD and no clear autosomal dominant inheritance pattern as this purine-rich region is usually poorly covered through high throughput sequencing. *RPGR* is a major gene associated

with X-linked RP (RP3, OMIM #300029) and CORD (CORD-XL1, OMIM #3040207-8% in IRD cohorts) with 80% of variants identified in exon *ORF15* [125–128].

3.1 Next generation sequencing

Initially, targeted NGS of 351 genes known or putative to be associated with IRDs (<https://sph.uth.edu/retnet/sum-dis.htm>), in collaboration with a company (IntegraGen, Evry, France), on *RPGR-ORF15* prescreened samples were performed to identify the underlying gene defect(s) of studied IRD patients[33]. NGS was done as following: a)Library preparation: first a custom-made oligonucleotide probe library in a TWIST silicon platform (TWIST bioscience, South San Francisco, USA) was designed to capture the exons of 351 genes and flanking intronic regions (Table 5) including known genes and candidate genes associated with IRD. b)Cluster generation: the library was loaded into a flow cell (SureSelect oligo probe, Agilent Courtaboeuf, France) where DNA fragments were captured on a lawn of surface-bound oligos complementary to the library adapters. Each fragment was then amplified into distinct, clonal clusters through bridge amplification (6 PCR cycles enrichment and 14 cycles PCR amplification). When cluster generation was completed, the templates were ready for sequencing. c)High throughput sequencing: Illumina NovaSeq technology uses a reversible terminator-based method that detects single bases as they are incorporated into DNA template strands generating 100 bp paired-end reads (Illumina, San Diego, USA). d)Data analysis: Image analysis was performed using Illumina real time analysis (v.3.4.4), then sequence reads were aligned to a reference human genome (UCSC hg38) using BWA-MEM alignment algorithm.

All bioinformatic pipeline with at the end-stage a variant calling were available on a web-based interface (SIRIUS: <https://integragen.com/fr/bioinformatique/sirius>) and in form of excel-sheets. Only nonsense, missense, canonical splice site and some known deep intronic variants, deletion et/or insertion variants were investigated first. If absent, filtering was enlarged to deep intronic, synonymous, 3' and 5'-UTR variants. Based on AD or AR XL pattern of inheritance, minor allele frequency inferior or equal to 0.005 or 0.001, respectively, in 1000Genomes (<http://www.1000genomes.org/>), Exome Aggregation Consortium (ExAC) (<http://exac.broadinstitute.org/>) and Genome Aggregation Database (gnomAD) (<http://gnomad.broadinstitute.org/>) were considered for analysis, as previously reported[129]. Pathogenicity was predicted for each remaining missense variant with multiple bioinformatic tools imbedded in AlamutTM software (<https://www.sophiagenetics.com/platform/alamut-visual-plus/>): Polymorphism Phenotyping v2 (PolyPhen2) <http://genetics.bwh.harvard.edu/pph2/>), Sorting Intolerant From Tolerant (SIFT) (<http://sift.jcvi.org/>) and MutationTaster (<http://www.mutationtaster.org/>). Variants predicted to be not disease-causing by PolyPhen2 and SIFT were not kept. Amino acid conservation across 100 species was evaluated with the UCSC Genome Browser (<http://genome.ucsc.edu/index.html>; Human GRCh38/hg38 Assembly). Non-canonical splice site variants were assessed with multiple algorithms imbedded in AlamutTM and additionally by SpliceAI[130]. All variants were then classified in accordance with standards of American College of Medical Genetics and Genomics (ACMG)[131,132].

Table 5. List of the 351 genes included in the targeted NGS panel performed to this cohort of patients.

	Gene	chromosomal localization	Full name
1	<i>ABCA4</i>	1p22.1	ATP binding cassette subfamily A member 4
2	<i>ABHD12</i>	20p11.21	abhydrolase domain containing 12, lysophospholipase
3	<i>ACBD5</i>	10p12.1	acyl-CoA binding domain containing 5
4	<i>ADAM9</i>	8p11.22	ADAM metallopeptidase domain 9
5	<i>ADAMTS18</i>	6q23.1	ADAM metallopeptidase with thrombospondin type 1 motif 18
6	<i>ADIPOR1</i>	1q32.1	adiponectin receptor 1
7	<i>ADGRV1</i>	5q14.3	adhesion G protein-coupled receptor V1
8	<i>AGBL5</i>	2p23.3	ATP/GTP binding protein like 5
9	<i>AHI1</i>	6q23.	Abelson helper integration site 1
10	<i>AIPL1</i>	17p13.2	aryl hydrocarbon receptor interacting protein like 1
11	<i>ALMS1</i>	2p13.1	ALMS1 centrosome and basal body associated protein
12	<i>ANKRD34C</i>	15q25.1	ankyrin repeat domain 34C
13	<i>ARFGAP2</i>	11p11.2	ADP ribosylation factor GTPase activating protein 2
14	<i>ARHGEF16</i>	1p36.32	Rho guanine nucleotide exchange factor 16
15	<i>ARHGEF18</i>	19p13.2	Rho/Rac guanine nucleotide exchange factor 18
16	<i>ARHGEF17</i>	11q13.4	Rho guanine nucleotide exchange factor 17
17	<i>ARHGEF38</i>	4q24	Rho guanine nucleotide exchange factor 38
18	<i>ARL13B</i>	3q11.1-q11.2	ADP ribosylation factor like GTPase 13B
19	<i>ARL2BP</i>	16q13	ADP ribosylation factor like GTPase 2 binding protein
20	<i>ARL3</i>	10q24.32	ADP ribosylation factor like GTPase 3
21	<i>ARL6</i>	3q11.2	ADP ribosylation factor like GTPase 6
22	<i>ARMC9</i>	2q37.1	armadillo repeat containing 9
23	<i>ARSG</i>	17q24.2	arylsulfatase G
24	<i>ASRGL1</i>	11q12.3	asparaginase and isoaspartyl peptidase 1
25	<i>ATF6</i>	1q23.3	activating transcription factor 6
26	<i>ATL2</i>	2p22.2-p22.1	atlastin GTPase 2
27	<i>ATXN7</i>	3p14.1	ataxin 7
28	<i>BBIP1</i>	10q25.2	BBSome interacting protein 1
29	<i>BBS1</i>	11q13.2	Bardet-Biedl syndrome 1
30	<i>BBS10</i>	12q21.2	Bardet-Biedl syndrome 10
31	<i>BBS12</i>	4q27	Bardet-Biedl syndrome 12
32	<i>BBS2</i>	16q13	Bardet-Biedl syndrome 2
33	<i>BBS4</i>	15q24.1	Bardet-Biedl syndrome 4

34	<i>BBS5</i>	2q31.1	Bardet-Biedl syndrome 5
35	<i>BBS7</i>	4q27	Bardet-Biedl syndrome 7
36	<i>BBS9</i>	7p14.3	Bardet-Biedl syndrome 9
37	<i>BCL9</i>	1q21.2	BCL9 transcription coactivator
38	<i>BEST1</i>	11q12.3	bestrophin 1
39	<i>BFSP1</i>	20p12.1	beaded filament structural protein 1
40	<i>C16orf46</i>	16q23.2	chromosome 16 open reading frame 46
41	<i>C1QTNF5</i>	11q23.3	C1q and TNF related 5
42	<i>CFAP410</i>	21q22.3	cilia and flagella associated protein 410
43	<i>C2orf71= PCARE</i>	2p23.2	chromosome 2 open reading frame 71
44	<i>CPLANE1</i>	5p13.2	ciliogenesis and planar polarity effector 1
45	<i>C8orf37</i>	8q22.1	chromosome 8 open reading frame 37
46	<i>CA4</i>	17q23.1	carbonic anhydrase 4
47	<i>CABP4</i>	11q13.2	calcium binding protein 4
48	<i>CACNA1F</i>	Xp11.23	calcium voltage-gated channel subunit alpha1 F
49	<i>CACNA2D4</i>	12p13.33	calcium voltage-gated channel auxiliary subunit alpha2delta 4
50	<i>CALHM3</i>	10q24.33	calcium homeostasis modulator 3
51	<i>CAPN5</i>	11q13.5	calpain 5
52	<i>CAPN7</i>	3p25.1	calpain 7
53	<i>CC2D2A</i>	4p15.32	coiled-coil and C2 domain containing 2A
54	<i>CCDC51</i>	3p21.31	coiled-coil domain containing 51, <i>putative</i>
55	<i>CCT2</i>	12q15	chaperonin containing TCP1 subunit 2
56	<i>CCZ1B</i>	7p22.1	CCZ1 homolog B, vacuolar protein trafficking and biogenesis associated
57	<i>CDH16</i>	16q22.1	cadherin 16
58	<i>CDH3</i>	16q22.1	cadherin 3
59	<i>CDH23</i>	10q22.1	cadherin related 23
60	<i>CDHR1</i>	10q23.1	cadherin related family member 1
61	<i>CDK5RAP3</i>	17q21.32	CDK5 regulatory subunit associated protein 3
62	<i>CENPN</i>	16q23.2	centromere protein N
63	<i>CEP164</i>	11q23.3	centrosomal protein 164
64	<i>CEP250</i>	20q11.22	centrosomal protein 250
65	<i>CEP290</i>	12q21.32	centrosomal protein 290
66	<i>CEP78</i>	9q21.2	centrosomal protein 78
67	<i>CERKL</i>	2q31.3	ceramide kinase like
68	<i>CFH</i>	1q31.3	complement factor H
69	<i>CHM</i>	Xq21.2	CHM Rab escort protein

70	<i>CLCC1</i>	1p13.3	chloride channel CLIC like 1
71	<i>CIC</i>	19q13.2	capicua transcriptional repressor
72	<i>CLN3</i>	16p12.1	CLN3 lysosomal/endosomal transmembrane protein, battenin
73	<i>CLN8</i>	8p23.3	CLN8 transmembrane ER and ERGIC protein
74	<i>CLRN1</i>	3q25.1	clarin 1
75	<i>CLUAP1</i>	16p13.3	clusterin associated protein 1
76	<i>CNGA1</i>	4p12	cyclic nucleotide gated channel subunit alpha 1
77	<i>CNGA3</i>	2q11.2	cyclic nucleotide gated channel subunit alpha 3
78	<i>CNGB1</i>	16q21	cyclic nucleotide gated channel subunit beta 1
79	<i>CNGB3</i>	8q21.3	cyclic nucleotide gated channel subunit beta 3
80	<i>CNNM4</i>	2q11.2	cyclin and CBS domain divalent metal cation transport mediator 4
81	<i>COL11A1</i>	1p21.1	collagen type XI alpha 1 chain
82	<i>COL2A1</i>	12q13.11	collagen type II alpha 1 chain
83	<i>COL9A1</i>	6q13	collagen type IX alpha 1 chain
84	<i>CRB1</i>	1q31.3	crumbs cell polarity complex component 1
85	<i>CROCC</i>	1p36.13	ciliary rootlet coiled-coil, rootletin
86	<i>CRTAC1</i>	10q24.2	cartilage acidic protein 1
87	<i>CRX</i>	19q13.33	cone-rod homeobox
88	<i>CSPP1</i>	8q13.1-q13.2	centrosome and spindle pole associated protein 1
89	<i>CTDP1</i>	18q23	CTD phosphatase subunit 1
90	<i>CTNNA1</i>	5q31.2	catenin alpha 1
91	<i>CWC27</i>	5q12.3	CWC27 spliceosome associated cyclophilin
92	<i>CYP4V2</i>	4q35.1-q35.2	cytochrome P450 family 4 subfamily V member 2
93	<i>DHDDS</i>	1p36.11	dehydrodolichyl diphosphate synthase subunit
94	<i>DHX32</i>	10q26.2	DEAH-box helicase 32
95	<i>DHX38</i>	16q22.2	DEAH-box helicase 38
96	<i>DNAJC17</i>	15q15.1	DnaJ heat shock protein family (Hsp40) member C17
97	<i>DNMBP</i>	10q24.2	dynamamin binding protein
98	<i>DRAM2</i>	1p13.3	DNA damage regulated autophagy modulator 2
99	<i>DTHD1</i>	4p14	death domain containing 1
100	<i>DSCAML1</i>	11q23.3	DS cell adhesion molecule like 1
101	<i>EFEMP1</i>	2p16.1	EGF containing fibulin extracellular matrix protein 1
102	<i>ELOVL4</i>	6q14.1	ELOVL fatty acid elongase 4
103	<i>EMC1</i>	1p36.13	ER membrane protein complex subunit 1
104	<i>EML4</i>	2p21	EMAP like 4
105	<i>EXOSC2</i>	9q34.12	exosome component 2

106	<i>EYS</i>	6q12	eyes shut homolog
107	<i>EZR</i>	6q25.3	ezrin
108	<i>TLCD3B</i>	16p11.2	TLC domain containing 3B
109	<i>FAM71A</i>	1q32.3	family with sequence similarity 71 member A
110	<i>FAM171A1</i>	10p13	family with sequence similarity 171 member A1
111	<i>FAM98B</i>	15q14	family with sequence similarity 98 member B
112	<i>FDFT1</i>	8p23.1	farnesyl-diphosphate farnesyltransferase 1
113	<i>FAM161A</i>	2p15	FAM161 centrosomal protein A
114	<i>FLVCR1</i>	1q32.3	FLVCR heme transporter 1
114	<i>FOXI2</i>	10q26.2	forkhead box 12
116	<i>FUT5</i>	19p13.3	fucosyltransferase 5
117	<i>GABRR1</i>	6q15	gamma-aminobutyric acid type A receptor subunit rho1
118	<i>FZD4</i>	11q14.2	frizzled class receptor 4
119	<i>GDF6</i>	8q22.1	growth differentiation factor 6
120	<i>GNAT1</i>	3p21.31	G protein subunit alpha transducin 1
121	<i>GNAT2</i>	1p13.3	G protein subunit alpha transducin 2
122	<i>GNB1L</i>	22q11.21	G protein subunit beta 1 like
123	<i>GNB3</i>	12p13.31	G protein subunit beta 3
124	<i>GNPTG</i>	16p13.3	N-acetylglucosamine-1-phosphate transferase subunit gamma
125	<i>ADGRA3=GPR125</i>	4p15.2	adhesion G protein-coupled receptor A3
126	<i>GPR179</i>	17q12	G protein-coupled receptor 179
127	<i>GPR45</i>	2q12.1	G protein-coupled receptor 45
128	<i>GRID2</i>	4q22.1-q22.2	glutamate ionotropic receptor delta type subunit 2
129	<i>GRK1</i>	13q34	G protein-coupled receptor kinase 1
130	<i>GRM6</i>	5q35.3	glutamate metabotropic receptor 6
131	<i>GUCA1A</i>	6p21.1	guanylate cyclase activator 1A
132	<i>GUCA1B</i>	6p21.1	guanylate cyclase activator 1B
133	<i>GUCY2D</i>	17p13.1	guanylate cyclase 2D, retinal
134	<i>GYS1</i>	19q13.33	glycogen synthase 1
135	<i>HARS1</i>	5q31.3	HISTIDYL-tRNA SYNTHETASE 1
136	<i>HDAC4</i>	2q37.3	histone deacetylase 4
137	<i>HGSNAT</i>	8p11.21-p11.1	heparan-alpha-glucosaminide N-acetyltransferase
138	<i>HK1</i>	10q22.1	hexokinase 1
139	<i>HMCN1</i>	1q25.3-q31.1	hemicentin 1
140	<i>HNRNPR</i>	1p36.12	heterogeneous nuclear ribonucleoprotein R
141	<i>IDH3A</i>	15q25.1	isocitrate dehydrogenase (NAD(+)) 3 catalytic subunit alpha

142	<i>IDH3B</i>	20p13	isocitrate dehydrogenase (NAD(+)) 3 non-catalytic subunit beta
143	<i>IFT27</i>	22q12.3	intraflagellar transport 27
144	<i>IFT88</i>	13q12.11	intraflagellar transport 88
145	<i>IFT43</i>	14q24.3	intraflagellar transport 43
146	<i>IFT81</i>	12q24.11	intraflagellar transport 81
147	<i>IFT122</i>	3q21.3-q22.1	intraflagellar transport 122
148	<i>IFT140</i>	16p13.3	intraflagellar transport 140
149	<i>IFT172</i>	2p23.3	intraflagellar transport 172
150	<i>IMPDH1</i>	7q32.1	inosine monophosphate dehydrogenase 1
151	<i>IMPG1</i>	6q14.1	interphotoreceptor matrix proteoglycan 1
152	<i>IMPG2</i>	3q12.3	interphotoreceptor matrix proteoglycan 2
153	<i>INPP5E</i>	9q34.3	inositol polyphosphate-5-phosphatase E
154	<i>INVS</i>	9q31.1	inversin
155	<i>IQCB1</i>	3q13.33; 3q21.1	IQ motif containing B1
156	<i>IRX5</i>	16q12.2	iroquois homeobox 5
157	<i>ITIH2</i>	10p14	inter-alpha-trypsin inhibitor heavy chain 2
158	<i>ITM2B</i>	13q14.2	integral membrane protein 2B
159	<i>KCNJ13</i>	2q37.1	potassium inwardly rectifying channel subfamily J member 13
160	<i>KCNV2</i>	9p24.2	potassium voltage-gated channel modifier subfamily V member 2
161	<i>KIAA1549</i>	7q34	KIAA1549
162	<i>KIAA2026</i>	9p24.1	KIAA2026
163	<i>KIZ</i>	20p11.23	kizuna centrosomal protein
164	<i>KLHL7</i>	7p15.3	kelch like family member 7
165	<i>KRT26</i>	17q21.2	keratin 26
166	<i>KSS</i>	mtDNA	KEARNS-SAYRE SYNDROME protein
167	<i>LAMA1</i>	18p11.31	laminin subunit alpha 1
168	<i>LARGE1</i>	22q12.3	LARGE xylosyl- and glucuronyltransferase 1
169	<i>LCA5</i>	6q14.1	lebercilin LCA5
171	<i>LIG3</i>	17q12	DNA ligase 3
172	<i>LRAT</i>	4q32.1	lecithin retinol acyltransferase
173	<i>LRIT3</i>	4q25	leucine rich repeat, lg-like and transmembrane domains 3
174	<i>LRP5</i>	11q13.2	LDL receptor related protein 5
175	<i>LZTFL1</i>	3p21.31	leucine zipper transcription factor like 1
176	<i>MAK</i>	6p24.2	male germ cell associated kinase
177	<i>MAN2C1</i>	15q24.2	mannosidase alpha class 2C member 1
178	<i>MAPKAPK3</i>	3p21.2	MAPK activated protein kinase 3

179	<i>MERTK</i>	2q13	MER proto-oncogene, tyrosine kinase
180	<i>MFRP</i>	11q23.3	membrane frizzled-related protein
181	<i>MFSD8</i>	4q28.2	major facilitator superfamily domain containing 8
182	<i>MiR-204</i>	9q21.12	microRNA 204
183	<i>MKKS</i>	20p12.2	McKusick-Kaufman syndrome
184	<i>MKS1</i>	17q22	MKS transition zone complex subunit 1
185	<i>MPRIIP</i>	17p11.2	myosin phosphatase Rho interacting protein
186	<i>MT-ATP6</i>	mtDNA	mitochondrially encoded ATP synthase 6
187	<i>MT-TH</i>	mtDNA	mitochondrially encoded tRNA histidine
188	<i>MT-TP</i>	mtDNA	mitochondrially encoded tRNA proline
189	<i>MT-TS2</i>	mtDNA	mitochondrially encoded tRNA serine 2 (AGU/C)
190	<i>MTTP</i>	mtDNA	microsomal triglyceride transfer protein
191	<i>MVK</i>	12q24.11	mevalonate kinase
192	<i>MYO7A</i>	11q13.5	myosin VIIA
193	<i>NAALADL1</i>	11q13.1	N-acetylated alpha-linked acidic dipeptidase like 1
194	<i>NBAS</i>	2p24.3	NBAS subunit of NRZ tethering complex
195	<i>NDP</i>	Xp11.3	norrin cystine knot growth factor NDP
196	<i>NDRG4</i>	16q21	NDRG family member 4
197	<i>NEK2</i>	1q32.3	NIMA related kinase 2
198	<i>NEUROD1</i>	2q31.3	neuronal differentiation 1
199	<i>NMNAT1</i>	1p36.22	nicotinamide nucleotide adenyltransferase 1
200	<i>NPHP1</i>	2q13	nephrocystin 1
201	<i>NPHP3</i>	3q22.1	nephrocystin 3
202	<i>NPHP4</i>	1p36.31	nephrocystin 4
203	<i>NR2E3</i>	15q23	nuclear receptor subfamily 2 group E member 3
204	<i>NRL</i>	14q11.2-q12	neural retina leucine zipper
205	<i>NRP1</i>	10p11.22	neuropilin 1
206	<i>NUMB</i>	14q24.2-q24.3	NUMB endocytic adaptor protein
207	<i>NYX</i>	Xp11.4	nyctalopin
208	<i>OAT</i>	10q26.13	ornithine aminotransferase
209	<i>OFD1</i>	Xp22.2	OFD1 centriole and centriolar satellite protein
210	<i>OPN1LW</i>	Xq28	opsin 1, long wave sensitive
211	<i>OPN1MW</i>	Xq28	opsin 1, medium wave sensitive
212	<i>OR2W3</i>	1q44	olfactory receptor family 2 subfamily W member 3
213	<i>OTOGL</i>	12q21.31	otogelin like
214	<i>OTX2</i>	14q22.3	orthodenticle homeobox 2

215	<i>PAF1</i>	19q13.2	PAF1 homolog, Paf1/RNA polymerase II complex component
216	<i>PANK2</i>	20p13	pantothenate kinase 2
217	<i>PCDH15</i>	10q21.1	protocadherin related 15
218	<i>PCYT1A</i>	3q29	phosphate cytidyltransferase 1, choline, alpha
219	<i>PDE4DIP</i>	1q21.2	phosphodiesterase 4D interacting protein
220	<i>PDE6A</i>	5q32	phosphodiesterase 6A
221	<i>PDE6B</i>	4p16.3	phosphodiesterase 6B
222	<i>PDE6C</i>	10q23.33	phosphodiesterase 6C
223	<i>PDE6D</i>	2q37.1	phosphodiesterase 6D
224	<i>PDE6G</i>	17q25.3	phosphodiesterase 6G
225	<i>PDE6H</i>	12p12.3	phosphodiesterase 6H
226	<i>PEX1</i>	7q21.2	peroxisomal biogenesis factor 1
227	<i>PEX2</i>	8q21.13	peroxisomal biogenesis factor 2
228	<i>PEX7</i>	6q23.3	peroxisomal biogenesis factor 7
229	<i>PHYH</i>	10p13	phytanoyl-CoA 2-hydroxylase
230	<i>PITPNM3</i>	17p13.2-p13.1	PITPNM family member 3
231	<i>PLA2G5</i>	1p36.13	phospholipase A2 group V
232	<i>PLD4</i>	14q32.33	phospholipase D family member 4
233	<i>PLK4</i>	4q28.1	polo like kinase 4
234	<i>PLEKHB1</i>	11q13.4	pleckstrin homology domain containing B1
235	<i>PNPLA6</i>	19p13.2	patatin like phospholipase domain containing 6
236	<i>POC1B</i>	12q21.33	POC1 centriolar protein B
237	<i>POC5</i>	5q13.3	POC5 centriolar protein
238	<i>PODNL1</i>	19p13.12	podocan like 1
239	<i>POMGNT1</i>	1p34.1	protein O-linked mannose N-acetylglucosaminyltransferase 1 (beta 1,2-)
240	<i>POMZP3</i>	7q11.23	POM121 and ZP3 fusion
241	<i>PPP1R21</i>	2p16.3	protein phosphatase 1 regulatory subunit 21, <i>putative</i>
242	<i>PRCD</i>	17q25.1	photoreceptor disc component
243	<i>PRDM13</i>	6q16.2	PR/SET domain 13
244	<i>PROM1</i>	4p15.32	prominin 1
245	<i>PRPF3</i>	1q21.2	pre-mRNA processing factor 3
246	<i>PRPF31</i>	19q13.42	pre-mRNA processing factor 31
247	<i>PRPF4</i>	9q32	pre-mRNA processing factor 4
248	<i>PRPF6</i>	20q13.33	pre-mRNA processing factor 6
249	<i>PRPF8</i>	17p13.3	pre-mRNA processing factor 8
250	<i>PRPH2</i>	6p21.1	peripherin 2

251	<i>PRPS1</i>	Xq22.3	phosphoribosyl pyrophosphate synthetase 1
252	<i>PRTFDC1</i>	10p12.1	phosphoribosyl transferase domain containing 1
253	<i>RAB28</i>	4p15.33	RAB28, member RAS oncogene family
254	<i>RAX2</i>	19p13.3	retina and anterior neural fold homeobox 2
255	<i>RBP3</i>	10q11.22	retinol binding protein 3
256	<i>RBP4</i>	10q23.33	retinol binding protein 4
257	<i>RCBTB1</i>	13q14.2	RCC1 and BTB domain containing protein 1
258	<i>RD3</i>	1q32.3	retinal degeneration 3, GUCY2D regulator
259	<i>RDH5</i>	12q13.2	retinol dehydrogenase 5
260	<i>RDH11</i>	14q24.1	retinol dehydrogenase 11
261	<i>RDH12</i>	14q24.1	retinol dehydrogenase 12
262	<i>REEP6</i>	19p13.3	receptor accessory protein 6
263	<i>RGR</i>	10q23.1	retinal G protein coupled receptor
264	<i>RGS9</i>	17q24.1	regulator of G protein signaling 9
265	<i>RGS9BP</i>	19q13.11	regulator of G protein signaling 9 binding protein
266	<i>RHO</i>	3q22.1	rhodopsin
267	<i>RIMS1</i>	6q13	regulating synaptic membrane exocytosis 1
268	<i>RLBP1</i>	15q26.1	retinaldehyde binding protein 1
269	<i>ROM1</i>	11q12.3	retinal outer segment membrane protein 1
270	<i>RP1</i>	8q11.23-q12.1	RP1 axonemal microtubule associated
271	<i>RP1L1</i>	8p23.1	RP1 like 1
272	<i>RP2</i>	Xp11.3	RP2 activator of ARL3 GTPase
273	<i>RP9</i>	7p14.3	RP9 pre-mRNA splicing factor
274	<i>RPE65</i>	1p31.3	retinoid isomerohydrolase RPE65
275	<i>RPGR</i>	Xp11.4	retinitis pigmentosa GTPase regulator
276	<i>RPGRIP1</i>	14q11.2	RPGR interacting protein 1
277	<i>RPGRIP1L</i>	16q12.2	RPGRIP1 like
278	<i>RS1</i>	Xp22.13	retinoschisin 1
279	<i>SAG</i>	2q37.1	S-antigen visual arrestin
280	<i>SASH1</i>	6q24.3-q25.1	SAM and SH3 domain containing 1
281	<i>SCAPER</i>	15q24.3	S-phase cyclin A associated protein in the ER
282	<i>SCLT1</i>	4q28.2	sodium channel and clathrin linker 1
283	<i>SDCCAG8</i>	1q43-q44	SHH signaling and ciliogenesis regulator SDCCAG8
284	<i>SEMA4A</i>	1q22	semaphorin 4A
285	<i>SEMA6B</i>	19p13.3	semaphorin 6B
286	<i>SF3B2</i>	11q13.1	splicing factor 3b subunit 2

287	<i>SFRP5</i>	10q24.2	secreted frizzled related protein 5
288	<i>SH3RF3</i>	2q13	SH3 domain containing ring finger 3
289	<i>SIK2</i>	11q23.1	salt inducible kinase 2
290	<i>SLC24A1</i>	15q22.31	solute carrier family 24 member 1
291	<i>SLC7A14</i>	3q26.2	solute carrier family 7 member 14
292	<i>SLC37A3</i>	7q34	solute carrier family 37 member 3
293	<i>SLC6A6</i>	3p25.1	solute carrier family 6 member 6
294	<i>SAMD11</i>	1p36.33	sterile alpha motif domain containing 11
295	<i>SNRNP200</i>	2q11.2	small nuclear ribonucleoprotein U5 subunit 200
296	<i>SPATA7</i>	14q31.3	spermatogenesis associated 7
297	<i>SPP2</i>	2q37.1	secreted phosphoprotein 2
298	<i>SPTBN1</i>	2p16.2	spectrin beta, non-erythrocytic 1
299	<i>SRD5A3</i>	4q12	steroid 5 alpha-reductase 3
300	<i>SYNE1</i>	6q25.2	spectrin repeat containing nuclear envelope protein 1
301	<i>SYNE2</i>	14q23.2	spectrin repeat containing nuclear envelope protein 2
302	<i>SYTL4</i>	Xq22.1	synaptotagmin like 4
303	<i>TEAD1</i>	11p15.3	TEA domain transcription factor 1
304	<i>TGM2</i>	20q11.23	transglutaminase 2
305	<i>TIMP3</i>	22q12.3	TIMP metalloproteinase inhibitor 3
306	<i>TMED7</i>	5q22.3	transmembrane p24 trafficking protein 7
307	<i>TMEM216</i>	11q12.2	transmembrane protein 216
308	<i>TMEM237</i>	2q33.1	transmembrane protein 237
309	<i>TOPORS</i>	9p21.1	TOP1 binding arginine/serine rich protein, E3 ubiquitin ligase
310	<i>TRAPPC9</i>	8q24.3	trafficking protein particle complex 9
311	<i>TRIM32</i>	9q33.1	tripartite motif containing 32
312	<i>TRNAU1AP</i>	1p35.3	tRNA selenocysteine 1 associated protein 1, <i>putative</i>
313	<i>TRNT1</i>	3p26.2	tRNA nucleotidyl transferase 1
314	<i>TRPM1</i>	15q13.3	transient receptor potential cation channel subfamily M member 1
315	<i>TSPAN11</i>	12p11.21	tetraspanin 11
316	<i>TSPAN12</i>	7q31.31	tetraspanin 12
317	<i>TTC28</i>	22q12.1	tetratricopeptide repeat domain 28
318	<i>TTC8</i>	14q31.3	tetratricopeptide repeat domain 8
319	<i>TTL5</i>	14q24.3	tubulin tyrosine ligase like 5
320	<i>TTPA</i>	8q12.3	alpha tocopherol transfer protein
321	<i>TUB</i>	11p15.4	TUB bipartite transcription factor
322	<i>TUBB4B</i>	9q34.3	tubulin beta 4B class IVb

323	<i>TUBGCP4</i>	15q15.3	tubulin gamma complex associated protein 4
324	<i>TUBGCP6</i>	22q13.33	tubulin gamma complex associated protein 6
325	<i>TULP1</i>	6p21.31	TUB like protein 1
326	<i>UBAP1L</i>	15q22.31	ubiquitin associated protein 1 like
327	<i>UNC119</i>	17q11.2	unc-119 lipid binding chaperone
328	<i>USH1C</i>	11p15.1	USH1 protein network component harmonin
329	<i>USH1G</i>	17q25.1	USH1 protein network component sans
330	<i>USH2A</i>	1q41	usherin
331	<i>USP16</i>	21q21.3	ubiquitin specific peptidase 16
332	<i>USP38</i>	4q31.21	ubiquitin specific peptidase 38
333	<i>VAX2</i>	2p13.3	ventral anterior homeobox 2
334	<i>VCAN</i>	5q14.2-q14.3	versican
335	<i>VPS13B</i>	8q22.2	vacuolar protein sorting 13 homolog B
336	<i>WASF3</i>	13q12.13	WASP family member 3
337	<i>WHRN</i>	9q32	whirlin
338	<i>WDPCP</i>	2p15	WD repeat containing planar cell polarity effector
339	<i>WDR19</i>	4p14	WD repeat domain 19
340	<i>WDR34=DYNC2I2</i>	9q34.11	dynein 2 intermediate chain 2
341	<i>WDR36</i>	5q22.1	WD repeat domain 36
342	<i>WDR48</i>	3p22.2	WD repeat domain 48
343	<i>PIK3R4</i>	3q22.1	PHOSPHATIDYLINOSITOL 3-KINASE, REGULATORY SUBUNIT 4
344	<i>XPNPEP2</i>	Xq26.1	X-prolyl aminopeptidase 2, <i>putative</i>
345	<i>ZC3H4</i>	19q13.32	zinc finger CCCH-type containing 4
346	<i>ZNF10</i>	12q24.33	zinc finger protein 10
346	<i>ZNF408</i>	11p11.2	zinc finger protein 408
347	<i>ZNF423</i>	16q12.1	zinc finger protein 423
348	<i>ZNF513</i>	2p23.3	zinc finger protein 513
349	<i>ZNF780A</i>	19q13.2	zinc finger protein 780A
350	<i>ZNF821</i>	16q22.2	zinc finger protein 821
351	<i>AZine1</i>	X	<i>putative</i>

3.2. Whole Exome Sequencing

When no putative disease-causing variant was identified, WES was applied for the affected proband(s) and unaffected family member(s), in collaboration with a company (IntegraGen) or with a research platform (IGBMC, Strasbourg, France). In summary, for IntegraGen, the exons, 5'UTR and 3'UTR included, and flanking intronic regions of DNA samples were captured with in-solution enrichment methodology (SureSelect Clinical Research Exome, Agilent, Massy,

France)[133] with the biotinylated oligonucleotide probe library. The paired-end 75 bases were massively sequenced on sequencer. For the lab (IGBMC), a pre-capture and post-capture PCR amplification was performed. Image analysis and bases calling were performed with a pipeline (Consensus Assessment of Sequence and Variation [CASAVA] 1.8, Illumina; CASAVA 1.8.2, Illumina).

Variant annotation was provided by an in-house pipeline (IntegraGen; Polypipeline, IGBMC) and results were available in the PolyWeb website (<http://polyweb.igbmc.fr/>; IGBMC) and in tabulated text files tables. Approximately 60,000 SNVs and InDels, were provided per sample or family in tabulated text files. For IGBMC, variant annotation were available in the PolyWeb website (<http://polyweb.igbmc.fr/>) and also in tabulated text files.

To identify the novel gene defect(s) with WES data, a stringent filtering was applied. As describe above for targeted NGS, expecting autosomal recessive, autosomal dominant or X-linked mode of inheritance, only nonsense, missense, splice site, or small deletion or insertion variants were kept. Based on autosomal recessive or autosomal dominant/X-linked mode of inheritance, minor allele frequency had to be inferior or equal to 0.005 or 0.001, respectively, in EVS, HapMap, 1000Genomes, dbSNP, ExAC and gnomAD. Pathogenicity for each missense variant was predicted with three bioinformatic tools imbedded in AlamutTM software: PolyPhen2, SIFT and MutationTaster. Variants predicted to be not disease-causing by PolyPhen2 and SIFT were not kept. Amino acid conservation across 100 species was evaluated with the UCSC Genome Browser (Human GRCh38/hg38 Assembly). “Highly conserved” means the amino acid or nucleotide for intronic variant is conserved across species; “Moderately conserved” amino acid or nucleotide variations were observed less than 5 times among species at this position but amino acid/nucleotide residue is conserved in primates; “Weakly conserved” when amino acid/nucleotide variation was observed 5 to 7 times among species at this position but amino acid residue is conserved in primates. Non-canonical splice site variants were assessed with multiple algorithms imbedded in AlamutTM and additionally by SpliceAI[130]. All variants were then classified in accordance with standards of American College of Medical Genetics and Genomics (ACMG)[131,132].

3.3. Retinal expression databases

For candidate genes, human and mouse retinal expression are analyzed with mouse[134,135] and human[136,137] transcriptomic databases. Mouse databases include the *rd1* mouse model characterized by mutations in *Pde6b* which lead to progressive rod then cone photoreceptor degeneration with a complete loss of rod photoreceptors by postnatal day 30[135]. Therefore, a decreased expression in the *rd1* mouse model compared to wild-type mice suggests that the candidate gene is expressed in rod photoreceptors. Another mouse model is the *Nrl* knock-out, characterized by the absence of rod photoreceptors at the presence of cone photoreceptors. In this database, the absence of expression of candidate gene is indicative of a rod-specific expression[121]. Roska database (<http://www.fmi.ch/roska.data/>) from transgenic mice expressing reporter genes specific of a retinal cell type was also consulted[134]. Expression values above 20 are considered as significant. Inner retinal layer expression was assessed through Retinal Bipolar Neuron Drop-seq database (https://singlecell.broadinstitute.org/single_cell/study/SCP3/retinal-bipolar-neuron-drop-seq#study-summary), developed by Shekhar and coll[137]. Human retinal transcriptomic databases included Farkas and coll. database

(<https://oculargenomics.meei.harvard.edu/retinal-transcriptome/>) of normal retinal expression[119]. Information about protein localization and function are investigated in Human Protein Atlas (<https://www.proteinatlas.org/>)[120]. Details regarding protein domains, localization and function were investigated in UniProt (<https://www.uniprot.org/>) and PubMed databases (<https://www.ncbi.nlm.nih.gov/pubmed/>). We also checked a protein-protein interaction database (<https://string-db.org/>) [138,139] to find known protein partners potentially implicated in the pathogenesis of IRD.

3.4. Confirmation and segregation of variants

Variants obtained from targeted NGS/WES were confirmed by bidirectional Sanger sequencing of exons and their intronic boundaries of the given gene. When a CNV was identified, MLPA was performed with a kit (SALSA MLPA kit gene specific, MRC Holland, Amsterdam, The Netherlands). If a MLPA probe was unavailable, a quantitative PCR was performed to study CNVs. For each exon of a gene, 10 ng of genomic DNA, 0.2 μ M of each primer (forward and reverse) and 10 μ l of mix from a kit (Power SYBR™ Green PCR Master mix, ThermoFisher Scientific, Waltham, Massachusetts, USA) were mixed in triplicates. For each qPCR plate, a housekeeping gene (*GAPDH* or *ACTB*) was also amplified in triplicate in order to normalize the results. A genomic DNA known to have no CNV for the given gene was used as a control. The samples were first incubated at 50°C during 2 min, then 15s at 95°C. During 41 cycles, the temperature changed between 15 sec at 95°C and 1 min at 60°C. Then, samples were heated at 95°C during 15 sec, 60°C during 15 sec to cool down at 10°C. A comparative C_T method was performed to analyze the results. An average of each triplicate was calculated. For each individual and for each exon of the candidate gene, the C_T value was normalized with the C_T value of *GAPDH* ($\Delta C_T = C_T$ (candidate gene) – C_T (*GAPDH/ACTB*)). Each ΔC_T was normalized to the control individual with no CNV ($\Delta\Delta C_T = \Delta C_T$ (patient) - ΔC_T (control)). Finally, a relative quantification was calculated with this formula: $2^{-\Delta\Delta C_T}$. A calculated value of ≤ 0.8 or ≥ 1.3 , was suggestive of a loss or a gain, respectively.

When family members of affected individuals were available for genetic studies, the same analysis for variants was performed on their DNA samples in order to identify the biallelic segregation and the origin of each allele (paternal/maternal/de novo).

The overall genotyping workflow is presented on Fig.18.

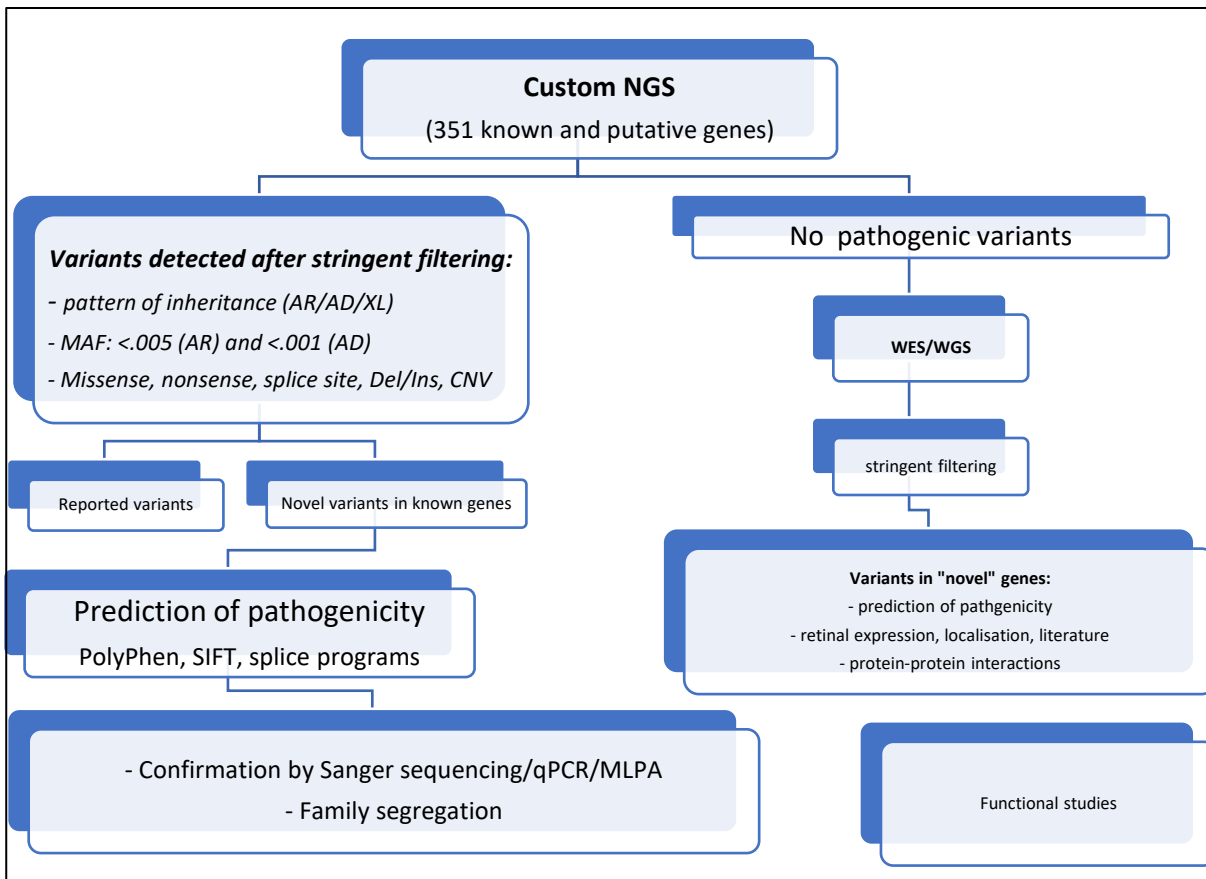


Figure 18 Workflow.

4. Expression analysis of candidate genes

4.1 RNA *in situ* hybridization

For retinal sections, adult mice C57BL/6JRj (Janvier, Genest Saint Isle, France) were sacrificed by cervical dislocation, eyes were collected, drilled at the ora serrata, and fixed for 1 hour in 4% paraformaldehyde before being dehydrated in 30% sucrose phosphate-buffered saline (PBS) solution. Thereafter, eyes were embedded in 7% gelatin/10% sucrose PBS and frozen in -40°C isopentane. Tissues were cut with a cryostat (MICROM HM 560, ThermoFisher Scientific) in 20 μm or 10 μm sections. Human donor eyes without known history of retinal diseases were collected through the Minnesota Lions Eye bank after due consent in accordance with the Declaration of Helsinki. The posterior segment was dissected, postfixed, dehydrated, embedded, and sectioned as described above for the mouse retinas. RNA probes which amplify exons 3 to 4 or exons 9 to 10 of mouse *Azine7* were designed (GeneCust, Dudelange, Luxembourg) and cloned in a vector (pBluescript II SK+, GeneCust) as previously described[140]. *NotI* and *KpnI* restrictions enzymes were used to linearize the plasmid. RNA *in situ* hybridization studies were performed as reported previously[140].

4.2 Immuno histofluorescence

Mouse and human retinal sections were incubated overnight with primary rabbit anti-Azine7 (Sigma-Aldrich, Darmstadt, Germany), rabbit anti-SOX9 (Sigma-Aldrich), mouse anti-glutamine synthetase (Sigma-Aldrich), antibodies at dilutions of 1:500, and 1:1,000. Thereafter, sections

were washed 3 times for 5 min each in 1× phosphate-buffered saline (PBS) and then incubated with donkey anti-rabbit Alexa Fluor 488 (Jackson ImmunoResearch Laboratories, Baltimore, MD) and donkey anti-mouse Cy3 (Jackson Immunoresearch Laboratories) secondary antibodies and 4,6-diamidino-2-phenylindole (DAPI; Euromedex, Souffelweyersheim, France) at a dilution 1:1000 each for 1 hour at room temperature. Controls were performed with only the use of secondary antibodies. Sections were washed 3 times for 5 min in PBS and mounted with coverslips (Mowiol 4-88; Sigma-Aldrich). Confocal fluorescence microscopy images were taken (model FV1000; Olympus, Hamburg, Germany).

4.3 Western blot

A solution of 50 µg/ml human recombinant RBP4 (Sigma- Aldrich,; #SRP6038) was prepared in 1xTris-buffered saline. Patient's and healthy control sera as well as a recombinant RBP4 solution were diluted 1:100 in Tris-buffered saline containing 0.5% NP40 and 1% Triton and then boiled at 100°C for 5 min. Fifteen µl of diluted sera and RBP4 were mixed with 13 µl of 6x Tris-buffered saline containing 500 mM/l dithiothreitol, 10% SDS, 50% glycerol and 0.5% bromophenol blue and then adjusted to a total volume of 45 µl with H₂O. Samples and molecular-weight size markers were loaded in the wells of Mini-Protean® TGX 4-15% gel (BioRad, Hercules, USA) and then electrophoresed for 1 h at 150 V in a Tris-glycine running buffer. The transfer on PVDF membrane (BioRad, #1704156) were made in Trans-Blot Turbo Transfer System® (BioRad). The membrane was fixed with a 5% non-fat milk and then incubated with primary polyclonal rabbit anti-human RBP4 antibody (Agilent Dako, Santa Clara, USA; #A004002-2) diluted 1:1000 at 4°C overnight. Loading control was performed using anti-transferrin monoclonal antibody (Abcam, Discovery Drive, Cambridge Biomedical Campus, Cambridge, UK, ab109503). The next day the membrane was washed with PBS and incubated for 1 h at room temperature with a secondary HRP-conjugated antibody (Jackson ImmunoResearch, Ely, UK; #11-035-003) diluted 1:1000, rinsed with PBS, incubated with Pierce ECL plus blotting substrate (ThermoFisher Scientific, Waltham, USA; #32134) for 5 min and then visualized in Vilber Lourmat-Fusion-Fx7 Superbright Transilluminator (Fisher Scientific).

Results

1. Epidemiological picture of REFERET inherited retinal disorder cohort analyzed by targeted next generation sequencing

The overall cohort of patients tested by targeted customized NGS is currently encompassing 1519 proband samples. Overall, during my PhD, I have analyzed 768 samples by this technique.

1.1 Phenotypes

Among these samples, 484 cases corresponded to male patients who had been pre-screened by Sanger sequencing for mutations in the exon *ORF15* of *RPGR* and revealed no variant. *ORF15* is a highly repetitive, variable purine rich DNA sequence poorly covered by standard NGS methods[141]. Variants in this region are a major cause of XL IRDs. The remaining patients (n=284) corresponded to females. Most of these IRD cases were clinically diagnosed with RCD

(n=670, 87%) (Fig.19). The subsequent analyses are focused on this subgroup of IRD, as it is predominant.

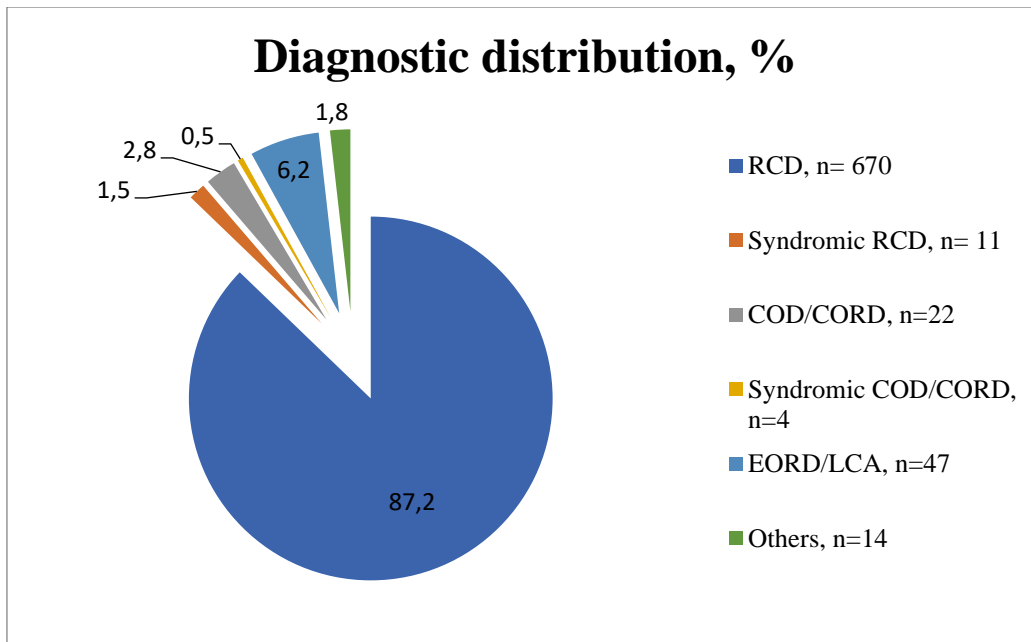


Figure 19. Presumed clinical diagnostic distribution in the cohort of 768 IRD patients: 87.2% of assessed cases had RCD.

1.2 Genotypes

Our genetic analyses showed variants in *USH2A*, *RPI* and *EYS* as major genetic defects underlying RCD, accounting for 12, 6.7 and 6.5% cases respectively, followed by *RHO*, *PDE6B*, *PRPH2*, *RPGR* and other genes, with a lower proportion (Fig.20). Unsolved cases accounted for 25%.

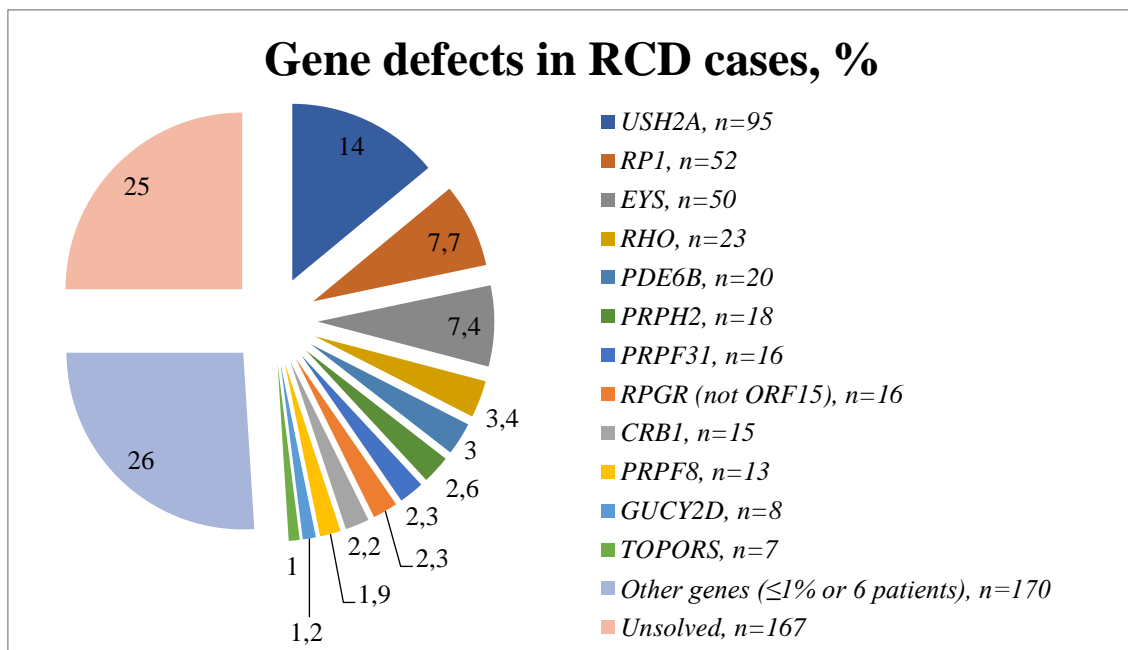


Figure 20. Gene defects in RCD (n=670) cases (all patterns of inheritance confounded). The most commonly mutated genes are *USH2A*, *RPI* and *EYS*.

In solved cases of autosomal recessive rod-cone dystrophies (n=398), gene defects were most frequently found in *USH2A*, *EYS* and *PDE6B* (Fig.21).

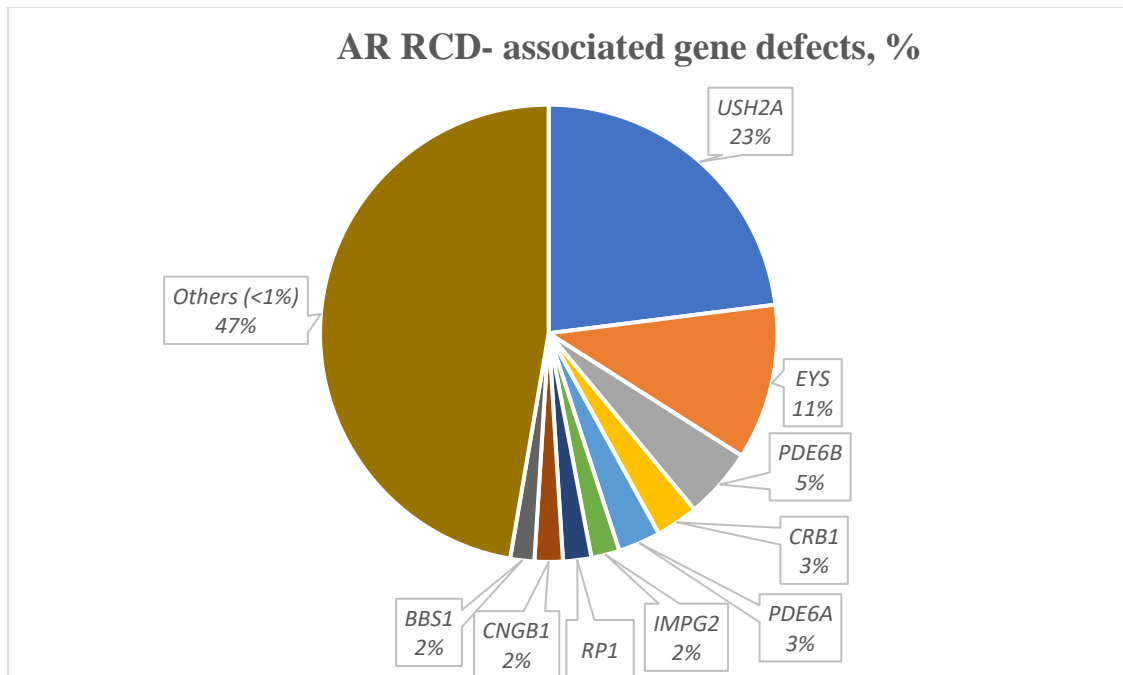


Figure 21. Gene defects found in solved autosomal recessive rod-cone dystrophy cases. Most commonly mutated genes are *USH2A*, *EYS* and *PDE6B*.

In solved cases of autosomal dominant RCD (n=122), gene defects were found predominantly in *RHO*, *RP1* and *PRPH2* (Fig.22). Altogether, variants in all splicing factors (*PRPFx* and *SNRNP200*) were the most frequent (n=30 or 24,5%).

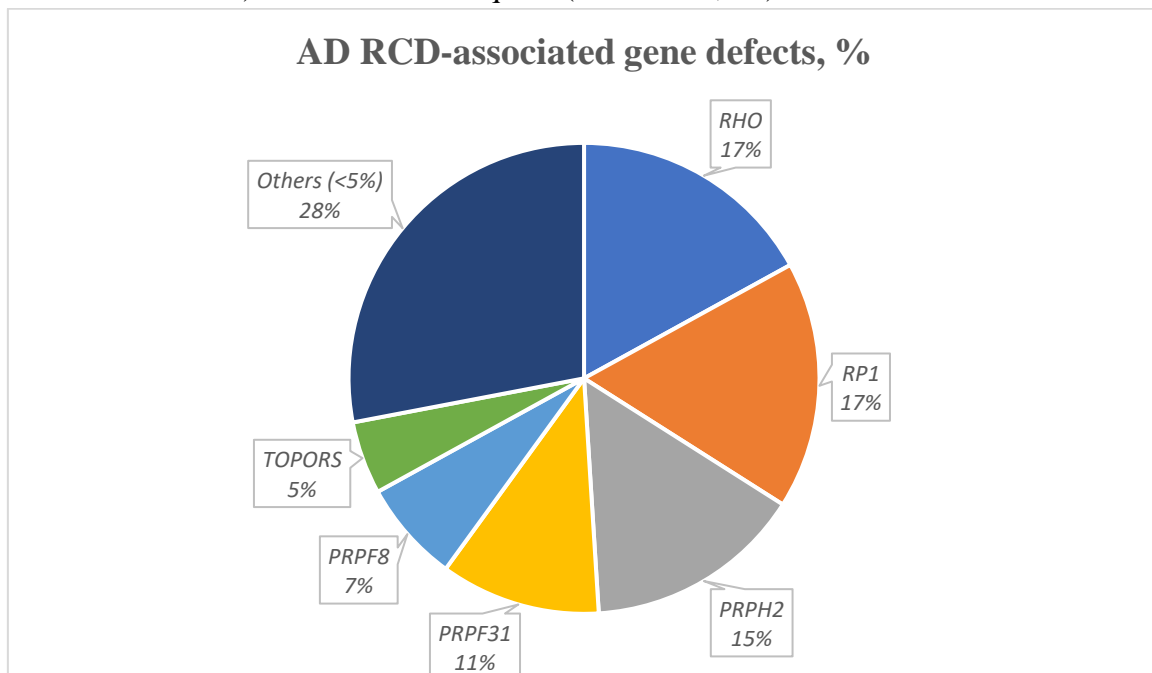


Figure 22. Gene defects in solved autosomal dominant cases. Most commonly mutated genes are *RHO*, *RP1*, *PRPH2* and *PRPF31*.

In solved XL RCD cases (n=23), *RPGR* gene defects were found in 74% of samples and *RP2* in 26%.

1.3 Post hoc analysis: changes in assumed inheritance pattern; critical review of initial clinical diagnosis

Only solved cases were considered for this analysis. In the solved simplex cases (n= 343), 17% were AD, 80% were AR and 3% were XL. In the cases with presumed AD mode of inheritance (n=58), 88% were indeed AD, 10% were AR and 2% were XL. Noteworthy, in cases presumed AD and finally solved as AR, biallelic gene defects were found in *SAG* (n=2), *USH2A* (n=2), *HGSNAT* (n=1), *PDE6B* (n=1), *RPI* (n=1). In the cases with presumed AR mode of inheritance (n=131), 90% were indeed AR, 5% were XL and 5% were AD. In the latter cases, gene defects in *BEST1* (n=2, both ADVIRC cases), *PRPF31*, *RPI* and *PRPH2* were found. In the cases with presumed XL mode of inheritance (n=11), 55% were indeed XL, 36% were AD (*IMPG2*, *RHO*, *PRPF31*) and 9% were AR (Fig.23).

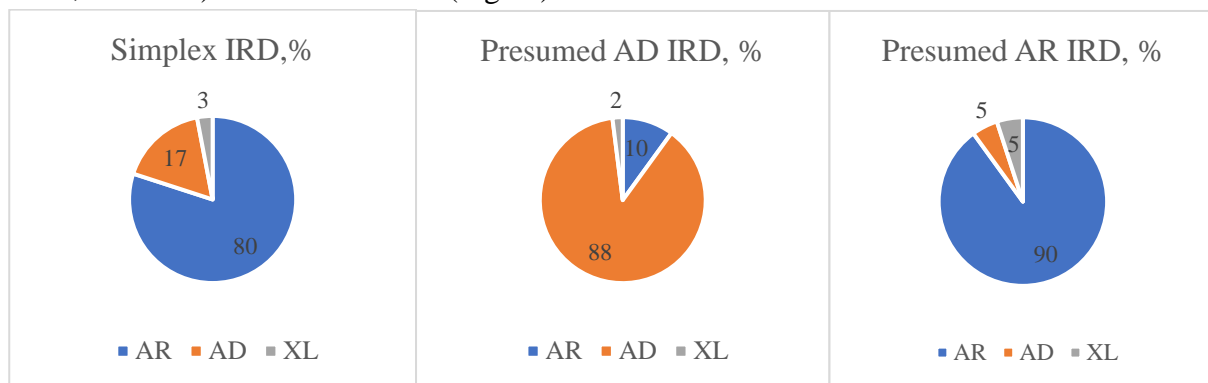


Figure 23. Post-hoc analysis of inheritance pattern.

1.4 Unsolved cases

Overall, 201 cases (26%) remained genetically unsolved after NGS panel analysis. In these cases, for 133 samples (66%) no disease causing variants were identified. For 47 samples (23%), only one previously reported variant in a known IRD-associated gene with recessive transmission was found. Variants in candidate genes of interest for our team was identified in 21 samples (11%).

2. Gene defect identification by Whole Exome Sequencing

A previous PhD student, Cécile Méjécase, has been working on 43 families with IRD, analyzed by targeted NGS and subsequently by WES. I continued working on unsolved cases from this cohort. The strategy of analysis was the following:

- the raw data were re-aligned to hg19 and the variants were re-annotated using the up-to-date databases through a bioinformatic pipeline developed in collaboration with the bioinformatic engineer from our team, Julien Navarro;
- I subsequently undertook the re-analysis of these data;
- I implemented the C. Méjécase's strategy by analysing copy number variations, some structural variants[142,143], and more recently published variants, in yet unsolved families.

2.1 Whole Exome Sequencing identified a known pathogenic variant in F163

A previously reported homozygous variant in *TULP1*: c.1496-6C>A was found in this family. This variant is annotated class 4 according to the ACMG (PP5, PM2, BP4). The proband's mother is heterozygous for this variant (Fig.24). Non-canonical splice site variants were not considered in the previous data analytic paradigm. This variant has been reported several times in severe arRCD [144–148].

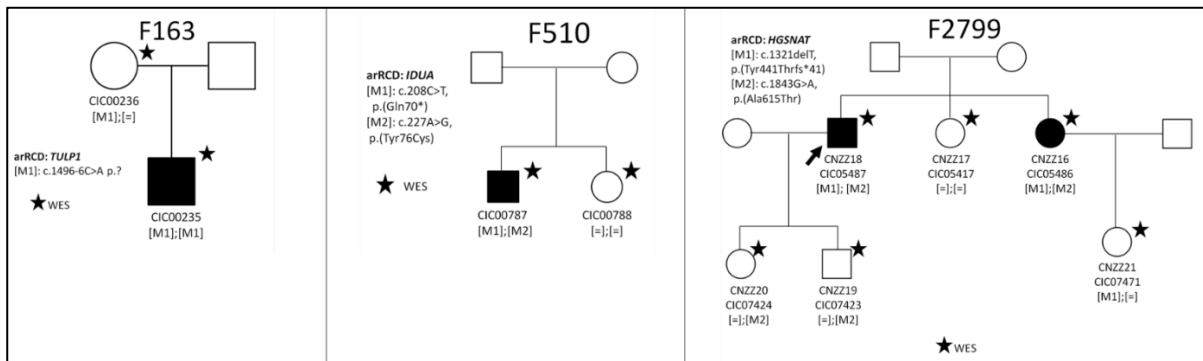


Figure 24. Pedigrees and variant segregation in families solved by WES.

2.2 Whole Exome Sequencing identified a known hypomorphic variant leading to isolated IRD in F510

Compound heterozygous variants in *IDUA* were found (Fig.24): c.208T>C p.(Gln70*) and c.227A>G p.(Tyr76Cys). The first variant is class 5 according to the ACMG and recurrent [149], the latter is considered as hypomorphic[150]. Variants *IDUA* are usually associated with a severe multisystemic disorder, mucopolysaccharidosis type I (Scheie and Hurler syndrome, OMIM # 607014, 607015, 607016), with RCD described in some cases[151–153]. The hypomorphic nature of the missense variant could probably explain the absence of obvious systemic clinical signs of mucopolysaccharidosis in our patient, although caution should be added to this statement and the patient is currently under more extensive clinical and biochemical evaluation.

2.3 Whole Exome Sequencing identified a known hypomorphic variant leading to isolated IRD in F2799.

Compound heterozygous variants in *HGSNAT* were found (Fig.24): a novel class 5 variant c.1321delT p.(Tyr441Thrfs*41) and an hypomorphic retina-specific recurrent variant c.1843G>A p.(Ala615Thr)[154–156]. *HGSNAT* is linked with a multisystemic disorder, mucopolysaccharidosis IIIC (OMIM # 252930) including a constant retinal degeneration but also with isolated retinal degeneration (RP73, OMIM # 616544)[157].

3. Specific and unusual genotype-phenotype associations identified by next generation sequencing technologies

3.1. Isolated retinal degeneration linked with *CLN3*

Mutations in *CLN3* typically lead to the juvenile form of neuronal ceroid lipofuscinosis (JNCL), also known as Batten disease (MIM# 204200)[158], a severe neurometabolic disease with

brain ceroid accumulation leading to neurodegeneration[159]. Few cases with *CLN3* mutations were recently reported having an isolated retinal degeneration[160].

CLN3 pathogenic variants were present in all clinical subsets of IRD explored on our NGS panel. Additionally, family F1517, undiagnosed by previous versions of targeted NGS panel, which did not include *CLN3*, was investigated by WES and two pathogenic variants in this gene were detected: ex.8_ex.9 del 1.02kb and c.461-3 C>A, p?. These two variants were confirmed by Sanger sequencing and qPCR and cosegregated with the phenotype. To perform genotype-phenotype correlations of patients with *CLN3* pathogenic variants, we investigated the whole cohort of IRD cases who undergone NGS screening.

We identified fifteen cases from eleven unrelated families harboring biallelic *CLN3* variants. It led to a publication in JAMA Ophthalmology[161], followed by editorial discussion[162]. We received comments from readers[163] and realized a Reply[164]. The work was also presented at Francophone Society of Ophthalmic Genetics (SGOF) in 2019.

Retinal Phenotype of Patients With Isolated Retinal Degeneration Due to *CLN3* Pathogenic Variants in a French Retinitis Pigmentosa Cohort

Vasily M. Smirnov, MD; Marco Nassisi, MD; Cyntia Solis Hernandez, MD; Cécile Méjécase, PhD; Said El Shamiéh, PhD; Christel Condroyer, BSc; Aline Antonio, BSc; Isabelle Meunier, MD, PhD; Camille Andrieu, MSc; Sabine Defoort-Dhellemmes, MD; Saddek Mohand-Said, MD, PhD; José-Alain Sahel, MD; Isabelle Audo, MD, PhD; Christina Zeitz, PhD

IMPORTANCE Biallelic variants in *CLN3* lead to a spectrum of diseases, ranging from severe neurodegeneration with retinal involvement (juvenile neuronal ceroid lipofuscinosis) to retina-restricted conditions.

OBJECTIVE To provide a detailed description of the retinal phenotype of patients with isolated retinal degeneration harboring biallelic *CLN3* pathogenic variants and to attempt a phenotype-genotype correlation associated with this gene defect.

DESIGN, SETTING, AND PARTICIPANTS This retrospective cohort study included patients carrying biallelic *CLN3* variants extracted from a cohort of patients with inherited retinal disorders (IRDs) investigated at the National Reference Center for Rare Ocular Diseases of the Centre Hospitalier National d'Ophtalmologie des Quinze-Vingts from December 2007 to August 2020. Data were analyzed from October 2019 to August 2020.

MAIN OUTCOME AND MEASURES Functional (best-corrected visual acuity, visual field, color vision, and full-field electroretinogram), morphological (multimodal retinal imaging), and clinical data from patients were collected and analyzed. Gene defect was identified by either next-generation sequencing or whole-exome sequencing and confirmed by Sanger sequencing, quantitative polymerase chain reaction, and cosegregation analysis.

RESULTS Of 1533 included patients, 843 (55.0%) were women and 690 (45.0%) were men. A total of 15 cases from 11 unrelated families harboring biallelic *CLN3* variants were identified. All patients presented with nonsyndromic IRD. Two distinct patterns of retinal disease could be identified: a mild rod-cone degeneration of middle-age onset (n = 6; legal blindness threshold reached by 70s) and a severe retinal degeneration with early macular atrophic changes (n = 9; legal blindness threshold reached by 40s). Eleven distinct pathogenic variants were detected, of which 4 were novel. All but 1, p.(Arg405Trp), *CLN3* point variants and their genotypic associations were clearly distinct between juvenile neuronal ceroid lipofuscinosis and retina-restricted disease. Mild and severe forms of retina-restricted *CLN3*-linked IRDs also had different genetic background.

CONCLUSIONS AND RELEVANCE These findings suggest *CLN3* should be included in next-generation sequencing panels when investigating patients with nonsyndromic rod-cone dystrophy. These results document phenotype-genotype correlations associated with specific variants in *CLN3*. However, caution seems warranted regarding the potential neurological outcome if a pathogenic variant in *CLN3* is detected in a case of presumed isolated IRD for the onset of neurological symptoms could be delayed.

JAMA Ophthalmol. doi:10.1001/jamaophthalmol.2020.6089
Published online January 28, 2021.

- [+ Invited Commentary](#)
- [+ Related article](#)
- [+ Supplemental content](#)

Author Affiliations: Author affiliations are listed at the end of this article.

Corresponding Author: Isabelle Audo, MD, PhD (isabelle.audo@inserm.fr), and Christina Zeitz, PhD (christina.zeitz@inserm.fr). Sorbonne Université, INSERM, Centre national de la recherche scientifique, Institut de la Vision, 17 rue Moreau, Paris 75012, France.

© 2021 American Medical Association. All rights reserved.

E1

Inherited retinal diseases (IRDs) are a clinically and genetically heterogeneous group of disorders, the most frequent of which being rod-cone dystrophy, also known as retinitis pigmentosa, with a prevalence of about 1:4000.¹ The vast majority of cases are nonsyndromic, with the disease restricted to the retina. A lesser number of cases are syndromic and encompass a continuum of clinical manifestations, from retinopathy with subtle extraocular signs to multisystemic disorders.^{2,3} Both syndromic and nonsyndromic forms are characterized by a large genetic heterogeneity with more than 100 genes potentially implicated.⁴ Moreover, recent advances in high-throughput sequencing, including comprehensive targeted next-generation panels, have underlined genotypic overlaps—cases of restricted retinal disease being associated with variants in genes also implicated in syndromic IRD.^{1,5,6} For instance, pathogenic variants in a major ciliopathy-associated gene, *USH2A*, account for about 20% of cases of isolated autosomal-recessive retinitis pigmentosa.⁷⁻⁹

Another example is *CLN3* (OMIM 607042), a ubiquitously expressed gene, variants of which have recently been associated with isolated retinal degeneration in 5 patients.¹⁰ Variants in *CLN3* typically lead to the juvenile form of neuronal ceroid lipofuscinosis (JNCL), also known as Batten disease or Vogt-Spielmeyer disease (OMIM 204200),¹¹ a severe neuro-metabolic disease with brain ceroid accumulation leading to neurodegeneration.¹² Neuronal ceroid lipofuscinosis (NCL) is in fact a genetically heterogeneous group of metabolic disorders with lysosomal enlargement and ceroid material accumulation.¹² Pathogenic variants in 13 genes, namely *PPT1* (OMIM 600722), *TPP1* (OMIM 607998), *CLN3*, *CLN5* (OMIM 608102), *CLN6* (OMIM 606725), *MFSD8* (OMIM 611124), *CLN8* (OMIM 607837), *CTSD* (OMIM 116840), *DNAJC5* (OMIM 611203), *CTSF* (OMIM 603539), *ATPI3A2* (OMIM 610513), *GRN* (OMIM 138945), and *KCTD7* (OMIM 611725), are known to cause NCL.¹² NCL affects 1:100 000 live births worldwide.¹³ JNCL linked to *CLN3* pathogenic variants accounts for approximately 13% of childhood-onset NCL.¹⁴ In its classic form, visual loss starts as early as age 5 to 6 years and precedes cognitive and motor regression.^{12,15} The earliest symptoms are poor vision, overlooking, bad color discrimination, and sometimes night blindness.¹⁶⁻¹⁸ Inner retinal dysfunction concomitant with the outer layer degeneration is a peculiar feature of the retinal dystrophy associated with JNCL.¹⁶⁻¹⁸

In this study, we provide further details on the retinal phenotype and novel pathogenic variants in a cohort of patients with IRD harboring biallelic *CLN3* variants and evaluate phenotype-genotype correlations.

Methods

Research procedures adhered to the tenets of the Declaration of Helsinki and were approved by the local ethics committee (Comité de Protection des Personnes Ile de France 5). Prior to testing, written informed consent was obtained from each study participant. No compensation or incentives were offered to individuals to participate in the study.

Key Points

Question Is there any phenotype-genotype correlation in patients harboring biallelic pathogenic variants in *CLN3*?

Findings In a French cohort of 1533 patients with inherited retinal disorders (IRDs), 15 patients (1.0%) had retina-restricted *CLN3*-linked disease covering 2 phenotypes: mild ($n = 6$) and severe ($n = 9$) retinal degeneration with macular atrophy. The genetic background (variant/genotype) underlying the mild and the severe retina-restricted forms of *CLN3*-associated IRD was clearly distinct from neuronal ceroid lipofuscinosis.

Meaning These results suggest that most patients harboring pathogenic variants in *CLN3* might have a phenotype and a prognosis predicted from the genetic background.

Clinical Studies

The sporadic and familial cases affected with IRD were clinically investigated at the National Reference Center for Rare Ocular Diseases of the Centre Hospitalier National d'Ophthalmologie des Quinze-Vingts. Ophthalmic examination of affected individuals was performed as previously described.¹⁹ Patients' data were collected from December 2007 to August 2020 and analyzed from October 2019 to August 2020. Information about genetic analyses can be found in the eMethods and eFigures 1 and 2 in the Supplement.

Statistical Analysis

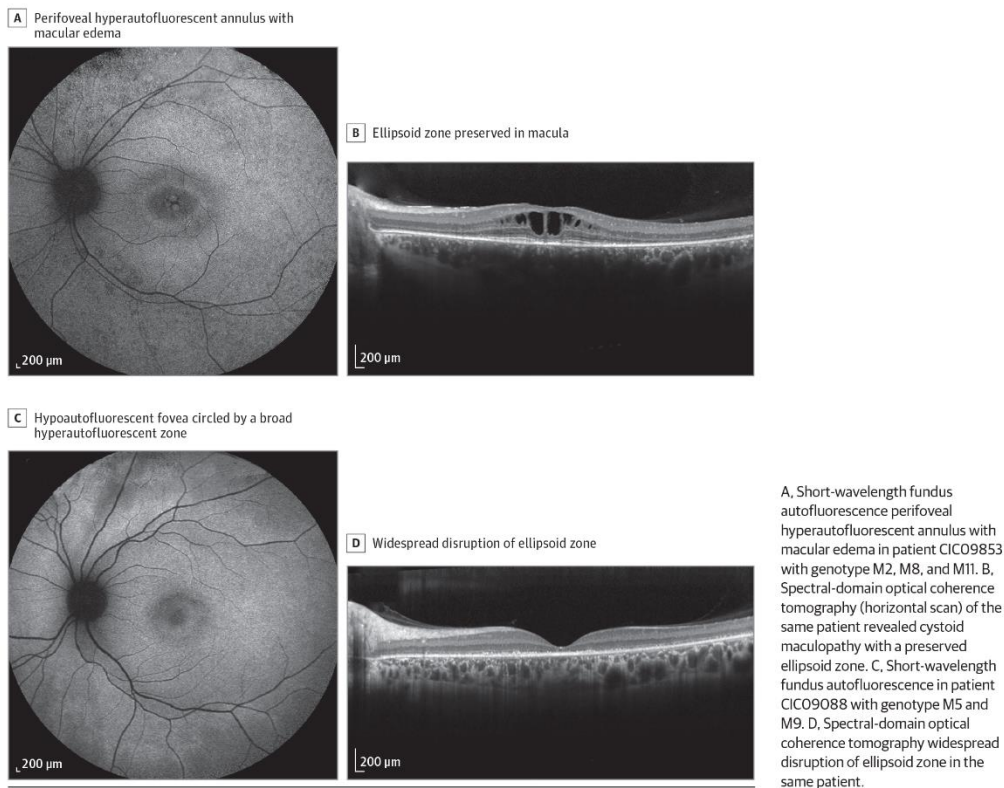
Best-corrected visual acuity (BCVA) variables were expressed in logMAR, then mean BCVA between eyes (right eye and left eye) was calculated and then used for further analysis (no significant difference between both eyes was found with a 2-tailed Wilcoxon signed rank test). Given the small number of samples, we did not perform a regression analysis for BCVA decline but only plotted individual mean BCVA on a graph.

Two phenotypic groups of patients (group A, mild; group B, severe) were separated on the basis of the following criteria: age of onset of the first symptoms, progression of BCVA, and presence of macular atrophy. Kaplan-Meier survival curves were plotted for mean BCVA of 1.3 logMAR or greater (20/400 Snellen equivalent; the legal blindness threshold in France). The difference between the curves from each phenotypic group was determined using a 2-sided log-rank test. Significance was set at $P < .05$. Clinical variables were analyzed using SPSS Statistics software version 21.0 (IBM).

Results

Of 1533 patients with IR from a large French cohort, 843 (55.0%) were women and 690 (45.0%) were men. A total of 15 affected patients with nonsyndromic IRD, including 10 men and 5 women aged 19 to 65 years from 11 unrelated families, were identified with biallelic *CLN3* variants. None of the 15 patients had neurological symptoms besides patient CICO0350, a woman in her 70s with extrapyramidal adverse effects from neuroleptic treatment given for depression, according to the neurologist.

Figure 1. Example of Milder (A and B) and Severe (C and D) Forms of *CLN3*-Related Isolated Retinal Degeneration



Ocular findings are summarized in **Figure 1** and eFigures 3 to 12 in the **Supplement**. Retinal findings from patients fall into 2 categories. In group A, 6 patients presented with mild retinal degeneration of middle-age onset (**Figure 1A and B**). Subjective symptoms appeared in individuals between their 20s and 40s. BCVA was relatively preserved (mean [range] BCVA, 20/32 [20/20 to 20/100]). Goldman visual field showed a general constriction of all isopters along with preservation of temporal crescent in 2 patients; no patient had absolute central scotoma. For the color vision defects, 4 patients exhibited a tritan axis, 1 patient had normal color vision, and 1 patient was not tested (**Table 1**). Fundus features included a waxy pallor of the optic disc, retinal vessel narrowing, midperipheral grayish discoloration, and sparse bone spicule-like pigmentation (eFigure 3 in the **Supplement**). Short-wavelength fundus autofluorescence showed a hyperautofluorescent ring in the posterior pole along with dark foveal dots in older patients (**Figure 1A**) (eFigure 3 in the **Supplement**). Spectral-domain optical coherence tomography (SD-OCT) revealed a variable extramacular outer retinal layer disruption. Foveal ellipsoid line was spared in 4 patients (**Figure 1B**) and disrupted or absent in 2 patients (eFigure 3 in the **Supplement**). Patients CICO8027, CICO8140

(eFigure 3 in the **Supplement**), and CICO9853 (**Figure 1B**) had cystoid macular changes in the progression of their disease. Electroretinogram (ERG) recordings were available for 5 patients in this group. Both rod and cone responses were undetectable in 3 patients (CICO0350, CICO8140, and CICO9152). It revealed a generalized rod-cone dysfunction with severely reduced or abolished dark-adapted responses and more preserved light-adapted responses in 2 patients (CICO2713 and CICO9853) (**Table 1**) (eFigure 5 in the **Supplement**).

In group B, 9 patients had a more severe retinal degeneration with macular atrophic changes (**Figure 1C and D**) (eFigure 4 in the **Supplement**). The onset of symptoms was earlier (age 10 to 20 years) than in group A, and BCVA was lower (mean [range] BCVA, 20/400 [20/160 to counting fingers]). For the Goldman visual field, 4 patients (CICO1168, CICO1170, CICO9088, and 1037229) exhibited central scotomata along with peripheral isopter constriction; 4 patients had an isopter constriction with residual temporal crescents (CICO0166, CICO1169, CICO8274, and CICO3517); and visual field was lacking for 1 patient (CICO5890) (**Table 1**). For color vision, 3 patients displayed a tritan axis, 1 patient had a deutan axis, and 1 patient had the color confusion errors without any axis;

Table 1. Clinical Characteristics of Patients With CLN3-Associated Retina-Restricted Diseases

Family	Patient	Sex	Age, y	Symptoms and comorbidities	BCVA, Snellen		Anterior segment	Fundus examination	SW-FAF	SD-OCT	Goldman visual field ^a	Farnsworth 15 Hue	Full-field ERG
					First examination	Last examination							
Mild retinal degeneration													
F234	CIC00350	F	55	Night blindness that developed in 40s; severe visual loss that developed in 50s; extrapyramidal syndrome that developed in 70s (medication associated: olanzapine, sertraline)	20/100 OD; 20/200 OS	Age 76 y; LP OD; LP OS	Unilateral high myopia in the left eye (~7.50); left eye amblyopia from childhood	Optic disc pallor; vessel narrowing; posterior pole patchy choriorretinal atrophy; sparse bone spicule-like pigmentation in midperiphery	Global loss of autofluorescence; perifoveal hyperautofluorescent ring; round patches of hypoautofluorescence at the posterior pole	Widespread outer layer disappearance; indistinct retinal layering; thinning of the hypoautofluorescent choriocapillaris	V4e constricted to 5°	Tritan	Undetectable at age 55 y
F976	CIC02713	F	65	Night blindness that developed in 40s; good vision	20/25 OD; 20/25 OS	Age 69 y; 20/25 OD; 20/25 OS	Normal	Optic disc pallor; retinal vessel narrowing; macula seems normal; midperipheral retina grayish and atrophic; confluent bone spicule-like pigmentation	Perifoveal annulus; granularity and round hypoautofluorescent patches in the midperiphery	Outer retinal layers preserved in fovea, interrupted choroidal thinning; epiretinal membrane	III4e constricted to 15°	Tritan	Dark-adapted ERG undetectable; light-adapted ERG severely reduced
F4480	CIC08027	M	34	Night blindness that developed in 20s; visual acuity loss and photophobia that developed in 30s	20/50 OD; 20/20 OS	Age 39 y; 20/63 OD; 20/25 OS	Normal	Optic disc pallor; retinal vessel narrowing; celophane light reflex from maculae; sparse bone spicule-like pigments and patchy choriorretinal atrophy in the midperiphery	Hypoautofluorescence from the fovea; perifoveal hyperautofluorescent ring; patchy hypoautofluorescence in the midperiphery	Outer retinal layers preserved at the fovea, interrupted microcystic intraretinal changes in the right eye; epiretinal membrane	III4e constricted to 10°; large temporal crescents at III4e	NA	Dark-adapted ERG undetectable; light-adapted ERG severely reduced
F4545	CIC08140	M	37	Night blindness that developed when younger than 10 y; visual acuity loss that developed in 20s	20/50 OD; 20/50 OS	Age 44 y; 20/25 OD; 20/50 OS	Posterior subcapsular cataract in both eyes; surgery at age 38 y	Optic disc pallor; retinal vessel narrowing; macular atrophy; dense bone spicule-like pigmentation and patchy choriorretinal atrophy in the midperiphery	Global hypoautofluorescence within the posterior pole; round patches of hypoautofluorescence in the midperiphery	Outer retinal layers preserved at the fovea, interrupted microcystic intraretinal changes in both eyes	III4e constricted to 15°	Tritan	Undetectable at age 42 y

(continued)

Table 1. Clinical Characteristics of Patients With CLN3-Associated Retina-Restricted Diseases (continued)

Family	Patient	Sex	Age, y	Symptoms and comorbidities	BCVA, Snellen	First examination	Last examination	Anterior segment	Fundus examination	SW-FAF	SD-OCT	Goldman visual field ^a	Farnsworth 15 Hue	Full-field ERG
F5230	CIC09152	M	37	Night blindness that developed when younger than 10 y; congenital right esotropia	NA	NA	Age 37 y: 20/40 OD; 20/32 OS	Keratoconus; with rigid contact lens carrier; clear lens	Optic disc pallor; retinal vessel narrowing; posterior pole patchy choriorretinal atrophy; fovea looks darkened; pigment clumping in the midperiphery	Central area of granular hypoautofluorescence (tiny black dots), involving the fovea and parafovea; large perimacular halo of hyperautofluorescence; patchy hypoautofluorescence in the midperiphery	Outer layer disappearance; hyperreflective subretinal dots	V4e constricted to 10°; temporal crescent	Tritan	Undetectable
F5662	CIC09853	M	35	Night blindness that developed in 20s; acetazolamide intake for microcystic retinal edema	20/50 OD; 20/40 OS	20/50 OD; 20/40 OS	Age 38 y: 20/40 OD; 20/50 OS	Normal	Disc and vessels seem normal; abnormal macular sheen; no obvious peripheral retinal changes	Perifoveal ring of hyperautofluorescence; granular hypoautofluorescence in the midperiphery	Outer retinal layers preserved in fovea, interrupted outside; microcystic retinal edema	III4e constricted to 10°	Normal	Dark-adapted ERG undetectable; light-adapted ERG severely reduced
Severe retinal degeneration														
F122	CIC00166	M	34	Night blindness and visual loss that developed in 20s	20/100 OD; 20/125 OS	20/100 OD; 20/125 OS	Age 37 y: 20/200 OD; 20/160 OS	Normal	Normal optic disc and retinal vessels; yellowish atrophic macular dots; sparse bone spicule-like pigmentation and perivascular pigmentary cuffs in midperiphery	Central area of granular hypoautofluorescence (tiny black dots), involving the fovea and parafovea	Widespread outer layers disappearance; hyperreflective subfoveal deposits	V4e constricted to 15°; temporal crescent	Tritan	Undetectable dark-adapted 0.01 and 3.0 ERG; electronegative dark-adapted 10.0 ERG (b/a ratio, 0.98); light-adapted ERG severely reduced

(continued)

Table 1. Clinical Characteristics of Patients With *CLN3*-Associated Retina-Restricted Diseases (continued)

Family	Patient	Sex	Age, y	Symptoms and comorbidities	BCVA, Snellen		Anterior segment	Fundus examination	SW-FAF	SD-OCT	Goldman visual field ^a	Famsworth 15 Hue	Full-field ERG
					First examination	Last examination							
F699	CIC01170	F	35	Night blindness and visual acuity loss that developed in 20s	20/400 OD; 20/400 OS	Age 38 y; 20/400 OD; 20/500 OS	Normal	Temporal optic disc pallor; yellowish macula with abnormal sheen and some pigmentary clumps; patchy chorioretinal atrophy and sparse bone spicule-like pigments in midperiphery	Hyperautofluorescence of the fovea; hypoautofluorescence and granularity of fovea; large perimacular halo of increased autofluorescence; patchy hypoautofluorescence of the midperiphery	Widespread outer layer disappearance; indistinct retinal layering; epimacular membrane	Absolute V4e central scotoma constricted to 5°; peripheral V4e constricted to 50°	Dyschromatopsia without axis	Undetectable at age 40 y
	CIC01169	M	25	Night blindness and visual acuity loss that developed when younger than 10 y	20/200 OD; 20/200 OS	Age 32 y; CF OD; 20/400 OS	Normal	Temporal optic disc pallor; yellowish macula with atrophic changes; patchy chorioretinal atrophy and sparse bone spicule-like pigmentation in midperiphery	Hyperautofluorescence of the fovea; hypoautofluorescence and granularity of fovea; large perimacular halo of hyperautofluorescence; patchy hypoautofluorescence of the midperipheral retina	Widespread outer layer disappearance; indistinct retinal layering; epimacular membrane	V4e constricted to 15°; temporal crescent at V4e	NA	Undetectable at age 32 y
	CIC01168	M	30	Night blindness and visual acuity loss that developed when younger than 10 y; neurological examination and brain MRI were normal at age 10 y; no vacuolated lymphocytes; death at 40 y from unspecified complications of long-term alcohol use	CF OD; CF OS	NA	Normal	Temporal optic disc pallor; yellowish macula with dark foveola and some pigmentary clumps; celophane light reflex; patchy chorioretinal atrophy and sparse bone spicule-like pigment in the midperiphery	Hyperautofluorescence of the fovea; hypoautofluorescence and granularity of the fovea; large perifoveal hyperautofluorescent halo; patchy hypoautofluorescence of the midperiphery	Widespread outer layer disappearance; indistinct retinal layering	Small temporal crescent at V4e	NA	Undetectable at age 30 y

(continued)

Table 1. Clinical Characteristics of Patients With *CLN3*-Associated Retina-Restricted Diseases (continued)

Family	Patient	Sex	Age, y	Symptoms and comorbidities	BCVA, Snellen	First examination	Last examination	Anterior segment	Fundus examination	SW-FAF	SD-OCT	Goldman visual field ^a	Famsworth 15 Hue	Full-field ERG
F1517	CIC03517	F	23	Night blindness that developed when younger than 10 y; photophobia that developed in 20s	20/160 OD; 20/160 OS	Age 32 y: HM OD; CF OS	High myopia (-18.0 OU); posterior subcapsular cataract in both eyes	Optic disc pallor; retinal vessel narrowing; atrophic maculae; sparse bone spicule-like pigments and patchy chorioretinal atrophy in the midperiphery	Hyperautofluorescence of the outer layer fovea; central area of granular hyperautofluorescence (tiny black dots) involving the fovea and parafovea; large perimacular halo of hyperautofluorescence	Widespread outer layer disappearance; indistinct retinal layering; developed a type 2 choroidal neovascular membrane (eFigure 6 in the Supplement)	V4e constricted to 5°; temporal crescent	Deutan	Undetectable dark-adapted 0.01 ERG, reduced; electronegative dark-adapted 3.0 and 10.0 ERG (b/a ratio, 0.75); light-adapted 3.0 and 30-Hz flicker ERG present, reduced, and delayed; ERG became undetectable at age 28 y	
	CIC05890	M	19	Night blindness that developed when younger than 10 y; recent photophobia	NA	Age 19 y: CF OU	High myopia (-15.0 OU); posterior subcapsular cataract in both eyes	Optic disc pallor; retinal vessel narrowing; atrophic maculae; celtophane light reflex; sparse bone spicule-like pigmentation and patchy chorioretinal atrophy in the midperiphery	Central area of granular hyperautofluorescence (tiny black dots) involving the fovea and parafovea; large perimacular halo of hyperautofluorescence	Widespread outer layer disappearance; hyperreflective subfoveal deposit	NA	NA	NA	
F4639	CIC08274	M	33	Night blindness and photophobia that developed when younger than 10 y; visual acuity loss that developed in 20s	20/400 OD; 20/800 OS	NA	Posterior subcapsular cataract in the right eye	Optic disc pallor and cupping; retinal vessels narrowing; pigmentary clumping in the macula and midperiphery	Round patches of atrophy (black holes) at the fovea, perifoveal hyperautofluorescent ring; round patches of hyperautofluorescence in the midperiphery	Outer layer disappearance; hyperreflective subretinal dots	V4e constricted to 20°; temporal crescents	NA	Undetectable at age 33 y	

Table 1. Clinical Characteristics of Patients With *CLN3*-Associated Retina-Restricted Diseases (continued)

Family	Patient	Sex	Age, y	Symptoms and comorbidities	BCVA, Snellen		Anterior segment	Fundus examination	SW-FAF	SD-OCT	Goldman visual field ^a	Farnsworth 15 Hue	Full-field ERG
					First examination	Last examination							
F5189	CIC09088	F	38	Night blindness that developed in the 20s; visual acuity loss that developed in the 30s	20/250 OD; 20/250 OS	Age 42 y; 20/250 OD; 20/320 OS	Normal	Retinal vessels narrowing; macular depigmentation and atrophic changes; no pigmentary clumping	Central area of granular hypoautofluorescence (tiny black dots) involving the fovea and parafovea	Outer layer disappearance; hyperreflective subretinal dots	Absolute central scotoma of 5° at V4e; relative central scotoma of 30° at III1e; conserved peripheral isopters	Tritan	Dark-adapted ERG undetectable; light-adapted ERG severely reduced
	1037229	M	37	Night blindness that developed in 20s; visual acuity loss that developed in 30s	20/32 OD; 20/40 OS	Age 42 y; 20/63 OD; 20/125 OS	Normal	Retinal vessels narrowing; macular depigmentation and atrophic changes; no pigmentary clumping	Hyperautofluorescence of the foveola; central area of granular hypoautofluorescence (tiny black dots) involving the fovea and parafovea; irregular hypoautofluorescent patches in the midperiphery	Outer layer disappearance; hyperreflective subretinal dots	Relative central scotoma of 30° at III1e; conserved peripheral isopters	Tritan	Dark-adapted ERG undetectable; light-adapted ERG severely reduced

Abbreviations: BCVA, best-corrected visual acuity; CF, counting fingers; ERG, electroretinography; HM, hand motion; LP, light perception; MRI, magnetic resonance imaging; NA, not available; SD-OCT, spectral-domain optical coherence tomography; SW-FAF, short-wavelength fundus autofluorescence.

^a Isopter V4e: absolute visual field defect; isopter III1e: relative visual field defect (both requested in France for legal purposes).

4 patients could not be tested because they had a very low BCVA (Table 1). Fundus exhibited more widespread chorioretinal dystrophic changes, and all patients had atrophic changes with yellowish discoloration of the macula (particularly prominent in patients CICO1168, CICO1169, and CICO1170) along with grayish discoloration and subtle pigment migrations in the mid-peripheral retina (eFigure 4 in the Supplement). Optic disc pallor and retinal vessel narrowing were present in variable degrees but less obvious than in group A. SD-OCT revealed macular and extramacular outer retinal layer loss. Inner retinal layering was preserved; there was no visible alteration of the inner nuclear layer or the retinal nerve fiber layer thickness. A total of 7 patients had changes at the vitreoretinal interface; either an epiretinal membrane or retinal striae at the level of internal limiting membrane was also seen at funduscopy (eFigure 4 in the Supplement). Short-wavelength fundus autofluorescence showed a macula of decreased autofluorescence in all patients surrounded by a large isoautofluorescent or hyperautofluorescent ring at the posterior pole with indistinct borders and patchy hypoautofluorescence outside the vascular arcades. In younger patients (Figure 1C) (eFigure 4 in the Supplement), macular hypoautofluorescence took a dotted, moth-eaten appearance while the extramacular retina looked isoautofluorescent. In more advanced cases (eFigure 4 in the Supplement), the fovea and extramacular retina were profoundly hypoautofluorescent and left between them an isoautofluorescent or slightly hyperautofluorescent ring. A total of 5 patients had undetectable ERG at the first assessment (Table 1). Patient CICO0166 had no response at the dark-adapted 0.01 ERG and dark-adapted 3.0 ERG but had a peculiar dark-adapted 10.0 ERG with reduced b/a ratio. Light-adapted ERG responses (light-adapted 3.0 ERG; light-adapted 30-Hz flicker ERG) were severely reduced (eFigure 5 in the Supplement). Patient CICO3517 had a clearly electro-negative ERG (b wave less than a wave) with a reduced a wave; 5 years later, ERG became undetectable (eFigure 5 in the Supplement).

CLN3 variants are summarized in Table 2.^{10,11,20-22} Briefly, 11 variants in *CLN3* were found, of which 4 were novel: the c.443_445del and c.906+15C>G variants identified in patient CICO9853 and variants c.938T>C p.(Leu313Pro) and c.1225A>G p.(Met409Val) in patients CICO0166 and CICO2713. All but 1 novel variant (c.906+15C>G, p.?) were classified as pathogenic or likely pathogenic in accordance with American College of Medical Genetics and Genomics standards.²³

Follow-up

All averaged BCVA measurements were plotted with age (eFigure 6 in the Supplement). All patients experienced a progressive BCVA reduction. Kaplan-Meier survival curves showing the survival distribution of BCVA of 1.3 logMAR or greater (20/400 Snellen equivalent; legal blindness threshold) were significantly different between the 2 phenotypic groups. A total of 3 of 6 patients from group A (50%) reached the legal blindness threshold by their 70s. A total of 11 patients from group B (70%) reached the legal blindness threshold by their 40s. Long-term follow-up data were available for patients CICO3517 (eFigure 7 in the Supplement), CICO0350 (eFigure 8 in the

Supplement), and patients from families F699 (eFigures 9 to 11 in the Supplement) and F5189 (eFigures 12 and 13 in the Supplement).

Discussion

We report here 15 patients with isolated retinal degeneration presenting with biallelic variants in *CLN3*. A total of 11 distinct variants were found in this study, of which 4 were novel. To our knowledge, this is the largest series of patients with isolated *CLN3*-linked IRD reported so far. Biallelic *CLN3* variants are usually associated with a severe neurometabolic disorder, JNCL.¹¹ The classic form of the disease begins by visual symptoms between ages 4 and 6 years, months prior to the onset of neurological symptoms.¹²

Recent studies reported patients with isolated retinal degeneration and biallelic *CLN3* variants.^{10,20,24,25} Our clinical data are mostly in line with these reports, with a further distinction of 2 phenotypic groups. Group A is characterized by a mild course of rod-cone degeneration, with an onset of symptoms between ages 20 and 40 years, a relatively preserved posterior pole and thus better visual acuity, and a slow progression, reaching legal blindness by the 70s. Group B shows more severe retinal degeneration with early macular atrophy, an onset of symptoms in the 10s or early 20s, rapid visual acuity loss, and legal blindness being reached by their 40s. Of note, there was no high prevalence of cystoid macular changes in our series (only 3 of 15 patients), in contrast with previous reports.²⁰

Interestingly, cases from 2 families showed retinal findings reminiscent of JNCL with an additional inner retinal dysfunction to photoreceptor disease characteristic of JNCL-associated retinopathy.¹⁶ SD-OCT findings in JNCL-associated retinopathy may also include macular outer nuclear layer and ellipsoid zone disruption along with inner nuclear layer thinning.¹⁸ This latter change was not found in patients with isolated IRD in this study. The presence of striated macular pattern, found in 7 patients in this series, is another confounding feature. The radial macular striae at the vitreoretinal interface (either with or without evidence of epiretinal membrane on OCT) are a common finding in JNCL.¹⁷ However, unlike JNCL, the first symptoms of retinal degeneration in these patients occurred later, by the end of the second decade of life.

CLN3 is located in 16p12.1 (Figure 2) and encodes battenin. It is expressed in all retinal cell types, but the immunohistochemical staining is more intense in Müller cells, bipolar cells, and the inner segment of photoreceptors.²⁶

Battenin is a transmembrane protein containing 438 amino acids (eFigure 14 in the Supplement). The protein has not been crystallized yet; the topology is predicted in silico.²⁷⁻²⁹ Second cytoplasmic loop and C-terminal domain contain the lysosomal targeting motifs, responsible for correct addressing of battenin from the Golgi apparatus to lysosome.^{30,31} The exact cellular function of battenin is still unclear but appears to be linked with vesicular addressing and trafficking, posttranslational protein modification, autophagy, and overall lysosomal function.^{29,32,33} Variants involved in nonsyndromic reti-

Table 2. CLN3 Variants in Study Cohort

Symbol	Location	Sequence variation	Protein change	ACMG interpretation	Comments	Source
M8	Exon 7	c.443_445del ^a	p.(Val148del) ^a	Likely pathogenic (IV: PM1, PM2, PM3, PM4, BP5)	rs752130042 gnomAD: MAF 0.00001592; never observed at homozygous state; allele count 4	This cohort
M1	Intron 7	c.461-3C>G	p.?	Pathogenic (II: PS4, PP1-S, PM2, PM3, PP1)	rs181995380 gnomAD: MAF 0.000004311; never observed at homozygous state; allele count 1; reported only compound heterozygous; led to abnormal transcription; homozygous in patient C1C0350 ^a	Ku et al, ²⁰ 2017
M2	Intron 7_Intron 9	Ex8.9del of 1.02 kilobase pairs (c.461-280_677+382del)	p.?	Pathogenic (Ia: PV51, PS3, PS4, PP1-S, PM1, PM2, PM3, PP1-M, PP1)	Reported usually as Ex7.8del (exon 1 in 5' untranslated region omitted); most frequent	Lerner et al, ¹¹ 1995
M7	Exon 12	c.868G>T	p.(Val290Leu)	Pathogenic (IIa: PS4, PM1, PM2, PM3)	rs3690087702 gnomAD: MAF 0.000007953; never observed at homozygous state; allele count 2	Wang et al, ¹⁰ 2014
M10	Exon12	c.883G>A	p.(Glu295Lys)	Pathogenic (IIa: PS4, PM1, PM2, PM3, PP2, PP3)	rs121434286 gnomAD: MAF 0.00002475; never observed at homozygous state; allele count 7	Munroe et al, ²¹ 1997
M11	Intron 12	c.906+15C>G ^a	p.?	Uncertain significance (PM2, PM3, PP2)	Unknown; new splicing donor site predicted: SpliceSiteFinder: 0→73 [0-100]; MaxEntScan: 0→4.7 [0-12]	This cohort
M5	Exon 13	c.938T>C ^a	p.(Leu313Pro) ^a	Likely pathogenic (IV: PM1, PM2, PM3, PM6, PP2, PP3)	rs141816714 gnomAD: MAF 0.00003544; never observed at homozygous state; allele count 10; PolyPhen-2: probably damaging; SIFT: damaging; MutationTaster: disease causing	This cohort
M3	Exon 14	c.1000C>T	p.(Arg334Cys)	Pathogenic (II: PS4, PM1, PM2, PM3, PS1, PP2, PP3)	rs386833694 gnomAD: MAF 0.000004011; never observed at homozygous state; allele count 1	Munroe et al, ²¹ 1997
M9	Intron 14	c.1056+3A>C	p.?	Pathogenic (Ia: PV51, PS3, PS4, PP1-S, PM1, PM2, PM3, PP1-M, PP1)	rs386833698; no frequency data	Lojewski et al, ²² 2014
M4	Exon 16	c.1213C>T	p.(Arg405Trp)	Pathogenic (IIa: PS4, PM1, PM2, PM3, PP2, PP3)	rs139842473 gnomAD: MAF 0.00006742; never observed at homozygous state; allele count 19	Wang et al, ¹⁰ 2014
M6	Exon 16	c.1225A>G ^a	p.(Met409Val) ^a	Likely pathogenic (IV: PM1, PM2, PM3, PP3)	rs776443981 gnomAD: MAF 0.00003902; never observed at homozygous state; allele count 11; PolyPhen-2: probably damaging; SIFT: deleterious; MutationTaster: disease causing	This cohort

Abbreviations: ACMG, American College of Medical Genetics and Genomics; MAF, minor allele frequency; SIFT, Sorting Intolerant From Tolerant.
^a Novel variant.

tion including *CLN3* and 2 point variants,³⁶ c.560G>C (p.Gly187Ala)³⁴ and c.988G>T (p.Val330Phe).²¹ The delayed-onset JNCL (with visual and neurological symptoms by age 8 to 10 years) was reported in a small number of patients with compound heterozygous variants in *CLN3*, including the common Ex8_9del and Ex10_13del or c.553+1G>C in trans.¹¹ Protracted-onset JNCL (neurological symptoms occur years later after initial visual involvement) is also described with compound heterozygous variants, including the Ex8_9del as one allele and the following variations as the second allele: c.1A>C, c.302T>C p.(Leu101Pro), c.509T>C p.(Leu170Pro), c.883G>A p.(Glu295Lys), or c.1000C>T p.(Arg334His) or with c.597C>A p.(Tyr199*) in a homozygous state.³⁷

CLN3-Associated Isolated Retinal Degeneration

Milder forms of retinal degeneration (group A) are associated with homozygous point variants affecting the lysosomal targeting motifs of battenin, ie, c.1225A>G p.(Met409Val) and c.1213C>T p.(Arg405Trp),¹⁰ presumably precluding a normal trafficking of battenin to the lysosome. Similarly, the homozygous c.461-3C>G variant, which is probably a leaky variant with decreased but persistent expression, is associated with a milder phenotype.²⁰ A mild phenotype is also found in genotypes associating the common Ex8_9del and the following point variants: c.837+5G>A, c.988G>A p.(Val330Ile),²⁰ c.175G>A p.,²⁵ and c.906+15C>G p./c.443_445del p.(Val148del). In the latter case (patient C1C09853), one of the variants (c.443_445del) is predicted to be deleterious in silico and the second (c.906+15C>G) is of uncertain significance. More severe and earlier-onset forms of isolated retinal degeneration (group B) occur in homozygous and compound point biallelic variants of *CLN3* coding sequence but also when an intronic variant (c.375-3C>G, c.461-3C>G) is associated with Ex8_9del in trans.

Three point variants—c.565G>C p.(Gly189Arg), c.883G>A p.(Glu295Lys), and c.883G>T p.(Glu295*)—are reported both in JNCL and isolated retinal disease.^{10,20,21,34,38} More specifically, compound heterozygous association of these variants with Ex8_9del give rise to JNCL, while isolated retinal phenotype is seen if any of these variants is in trans with another point variant, specific for only retinal involvement (eTable in the Supplement). Another intronic variant, c.1056+3A>C, was previously reported only in JNCL in association with the c.1247A>G variant³⁴ or with Ex2_5del.¹⁷ We found this intronic variant in 2 affected members of the family F5189 along with c.938C>T p.(Leu313Pro). The latter variant, homozygous in patient C1C00166, also led to isolated retinal degeneration.

Of note, phenotype-genotype correlations in *CLN3* variants are imperfect, and caution should be given to a falsely reassuring retina-restricted diagnosis. Although none of these patients manifested *CLN3*-related neurological symptoms (including a woman in her 70s who only manifested extrapyramidal iatrogenic symptoms according to the neurologist), a 2017 report mentioned 2 siblings with an initial isolated

retinal disease carrying the homozygous c.1213C>T p.(Arg405Trp) variant (Figure 3) who developed neurological symptoms reminiscent of NCL in their 30s.³⁹ The p.(Arg405Trp) variant was first reported in isolated retinal disease, both as homozygous and compound heterozygous with Ex8_9del in trans.^{10,20,40} In our series, 3 patients harbored the p.(Arg405Trp) variant, either with Ex8_9del or c.883G>A and c.1000C>T missense variants in trans. None of them have had extraocular involvement to date, but the patients are younger than 40 years. A very protracted course of ceroid lipofuscinosis, compatible with the diagnosis of Kufs disease (adult-onset ceroid lipofuscinosis),⁴¹⁻⁴³ is in the spectrum of clinical manifestations of biallelic *CLN3* variants. Thus, the long-term prognosis for development of the neurologic condition is very difficult if impossible to predict for these cases carrying *CLN3* variants.

Limitations

Our study has some limitation. Biases from retrospective analyses of the collected data are obvious. Due to the limited number of cases, we could not realize a statistical analysis of phenotype-genotype correlations. Larger series with meta-analysis of previously published data should be performed to better understand the pathology and phenotype-genotype correlations. Functional studies of novel *CLN3* variants could also be beneficial for deciphering the retinal degeneration pathophysiological mechanism.

To date, both JNCL and *CLN3*-associated isolated retinal degeneration are untreatable conditions.⁴⁴ Gene replacement approaches in animals showed efficacy and safety both through systemic administration for neurological disease⁴⁵ and through intraocular delivery for retinal degeneration.⁴⁶ A phase 1/2 gene therapy study in human is under way to evaluate intrathecal injection of AAV9-*CLN3* in pediatric patients with JNCL.⁴⁷ Isolated retinal degeneration linked with *CLN3* variants could also be a good target for intraocular gene delivery due to the simplicity of tissue access and functional assessment.

Conclusions

Biallelic *CLN3* variants are responsible for a spectrum of diseases, varying from severe neurodegeneration to retina-restricted disease. These findings support adding *CLN3* to NGS panels investigating presumed cases with IRD.⁴⁸ Phenotype-genotype correlations can be drawn, but more data are needed to refine them. Caution should be taken regarding potential neurological outcome, and a long-term follow-up for patients with apparent retina-restricted disease linked with *CLN3* variants is required. A better understanding of phenotype-genotype correlations would serve as a basis for the development of a *CLN3* gene therapy.

ARTICLE INFORMATION

Accepted for Publication: October 1, 2020.

Published Online: January 28, 2021.
doi:10.1001/jamaophthalmol.2020.6089

Author Affiliations: Sorbonne Université, INSERM, Centre national de la recherche scientifique, Institut

de la Vision, Paris, France (Smirnov, Nassisi, Solis Hernandez, Méjécase, El Shami, Condroyer, Antonio, Sahel, Audo, Zeitz); Université de Lille, Faculté de Médecine, Lille, France (Smirnov);

Exploration de la Vision et Neuro-Ophthalmologie, CHU de Lille, Lille, France (Smirnov, Defoort-Dhellemmes); Institute of Ophthalmology, University College London, London, United Kingdom (Mégécase, Audo); Department of Medical Laboratory Technology, Faculty of Health Sciences, Beirut Arab University, Beirut, Lebanon (El Shamieh); Institute for Neurosciences Montpellier, INSERM UI051, University of Montpellier, Montpellier, France (Meunier); National Center for Rare Genetic Retinal Dystrophies, Hôpital Guy de Chauliac, Montpellier, France (Meunier); Centre Hospitalier National d'Ophthalmologie des Quinze-Vingts, INSERM-DHOS CIC 1423, Paris, France (Andrieu, Mohand-Said, Sahel, Audo); Fondation Ophthalmologique Adolphe de Rothschild, Paris, France (Sahel); Académie des Sciences, Institut de France, Paris, France (Sahel); Department of Ophthalmology, The University of Pittsburgh School of Medicine, Pittsburgh, Pennsylvania (Sahel).

Author Contributions: Drs Audo and Zeitz had full access to all of the data in the study and take responsibility for the integrity of the data and the accuracy of the data analysis. Drs Audo and Zeitz contributed equally to the article.

Study concept and design: Smirnov, Audo, Zeitz.

Acquisition, analysis, or interpretation of data: Smirnov, Nassisi, Solis Hernandez, Mégécase, El Shamieh, Condroyer, Antonio, Meunier, Andrieu, Defoort-Dhellemmes, Mohand-Said, Sahel, Audo. **Drafting of the manuscript:** Smirnov, Meunier, Defoort-Dhellemmes.

Critical revision of the manuscript for important intellectual content: Smirnov, Nassisi, Solis Hernandez, Mégécase, El Shamieh, Condroyer, Antonio, Meunier, Andrieu, Mohand-Said, Sahel, Audo, Zeitz.

Statistical analysis: Smirnov, Nassisi, El Shamieh. **Obtained funding:** Sahel, Audo, Zeitz.

Administrative, technical, or material support: Condroyer, Andrieu, Mohand-Said, Audo, Zeitz. **Study supervision:** Defoort-Dhellemmes, Sahel, Audo, Zeitz.

Conflict of Interest Disclosures: Dr Sahel has received personal fees from Pixium Vision, GenSight Biologics, SparingVision, Prohesea, and Chronolife. Dr Audo is a consultant for SparingVision and Novartis. No other disclosures were reported.

Funding/Support: This work was supported by grants from LabEx LifeSenses, IHU FOReSIGHT, and Fondation Fighting Blindness. Dr Smirnov was supported by RHU-Light 4 Deaf. Dr Nassisi was supported by RHU-Light 4 Deaf and a fellowship award from Fondation Fighting Blindness. Dr Mégécase was supported by Fondation de France.

Role of the Funder/Sponsor: The funders had no role in the design and conduct of the study; collection, management, analysis, and interpretation of the data; preparation, review, or approval of the manuscript; and decision to submit the manuscript for publication.

Additional Contributions: We thank the patients and their families for their participation in the study as well as the clinical staff from the Clinical Investigation Center 1423.

REFERENCES

1. Verbakel SK, van Huet RAC, Boon CJF, et al. Non-syndromic retinitis pigmentosa. *Prog Retin Eye*

Res. 2018;66:157-186. doi:10.1016/j.preteyeres.2018.03.005

2. Abu Diab A, Altalbishi A, Rosin B, et al. The combination of whole-exome sequencing and clinical analysis allows better diagnosis of rare syndromic retinal dystrophies. *Acta Ophthalmol*. 2019;97(6):e877-e886. doi:10.1111/aos.14095

3. Wang X, Feng Y, Li J, et al. Retinal diseases caused by mutations in genes not specifically associated with the clinical diagnosis. *PLoS One*. 2016;11(10):e0165405. doi:10.1371/journal.pone.0165405

4. Daiger SP; The University of Texas Health Science Center. RetNet: Retinal Information Network. Accessed August 28, 2020. <https://sph.uth.edu/retnet/>

5. Karali M, Testa F, Brunetti-Pierri R, et al. Clinical and genetic analysis of a European cohort with pericentral retinitis pigmentosa. *Int J Mol Sci*. 2019;21(1):E86. doi:10.3390/ijms21010086

6. Estrada-Cuzcano A, Koenekoop RK, Senechal A, et al. *BB51* mutations in a wide spectrum of phenotypes ranging from nonsyndromic retinitis pigmentosa to Bardet-Biedl syndrome. *Arch Ophthalmol*. 2012;130(11):1425-1432. doi:10.1001/archophthalmol.2012.2434

7. Seyedahmadi BJ, Rivolta C, Keene JA, Berson EL, Dryja TP. Comprehensive screening of the *USH2A* gene in Usher syndrome type II and non-syndromic recessive retinitis pigmentosa. *Exp Eye Res*. 2004;79(2):167-173. doi:10.1016/j.exer.2004.03.005

8. Ávila-Fernández A, Cantalapiedra D, Aller E, et al. Mutation analysis of 272 Spanish families affected by autosomal recessive retinitis pigmentosa using a genotyping microarray. *Mol Vis*. 2010;16:2550-2558.

9. McGee TL, Seyedahmadi BJ, Sweeney MO, Dryja TP, Berson EL. Novel mutations in the long isoform of the *USH2A* gene in patients with Usher syndrome type II or non-syndromic retinitis pigmentosa. *J Med Genet*. 2010;47(7):499-506. doi:10.1136/jmg.2009.075143

10. Wang F, Wang H, Tuan H-F, et al. Next generation sequencing-based molecular diagnosis of retinitis pigmentosa: identification of a novel genotype-phenotype correlation and clinical refinements. *Hum Genet*. 2014;133(3):331-345. doi:10.1007/s00439-013-1381-5

11. Lerner TJ, Boustany R-MN, Anderson JW, et al; The International Batten Disease Consortium. Isolation of a novel gene underlying Batten disease. *CLN3*. *Cell*. 1995;82(6):949-957. doi:10.1016/0092-8674(95)90274-0

12. Mole SE, Williams RE. Neuronal ceroid-lipofuscinoses. In: Adam MP, Ardinger HH, Pagon RA, et al, eds. *GeneReviews*. University of Washington; 1993. Accessed November 24, 2019. <https://www.ncbi.nlm.nih.gov/books/NBK1428/>

13. Geraets RD, Koh SY, Hastings ML, Kielian T, Pearce DA, Weimer JM. Moving towards effective therapeutic strategies for neuronal ceroid lipofuscinosis. *Orphanet J Rare Dis*. 2016;11(1):40. doi:10.1186/s13023-016-0414-2

14. Santorelli FM, Garavaglia B, Cardona F, et al. Molecular epidemiology of childhood neuronal ceroid-lipofuscinosis in Italy. *Orphanet J Rare Dis*. 2013;8:19. doi:10.1186/1750-1172-8-19

15. Mink JW, Augustine EF, Adams HR, Marshall FJ, Kwon JM. Classification and natural history of the

neuronal ceroid lipofuscinoses. *J Child Neurol*. 2013;28(9):1101-1105. doi:10.1177/0883073813494268

16. Weleber RG. The dystrophic retina in multisystem disorders: the electroretinogram in neuronal ceroid lipofuscinoses. *Eye (Lond)*. 1998;12(pt 3b):580-590. doi:10.1038/eye.1998.148

17. Wright GA, Georgiou M, Robson AG, et al. Juvenile Batten disease (*CLN3*): detailed ocular phenotype, novel observations, delayed diagnosis, masquerades, and prospects for therapy. *Ophthalmol Retina*. 2020;4(4):433-445. doi:10.1016/j.oret.2019.11.005

18. Preising MN, Abura M, Jäger M, Wassill K-H, Lorenz B. Ocular morphology and function in juvenile neuronal ceroid lipofuscinosis (*CLN3*) in the first decade of life. *Ophthalmic Genet*. 2017;38(3):252-259. doi:10.1080/13816810.2016.1210651

19. Audo I, Friedrich A, Mohand-Said S, et al. An unusual retinal phenotype associated with a novel mutation in *RHO*. *Arch Ophthalmol*. 2010;128(8):1036-1045. doi:10.1001/archophthalmol.2010.162

20. Ku CA, Hull S, Arno G, et al. Detailed clinical phenotype and molecular genetic findings in *CLN3*-associated isolated retinal degeneration. *JAMA Ophthalmol*. 2017;135(7):749-760. doi:10.1001/jamaophthalmol.2017.1401

21. Munroe PB, Mitchison HM, O'Rawe AM, et al. Spectrum of mutations in the Batten disease gene, *CLN3*. *Am J Hum Genet*. 1997;61(2):310-316. doi:10.1086/514846

22. Lojewski X, Staropoli JF, Biswas-Légrand S, et al. Human iPSC models of neuronal ceroid lipofuscinosis capture distinct effects of *TPP1* and *CLN3* mutations on the endocytic pathway. *Hum Mol Genet*. 2014;23(8):2005-2022. doi:10.1093/hmg/ddt596

23. Richards S, Aziz N, Bale S, et al; ACMG Laboratory Quality Assurance Committee. Standards and guidelines for the interpretation of sequence variants: a joint consensus recommendation of the American College of Medical Genetics and Genomics and the Association for Molecular Pathology. *Genet Med*. 2015;17(5):405-424. doi:10.1038/gim.2015.30

24. Carss KJ, Arno G, Erwood M, et al; NIH-Rare BioResource Rare Diseases Consortium. Comprehensive rare variant analysis via whole-genome sequencing to determine the molecular pathology of inherited retinal disease. *Am J Hum Genet*. 2017;100(1):75-90. doi:10.1016/j.ajhg.2016.12.003

25. Chen FK, Zhang X, Eintracht J, et al. Clinical and molecular characterization of non-syndromic retinal dystrophy due to c.175G>A mutation in ceroid lipofuscinosis neuronal 3 (*CLN3*). *Doc Ophthalmol*. 2019;138(1):55-70. doi:10.1007/s10633-018-9665-7

26. Katz ML, Gao CL, Prabhakaram M, Shibuya H, Liu PC, Johnson GS. Immunohistochemical localization of the Batten disease (*CLN3*) protein in retina. *Invest Ophthalmol Vis Sci*. 1997;38(11):2375-2386.

27. Cotman SL, Staropoli JF. The juvenile Batten disease protein, *CLN3*, and its role in regulating anterograde and retrograde post-Golgi trafficking. *Clin Lipidol*. 2012;7(1):79-91. doi:10.2217/clp.11.70

28. Nugent T, Mole SE, Jones DT. The transmembrane topology of Batten disease protein *CLN3* determined by consensus computational prediction constrained by experimental data. *FEBS*

- Letts. 2008;582(7):1019-1024. doi:10.1016/j.febslet.2008.02.049
29. Mirza M, Vainshtein A, DiRonza A, et al. The *CLN3* gene and protein: what we know. *Mol Genet Genomic Med*. 2019;7(12):e859. doi:10.1002/mgg3.859
30. Kytälä A, Ihrke G, Vesa J, Schell MJ, Luzio JP. Two motifs target Batten disease protein *CLN3* to lysosomes in transfected nonneuronal and neuronal cells. *Mol Biol Cell*. 2004;15(3):1313-1323. doi:10.1091/mbc.e03-02-0120
31. Kytälä A, Yliannala K, Schu P, Jalanko A, Luzio JP. AP-1 and AP-3 facilitate lysosomal targeting of Batten disease protein *CLN3* via its dileucine motif. *J Biol Chem*. 2005;280(11):10277-10283. doi:10.1074/jbc.M411862200
32. Yasa S, Modica G, Sauvageau E, Kaleem A, Hermey G, Lefrançois S. *CLN3* regulates endosomal function by modulating Rab7A-effector interactions. *J Cell Sci*. 2020;133(6):jcs234047. doi:10.1242/jcs.234047
33. Metcalf DJ, Calvi AA, Seaman MNJ, Mitchison HM, Cutler DF. Loss of the Batten disease gene *CLN3* prevents exit from the TGN of the mannose 6-phosphate receptor. *Traffic*. 2008;9(11):1905-1914. doi:10.1111/j.1600-0854.2008.00807.x
34. Kousi M, Lehesjoki A-E, Mole SE. Update of the mutation spectrum and clinical correlations of over 360 mutations in eight genes that underlie the neuronal ceroid lipofuscinoses. *Hum Mutat*. 2012;33(1):42-63. doi:10.1002/humu.21624
35. de los Reyes E, Dyken PR, Phillips P, et al. Profound infantile neuroretinal dysfunction in a heterozygote for the *CLN3* genetic defect. *J Child Neurol*. 2004;19(1):42-46. doi:10.1177/08830738040190010703
36. Pebrel-Richard C, Debost-Légrand A, Eymard-Pierre E, et al. An unusual clinical severity of 16p11.2 deletion syndrome caused by unmasked recessive mutation of *CLN3*. *Eur J Hum Genet*. 2014;22(3):369-373. doi:10.1038/ejhg.2013.141
37. Sarpong A, Schottmann G, Rütger K, et al. Protracted course of juvenile ceroid lipofuscinosis associated with a novel *CLN3* mutation (p.Y199X). *Clin Genet*. 2009;76(1):38-45. doi:10.1111/j.1399-0004.2009.01179.x
38. Bell CJ, Dinwiddie DL, Miller NA, et al. Carrier testing for severe childhood recessive diseases by next-generation sequencing. *Sci Transl Med*. 2011;3(65):65ra4. doi:10.1126/scitranslmed.3001756
39. Kuper WFE, van Alfen C, van Eck L, et al. A case of unexpected adult-onset neurologic decline in *CLN3*-associated retinal degeneration. *JAMA Ophthalmol*. 2017;135(12):1451-1453. doi:10.1001/jamaophthalmol.2017.4353
40. Stone EM, Andorf JL, Whitmore SS, et al. Clinically focused molecular investigation of 1000 consecutive families with inherited retinal disease. *Ophthalmology*. 2017;124(9):1314-1331. doi:10.1016/j.ophtha.2017.04.008
41. Berkovic SF, Carpenter S, Andermann F, Andermann E, Wolfe LS. Kufs' disease: a critical reappraisal. *Brain*. 1988;111(pt 1):27-62. doi:10.1093/brain/111.1.27
42. Tyynelä J, Lehesjoki A-E. Kufs or not Kufs: challenging diagnostics of a rare adult-onset neurodegenerative disease. *Brain*. 2019;142(1):2-5. doi:10.1093/brain/awy312
43. Berkovic SF, Oliver KL, Canafoglia L, et al. Kufs disease due to mutation of *CLN6*: clinical, pathological and molecular genetic features. *Brain*. 2019;142(1):59-69. doi:10.1093/brain/awy297
44. Mole SE, Anderson G, Band HA, et al. Clinical challenges and future therapeutic approaches for neuronal ceroid lipofuscinosis. *Lancet Neurol*. 2019;18(1):107-116. doi:10.1016/S1474-4422(18)30368-5
45. Bosch ME, Aldrich A, Fallet R, et al. Self-complementary AAV9 gene delivery partially corrects pathology associated with juvenile neuronal ceroid lipofuscinosis (*CLN3*). *J Neurosci*. 2016;36(37):9669-9682. doi:10.1523/JNEUROSCI.1635-16.2016
46. Wiley LA, Burnight ER, Drack AV, et al. Using patient-specific induced pluripotent stem cells and wild-type mice to develop a gene augmentation-based strategy to treat *CLN3*-associated retinal degeneration. *Hum Gene Ther*. 2016;27(10):835-846. doi:10.1089/hum.2016.049
47. Gene therapy for children with *CLN3* Batten disease. ClinicalTrials.gov identifier: NCT03770572. Updated March 25, 2020. Accessed August 28, 2020. <https://clinicaltrials.gov/ct2/show/NCT03770572>
48. Turriff AE, Cukras CA, Brooks BP, Huryn LA. Considerations in multi-gene panel testing in pediatric ophthalmology. *J AAPOS*. 2019;23(3):163-165.e1. doi:10.1016/j.jaapos.2019.01.008

The comment from readers and our reply are following.

Letters

COMMENT & RESPONSE

Challenges of Phenotype-Genotype Correlations in Rare Diseases

To the Editor We were interested to read the recent article by Smirnov et al.¹ This excellent article described ophthalmologic phenotypes in *CLN3* disease. It also raised important questions about prior reports of genotype-phenotype associations in *CLN3* disease.

The authors nicely illustrate the complexity of genotype-phenotype associations in *CLN3* disease (Figure 3¹). However, some of the information included from the literature did not match our understanding of those same publications.

The authors list 4 genotypes associated with severe *CLN3* disease. We have concerns with the classification of each of these individuals:

1. One had a 1.7-megabase pair deletion in *CLN3* in trans with the common 1-kilobase pair (kb) deletion in addition to 16p11.2 deletion syndrome (reference 36 in original study¹). The 16p11.2 deletion is associated with an autistic phenotype that is possibly responsible for the more severe phenotype. Because of the potential impact of cooccurring genetic disorders, we suggest that discussions of the *CLN3* phenotype exclude individuals with disease-causing variants in multiple genes.
2. One had the common 1-kb deletion on one allele but no variant identified on the other allele. This individual had profound neurologic symptoms at age 5 months with features that are not seen in *CLN3* disease (reference 35 in original study).¹ Additionally, there was no histological evidence for *CLN3* disease on electron microscopy. For these reasons, we do not think that the reported symptoms are consistent with *CLN3* disease.
3. One had p.Gly187Ala in trans with the 1-kb common deletion and was reported to have a classic, not severe, juvenile neuronal ceroid lipofuscinosis (JNCL) phenotype (reference 34 in original study).¹
4. One had p.Val330Phe in trans with the 1-kb common deletion and also was reported to have classic, not severe, JNCL (reference 21 in original study).¹ We have reported a different individual with the same genotype who also had classic JNCL.²

The relative lack of published quantitative phenotype data in *CLN3* disease in combination with the use of poorly defined, subjective terms, such as delayed onset and protracted course throughout the literature, pose challenges to data aggregation. Variants previously reported may not include accurate reporting of phenotypic severity. In addition, these terms

are often used interchangeably but may actually reflect different phenotypes. These challenges illustrate the need for better quantitative phenotype data in *CLN3* disease. We commend Smirnov et al¹ for providing such quantitative data about ophthalmological involvement in *CLN3* disease.

Margaux C. Masten, BA
Erika F. Augustine, MD, MS
Jonathan W. Mink, MD, PhD

Author Affiliations: University of Rochester, Rochester, New York (Masten, Augustine, Mink); Kennedy Krieger Institute, Baltimore, Maryland (Augustine).

Corresponding Author: Margaux C. Masten, BA, University of Rochester, 601 Elmwood Ave, Rochester, NY 14642 (margaux_masten@urmc.rochester.edu).

Published Online: October 28, 2021. doi:10.1001/jamaophthalmol.2021.4372

Conflict of Interest Disclosures: Dr Augustine has received grants from Abeona Therapeutics, National Institutes of Health, and Batten Disease Support and Research Association; personal fees from Beyond Batten Disease Foundation; and consultation fees paid to her institution from Taysha Gene Therapies, Neurogene, and Amicus Therapeutics; and has a copyright for the Unified Batten Disease Rating Scale. Dr Mink has received personal fees from Neurogene, Amicus Therapeutics, and Taysha Gene Therapies and has a copyright for the Unified Batten Disease Rating Scale. No other disclosures were reported.

1. Smirnov VM, Nassisi M, Solis Hernandez C, et al. Retinal phenotype of patients with isolated retinal degeneration due to *CLN3* pathogenic variants in a French retinitis pigmentosa cohort. *JAMA Ophthalmol*. 2021;139(3):278-291. doi:10.1001/jamaophthalmol.2020.6089

2. Kwon JM, Adams H, Rothberg PG, et al. Quantifying physical decline in juvenile neuronal ceroid lipofuscinosis (Batten disease). *Neurology*. 2011;77(20):1801-1807. doi:10.1212/WNL.0b013e318237f649

In Reply We recognize that p.Gly187Ala¹ and p.Val330Phe² variants in trans with the common 1-kilobase pair deletion were erroneously classified in the severe neuronal ceroid lipofuscinosis (NCL) group and should be considered to be associated with the classic *CLN3*-associated NCL. We apologize for this error in our article.³ This error was discovered by Masten et al and reported in their comment on our article.

This error does not affect our results, statistically significant and nonsignificant data, interpretation of our findings, or conclusion of our article. The discussion about *CLN3*-associated NCL severity is based on analysis of all reported cases and had 2 objectives, which are not altered by the reported error:

1. To demonstrate that *CLN3*-associated isolated retinal degeneration has a broad spectrum of severity which, to some extent, mirrors the spectrum of *CLN3*-associated NCL.
2. To show that the genotypes are distinct between the juvenile form of NCL and *CLN3*-associated isolated retinal degeneration.

The relevant article text and Figure 3 have been corrected online.⁴ To the best of our knowledge and after revision, there are no other errors in the article, figures, tables, and Supplement.

Vasily M. Smirnov, MD
Christina Zeitz, PhD
Isabelle Audo, MD, PhD

Author Affiliations: Sorbonne Université, INSERM, CNRS, Institut de la Vision, Paris, France (Smirnov, Zeitz, Audo); Université de Lille, Faculté de Médecine, Lille, France (Smirnov); Exploration de la Vision et Neuro-Ophthalmologie, CHU de Lille, Lille, France (Smirnov); Centre Hospitalier National d'Ophthalmologie des Quinze-Vingts, INSERM-DHOS CIC 1423, Paris, France (Audo); Institute of Ophthalmology, University College London, London, United Kingdom (Audo).

Corresponding Author: Isabelle Audo, MD, PhD (isabelle.audo@inserm.fr), and Christina Zeitz, PhD (christina.zeitz@inserm.fr), Sorbonne Université, INSERM, CNRS, Institut De La Vision, 17 Rue Moreau, Paris 75012, France.

Published Online: October 28, 2021. doi:10.1001/jamaophthalmol.2021.4375

Conflict of Interest Disclosures: Dr Audo has received grants from LabEx LifeSenses, IHU FReSIGHT, Foundation Fighting Blindness, and RHU-Light 4 Deaf and has consulted for Novartis, SparingVision, Biogen, and Roche. No other disclosures were reported.

1. Kousi M, Lehesjoki A-E, Mole SE. Update of the mutation spectrum and clinical correlations of over 360 mutations in eight genes that underlie the neuronal ceroid lipofuscinoses. *Hum Mutat*. 2012;33(1):42-63. doi:10.1002/humu.21624
2. Munroe PB, Mitchison HM, O'Rawe AM, et al. Spectrum of mutations in the Batten disease gene, *CLN3*. *Am J Hum Genet*. 1997;61(2):310-316. doi:10.1086/514846
3. Smirnov VM, Nassisi M, Solis Hernandez C, et al. Retinal phenotype of patients with isolated retinal degeneration due to *CLN3* pathogenic variants in a French retinitis pigmentosa cohort. *JAMA Ophthalmol*. 2021;139(3):278-291. doi:10.1001/jamaophthalmol.2020.6089
4. Error in classification of variants. Correction. *JAMA Ophthalmol*. Published online October 28, 2021. doi:10.1001/jamaophthalmol.2021.4737

CORRECTION

Error in a Supplement: In the article titled "Refractive Outcomes After Immediate Sequential vs Delayed Sequential Bilateral Cataract Surgery," published online July 1, 2021, and also in the August 2021 issue of *JAMA Ophthalmology*,¹ there was a formatting error in Supplement 2 listing the IRIS Research Analytic Center Consortium members. The supplement was corrected online. This article was also previously corrected on August 18, 2021.

1. Owen JP, Blazes M, Lacy M, et al; IRIS Research Analytic Center Consortium. Refractive outcomes after immediate sequential vs delayed sequential bilateral cataract surgery. *JAMA Ophthalmol*. Published online July 1, 2021. doi:10.1001/jamaophthalmol.2021.2032

Correction to X-Axis in Figure: In the Original Investigation titled "Rates of Myopia Development in Young Chinese Schoolchildren During the Outbreak of COVID-19," published online September 16, 2021, in *JAMA Ophthalmology*,¹ the x-axis labels in Figure 2B have been corrected. This article was corrected online.

1. Hu Y, Zhao F, Ding X, et al. Rates of myopia development in young Chinese schoolchildren during the outbreak of COVID-19. *JAMA Ophthalmol*. Published online September 16, 2021. doi:10.1001/jamaophthalmol.2021.3563

Error in Classification of Variants: In the Original Investigation titled "Retinal Phenotype of Patients With Isolated Retinal Degeneration Due to *CLN3* Pathogenic Variants in a French Retinitis Pigmentosa Cohort,"¹ published online January 28, 2021, and in the March 2021 issue of *JAMA Ophthalmology*, 2 variants were erroneously classified in the severe neuronal ceroid lipofuscinosis (NCL) group instead of the classic *CLN3*-associated NCL. The Discussion section and Figure 3 were updated. None of the study's conclusions were affected. The article was corrected online.²

1. Smirnov VM, Nassisi M, Solis Hernandez C, et al. Retinal phenotype of patients with isolated retinal degeneration due to *CLN3* pathogenic variants in a French retinitis pigmentosa cohort. *JAMA Ophthalmol*. 2021;139(3):278-291. doi:10.1001/jamaophthalmol.2020.6089
2. Smirnov VM, Zeitz C, Audo I. Challenges of phenotype-genotype correlations in rare diseases—reply. *JAMA Ophthalmol*. Published online October 28, 2021. doi:10.1001/jamaophthalmol.2021.4375

3.2. High dose vitamin A improves retinal function in *RBP4*-related fundus albipunctatus

Inborn metabolism errors can also be responsible for a subset of IRD. Some of them are caused by dysfunction of cellular organelles: peroxysomopathies (e.g. Refsum disease[165,166]), lysosomopathies (e.g. mucopolysaccharidoses[153]) and mitochondrial cytopathies (e.g. Kearns-Sayre syndrome[167]) and can also include a retinal dystrophy in their clinical spectrum. Nucleic acid, protein, lipid and small molecules (e.g. vitamins) transport and metabolism errors lead in some cases to IRD as well. Ocular involvement (IRD and developmental abnormalities) are usually a part of vitamin A metabolism abnormalities. Indeed, the retinol is the major component of the visual cycle[168] and also an ocular development regulator[169].

Patient CIC08621 in our cohort presenting an unusual retinal phenotype with early onset night blindness and fine white dots on fundus examination was found to harbor a novel homozygous pathogenic variant in *RBP4*: c.255G>A, p.(Trp85*), resulting in the absence of the major blood carrier of vitamin A. This patient was treated with high-dose retinol palmitate and his visual function improved.

This work was published in the International Journal of Molecular Sciences[170] and also presented at the International Society for Genetic Eye Diseases and Retinoblastoma (ISGEDR) in 2021.



Case Report

Large Benefit from Simple Things: High-Dose Vitamin A Improves *RBP4*-Related Retinal Dystrophy

Vasily M. Smirnov ^{1,2,3} , Baptiste Wilmet ¹, Marco Nassisi ¹, Christel Condroyer ¹, Aline Antonio ¹, Camille Andrieu ⁴, Céline Devisme ⁴, Serge Sancho ⁴, José-Alain Sahel ^{1,4,5}, Christina Zeitz ^{1,*} and Isabelle Audo ^{1,4,*}

- ¹ Sorbonne Université, INSERM, CNRS, Institut de la Vision, F-75012 Paris, France; vasily.smirnov@inserm.fr (V.M.S.); baptiste.wilmet@inserm.fr (B.W.); marco.nassisi@inserm.fr (M.N.); christel.condroyer@inserm.fr (C.C.); aline.antonio@inserm.fr (A.A.); j.sahel@gmail.com (J.-A.S.)
- ² Faculté de Médecine, Université de Lille, F-59000 Lille, France
- ³ Exploration de la Vision et Neuro-Ophthalmologie, CHU de Lille, F-59000 Lille, France
- ⁴ Centre Hospitalier National d’Ophthalmologie des Quinze-Vingts, National Rare Disease Center REFERET and INSERM-DGOS CIC 1423, F-75012 Paris, France; candrieu@15-20.fr (C.A.); cdevisme@15-20.fr (C.D.); ssancho@15-20.fr (S.S.)
- ⁵ Department of Ophthalmology, University of Pittsburgh School of Medicine, Pittsburg, PA 15213, USA
- * Correspondence: christina.zeitz@inserm.fr (C.Z.); isabelle.audo@inserm.fr (I.A.); Tel.: +33-1-53-462-540 (C.Z.); +33-1-53-462-542 (I.A.)



Citation: Smirnov, V.M.; Wilmet, B.; Nassisi, M.; Condroyer, C.; Antonio, A.; Andrieu, C.; Devisme, C.; Sancho, S.; Sahel, J.-A.; Zeitz, C.; et al. Large Benefit from Simple Things: High-Dose Vitamin A Improves *RBP4*-Related Retinal Dystrophy. *Int. J. Mol. Sci.* **2022**, *23*, 6590. <https://doi.org/10.3390/ijms23126590>

Academic Editor: Jan Wijnholds

Received: 22 April 2022

Accepted: 7 June 2022

Published: 13 June 2022

Publisher’s Note: MDPI stays neutral with regard to jurisdictional claims in published maps and institutional affiliations.



Copyright: © 2022 by the authors. Licensee MDPI, Basel, Switzerland. This article is an open access article distributed under the terms and conditions of the Creative Commons Attribution (CC BY) license (<https://creativecommons.org/licenses/by/4.0/>).

Abstract: Inherited retinal diseases (IRD) are a group of heterogeneous disorders, most of which lead to blindness with limited therapeutic options. Pathogenic variants in *RBP4*, coding for a major blood carrier of retinol, retinol-binding protein 4, are responsible for a peculiar form of IRD. The aim of this study was to investigate if retinal function of an *RBP4*-related IRD patient can be improved by retinol administration. Our patient presented a peculiar white-dot retinopathy, reminiscent of vitamin A deficient retinopathy. Using a customized next generation sequencing (NGS) IRD panel we discovered a novel loss-of-function homozygous pathogenic variant in *RBP4*: c.255G >A, p.(Trp85*). Western blotting revealed the absence of RBP4 protein in the patient’s serum. Blood retinol levels were undetectable. The patient was put on a high-dose oral retinol regimen (50,000 UI twice a week). Subjective symptoms and retinal function markedly and sustainably improved at 5-months and 1-year follow-up. Here we show that this novel IRD case can be treated by oral retinol administration.

Keywords: inherited retinal degeneration; fundus albipunctatus; retinol-binding protein; RBP4; retinol treatment

1. Introduction

Inherited retinal diseases are a heterogeneous group of disorders, the most common of which—retinitis pigmentosa—progresses towards blindness with limited therapeutic options. Some rare forms of IRD, linked with inborn defects of small molecule metabolism can benefit from metabolic and/or dietary treatment [1,2]. For instance, vitamin A and E intake improves vision in patients with abetalipoproteinemia (OMIM# 200100), a hereditary defect of fat-soluble vitamin absorption and transport [3]. Dietary arginine restriction and vitamin B6 intake can reduce blood ornithine level and slow retinal degeneration in patients with gyrate atrophy (OMIM#258870) [4,5]. Low phytanic acid diet may slow retinal degeneration progression rates in adult Refsum disease (OMIM#266500) [6,7].

Retinol-binding protein 4 (RBP4, Uniprot#Q5VY30) is a major blood transporter of retinol from hepatocyte to target organs. Pathogenic variants in *RBP4* are associated with both ocular developmental abnormalities and retinal degeneration (OMIM#615147). Ocular developmental abnormalities range from a mild iris coloboma to micro- and anophthalmia. Retinal degeneration consists of a rod–cone dystrophy, also known as retinitis pigmentosa.

We report here that high-dose vitamin A is able to improve visual function in a new case of *RBP4*-associated retinopathy.

2. Results

2.1. Detailed Case Description

A male patient of Algerian ancestry was initially assessed at age 12 years. He had decreased visual acuity and progressive night blindness since early childhood. Best corrected visual acuity was 20/32 for both eyes with spectacle correction $-0.50(-1.0)5^\circ$ in the right eye (RE) and $-0.75(-0.25)170^\circ$ in the left eye (LE).

Goldman kinetic visual field tested on V4e, V1e, and V1e targets was normal while the III1e and smaller targets were not perceived by the patient (Figure S1 in Supplementary Data). Automated static perimetry showed a pericentral ring scotoma. Dark-adapted responses (DA0.01) of ISCEV standard full-field electroretinogram (ffERG) were undetectable while DA3.0 and DA10.0 revealed severely reduced and delayed responses; light-adapted responses (LA3.0 and LA3.0 flicker) were severely reduced with implicit time shift in keeping with generalized rod-cone dysfunction (Figure S2 in Supplementary Data). Full Stimulus Threshold (FST) revealed severely reduced threshold for the white stimulus (Figure S3 in Supplementary Data). Fundus examination revealed numerous white dots scattered over the mid and far periphery with no pigmentary or atrophic retinal changes (Figure 1A and Figure S4 in Supplementary Data). On infrared reflectance (IRR) imaging, both maculae were granular (Figure 1B). Increased image averaging on short-wave fundus autofluorescence (SWAF) revealed an ellipsoid-shaped ring of increased autofluorescence around the fovea on an overall hypoautofluorescent background (Figure 1C). Near-infrared fundus autofluorescence (NIRAF) imaging also showed a reduced signal (Figure 1D). Spectral domain optical coherence tomography (SD-OCT) centered on the fovea revealed an hyporeflective irregular ellipsoid zone (EZ) (Figure 1E). The outer nuclear layer (ONL) thickness was preserved with an unusual hyper reflective band on both sides of the fovea (Figure 1F, yellow arrows). SD-OCT performed through the peripheral white dots revealed hyperreflective dots above the retinal pigment epithelium (RPE), interrupting the EZ (Figure 1G, white arrows).

A general examination was performed to detect any vitamin A deficiency-related alterations. The only skin issue was subtle acne vulgaris on the forehead. Past medical history was unremarkable and the patient declined any dietary restrictions.

2.2. Genetic and Functional Studies

The family consisted of unaffected first-degree-cousin parents of Algerian descent and two unaffected sisters (Figure 2A). Targeted NGS identified a novel homozygous nonsense variant c.255G >A, p.(Trp85*) in *RBP4* which co-segregated with disease in this family. This variant was classified as pathogenic 1a (PVS1, PP1-S, PM2) in accordance with ACMG standards [8]. Western blot analysis revealed the absence of the RBP4 protein band in the serum of the patient (Figure 2B). Blood retinol level was also undetectable.

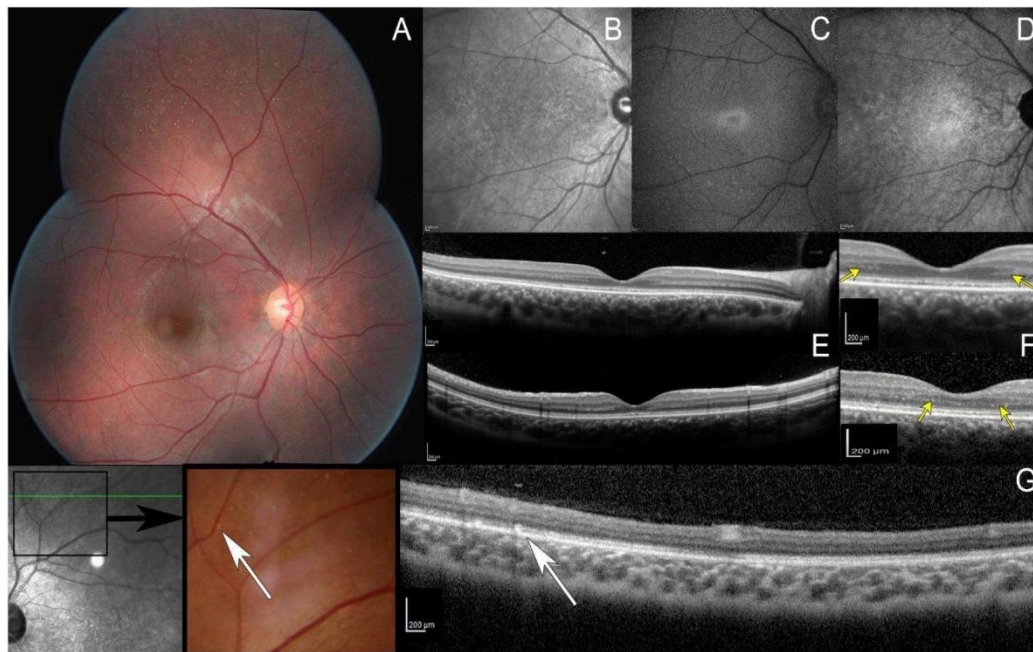


Figure 1. Multimodal retinal imaging. (A) Fundus photo, multiple white dots scattered over the midperipheral retina. Note the absence of intraretinal pigment migration and the lack of retinal vessel attenuation. (B) Infrared reflectance image, macular granularity. (C) Short-wavelength fundus autofluorescence imaging obtained with significant averaging due to the generalized reduced autofluorescence, small peri-foveal hyperautofluorescent ring with indistinct borders. (D) Near infrared fundus autofluorescence, small hypoautofluorescent dots. (E,F) spectral domain optic coherence tomography (SD-OCT, top: horizontal scan; and bottom: vertical scan), hypo reflective and fragmented ellipsoid zone with no interdigitation zone; preserved outer nuclear layer thickness with an unusual hyper reflective band on both sides of the fovea (yellow arrows). (G) OCT (scan passing through white dots, white arrows), hyperreflective dots above the retinal pigment epithelium with a focal interruption of the ellipsoid zone.

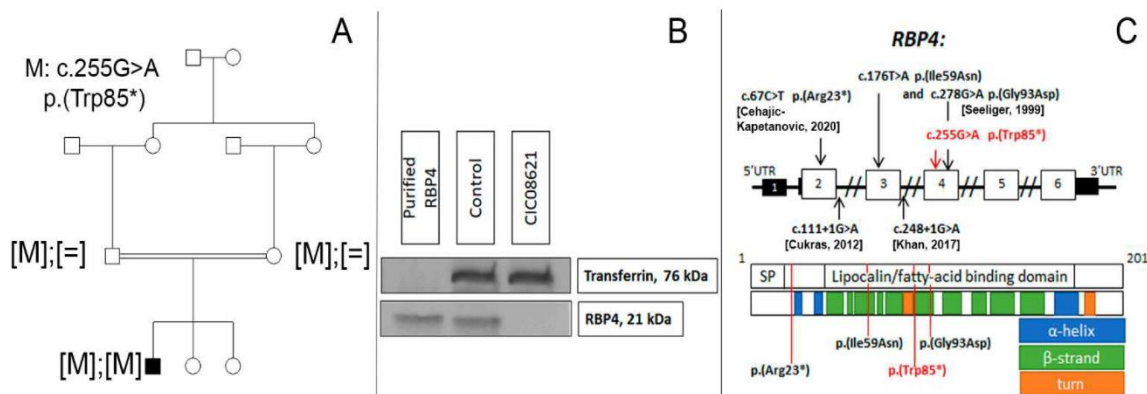


Figure 2. (A) Novel biallelic *RBP4* variant co-segregating with the disease. (B) Western blot analysis showing the absence of *RBP4* in peripheral blood of our patient (CIC08621) carrying the homozygous nonsense variant in *RBP4*, compared to an unaffected control and recombinant *RBP4*. Transferrin is used as serum loading control. (C) *RBP4* gene and protein structure. SP—signal peptide domain. Disulfide bonds (22-178, 88-192, 138-147) are not shown. Previously reported and novel (in red) variants linked with inherited retinal degeneration [9,10].

2.3. Treatment and Follow-Up

After discussion with the patient and his parents and their informed consent, high-dose oral vitamin A was initiated with retinol palmitate, 50,000 UI twice a week. Liver function was monitored. Five months after initiation of the treatment, the patient reported a significant subjective night vision improvement and a better tolerance of light-to-dark transitions. There was an improvement in FST at this time point (+25% in RE and 40% in LE, respectively) sustained at 1-year follow-up (Figure 3 and Figure S3 in Supplementary Data), while visual acuity, ERG, and retinal imaging (more specifically, white dots, ONL and EZ aspects) remained unchanged. We also observed a marked visual field improvement: III1e and III1e targets became perceived by the patient (Figure S1 in Supplementary Data). There were no signs of general retinol toxicity and liver function remained normal.

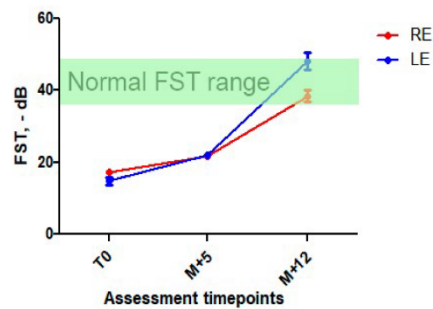


Figure 3. Full stimulus threshold before and after high-dose vitamin A intake. Mean FST \pm SD at first assessment, at M + 5 and M + 12 follow-up. A significant improvement in FST was observed at M + 5 (25 and 40% decrease) and was sustained at M + 12 (123 et 215% in RE and LE, respectively). In green, normal FST range [11,12].

3. Discussion

The visual system is highly dependent upon retinol supply. Retinoids are essential for normal ocular development as a whole and for the maintenance of a normal tissue structure. Abnormalities in nutritional supply, storage, transport, delivery, or metabolism of retinoids are linked with a broad spectrum of developmental and degenerative diseases of the eye [13].

RBP4 is the major plasma carrier of retinol and retinoids. It forms a heterohexameric complex with transthyretin in the blood, a characteristic which protects small molecules of RBP4 (21k Da) from glomerular filtration [14]. There are two different pathways for retinoids to reach their target tissues. The main pathway depends upon RBP4, which is complexed to retinol (holo-RBP4) and then recognized and bond to a membrane retinoid receptor STRA6, located at the basal side of the RPE. STRA6 allows the internalization of retinol [15]. The minor pathway is under the control of the scavenger class B type I receptor (Sr-BI) which enables the absorption of the protein-free fraction of retinoids transported within circulating lipoprotein complexes and chylomicrons. In the absence of RBP4, this second low-rate route could be sufficient to provide retinoids to all other tissues except for the RPE, leading to a retinal disease [16–18].

Pathogenic variants in *RBP4* are responsible for rod–cone dystrophy associated with various degrees of microphthalmia, coloboma, and comedogenic acne. Only few patients harboring *RBP4* defects have been reported to date [9,10,19,20] (Figure 2C). Our patient presents a mild phenotype unlike patients harboring *RBP4* gene defects reported previously which could be explained in part by his young age (12 years) compared to the late adult cases with advanced retinal degeneration reported in the literature. The observed white dot retinopathy in our patient could be an early feature of progressive inherited retinal degeneration.

In contrast, our patient had a very unusual phenotype for *RBP4* deficiency. His ocular findings were reminiscent of fundus albipunctatus (FA, OMIM#136880) due to

the presence of night blindness, numerous peripheral white dots, and no signs of retinal degeneration. FA clinical phenotype is typically associated with pathogenic variants in *RDH5* (OMIM#601617). However, retinal white dots in our patient were less numerous and clearly not organized in a network pattern as in *RDH5*-retinopathy. The ERG was also different showing a generalized severe rod–cone dysfunction distinct from the Riggs-type ERG [21] classically associated with *RDH5*-retinopathy including normal cone function and cone-dominated dark-adapted responses. Retinol-dehydrogenase 5 is a visual cycle enzyme oxidizing 11-cis-retinol into 11-cis-retinal. The lack of enzyme activity leads to 11-cis and 13-cis retinyl esters accumulation which are thought to be the origin of the white dots in FA [22,23].

Another retinal disease very close to our patient's presentation is retinitis punctata albescens (RPA, OMIM#136880 or Bothnia dystrophy, OMIM#607475). White dots are usually present in the early stages of the disease and are due to an accumulation of all-trans-retinyl esters in the retinal pigment epithelium secondary to an impairment of the cellular retinaldehyde-binding protein 1 (CRABP1, Uniprot#P29762), slowing down the isomerization of all-trans-retinyl esters in 11-cis-retinol. Pathogenic variants in *RLBP1*, encoding CRABP1, are responsible for this phenotype. As its name implies, RPA is a progressive retinal degeneration. Unlike in our patient, RPA is characterized by moderate narrowing of the retinal vasculature, optic disc pallor, pigmentary changes, and peripheral scalloped areas of chorioretinal atrophy [24,25]. ERG responses in RPA are, however, closer to those of our patient, with severely affected rod responses and more preserved cone responses. A limited recovery of ERG responses after prolonged dark adaptation is also reported in RPA [26] as in *RDH5*-retinopathy. This was unfortunately not tested in our patient. White dots have also been described in *RHO* (OMIM#180380) [27], *PRPH2* (OMIM#179605) [28], *LRAT* (OMIM#604863) [29,30], and *RPE65* (OMIM#180069) [31,32] gene defects, but the phenotype in these cases is more severe and progressive; thus, delineating it from our patient's clinical picture.

Functional and morphological retinal changes in our patient were close to those reported in vitamin A deficient retinopathy (VAD). Functionally, generalized photoreceptor dysfunction with rod responses being more altered than cone responses is also characteristic for VAD [33,34]. White retinal dots can be a feature in VAD [33,34], but they are somewhat different in shape (indistinct borders) and hypoautofluorescent on SWAF [35]. Our case also presented intriguing finding with an additional hyperreflective band in the parafoveal region on OCT (Figure 2F). We hypothesize that this alteration could be a partial duplication of the outer plexiform layer and may be related to the important role of retinoids in retinal development [36].

Another inherited form of retinal degeneration linked with an altered absorption and biodistribution of vitamin A is abetalipoproteinemia (or Bassen–Kornzweig syndrome). Biallelic gene defects in *MTTP* (OMIM#157147), encoding Mitochondrial Triglyceride Transfer Protein (Uniprot#P55157) lead to impaired assembly and secretion of plasma lipoproteins that contain apolipoprotein B (very low- and low-density lipoproteins and chylomicrons). Lipoproteins facilitate absorption and carry a free fraction of fat-soluble vitamins (A, D, E, K). Upon reduced MTTP activity, there is a reduced retinol and tocopherol absorption, transport, and delivery to the target organs, including the eye, which results in retinal degeneration. Early treatment with high-dose vitamins A and E in patients with abetalipoproteinemia resulted in improvement in their retinal function and a slower retinal degeneration progression rate [3,37,38].

Oral administration of high-dose retinol palmitate has already shown to raise the level of free plasma retinol and retinyl esters in RBP4-deficient patients [39] but no visual outcome had been reported so far. Nevertheless, experimental studies report that *RBP4*^{-/-} mice are able to use alternative RBP-independent pathways for retinol supply to the retina with phenotypic rescue provided by a retinol-sufficient diet [17]. In order to compensate for the lack of RBP4-related retinol transport and attempt to enhance the free fraction of retinoids delivered via the slow RBP4-independent pathway, we decided to prescribe high

doses of retinol to our patient. After five months of high-dose oral vitamin A, the patient reported subjective improvement in dimly lighted environments which was supported by FST and kinetic perimetry changes from baseline. This effect further improved after one year follow-up.

Adverse and toxic effects of long-term high retinol intake are numerous including bone toxicity (hypercalcemia and osteoporosis), neurotoxicity (intracranial hypertension), and liver toxicity (liver enlargement, cirrhosis) [40]. Saturation of the RBP4-independent pathway of retinol delivery could also be detrimental for xanthophyll pigment uptake by the retina, as this slow pathway is competitive between retinol and lutein/zeaxanthin transport [41]. However, toxicity did not occur in patients with abetalipoproteinemia on prolonged high-dose retinol treatment, as the overall blood levels remained low [3]. Our patient did not experience any adverse effect after 1 year of retinol intake. Liver enzymes and blood calcium were normal. Long-term follow-up with close monitoring for vitamin A tolerability will determine whether high doses of retinol are able to prevent retinal degeneration.

4. Materials and Methods

4.1. Clinical Studies

The patient was clinically investigated at the national reference center for rare ocular diseases REFERET of the Centre Hospitalier National d'Ophtalmologie des Quinze-Vingts as previously described [42]. Briefly, best-corrected visual acuity (BCVA), refractive error, slit-lamp biomicroscopy, static and kinetic visual fields, full-field electroretinogram according to the standards of International Society for Clinical Electrophysiology of Vision [43] (Espion, Diagnosys LLC, Lowell, MA), fundus photography, spectral domain optical coherence tomography (Spectralis OCT, Heidelberg Engineering, Inc., Heidelberg, Germany), infrared and short-wavelength autofluorescence (Heidelberg Retinal Tomograph, Heidelberg Engineering, Inc.) were performed. Full stimulus threshold was assessed using achromatic full-field stimuli (Diagnosys Espion system, Diagnosys LLC, Lowell, MA, USA) as previously described [11,12].

4.2. Genetic Analysis

Blood samples from the index case and from his parents were collected for genetic research and genomic DNA was extracted as previously reported [44]. These DNA samples were stored and obtained from the NeuroSensCol DNA bank, for research in neuroscience (PI: JA Sahel, co-PI I Audo, partner with CHNO des Quinze-Vingts, Inserm and CNRS, certified NFS96-900). Targeted next generation sequencing (NGS) was performed in collaboration with an external company (IntegraGen, Evry, France) [45]. The *RBP4* (MIM#180250) variant selected after NGS was validated in the index case and relatives by Sanger sequencing (refseq: NM_001323517.1, primer sequences and conditions available on demand).

4.3. Western Blot

Western blot identification of RBP4 was performed as described in a previously published protocol [46]. Loading control was performed using anti-transferrin monoclonal antibody (Abcam, Discovery Drive, Cambridge Biomedical Campus, Cambridge, UK, ab109503).

5. Conclusions

We report here the first case of *RBP4*-related retinopathy manifesting as a white-dot retinopathy whose visual function improved after high-dose oral vitamin A intake. Such treatment should be considered in early stages of *RBP4*-related retinopathy. Future research will determine whether high level of vitamin A intake is able to reverse the phenotype sustainably.

Supplementary Materials: The following supporting information can be downloaded at: <https://www.mdpi.com/article/10.3390/ijms23126590/s1>.

Author Contributions: Conceptualization, C.Z., J.-A.S. and I.A.; methodology, B.W., M.N., C.C., A.A., C.A., C.D. and S.S.; validation, C.Z., J.-A.S., I.A., B.W., M.N., C.C., A.A., C.A., C.D. and S.S.; formal analysis, V.M.S., C.Z., J.-A.S., I.A., B.W., M.N., C.C., A.A., C.A., C.D. and S.S.; investigation, V.M.S., C.Z., I.A., B.W., M.N., C.C., A.A., C.A., C.D. and S.S.; resources, C.Z., J.-A.S. and I.A.; data curation, V.M.S., C.Z., J.-A.S., I.A., B.W., M.N., C.C., A.A., C.A., C.D. and S.S.; writing—original draft preparation, V.M.S.; writing—review and editing, V.M.S., C.Z. and I.A.; supervision, C.Z. and I.A.; funding acquisition, C.Z., J.-A.S. and I.A. All authors have read and agreed to the published version of the manuscript.

Funding: LABEX LIFESENSES [reference ANR-10-LABX-65] supported by French state funds managed by the Agence Nationale de la Recherche within the Investissements d’Avenir program [ANR-11-IDEX-0004-0]; IHU FOReSIGHT [ANR-18-IAHU-0001] supported by French state funds managed by the Agence Nationale de la Recherche within the Investissements d’Avenir program; funding from RHU-Light4deaf [ANR-15-RHU-0001]; Foundation Fighting Blindness center grant [C-CMM-0907-0428-INSERM04], BR-GE-0619-0761-INSERM and fellowship award (MN) [CD-CL-0619-0759-INSERM]. Retina France, U UNADEV (Union Nationale des Aveugles et Déficients Visuels) in partnership with ITMO NNP/AVIESAN (alliance nationale pour les sciences de la vie et de la santé) for research on visual disorders.

Institutional Review Board Statement: Research procedures adhered to the tenets of the Declaration of Helsinki and were approved by the local Ethics Committee (CPP, Ile de France V, Project number 06693, N°EUDRACT 2006-A00347-44, 11 December 2006).

Informed Consent Statement: Prior to testing, written informed consent was obtained from the parents and participant who was under 18. No compensation or incentive was offered to the subject to participate in the study.

Data Availability Statement: All data are contained within the article or Supplementary Materials.

Acknowledgments: The authors thank the family in the study and the clinical staff of National Rare Disease Center REFERET and INSERM-DGOS CIC 1423 for collecting phenotypic data. We are thankful to Robert Duvoisin for his English revisions.

Conflicts of Interest: The authors declare no conflict of interest.

References

- Grant, C.A.; Berson, E.L. Treatable Forms of Retinitis Pigmentosa Associated with Systemic Neurological Disorders. *Int Ophthalmol. Clin.* **2001**, *41*, 103–110. [[CrossRef](#)]
- Weleber, R.G.; Kurz, D.E.; Trzuppek, K.M. Treatment of Retinal and Choroidal Degenerations and Dystrophies: Current Status and Prospects for Gene-Based Therapy. *Ophthalmol. Clin. N. Am.* **2003**, *16*, 583–593. [[CrossRef](#)]
- Chowers, I.; Banin, E.; Merin, S.; Cooper, M.; Granot, E. Long-Term Assessment of Combined Vitamin A and E Treatment for the Prevention of Retinal Degeneration in Abetalipoproteinaemia and Hypobetalipoproteinaemia Patients. *Eye* **2001**, *15*, 525–530. [[CrossRef](#)] [[PubMed](#)]
- Balfoort, B.M.; Buijs, M.J.N.; Ten Asbroek, A.L.M.A.; Bergen, A.A.B.; Boon, C.J.F.; Ferreira, E.A.; Houtkoper, R.H.; Wagenmakers, M.A.E.M.; Wanders, R.J.A.; Waterham, H.R.; et al. A Review of Treatment Modalities in Gyrate Atrophy of the Choroid and Retina (GACR). *Mol. Genet. Metab.* **2021**, *134*, 96–116. [[CrossRef](#)] [[PubMed](#)]
- Casalino, G.; Pierro, L.; Manitto, M.P.; Michaelides, M.; Banello, F. Resolution of Cystoid Macular Edema Following Arginine-Restricted Diet and Vitamin B6 Supplementation in a Case of Gyrate Atrophy. *J. AAPOS* **2018**, *22*, 321–323. [[CrossRef](#)] [[PubMed](#)]
- Rüether, K.; Baldwin, E.; Casteels, M.; Feher, M.D.; Horn, M.; Kuranoff, S.; Leroy, B.P.; Wanders, R.J.; Wierzbicki, A.S. Adult Refsum Disease: A Form of Tapetoretinal Dystrophy Accessible to Therapy. *Surv. Ophthalmol.* **2010**, *55*, 531–538. [[CrossRef](#)]
- Benson, M.D.; MacDonald, I.M.; Sheehan, M.; Jain, S. Improved Electroretinographic Responses Following Dietary Intervention in a Patient with Refsum Disease. *JIMD Rep.* **2020**, *55*, 32–37. [[CrossRef](#)]
- Richards, S.; Aziz, N.; Bale, S.; Bick, D.; Das, S.; Gastier-Foster, J.; Grody, W.W.; Hegde, M.; Lyon, E.; Spector, E.; et al. Standards and Guidelines for the Interpretation of Sequence Variants: A Joint Consensus Recommendation of the American College of Medical Genetics and Genomics and the Association for Molecular Pathology. *Genet. Med.* **2015**, *17*, 405–424. [[CrossRef](#)]
- Seeliger, M.W.; Biesalski, H.K.; Wissinger, B.; Gollnick, H.; Gielen, S.; Frank, J.; Beck, S.; Zrenner, E. Phenotype in Retinol Deficiency Due to a Hereditary Defect in Retinol Binding Protein Synthesis. *Investig. Ophthalmol. Vis. Sci.* **1999**, *40*, 3–11.

10. Cehajic-Kapetanovic, J.; Jasani, K.M.; Shanks, M.; Clouston, P.; MacLaren, R.E. A Novel Homozygous c.67C>T Variant in Retinol Binding Protein 4 (RBP4) Associated with Retinitis Pigmentosa and Childhood Acne Vulgaris. *Ophthalmic. Genet.* **2020**, *41*, 288–292. [[CrossRef](#)]
11. Roman, A.J.; Cideciyan, A.V.; Aleman, T.S.; Jacobson, S.G. Full-Field Stimulus Testing (FST) to Quantify Visual Perception in Severely Blind Candidates for Treatment Trials. *Physiol. Meas.* **2007**, *28*, N51–N56. [[CrossRef](#)] [[PubMed](#)]
12. Klein, M.; Birch, D.G. Psychophysical Assessment of Low Visual Function in Patients with Retinal Degenerative Diseases (RDDs) with the Diagnosys Full-Field Stimulus Threshold (D-FST). *Doc. Ophthalmol.* **2009**, *119*, 217–224. [[CrossRef](#)] [[PubMed](#)]
13. Kiser, P.D.; Palczewski, K. Retinoids and Retinal Diseases. *Annu. Rev. Vis. Sci.* **2016**, *2*, 197–234. [[CrossRef](#)]
14. Monaco, H.L.; Rizzi, M.; Coda, A. Structure of a Complex of Two Plasma Proteins: Transthyretin and Retinol-Binding Protein. *Science* **1995**, *268*, 1039–1041. [[CrossRef](#)]
15. Kawaguchi, R.; Yu, J.; Honda, J.; Hu, J.; Whitelegge, J.; Ping, P.; Wiita, P.; Bok, D.; Sun, H. A Membrane Receptor for Retinol Binding Protein Mediates Cellular Uptake of Vitamin A. *Science* **2007**, *315*, 820–825. [[CrossRef](#)] [[PubMed](#)]
16. Quadro, L.; Hamberger, L.; Colantuoni, V.; Gottesman, M.E.; Blaner, W.S. Understanding the Physiological Role of Retinol-Binding Protein in Vitamin A Metabolism Using Transgenic and Knockout Mouse Models. *Mol. Asp. Med.* **2003**, *24*, 421–430. [[CrossRef](#)]
17. Quadro, L. Impaired Retinal Function and Vitamin A Availability in Mice Lacking Retinol-Binding Protein. *EMBO J.* **1999**, *18*, 4633–4644. [[CrossRef](#)] [[PubMed](#)]
18. Du, M.; Phelps, E.; Balangue, M.J.; Dockins, A.; Moiseyev, G.; Shin, Y.; Kane, S.; Otorola, L.; Ma, J.-X.; Farjo, R.; et al. Transgenic Mice Over-Expressing RBP4 Have RBP4-Dependent and Light-Independent Retinal Degeneration. *Investig. Ophthalmol. Vis. Sci.* **2017**, *58*, 4375–4383. [[CrossRef](#)] [[PubMed](#)]
19. Cukras, C.; Gaasterland, T.; Lee, P.; Gudiseva, H.V.; Chavali, V.R.M.; Pullakhandam, R.; Maranhao, B.; Edsall, L.; Soares, S.; Reddy, G.B.; et al. Exome Analysis Identified a Novel Mutation in the RBP4 Gene in a Consanguineous Pedigree with Retinal Dystrophy and Developmental Abnormalities. *PLoS ONE* **2012**, *7*, e50205. [[CrossRef](#)]
20. Khan, K.N.; Carss, K.; Raymond, F.L.; Islam, F.; Nihir BioResource-Rare Diseases Consortium, null; Moore, A.T.; Michaelides, M.; Arno, G. Vitamin A Deficiency Due to Bi-Allelic Mutation of RBP4: There's More to It than Meets the Eye. *Ophthalmic. Genet.* **2017**, *38*, 465–466. [[CrossRef](#)]
21. Riggs, L.A. Electroretinography in Cases of Night Blindness. *Am. J. Ophthalmol.* **1954**, *38*, 70–78. [[CrossRef](#)]
22. Driessen, C.A.; Winkens, H.J.; Hoffmann, K.; Kuhlmann, L.D.; Janssen, B.P.; Van Vugt, A.H.; Van Hooser, J.P.; Wieringa, B.E.; Deutman, A.F.; Palczewski, K.; et al. Disruption of the 11-Cis-Retinol Dehydrogenase Gene Leads to Accumulation of Cis-Retinals and Cis-Retinyl Esters. *Mol. Cell. Biol.* **2000**, *20*, 4275–4287. [[CrossRef](#)]
23. Jang, G.F.; Van Hooser, J.P.; Kuksa, V.; McBee, J.K.; He, Y.G.; Janssen, J.J.; Driessen, C.A.; Palczewski, K. Characterization of a Dehydrogenase Activity Responsible for Oxidation of 11-Cis-Retinol in the Retinal Pigment Epithelium of Mice with a Disrupted RDH5 Gene. A Model for the Human Hereditary Disease Fundus Albipunctatus. *J. Biol. Chem.* **2001**, *276*, 32456–32465. [[CrossRef](#)] [[PubMed](#)]
24. Burstedt, M.; Jonsson, F.; Köhn, L.; Burstedt, M.; Kivitalo, M.; Golovleva, I. Genotype-Phenotype Correlations in Bothnia Dystrophy Caused by *RLBP1* Gene Sequence Variations. *Acta Ophthalmol.* **2013**, *91*, 437–444. [[CrossRef](#)] [[PubMed](#)]
25. Dessalces, E.; Bocquet, B.; Bourien, J.; Zanlonghi, X.; Verdet, R.; Meunier, I.; Hamel, C.P. Early-Onset Foveal Involvement in Retinitis Punctata Albescens With Mutations in *RLBP1*. *JAMA Ophthalmol.* **2013**, *131*, 1314. [[CrossRef](#)]
26. Burstedt, M.S.I.; Sandgren, O.; Golovleva, I.; Wachtmeister, L. Effects of Prolonged Dark Adaptation in Patients with Retinitis Pigmentosa of Bothnia Type: An Electrophysiological Study. *Doc. Ophthalmol.* **2008**, *116*, 193–205. [[CrossRef](#)]
27. Souied, E.; Soubrane, G.; Benlian, P.; Coscas, G.J.; Gerber, S.; Munnich, A.; Kaplan, J. Retinitis Punctata Albescens Associated With the Arg135Trp Mutation in the Rhodopsin Gene. *Am. J. Ophthalmol.* **1996**, *121*, 19–25. [[CrossRef](#)]
28. Kajiwar, K.; Sandberg, M.A.; Berson, E.L.; Dryja, T.P. A Null Mutation in the Human Peripherin/RDS Gene in a Family with Autosomal Dominant Retinitis Punctata Albescens. *Nat. Genet.* **1993**, *3*, 208–212. [[CrossRef](#)]
29. Littink, K.W.; van Genderen, M.M.; van Schooneveld, M.J.; Visser, L.; Riemsdag, F.C.C.; Keunen, J.E.E.; Bakker, B.; Zonneveld, M.N.; den Hollander, A.I.; Cremers, F.P.M.; et al. A Homozygous Frameshift Mutation in *LRAT* Causes Retinitis Punctata Albescens. *Ophthalmology* **2012**, *119*, 1899–1906. [[CrossRef](#)]
30. Talib, M.; van Schooneveld, M.J.; van Duuren, R.J.G.; Van Cauwenbergh, C.; Ten Brink, J.B.; De Baere, E.; Florijn, R.J.; Schallij-Delfos, N.E.; Leroy, B.P.; Bergen, A.A.; et al. Long-Term Follow-Up of Retinal Degenerations Associated With *LRAT* Mutations and Their Comparability to Phenotypes Associated With *RPE65* Mutations. *Transl. Vis. Sci. Technol.* **2019**, *8*, 24. [[CrossRef](#)]
31. Schatz, P.; Preising, M.; Lorenz, B.; Sander, B.; Larsen, M.; Rosenberg, T. Fundus Albipunctatus Associated with Compound Heterozygous Mutations in *RPE65*. *Ophthalmology* **2011**, *118*, 888–894. [[CrossRef](#)]
32. Ramtohul, P.; Denis, D. *RPE65*-Mutation Associated Fundus Albipunctatus with Cone Dystrophy. *Ophthalmol. Retina* **2019**, *3*, 535. [[CrossRef](#)]
33. Apushkin, M.A.; Fishman, G.A. Improvement in Visual Function and Fundus Findings for a Patient with Vitamin A-Deficient Retinopathy. *Retina* **2005**, *25*, 650–652. [[CrossRef](#)] [[PubMed](#)]
34. Genead, M.A.; Fishman, G.A.; Lindeman, M. Fundus White Spots and Acquired Night Blindness Due to Vitamin A Deficiency. *Doc. Ophthalmol.* **2009**, *119*, 229–233. [[CrossRef](#)] [[PubMed](#)]
35. Aleman, T.S.; Garrity, S.T.; Brucker, A.J. Retinal Structure in Vitamin A Deficiency as Explored with Multimodal Imaging. *Doc. Ophthalmol.* **2013**, *127*, 239–243. [[CrossRef](#)]

36. Cvekl, A.; Wang, W.-L. Retinoic Acid Signaling in Mammalian Eye Development. *Exp. Eye Res.* **2009**, *89*, 280–291. [[CrossRef](#)]
37. MacGilchrist, A.J.; Mills, P.R.; Noble, M.; Foulds, W.S.; Simpson, J.A.; Watkinson, G. Abetalipoproteinaemia in Adults: Role of Vitamin Therapy. *J. Inherit. Metab. Dis.* **1988**, *11*, 184–190. [[CrossRef](#)]
38. Bishara, S.; Merin, S.; Cooper, M.; Azizi, E.; Delpre, G.; Deckelbaum, R.J. Combined Vitamin A and E Therapy Prevents Retinal Electrophysiological Deterioration in Abetalipoproteinaemia. *Br. J. Ophthalmol.* **1982**, *66*, 767–770. [[CrossRef](#)] [[PubMed](#)]
39. Biesalski, H.K.; Frank, J.; Beck, S.C.; Heinrich, F.; Illek, B.; Reifen, R.; Gollnick, H.; Seeliger, M.W.; Wissinger, B.; Zrenner, E. Biochemical but Not Clinical Vitamin A Deficiency Results from Mutations in the Gene for Retinol Binding Protein. *Am. J. Clin. Nutr.* **1999**, *69*, 931–936. [[CrossRef](#)]
40. Hathcock, J.N.; Hattan, D.G.; Jenkins, M.Y.; McDonald, J.T.; Sundaresan, P.R.; Wilkening, V.L. Evaluation of Vitamin A Toxicity. *Am. J. Clin. Nutr.* **1990**, *52*, 183–202. [[CrossRef](#)]
41. During, A.; Doraiswamy, S.; Harrison, E.H. Xanthophylls Are Preferentially Taken up Compared with β -Carotene by Retinal Cells via a SRBI-Dependent Mechanism. *J. Lipid Res.* **2008**, *49*, 1715–1724. [[CrossRef](#)]
42. Audo, I. An Unusual Retinal Phenotype Associated With a Novel Mutation in RHO. *Arch. Ophthalmol.* **2010**, *128*, 1036. [[CrossRef](#)]
43. McCulloch, D.L.; Marmor, M.F.; Brigell, M.G.; Hamilton, R.; Holder, G.E.; Tzekov, R.; Bach, M. ISCEV Standard for Full-Field Clinical Electroretinography (2015 Update). *Doc. Ophthalmol.* **2015**, *130*, 1–12. [[CrossRef](#)] [[PubMed](#)]
44. Audo, I.; Lancelot, M.; Mohand-Saïd, S.; Antonio, A.; Germain, A.; Sahel, J.; Bhattacharya, S.S.; Zeitz, C. Novel *C2orf71* Mutations Account for ~1% of Cases in a Large French ArRP Cohort. *Hum. Mutat.* **2011**, *32*, E2091–E2103. [[CrossRef](#)] [[PubMed](#)]
45. Audo, I.; Bujakowska, K.M.; Léveillard, T.; Mohand-Saïd, S.; Lancelot, M.-E.; Germain, A.; Antonio, A.; Michiels, C.; Saraiva, J.-P.; Letexier, M.; et al. Development and Application of a Next-Generation-Sequencing (NGS) Approach to Detect Known and Novel Gene Defects Underlying Retinal Diseases. *Orphanet. J. Rare Dis.* **2012**, *7*, 8. [[CrossRef](#)] [[PubMed](#)]
46. Graham, T.E.; Wason, C.J.; Blüher, M.; Kahn, B.B. Shortcomings in Methodology Complicate Measurements of Serum Retinol Binding Protein (RBP4) in Insulin-Resistant Human Subjects. *Diabetologia* **2007**, *50*, 814–823. [[CrossRef](#)]

3.3. Retinal degeneration in French patients harboring variants in *CLRN1*

Biallelic variants in *CLRN1* cause Usher syndrome (RCD and neurosensorial hearing loss) type 3 (USH3, MIM#276902) and non-syndromic RP (RP61, MIM #614180). Taking into account the very low prevalence of *CLRN1*-related USH3 syndrome and non-syndromic RP in non-Finnish European populations (<2%)[171], we compiled all our cases for a detailed study of retinal degeneration phenotype.

This work was accepted for an ARVO 2020 poster presentation. Unfortunately, ARVO 2020 meeting was canceled (COVID19 pandemic); finally, it was submitted as a video-presentation. It was subsequently published in *Investigative Ophthalmology and Visual Science*[172].

Retinal Phenotype of Patients with *CLRN1*-Associated Usher 3A Syndrome in French Light4Deaf Cohort

Vasily M. Smirnov,^{1,2} Marco Nassisi,¹ Saddek Mohand-Saïd,^{1,3} Crystel Bonnet,⁴⁻⁶ Anne Auboïs,³ Céline Devisme,³ Thilissa Dib,³ Christina Zeitz,¹ Natalie Loundon,^{7,8} Sandrine Marlin,⁸ Christine Petit,^{4-6,9} Bahram Bodaghi,¹⁰ José-Alain Sahel,^{1,3,11-13} and Isabelle Audo^{1,3,14}

¹Sorbonne Université, INSERM, CNRS, Institut de la Vision, Paris, France

²Université de Lille, Faculté de Médecine, Lille, France

³CHNO des Quinze-Vingts, Centre de Référence Maladies Rares REFERET and DHU Sight Restore, INSERM-DGOS CIC1423, Paris, France

⁴Unité de Génétique et Physiologie de l'Audition, Institut Pasteur, Paris, France

⁵Unité Mixte de Recherche en Santé 1120, INSERM, Paris, France

⁶Institut de l'Audition, Paris, France

⁷Otorhinolaryngologie Pédiatrique, APHP Hôpital Necker, Paris, France

⁸Centre de référence des Surdités Génétiques, Service de Génétique, APHP Hôpital Necker, Paris, France

⁹Collège de France, Paris, France

¹⁰Hôpital Pitié-Salpêtrière, Paris, France

¹¹Fondation Ophthalmologique Adolphe de Rothschild, Paris, France

¹²Department of Ophthalmology, University of Pittsburgh Medical School, Pittsburgh, Pennsylvania, United States

¹³Académie des Sciences-Institut de France, Paris, France

¹⁴Institute of Ophthalmology, University College of London, London, United Kingdom

Correspondence: Isabelle Audo, 17, Rue Moreau, 75012 Paris, France; isabelle.audo@inserm.fr

Received: November 28, 2020

Accepted: April 7, 2022

Published: April 28, 2022

Citation: Smirnov VM, Nassisi M, Mohand-Saïd S, et al. Retinal phenotype of patients with *CLRN1*-associated Usher 3A syndrome in French Light4Deaf cohort. *Invest Ophthalmol Vis Sci.* 2022;63(4):25. <https://doi.org/10.1167/iovs.63.4.25>

PURPOSE. Biallelic variants in *CLRN1* are responsible for Usher syndrome 3A and non-syndromic rod-cone dystrophy (RCD). Retinal findings in Usher syndrome 3A have not been well defined. We report the detailed phenotypic description of RCD associated with *CLRN1* variants in a prospective cohort.

METHODS. Patients were clinically investigated at the National Reference Center for rare ocular diseases at the Quinze-Vingts Hospital, Paris, France. Best-corrected visual acuity (BCVA) tests, Goldmann perimetry, full-field electroretinography (ffERG), retinal photography, near-infrared reflectance, short-wavelength and near-infrared autofluorescence, and optical coherence tomography (OCT) were performed for all patients.

RESULTS. Four patients from four unrelated families were recruited. Mean follow-up was 11 years for three patients, and only baseline data were available for one subject. Median BCVA at baseline was 0.2 logMAR (range, 0.3–0). ffERG responses were undetectable in all subjects. The III4e isopter of the Goldmann visual field was constricted to 10°. The retinal phenotype was consistent in all patients: small whitish granular atrophic areas were organized in a network pattern around the macula and in the midperiphery. OCT showed intraretinal microcysts in all patients. Upon follow-up, all patients experienced a progressive BCVA loss and further visual field constriction. Four distinct pathogenic variants were identified in our patients: two missense (c.144T>G, p.(Asn48Lys) and c.368C>A, p.(Ala123Asp)) and two frameshift variants (c.176del, p.(Gly59Valfs*13) and c.230dup, p.(Ala78Serfs*52)).

CONCLUSIONS. RCD in Usher 3A syndrome has some distinctive features. It is a severe photoreceptor dystrophy with whitish granular posterior pole appearance and cystic maculopathy.

Keywords: Usher 3 syndrome, retinal degeneration, natural history

Usher syndrome (USH) is the leading genetic cause of deafness and blindness and is inherited as an autosomal recessive trait. Its prevalence is estimated at 3 to 6 per 100,000.¹⁻⁴ USH is a clinically heterogeneous group of disorders with three main reported clinical subtypes associ-

ated with variable severity of deafness, vestibular dysfunction, and rod-cone dystrophy (RCD), a form of retinitis pigmentosa (RP).⁵ Usher syndrome type 1 (USH1), the most severe form of USH, includes bilateral profound congenital sensorineural hearing loss (SNHL), vestibular dysfunction,

Copyright 2022 The Authors
iovs.arvojournals.org | ISSN: 1552-5783

This work is licensed under a Creative Commons Attribution-NonCommercial-NoDerivatives 4.0 International License.



and RCD. Pathogenic variants in *MYO7A* (MIM *276903), encoding myosin VIIA, an unconventional myosin linked with intracellular movement,⁶ are the most common cause of USH1 and are responsible not only for USH1B (MIM #276900) but also for non-syndromic SNHL.⁷

Usher syndrome type 2 (USH2) is characterized by RCD and variable severity (mild to severe) of congenital SNHL without vestibular dysfunction.⁸ Biallelic variants in *USH2A* (MIM #608400), encoding usherin, a protein involved in periciliary membrane complex in photoreceptors and in interstereocilia ankle in the inner ear sensory cells,⁹ are the leading cause of USH2 (underlying USH2A, MIM #276901)¹⁰ and are also responsible for non-syndromic autosomal recessive RCD (RP39, MIM #613809).^{11–13}

Usher syndrome type 3 (USH3) was defined on the basis of audiological features in the 1970 and 1980s.^{1,4,15} It is characterized by progressive postlingual SNHL and variable (none to progressive) vestibular dysfunction. Language and motor development are normal in most subjects. Onset of progressive SNHL begins in the first decade of life. About 50% of patients are profoundly deaf by their 40s.¹⁶

Pathogenic variants in two genes have been associated with USH3: *CLRN1* (MIM #606397), which encodes clarin-1, a four transmembrane-domain protein with a possible role in sensory synapses¹⁷ (involved in USH3A, MIM #276902), and *HARS1* (MIM #142810), encoding histidyl-tRNA synthetase 1, catalyzing the ligation of histidine to its cognate tRNA¹⁸ (involved in USH3B, MIM #614504). Biallelic variants in *CLRN1* have also been reported in non-syndromic RCD (RP61, MIM #614180).¹⁹ Patients with *HARS1* variants are rare, and all present syndromic manifestations including cochleo-vestibular involvement,²⁰ axonal peripheral neuropathy consistent with Charcot-Marie-Tooth 2W syndrome (MIM #616625),^{21,22} and/or ataxia.²³

USH3A associated with *CLRN1* mutations is uncommon. It represents only 2% of all patients with Usher syndromes in non-Finnish European populations,²⁴ but it causes 40% to 45% of the Usher cases in Finland.²⁵ The most common pathogenic variant in the Finnish population is c.528 T>G, p.(Tyr176*), suggesting a founder effect. USH3A is also more common (about 10% of the Usher patients) in Israeli and Palestinian populations.²⁶ A founder pathogenic variant of *CLRN1* is also reported in Ashkenazi Jews (c.144T>G, p.(Asn48Lys)).^{27,28}

There are only a few reports describing the ophthalmological features of *CLRN1*-related USH3A due to the rarity of this disorder. A large study cohort that included 90 Finnish patients demonstrated that the clinical course of *CLRN1*-related syndromic RCD due to the founder variant c.528 T>G, p.(Tyr176*) was similar to that for USH1 and USH2 individuals with non-specific retinal imaging findings.²⁵ In a series of 10 non-Finnish USH3A patients, RCD was more severe and rapidly progressive compared to patients harboring *USH2A* gene defects.²⁹ The cone mosaic assessed by adaptive optics was normal within the four central retinal degrees with spared ellipsoid zone (EZ) in three USH3A patients.³⁰ In Ashkenazi Jewish patients harboring the c.144T>G, p.(Asn48Lys) founder pathogenic *CLRN1* variant, night blindness and visual field constriction appeared early in life (early childhood to late teens) in one third of patients prior to the auditory symptoms. One third of patients were legally blind (i.e., below 1.3 logMAR) by their 50s.²⁸

The aim of our study was to report the retinal phenotype of a series of French patients with *CLRN1*-related USH3A

and to compare it with previously reported European and Israeli/Palestinian cohorts.

PATIENTS AND METHODS

Clinical Investigation

Patients with a molecular diagnosis of USH were included in a large prospective cohort study of USH syndromes (Light4Deaf, NCT04665726, www.clinicaltrials.gov). Patients were clinically investigated at the National Reference Center for Rare Retinal Diseases of Quinze-Vingts Hospital, Paris, France. Ophthalmic examination was performed as previously described.³¹ Prior to testing, written informed consent, approved by the Comité de Protection des Personnes, was obtained from each study participant or their parents. The study protocol adhered to the tenets of the Declaration of Helsinki and was approved by the local ethics committee. The study was performed in compliance with Oviedo Convention and Treaty of Lisbon.

Genetic Analysis

For most patients, a multiplex amplicon panel (Fluidigm Access Array; Fluidigm Corporate, San Francisco, CA, USA) was applied as previously described²⁴ to analyze all coding and noncoding exons of the 10 USH genes: *MYO7A*, myosin VIIA (MIM #276903); *USH1C*, harmonin (MIM #605242); *CDH23*, cadherin 23 (MIM #605516); *PCDH15*, protocadherin 15 (MIM #605514); *USH1G*, sans (MIM #607696); *CIB2*, calcium- and integrin-binding 2 (MIM #605564); *USH2A*, usherin (MIM #608400); *ADGRV1*, adhesion G protein-coupled receptor V1 (MIM #602851); *WHRN*, whirlin (MIM #607928); *CLRN1*, clarin-1 (MIM #606397); and the USH2 modifier gene *PDZD7*, PZD domain-containing 7 (MIM #612971). For some individuals, direct Sanger sequencing of coding sequences and flanking intronic regions of *CLRN1* were performed.^{27,32} Family segregation of the identified variants was performed when possible. All patients harboring biallelic pathogenic variants in *CLRN1* were subsequently included in this study.

Clinical Data Collection

Clinical data were retrospectively collected from medical records. These included sex, age at time of diagnosis and examination, personal or family history, symptoms, best-corrected visual acuity (BCVA) assessed by the Early Treatment Diabetic Retinopathy Study (ETDRS) chart, refractive errors, slit-lamp biomicroscopy, Lanthony D-15 panel, Goldmann kinetic visual fields (VFs; Haag-Streit, Koeniz, Switzerland), full-field electroretinogram (ffERG; ColorDome, Diagnosys, Cambridge, UK), spectral-domain optical coherence tomography (SD-OCT), fundus photography, and short-wavelength fundus autofluorescence (SWAF) and near-infrared fundus autofluorescence (NIRAF) imaging (SPECTRALIS HRA-OCT; Heidelberg Engineering, Heidelberg, Germany). Structural changes were evaluated using Heidelberg Eye Explorer, version 1.9.10.0 (Heidelberg Engineering). We measured the horizontal and vertical diameters of the remaining central retina on three retinal imaging modalities: first, the preserved ellipsoid zone on SD-OCT scans passing through the fovea; second, the ring of increased autofluorescence on SWAF (SWAF-RIA); and, third, the area of preserved autofluorescence on NIRAF (NIRAF-

APA). For SD-OCT, the follow-up setting for horizontal and vertical images was used to ensure consistent measurements in serial images.

Statistical Analysis

Statistical analyses were performed using SPSS Statistics 21.0 (IBM, Chicago, IL, USA), with $P \leq 0.05$ considered statistically significant.

We applied the Wilcoxon signed-rank test for BCVA, NIRAF-APA, and EZ diameters to evaluate the agreement between eyes. We then averaged the two values for further analyses. The rate of annual progression for NIRAF-APA and EZ diameters was calculated as follows: (value on first visit – value on last visit)/(years of follow-up).

RESULTS

We identified four patients (two males and two females) with *CLRN1*-related USH3A in our Usher database comprised of 289 index patients in total, leading to a prevalence of 1.4% in our USH cohort. Three families were of African ancestry: F65 (CIC00088) from Algeria, F196 (CIC03005), and F2792 (CIC05477) from Ivory Coast. F937 (CIC02644) was of Ashkenazi Jewish descent.

The clinical data at first assessment are summarized in Table 1. Night blindness was the first symptom of disease, appearing at 10 to 12 years of age in all patients. The mean age at the initial examination was 18.5 years. The mean BCVA was 0.2 ± 0.08 logMAR. The Goldmann visual field at the III4e/V4e target was severely constricted in all patients. Subjects CIC03005 and CIC05477 had a residual temporal peripheral crescent of visual field at V4e target. Static perimetry showed a ring-shaped scotoma with variable preservation of foveal threshold. Color vision tests showed normal results (CIC02644), multiple without-axis errors (CIC00088 and CIC05477), or tritan axis dyschromatopsia (CIC03005). Full-field ERG was undetectable in all patients.

At slit-lamp examination, patients CIC00088 and CIC02644 had a posterior subcapsular cataract in each eye. Multimodal retinal imaging is presented in Figure 1. Fundus findings were typical of severe RP: waxy pallor of the optic disc, retinal vasculature narrowing, and pigmentary changes (Figs. 1A–1D). However, all patients presented an unusual whitish granularity of the midperipheral retina as a distinctive feature (Figs. 1A–1D, Supplementary Fig. S1). SWAF, NIRAF, and SD-OCT findings were typical of RP.

Long-term follow-up data were available for three patients (Table 2, Figs. 1A–1D, Figs. 2A–2C). BCVA was stable until 25 years of age and then gradually decreased (Fig. 2A). The peripheral visual field rapidly became constricted with relative preservation of central vision (Table 2). EZ and NIRAF-APA diameters decreased altogether but not completely in parallel (Figs. 2B, 2C). Cystic macular changes were observed in all patients on initial examination. Patient CIC05477 was assessed only once at 19 years of age. Unfortunately, the patient did not return for follow-up visits.

We identified four *CLRN1* variants (Fig. 3A, Supplementary Table S2): one duplication (c.230dup, p.(Ala78Serfs*52)²⁴); one deletion (c.176del, p.(Gly59Valfs*13)²⁴); and two missense (c.368C>A, p.(Ala123Asp)³³ and c.144T>G, p.(Asn48Lys)).¹⁷ All variants had been previously reported and were classified as pathogenic according to the

American College of Medical Genetics and Genomics guidelines.³⁴ Patient CIC02644 (Ashkenazi Jewish) was a compound heterozygous for c.176del, p.(Gly59Valfs*13) and c.144T>G, p.(Asn48Lys), the latter being a founder.^{23,24} The remaining three patients carried homozygous changes: patient CIC00088 carried the homozygous duplication (c.230dup, p.(Ala78Serfs*52)), whereas the other two patients (CIC03005 and CIC05477) carried the homozygous missense variant (c.368C>A, p.(Ala123Asp)). Two patients reported a history of parental consanguinity (CIC00088 and CIC05477). Parents of CIC03005 were born in the same village from Ivory Coast, but there was no identifiable parental consanguinity (Fig. 3B).

ENT data are summarized in the Table 1 but are beyond the scope of this study. Because the auditory and vestibular phenotype of patients harboring the aforementioned variants have already been reported, our study focused on the first documentation of retinal findings.

DISCUSSION

CLRN1-related USH3A is relatively rare in non-Finnish European populations. It accounts for 1.4% of our cohort of Usher patients. At present, there are only a few reports of audiological^{15,16,35} and retinal^{25,29,30} phenotypes in USH3A.

On initial examination, the RCD was severe in our patients. Despite a relatively preserved visual acuity, all patients had abnormal color vision with tritan or anarchic color vision defects. Visual field was severely constricted from the teen years; if initially present, the remaining temporal crescent disappeared within a decade on Goldmann perimetry. None of the studied patients had detectable fERG responses at presentation in their teen years.

The functional data of our patients were similar to those of previously reported series.^{25,28,29,36} In the largest USH3A ocular phenotype study of Finnish patients harboring the founder p.(Tyr176*) variant in *CLRN1*,²⁵ mean BCVA was 0.2 logMAR or better at 20 years of age, ranged from 0.2 to 0.6 logMAR at 30 years of age, and was equal or worse than 0.6 logMAR at 35 years. We observed the same rate of BCVA loss in our study (Fig. 2A). However, visual fields were more severely constricted in our patients, as two out of four had tubular fields without peripheral islands before 20 years of age, whereas in the Finnish cohort a similar stage was reached at an age of 30 years. More recent reports^{29,36} compared the progression of the retinal disease in subject with *CLRN1*-related USH3A and *USH2A*-related USH2A. The authors²⁹ concluded that *CLRN1*-associated retinal disease was more severe at a given age and was more rapidly progressing than *USH2A*-associated RCD.

The severity of retinal dysfunction in our cohort was mirrored by structural alterations. Only a small foveal island of outer retina was preserved. SWAF-RIA in the posterior pole was present at the initial visit in two of the four subjects (CIC00088 and CIC05477). It was faint and rapidly replaced by patches of hypo-autofluorescence due to rapid outer retinal atrophy. Poor outer retinal preservation was also apparent on the NIRAF imaging, with only a small remaining area of normal autofluorescence that rapidly diminished (e.g., –107 $\mu\text{m}/\text{y}$ on average for CIC02644). NIRAF alterations have been reported to precede SWAF alterations and have been found to better correlate with SD-OCT findings in RP.^{37,38} Indeed, the borders of NIRAF-APA usually coincide with the relative preservation of the EZ on SD-OCT.³⁷ We recog-

TABLE 1. Initial Clinical Features of Patients with *CLRN1*-Related USH3A

Patient, Sex, Ancestry	Age at First Examination (y)	Symptoms	BCVA (log/MAR) and Refraction	Anterior Segment	Fundus	SWAF	NIRAF	OCT	KP	SP MD/FT (RE/LE)	Color Vision	fERG	Remarks
CIC00088, M, Algerian	22	Hearing difficulties at 20 y; night blindness from 10 y	RE: 0.5; +1.50 (-1.25); 20° LE: 0.2; +1.50 (-1.25); 150°	Anterior polar cataract OU Cataract surgery at 34 y	Waxy disc pallor Vessel narrowing Whitish retina at posterior pole and whitish granularity of the midperipheral retina Bone spicules-like, paravascular pigmentary cuffs, coarse pigment clumps in midperiphery	Perifoveal RIA, patchy paramacular and midperipheral hypoAF	Small central APA	Small foveolar area of preserved EZ, outer retinal layers disorganization outside Microcystic maculopathy ILM thickening and irregular retinal surface	III4e constricted to 5° OU	17.9/15 16.7/22	Severe defect without axis (RE) Normal (LE)	Undetectable	Audiogram: middle and high-frequency losses MD REar: -55 dB MD LEar: -49 dB Hearing aids from 20 y
CIC02644, F, Ashkenazi Jewish	16	Mild hearing loss at 5 y; night blindness at 12 y	RE: 0; +1.75 (-2.0); 45° LE: 0.1; +1.75 (-2.0); 135°	Posterior subcapsular opacities OU	Waxy disc pallor Vessel narrowing Normal aspect of the macula Midperipheral whitish granularity, spotted AF loss in marble appearance Bone spicules, paravascular pigmentary cuffs, sparse pigmentary clumps in midperiphery	Narrow perifoveal RIA, patchy paramacular and midperipheral hypoAF, some punched-out AF loss in midperiphery	Small central APA	Foveal area of preserved EZ, disorganization of the outer retinal layers replaced by hyperreflective dots outside the fovea Microcystic maculopathy (in INL and OPL)	KP: III4e constricted to 10°	17.3/29 16.8/32	Normal (both eyes)	Undetectable	—

Investigative Ophthalmology & Visual Science

Patient, Sex, Ancestry	Age at First Examination (y)	Symptoms	BCVA (logMAR) and Refraction		Anterior Segment	Fundus	SWAF	NIRAF	OCT	KP	SP MD/FT (RE/LE)	Color Vision	ffERG	Remarks
			RE	LE										
CIC03005, F, Ivory Coast	17	Night blindness from 12 y	RE: 0.4; +3.0 (-0.75); 135° LE: 0.6; +2.0 (-0.75); 35°	Normal	Normal	Arteriolar narrowing Yellowish macula, microcystic maculopathy Whitish granularity of midperipheral retina, spotted marble appearance Bone spicule-like and paravascular pigmentary cuffs	SWAF: posterior pole globally hypoAF with foveolar hyperAF Patchy midperipheral hypoAF	Small central APA	Small foveolar area of preserved EZ, disorganized outer retinal layers outside the fovea Microcystic maculopathy ILM thickening and irregularity	V4e constricted to 60° + temporal crescent OU	18.8/15 24.3/12	Tritan defect (both eyes)	Undetectable	Seizures, valproate treatment
CIC05477, M, Ivory Coast	20	Progressive hearing loss starting at 7 y; night blindness at 10 y	RE: 0.1; +1.75 (-1.75); 15° LE: 0.2; +1.75 (-1.75); 170°	Normal	Normal	Arteriolar narrowing Normal aspect of the macula, midperipheral whitish granularity, spotted marble appearance Few bone spicule-like pigments in midperiphery	SWAF: well-circumscribed perifoveal RIA, patchy midperipheral hypoAF	Foveal APA	Foveal area of preserved EZ, disorganization of the outer retinal layers replaced by hyper-reflective dots outside the foveal region Microcystic maculopathy (in INL and OPL)	KP: V4e constricted to 20° + temporal crescent OU	21.2/22 21.6/21	Multiple errors without axis (both eyes)	Undetectable	Audiogram: severe middle and high-frequency loss MD REar: -100 dB MD LEar: -75 dB Normal speech Hearing aids from 7 y, cochlear implant at 21 y

KP, kinetic perimetry; SP, static perimetry; MD, mean deficit; FT, foveal threshold (dB); M, male; F, female; RE, right eye; LE, left eye; OU, both eyes; hypoAF, hypo-autofluorescence; hyperAF, hyper-autofluorescence; APA, area of preserved autofluorescence; REar, right ear; LEar, left ear; INL, inner nuclear layer; OPL, outer plexiform layer; ILM, internal limiting membrane (dB).

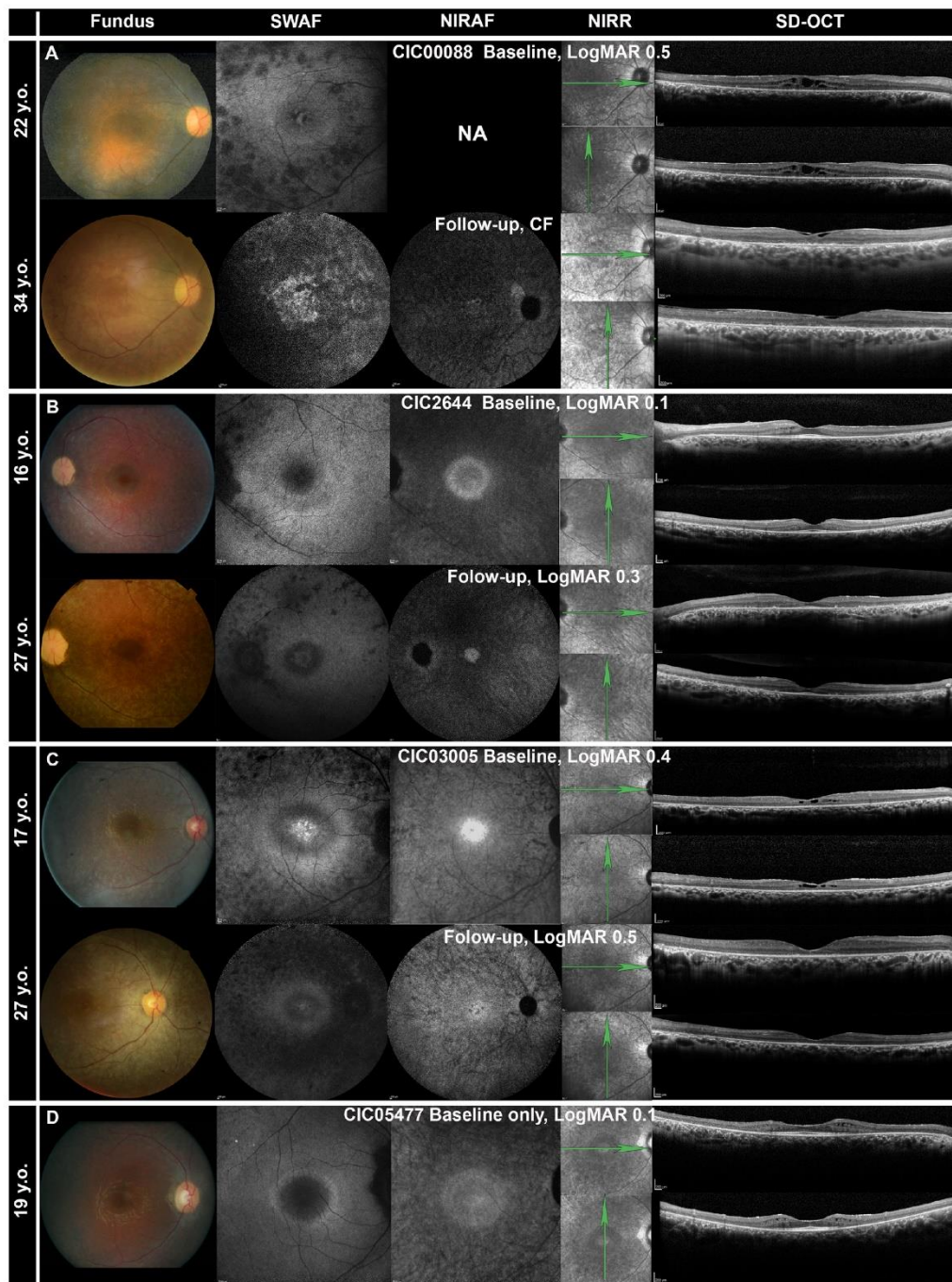


FIGURE 1. Multimodal retinal imaging in patients with *CLRN1* USH3A at first assessment and follow-up. Color fundus photography, SWAF, NIRAF, near-infrared reflectance (NIRR), and SD-OCT horizontal and vertical cross-section images. (A) Patient CIC00088, (B) Patient CIC2644, (C) Patient CIC03005, and (D) Patient CIC05477. All patients had classical signs of RP on fundus photography: optic disc pallor, arterial narrowing, and pigmentary changes. The distinctive feature was a granularity and whitishness of retina, present in all patients and prominent in CIC2644 and CIC03005. Only patient CIC05477 had a typical ring of increased autofluorescence on SWAF. The remaining cases show ill-defined perifoveal changes with hyper-autofluorescence (CIC03005) or iso-autofluorescence (CIC00088). On follow-up, hypo-autofluorescent zones increased. NIRAF showed a progressive narrowing of the area of preserved autofluorescence (APA) in the posterior pole, seen in CIC2644 and CIC03005. Patient CIC03005 had some black dots in APA suggestive of foveal outer retinal disruption. SD-OCT revealed various degrees of outer nuclear layer, EZ, and RPE preservation. There were multiple hyperreflective dots in the subretinal space, especially in patients with prominent whitishness of the retina (CIC2644 and CIC03005). All patients had microcystic macular changes. Patient CIC00088 developed an epimacular membrane. CF, counting fingers.

TABLE 2. Longitudinal Follow-Up of Patients with *CLRN1*-Related UHS3A

Patient	Follow-Up Period (y)	BCVA at Last Visit (logMAR), RE/LE; Age	Visual Field Progression	Color Vision at Last Visit	SWAF	NIRAF	OCT
CIC00088	12	CF/0.6; 34 y	Temporal crescents diminished and finally disappeared at the age 25. The central V4e isopter reduction was only of 5° over the 12 y.	Multiple without-axis errors appeared in RE, whereas the LE color vision remained unchanged.	RIA disappeared at age 25. Scalloped patches of midperipheral hypo-autofluorescence became larger and confluent, more advanced in the macular area (Fig. 1A).	APA disappearance at age 32 (Fig. 1A)	The EZ was preserved at the fovea at age 22 and disappeared at age 32 (Figs. 2B, 2C). Cystic maculopathy resolved at the same age. There was a thick epimacular membrane at the last visit (Fig. 1A). EZ was regularly decreasing for both the vertical (90 μm/y) and the horizontal (100 μm/y) diameters (Figs. 2B, 2C). Cystic macular changes appeared at 18 y and had been successfully treated by acetazolamide for 4 y. The treatment was then discontinued without recurrence of microcysts (Fig. 1B).
CIC02644	11	0.2/0.3; 27 y	Progressive loss and finally disappearance (at 24 y) of the temporal peripheral crescents. The extent of the central V4e isopter did not change. Mean defect was slowly worsening, with a loss of 5 dB in the RE (-18%) and 2 dB in the LE (-12%) compared with the first assessment.	Color vision was first normal but a tritan defect became obvious.	RIA disappeared at 24 y and was replaced by a large ring of hypo-autofluorescence	APA was regularly decreasing for both the vertical (115 μm/y) and the horizontal (102 μm/y) diameters (Figs. 2B, 2C).	The EZ was already disorganized on the first SD-OCT and remained unchanged. Irregular-shaped macular microcysts persisted at all visits despite the acetazolamide treatment (Fig. 1C)
CIC03005	9	0.5/0.5; 30 y	Kinetic visual field was normal under the age of 20 y. Temporal peripheral crescents disappeared at 24 y, and the isopter V4e became constricted to 10° at 25 y.	A tritan color vision defect was present at the first assessment and remained unchanged.	Unchanged	Unchanged	

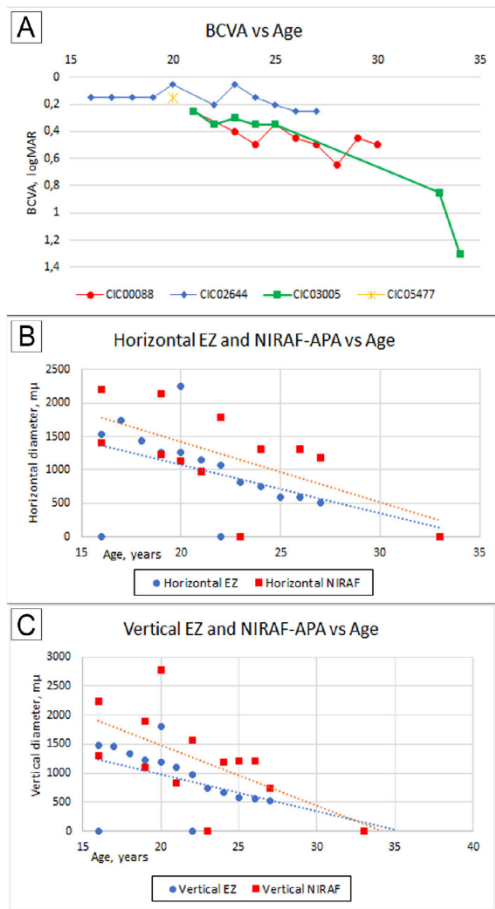


FIGURE 2. Longitudinal follow-up. (A) BCVA changes. (B) Horizontal EZ and NIRAF-APA changes. (C) Vertical EZ and NIRAF-APA changes.

nize, however, the difficulty of obtaining reliable NIRAF-APA measurements in late stages of RCD when NIRAF-APA limits become ill defined (e.g., in patient CIC03005) (Fig. 1C). This may explain some discrepancies between observed EZ and NIRAF-APA parameters. Previously published OCT data in *CLRN1*-*USH3A* patients²⁹ documented the progression of retinal thinning with age. Our study takes into account the EZ diameter, as it probably correlated better with the functional parameters.^{35,36} The loss of outer retinal layers on SD-OCT was in line with SWAF and NIRAF findings (e.g., $-76 \mu\text{m}/\text{y}$ on average for CIC02644). All of our patients had cystic macular changes in the course of our monitoring.

Of note, we found an unusual phenotype of *CLRN1* RCD consisting of a whitish granularity of the midperipheral retina giving a spotted marbled appearance that was present in all four patients. This finding was correlated with the presence of numerous hyperreflective dots in the subretinal space on SD-OCT, especially in patients with prominent whitishness of the retina (Figs. 1B, 1C; Supplementary Fig. 1). We hypothesize that it might be debris of degenerating photoreceptors and/or retinal pigment epithelium. Alternatively, we cannot exclude the possibility that the whitishness

could be a general feature of RCD at this time point. Indeed, our study involved patients of nearly the same age. This finding was not reported in the description of the Finnish or Ashkenazi Jewish cohorts^{25,26,29} or evident on published fundus photographs.^{30,39}

Patients CIC03005 and CIC05477, both from Ivory Coast ancestry and harboring the same homozygous variant c.368C>A, p.(Ala123Asp), were initially assessed by the end of their 20s. Foveal EZ and RPE were already disorganized in CIC03005 at 17 years of age, whereas there was a well-preserved foveal island of outer retina in CIC05477 at 19 years of age. These data suggest some phenotypic variability in *CLRN1*-related RCD, also common for other inherited retinal disorders.²⁸ This pathogenic variant was first reported in a French Canadian patient.³³ The retinal phenotype of this patient has not been published. Patients CIC03005 and CIC05477 did not report any common ancestor and were born in different Ivory Coast districts; however, a founder effect cannot be excluded considering an enrichment of this allele in the French Light4Deaf cohort.

The gene coding for clarin-1, *CLRN1*, is a four exon gene located on chromosome 3q25.1.^{27,40} Multiple transcripts have been reported for this gene,⁴⁰ but the major mRNA transcript variant, comprised of exons 0, 2, and 3 (RefSeq NM_174878.3), is expressed in the retina⁴¹ and encodes a protein of 232 amino acid residues (clarin-1 isoform a). A minor mRNA transcript, comprised of exons 1, 2, 3a, and 3b (RefSeq NM_052995.2), encodes a protein of 120 amino acid residues (clarin-1 isoform c). Clarin-1 is a small transmembrane protein belonging to the tetraspanin and claudin families. A major retinal isoform a is predicted to be comprised of four transmembrane domains and is glycosylated at Asn48 residue.¹⁷ Multiple sequence alignment algorithms have depicted a close similarity of clarin-1 with the voltage-dependent calcium channel gamma-2 subunit, *CACNG2* (MIM #602911), also known as stargazin.¹⁷ The putative function of clarin-1 in cells was deduced from this resemblance. Adato and colleagues¹⁷ speculated that clarin-1 may have a role in the structure and function of the ribbon synapse and in protein-protein bridging in the synaptic cleft. The protein is localized ubiquitously with higher levels in the spiral ganglion cells of the inner ear, in the olfactory epithelium, in the testis and in the retina. RNA in situ hybridization and single-cell RNA sequencing demonstrated the localization of mRNA transcripts in the inner nuclear layer and more precisely in the Müller cells for both mouse and human retinas.⁴²

The mechanism of *CLRN1*-related RCD remains unknown because there is no mouse model of clarin-1-associated RCD: knock-in and knock-out mice for *Clrn1* do not produce any detectable retinal disease.^{42,43} Plausible hypotheses for the discrepancy between human and mouse phenotypes have been formulated. First, it is possible that *CLRN1* expression does not follow the same spatial and temporal pattern across mammalian species. For example, there is a developmental downregulation of *Clrn1* expression in mouse retina and not in human.^{42,43} The absence of well-developed, actin-filled calyceal processes at the apical region of inner segments of mouse photoreceptors represents a second possibility.⁴⁴ As the Usher syndromes are a part of the ciliopathy spectrum, clarin-1 could take part in the structure or/and function of the photoreceptor connecting cilium; unfortunately, limited experimental data are available to support this hypothesis. A better understanding of the retinal localization and function of clarin-1 would be crucial for

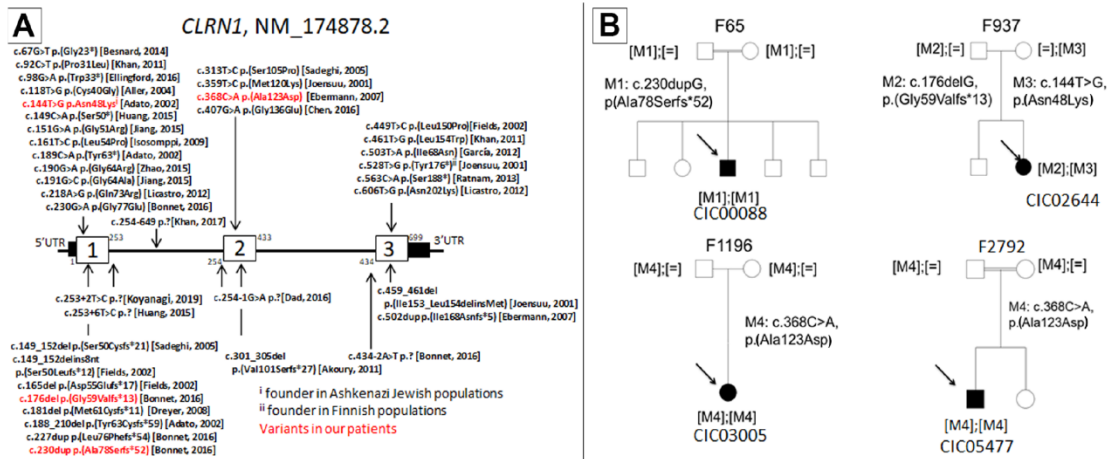


FIGURE 3. Pedigrees and variants in *CLRN1*. (A) Pathogenic variants are drawn in major retinal transcript coding for clarin-1 isoform a. Variants found in our cohort are shown in red. (B) Pedigrees. Two probands (F65, CIC00088; F2792, CIC05477) reported parental consanguinity. Both cases with the c.368C>A, p.(Ala123Asp) variant were from Ivory Coast ancestry.

translational research, such as developing gene replacement protocols, as *CLRN1* is a small gene, suitable for viral delivery, unlike other USH-related genes.⁴⁵

In contrast, the inner ear dysfunction phenotype could be obtained and rescued in mutant mice. Clarin-1 is essential for the morphogenesis and maintenance of the stereocilia hair bundle in auditory hair cells.⁴⁶ At the molecular level, the protein is supposed to be necessary for the regulation of actin cytoskeleton and of the F-actin core of the stereocilia hair cell.^{47,48} The stereocilia in *Clrn1* knock-out mice are poorly developed and disorganized.^{43,49} Viral-based gene augmentation therapy prevents early-onset deafness and limits the progression of SNHL in this model.⁴⁸

Two founder pathogenic variants have been reported and account for most cases: c.528T>G, p.(Tyr176*) in the Finnish population³² and c.144T>G, p.(Asn48Lys) in Ashkenazi Jews.¹⁷ Thirty-eight other disease-causing variants in *CLRN1* (Fig. 3A) have been reported to date (<http://www.hgmd.cf.ac.uk/>; <https://databases.lovd.nl/shared/variants/CLRN1/unique>), with missense and nonsense pathogenic variants being the most frequent.²⁴

Some genotype–phenotype associations related to *CLRN1* variants have been described. Amino acid changes found in the intra- and extracellular loops are thought to be more damaging than non-polar amino acid substitutions within the transmembrane domains that could give rise to non-syndromic RP61.¹⁹ As our patients were selected on the basis of their clinical phenotype and their number was small, we cannot come to conclusions. Larger cohorts of patients in collaborative projects would be necessary to explore genotype–phenotype correlations.

In summary, we have described relatively severe and rapidly progressive *CLRN1*-associated RCD with a distinctive retinal granularity and whitishness not previously reported (Fig. 1, Supplementary Fig. S1). It accounts for 1.4% of the cases in our large French USH cohort. Although the variants in *CLRN1* harbored by our patients have already been reported, the associated ocular phenotype has not.

Acknowledgments

The authors are grateful to Katia Marazova (Institut de la Vision, Paris, France) for her English revisions. The authors thank families participating in the study and the clinical staff from the National Center for Rare Diseases REFERET. DNA samples were obtained from the NeuroSensCol DNA bank, for research in neuroscience (PI, J.-A.S.; co-PI, I.A.; partner with CHNO des Quinze-Vingts, Inserm, and CNRS, certified NFS96-900).

Supported by funding from RHU-Light4deaf (ANR-15-RHU-0001) and LABEX LIFESENSES (ANR-10-LABX-65); French state funds managed by the Agence Nationale de la Recherche within the Investissements d'Avenir program (ANR-21-11-IDEX-0004-0); IHU FOReSIGHT (ANR-18-IAHU-0001), which is supported by French state funds managed by the Agence Nationale de la Recherche within the Investissements d'Avenir program; and Foundation Fighting Blindness center grant (C-CMM-0907-0428-INSERM04). The funding organizations had no role in the design or conduct of this research.

Presented as Poster #3033 (abstract #3362510) at ARVO 2020 (online).

Disclosure: V.M. Smirnov, None; M. Nassisi, None; S. Mohand-Said, None; C. Bonnet, None; A. Aubois, None; C. Devisme, None; T. Dib, None; C. Zeitz, None; N. Loundon, None; S. Marlin, None; C. Petit, None; B. Bodaghi, None; J.-A. Sahel, None; I. Audo, None

References

- Boughman JA, Vernon M, Shaver KA. Usher syndrome: definition and estimate of prevalence from two high-risk populations. *J Chronic Dis.* 1983;36(8):595–603.
- Hartong DT, Berson EL, Dryja TP. Retinitis pigmentosa. *Lancet.* 2006;368(9549):1795–1809.
- Keats BJ, Corey DP. The usher syndromes. *Am J Med Genet.* 1999;89(3):158–166.
- Kimberling WJ, Hildebrand MS, Shearer AE, et al. Frequency of Usher syndrome in two pediatric populations: implications for genetic screening of deaf and hard of hearing children. *Genet Med.* 2010;12(8):512–516.

5. Mathur PD, Yang J. Usher syndrome and non-syndromic deafness: functions of different whirlin isoforms in the cochlea, vestibular organs, and retina. *Hear Res.* 2019;375:14–24.
6. Heissler SM, Manstein DJ. Functional characterization of the human myosin-7a motor domain. *Cell Mol Life Sci.* 2012;69(2):299–311.
7. Weil D, Blanchard S, Kaplan J, et al. Defective myosin VIIA gene responsible for Usher syndrome type 1B. *Nature.* 1995;374(6517):60–61.
8. Bonnet C, El-Amraoui A. Usher syndrome (sensorineural deafness and retinitis pigmentosa): pathogenesis, molecular diagnosis and therapeutic approaches. *Curr Opin Neurol.* 2012;25(1):42–49.
9. Bhattacharya G, Kalluri R, Orten DJ, Kimberling WJ, Cosgrove D. A domain-specific usherin/collagen IV interaction may be required for stable integration into the basement membrane superstructure. *J Cell Sci.* 2004;117(2):233–242.
10. Eudy JD, Weston MD, Yao S, et al. Mutation of a gene encoding a protein with extracellular matrix motifs in Usher syndrome type IIa. *Science.* 1998;280(5370):1753–1757.
11. Seyedahmadi BJ, Rivolta C, Keene JA, Berson EL, Dryja TP. Comprehensive screening of the *USH2A* gene in Usher syndrome type II and non-syndromic recessive retinitis pigmentosa. *Exp Eye Res.* 2004;79(2):167–173.
12. Ávila-Fernández A, Cantalapiedra D, Aller E, et al. Mutation analysis of 272 Spanish families affected by autosomal recessive retinitis pigmentosa using a genotyping microarray. *Mol Vis.* 2010;16:2550–2558.
13. McGee TL, Seyedahmadi BJ, Sweeney MO, Dryja TP, Berson EL. Novel mutations in the long isoform of the *USH2A* gene in patients with Usher syndrome type II or non-syndromic retinitis pigmentosa. *J Med Genet.* 2010;47(7):499–506.
14. Nuutila A. Dystrophia retinae pigmentosa–dysacusis syndrome (DRD): a study of the Usher- or Hallgren syndrome. *J Genet Hum.* 1970;18(1):57–88.
15. Gorlin RJ, Tilsner TJ, Feinstein S, Duvall AJ. Usher's syndrome type III. *Arch Otolaryngol Chic Ill 1960.* 1979;105(6):353–354.
16. Sadeghi M, Cohn ES, Kimberling WJ, Tranebjaerg L, Möller C. Audiological and vestibular features in affected subjects with *USH3*: a genotype/phenotype correlation. *Int J Audiol.* 2005;44(5):307–316.
17. Adato A, Vreugde S, Joensuu T, et al. *USH3A* transcripts encode clarin-1, a four-transmembrane-domain protein with a possible role in sensory synapses. *Eur J Hum Genet.* 2002;10(6):339–350.
18. Abbott JA, Meyer-Schuman R, Lupo V, et al. Substrate interaction defects in histidyl-tRNA synthetase linked to dominant axonal peripheral neuropathy. *Hum Mutat.* 2018;39(3):415–432.
19. Khan MI, Kersten FFJ, Azam M, et al. *CLRN1* mutations cause nonsyndromic retinitis pigmentosa. *Opthalmology.* 2011 Jul 1;118(7):1444–1448.
20. Puffenberger EG, Jinks RN, Sougnez C, et al. Genetic mapping and exome sequencing identify variants associated with five novel diseases. *PLoS One.* 2012;7(1):e28936.
21. Vester A, Velez-Ruiz G, McLaughlin HM, et al. A loss-of-function variant in the human histidyl-tRNA synthetase (*HARS*) gene is neurotoxic in vivo. *Hum Mutat.* 2013;34(1):191–199.
22. Safka Brozkova D, Deconinck T, Griffin LB, et al. Loss of function mutations in *HARS* cause a spectrum of inherited peripheral neuropathies. *Brain J Neurol.* 2015;138(Pt 8):2161–2172.
23. Galatolo D, Kuo ME, Mullen P, et al. Bi-allelic mutations in *HARS1* severely impair histidyl-tRNA synthetase expression and enzymatic activity causing a novel multisystem ataxic syndrome. *Hum Mutat.* 2020;41(7):1232–1237.
24. Bonnet C, Riahi Z, Chantot-Bastaraud S, et al. An innovative strategy for the molecular diagnosis of Usher syndrome identifies causal biallelic mutations in 93% of European patients. *Eur J Hum Genet.* 2016;24(12):1730–1738.
25. Pakarinen L, Tuppurainen K, Laippala P, Mäntyjärvi M, Puhakka H. The ophthalmological course of Usher syndrome type III. *Int Ophthalmol.* 1995;19(5):307–311.
26. Khalaileh A, Abu-Diab A, Ben-Yosef T, et al. The genetics of Usher syndrome in the Israeli and Palestinian populations. *Invest Ophthalmol Vis Sci.* 2018;59(2):1095–1104.
27. Fields RR, Zhou G, Huang D, et al. Usher syndrome type III: revised genomic structure of the *USH3* gene and identification of novel mutations. *Am J Hum Genet.* 2002;71(3):607–617.
28. Ness SL, Ben-Yosef T, Bar-Lev A, et al. Genetic homogeneity and phenotypic variability among Ashkenazi Jews with Usher syndrome type III. *J Med Genet.* 2003;40(10):767–772.
29. Herrera W, Aleman TS, Cideciyan AV, et al. Retinal disease in Usher syndrome III caused by mutations in the *clarin-1* gene. *Invest Ophthalmol Vis Sci.* 2008;49(6):2651.
30. Ratnam K, Västinsalo H, Roorda A, Sankila E-MK, Duncan JL. Cone structure in patients with usher syndrome type III and mutations in the *Clarin 1* gene. *JAMA Ophthalmol.* 2013;131(1):67–74.
31. Audo I, Friedrich A, Mohand-Said S, Lancelot M-E, Antonio A, Moskova-Doumanova V, Poch O, Bhattacharya S, Sahel J-A, Zeitz C. An unusual retinal phenotype associated with a novel mutation in *RHO*. *Arch Ophthalmol.* 2010;128(8):1036–1045.
32. Joensuu T, Hämäläinen R, Yuan B, et al. Mutations in a novel gene with transmembrane domains underlie Usher syndrome type 3. *Am J Hum Genet.* 2001;69(4):673–684.
33. Ebermann I, Lopez I, Bitner-Glindzic M, Brown C, Koenekoop RK, Bolz HJ. Deafblindness in French Canadians from Quebec: a predominant founder mutation in the *USH1C* gene provides the first genetic link with the Acadian population. *Genome Biol.* 2007;8(4):R47.
34. Richards S, Aziz N, Bale S, et al. Standards and guidelines for the interpretation of sequence variants: a joint consensus recommendation of the American College of Medical Genetics and Genomics and the Association for Molecular Pathology. *Genet Med.* 2015;17(5):405–424.
35. Pakarinen L, Karjalainen S, Simola KOJ, Laippala P, Kaitalo H. Usher's syndrome type 3 in Finland. *Laryngoscope.* 1995;105(6):613–617.
36. Plantinga RF, Pennings RJE, Huygen PLM, et al. Visual impairment in Finnish Usher syndrome type III. *Acta Ophthalmol Scand.* 2006;84(1):36–41.
37. Duncker T, Tabacaru MR, Lee W, Tsang SH, Sparrow JR, Greenstein VC. Comparison of near-infrared and short-wavelength autofluorescence in retinitis pigmentosa. *Invest Ophthalmol Vis Sci.* 2013;54(1):585–591.
38. Nassisi M, Lavia C, Mohand-Said S, et al. Near-infrared fundus autofluorescence alterations correlate with swept-source optical coherence tomography angiography findings in patients with retinitis pigmentosa. *Sci Rep.* 2021;11(1):3180.
39. Ebermann I, Wilke R, Lauhoff T, Lübber D, Zrenner E, Bolz HJ. Two truncating *USH3A* mutations, including one novel, in a German family with Usher syndrome. *Mol Vis.* 2007;13:1539–1547.
40. Västinsalo H, Jalkanen R, Dinculescu A, et al. Alternative splice variants of the *USH3A* gene *Clarin 1* (*CLRN1*). *Eur J Hum Genet.* 2011;19(1):30–35.
41. Zallocchi M, Meehan DT, Delimont D, et al. Localization and expression of *clarin-1*, the *Clrn1* gene product, in auditory hair cells and photoreceptors. *Hear Res.* 2009;255(1–2):109–120.

42. Xu L, Bolch SN, Santiago CP, et al. *Clarin-1* expression in adult mouse and human retina highlights a role of Müller glia in Usher syndrome. *J Pathol.* 2020;250(2):195–204.
43. Geller SF, Guerin KI, Visel M, et al. CLRN1 is nonessential in the mouse retina but is required for cochlear hair cell development. *PLoS Genet*;5(8):e1000607.
44. Sahly I, Dufour E, Schietroma C, et al. Localization of Usher 1 proteins to the photoreceptor calyceal processes, which are absent from mice. *J Cell Biol.* 2012;199(2):381–399.
45. Dinculescu A, Stupay RM, Deng W-T, et al. AAV-mediated clarin-1 expression in the mouse retina: implications for USH3A gene therapy. *PLoS One.* 2016;11(2):e0148874.
46. Geng R, Melki S, Chen DH-C, et al. The mechanosensory structure of the hair cell requires clarin-1, a protein encoded by Usher syndrome III causative gene. *J Neurosci.* 2012;32(28):9485–9498.
47. Tian G, Zhou Y, Hajkova D, et al. Clarin-1, encoded by the Usher syndrome III causative gene, forms a membranous microdomain: possible role of clarin-1 in organizing the actin cytoskeleton. *J Biol Chem.* 2009;284(28):18980–18993.
48. Geng R, Omar A, Gopal SR, et al. Modeling and preventing progressive hearing loss in Usher syndrome III. *Sci Rep.* 2017;7(1):13480.
49. Geng R, Geller SF, Hayashi T, et al. Usher syndrome IIIA gene clarin-1 is essential for hair cell function and associated neural activation. *Hum Mol Genet.* 2009;18(15):2748–2760.

3.4. *TTL5* collaborative work

Gene defects in *TTL5* are linked with COD and CORD, but the condition is very rare. Only a small number of cases have been published to date. A collaborative work involving XV-XX hospital, Institut de la Vision, Fondation Rothschild, CHU de Lille, CHU de Montpellier, CHU de Strasbourg and Clinique Jules Verne, Nantes contributed to a publication of 5 novel cases and new genotype-phenotype associations in *TTL5*-linked COD/CORD. I collected and analyzed all the clinical data from six centers, performed a genotype-phenotype correlation and substantially (50%) contributed to the article published in International Journal of Molecular Sciences[173].



Article

Novel *TLL5* Variants Associated with Cone-Rod Dystrophy and Early-Onset Severe Retinal Dystrophy

Vasily Smirnov ^{1,2,3}, Olivier Grunewald ⁴, Jean Muller ^{5,6}, Christina Zeitz ³, Carolin D. Obermaier ⁷, Aurore Devos ⁸, Valérie Pelletier ⁹, Béatrice Bocquet ^{10,11}, Camille Andrieu ¹², Jean-Louis Bacquet ⁹, Elodie Lebretonchel ⁸, Saddek Mohand-Saïd ^{3,12}, Sabine Defoort-Dhellemmes ², José-Alain Sahel ^{3,12,13,14}, Héléne Dollfus ⁹, Xavier Zanlonghi ¹⁵, Isabelle Audo ^{3,12,16}, Isabelle Meunier ^{10,11}, Elise Boulanger-Scemama ¹³ and Claire-Marie Dhaenens ^{4,*}

- ¹ Université de Lille, Faculté de Médecine, 59037 Lille, France; vasily.smirnov@chru-lille.fr
- ² CHU Lille, Service d'Exploration Fonctionnelle de la Vision et de Neuro-Ophtalmologie, Hôpital Salengro, 59037 Lille, France; sabine.defoort@chru-lille.fr
- ³ Sorbonne Université, INSERM, CNRS, Institut de la Vision, 75012 Paris, France; christina.zeitz@inserm.fr (C.Z.); saddekms@gmail.com (S.M.-S.); jsahel@gmail.com (J.-A.S.); isabelle.audo@inserm.fr (I.A.)
- ⁴ Univ. Lille, Inserm, CHU Lille, U1172-LilNCog-Lille Neuroscience & Cognition, 59045 Lille, France; olivier.grunewald@chru-lille.fr
- ⁵ Laboratoire de Génétique Médicale, Institut de Génétique Médicale d'Alsace (IGMA), INSERM U1112, Fédération de Médecine Translationnelle de Strasbourg (FMTS), Université de Strasbourg UMRS_1112, 67000 Strasbourg, France; jeanmuller@unistra.fr
- ⁶ Laboratoire de Diagnostic Génétique, Hôpitaux Universitaires de Strasbourg, Institut de Génétique Médicale d'Alsace (IGMA), 67000 Strasbourg, France
- ⁷ Praxis für Humangenetik Tuebingen & Center for Genomics and Transcriptomics, CeGaT GmbH, 72076 Tuebingen, Germany; Carolin.Obermaier@humangenetik-tuebingen.de
- ⁸ Univ. Lille, CHU Lille, Service de Toxicologie et Génopathies, 59037 Lille, France; aurore.devos@chru-lille.fr (A.D.); elodie.lebretonchel@chru-lille.fr (E.L.)
- ⁹ Centre de Référence pour les Affections Rares en Génétique Ophtalmologiques, Hôpitaux Universitaires de Strasbourg, 67000 Strasbourg, France; valerie.pelletier@chru-strasbourg.fr (V.P.); jean-louis.bacquet@chru-strasbourg.fr (J.-L.B.); dollfus@unistra.fr (H.D.)
- ¹⁰ National Reference Centre for Inherited Sensory Diseases, University of Montpellier, Montpellier University Hospital, Sensene Care Network, ERN-EYE Network, 34295 Montpellier, France; beatrice.bocquet@inserm.fr (B.B.); isabelannemeunier@yahoo.fr (I.M.)
- ¹¹ Institute for Neurosciences of Montpellier (INM), INSERM, University of Montpellier, INSERM, 34295 Montpellier, France
- ¹² Centre Hospitalier National d'Ophtalmologie des Quinze-Vingts, INSERM-DHOS CIC 1423, 75012 Paris, France; candrieu@for.paris
- ¹³ Fondation Ophtalmologique Adolphe de Rothschild, 75019 Paris, France; eboulanger@for.paris
- ¹⁴ Department of Ophthalmology, The University of Pittsburgh School of Medicine, Pittsburgh, PA 15213, USA
- ¹⁵ Service d'Ophtalmologie, CHU de Rennes, 35000 Rennes, France; dr.zanlonghi@gmail.com
- ¹⁶ Institute of Ophthalmology, University College London, London EC1V 9EL, UK
- * Correspondence: claire-marie.dhaenens@inserm.fr; Tel.: +33-320-444-953



Citation: Smirnov, V.; Grunewald, O.; Muller, J.; Zeitz, C.; Obermaier, C.D.; Devos, A.; Pelletier, V.; Bocquet, B.; Andrieu, C.; Bacquet, J.-L.; et al. Novel *TLL5* Variants Associated with Cone-Rod Dystrophy and Early-Onset Severe Retinal Dystrophy. *Int. J. Mol. Sci.* **2021**, *22*, 6410. <https://doi.org/10.3390/ijms22126410>

Academic Editor: J. Fielding Hejtmančík

Received: 19 May 2021
Accepted: 9 June 2021
Published: 15 June 2021

Publisher's Note: MDPI stays neutral with regard to jurisdictional claims in published maps and institutional affiliations.



Copyright: © 2021 by the authors. Licensee MDPI, Basel, Switzerland. This article is an open access article distributed under the terms and conditions of the Creative Commons Attribution (CC BY) license (<https://creativecommons.org/licenses/by/4.0/>).

Abstract: Variants of the *TLL5* gene, which encodes tubulin tyrosine ligase-like family member five, are a rare cause of cone dystrophy (COD) or cone-rod dystrophy (CORD). To date, only a few *TLL5* patients have been clinically and genetically described. In this study, we report five patients harbouring biallelic variants of *TLL5*. Four adult patients presented either COD or CORD with onset in the late teenage years. The youngest patient had a phenotype of early onset severe retinal dystrophy (EOSRD). Genetic analysis was performed by targeted next generation sequencing of gene panels and assessment of copy number variants (CNV). We identified eight variants, of which six were novel, including two large multiexon deletions in patients with COD or CORD, while the EOSRD patient harboured the novel homozygous p.(Trp640*) variant and three distinct *USH2A* variants, which might explain the observed rod involvement. Our study highlights the role of *TLL5* in COD/CORD and the importance of large deletions. These findings suggest that COD or CORD patients lacking variants in known genes may harbour CNVs to be discovered in *TLL5*, previously

undetected by classical sequencing methods. In addition, variable phenotypes in *TLL5*-associated patients might be due to the presence of additional gene defects.

Keywords: *TLL5* gene; novel variants; large deletion; cone-rod dystrophy; early onset severe retinal dystrophy

1. Introduction

Cone and cone-rod dystrophies constitute a heterogeneous group of inherited retinal disorders primarily affecting cone photoreceptors. In cone dystrophies (COD), alterations are generally restricted to the cones, but can extend to the rod photoreceptors at a later stage [1]. COD begins in late childhood or early adult life with visual loss, abnormal colour vision, photophobia and central scotoma [2]. The fundus is variably altered, ranging from no alteration to bull's eye maculopathy. The retinal periphery is usually preserved. The optic discs show a variable degree of temporal pallor [2]. Cases of pure COD are very rare. Usually, there is a clinical continuum between COD and cone-rod dystrophies (CORD). The course of CORD is more severe than that of COD, but both disorders progress to complete blindness in most cases [3].

The estimated prevalence for nonsyndromic COD and CORD is between one in 30,000 and one in 40,000 [4], and all modes of Mendelian inheritance have been reported. They are highly genetically heterogeneous, but as COD and CORD overlap strongly in their clinical characteristics, the genetic descriptions of both entities are generally merged. Ten genes involved in autosomal dominant forms of COD/CORD, twenty-three genes involved in recessive forms and two genes involved in X-linked forms have been reported in the Retnet database (<https://sph.uth.edu/retnet/sum-dis.htm#B-diseases>, 21 January 2021 version). However, 30–50% of recessive or simplex COD/CORD cases remain unsolved [5–7].

In 2014, a new gene, *TLL5* (MIM 612268, RefSeq accession number NM_015072.4), which encodes tubulin tyrosine ligase-like family member five, was described in COD/CORD patients [8]. *TLL5* contains 32 exons, among which 31 encode a protein of 1281 amino acid residues. *TLL5* is highly expressed in the brain, testis, and retina [8–10] and is mainly involved in polyglutamylation, a posttranslational modification consisting of the addition of glutamic acids to a glutamate residue on targeted proteins within the primary cilium. Moreover, it glutamylates the glutamic acid and glycine repeated residues of RPRG^{ORF15} [11,12]. In the human retina, *TLL5* is mainly expressed in cones and at lower levels in rod photoreceptors [8].

Only 17 patients from 14 families with COD/CORD associated with *TLL5* gene defects have been described to date, and among these patients, 14 have been clinically detailed [8,13–17]. Here, we report a complete clinical description of five French patients presenting either COD/CORD or early-onset severe retinal dystrophy (EOSRD) linked to six novel pathogenic biallelic variants, among which two are large intragenic deletions in *TLL5*.

2. Results

2.1. Phenotypic Characterization

Here, we describe five individuals from five families with biallelic pathogenic variants in the *TLL5* gene, four patients with teenage onset COD/CORD and one patient (IA-CIC08269) with EOSRD. A summary of the clinical data is presented in Table 1.

Subject IA-CIC08269 was the second child of consanguineous parents (first-degree cousins). She had poor vision since early childhood and night blindness since 6 y.o. BCVA for both eyes was reduced to 20/50 at 7 y.o. The visual field to the IIIe target was constricted to 5°, while target IIe was not perceived. There was a tritan axis colour vision defect. The fERG response was undetectable under both scotopic and photopic conditions (Figure 1a(A)). Fundus examination revealed mild narrowing of the retinal vasculature and

some pigmentary changes around the fovea and outside the vascular arcades (Figure 1b). Only a small foveal island of the outer retinal layers (i.e., external limiting membrane (ELM) and ellipsoid zone (EZ)) was preserved on SD-OCT, with thinning of the outer nuclear layer (ONL). These foveal changes were correlated with a small perifoveal ring of increased autofluorescence on SWAF. The patient had been tested for hearing impairment at ages 8 and 9, and both audiograms were normal.

Four subjects (XZ-358338, IM-4476, HD-2011304 and EB-163150) shared nearly the same clinical presentation (Table 1 and Figure 1b). These patients reported poor visual acuity from their teenage years. Photophobia appeared in their third or fourth decade. They were all highly myopic. Visual field testing revealed absolute or relative central scotomata of small size (5° to 15°) and a preserved peripheral visual field. Colour vision testing revealed a tritan axis in all but one patient (IM-4476), who presented with severe dyschromatopsia. The ffERG was consistent with pure cone dysfunction in patients IM-4476 and EB-163150; combined cone-rod dysfunction was found in subjects XZ-358338 and HD-2011304 (Figure 1a (B,C)). Cataracts were observed in the oldest subject (EB-163150), and patient XZ-358338 had a phakic intraocular lens for myopia correction. Regarding the fundus aspects, all presented a depigmented round macular lesion with more or less distinct edges (bull's eye maculopathy), and all had myopic fundus changes (peripapillary atrophy and chorioretinal thinning in the posterior pole, Figure 1b). SWAF showed a round macular lesion of decreased autofluorescence with hyperautofluorescent edges and a small hyperautofluorescent foveal dot in subjects XZ-358338, IM-4476 and HD-2011304; subject EB-163150 had a dark fovea circled with an ill-limited ring of increased autofluorescence. NIR images showed an increased reflectance corresponding to the macular lesions. SD-OCT scans revealed various degrees of outer retinal (ONL and EZ) and RPE hyporeflectivity within the posterior pole. Subject XZ-358338 had a dome-shaped macula.

Two of the four adult patients had children (Supplementary Figure S1). For the other two, the absence of offspring was not investigated. It is therefore not known whether infertility was the cause.

2.2. Genotyping Results

Overall, we identified eight variations, of which six were novel, encompassing three missense and two nonsense variants, one splice site variant and two large multiexon deletions in *TTL5* (Table 2). All were classified as pathogenic or likely pathogenic according to the ACMG (American College of Medical Genetics and Genomics) criteria [18].

Among the single nucleotide variants, c.211C>T p.(Arg71*) was recently reported [17], and c.1920G>A p.(Trp640*) is novel. They are located in exon 4 (TLL domain) and exon 20 (CID domain) (Figure 2). Both variants are rare. Indeed, p.(Arg71*) is present in 0.00002% of the non-Finnish European population, while p.(Trp640*) has not been reported in gnomAD V2.1.1.

Table 1. Clinical characteristics of patients.

Patient, Sex	Symptoms	BCVA at First Visit	Refraction	Anterior Segment	Fundus	Colour Vision	Visual Field	fERG	SWAF	SD-OCT
IA-CIC08269, F	Night vision difficulties since 6 y.o. Bilateral decreased visual acuity	RE: 20/50 LE: 20/50 7 y.o.	+1.0(−1.5)/10° +1.0(−1.5)/75°	Normal	Normal optic discs Mild vascular narrowing Dark fovea, yellowish deposit with indistinct borders surrounding the fovea Whitish spots of chorio-retinal atrophy and coarse pigimentary migration in peripheral retina	Tritan defect	Kinetic perimetry: V4e: 145° horizontal and 120° vertical III4e: constricted to 5° IIe: not perceived OU	Undetectable scotopic- and photopic responses	Very narrow ring of increased autofluorescence	Outer retinal layers (EZ, ONL) disappearance outside the fovea
XZ-358338, M	Progressive visual loss since teens, Photophobia from age 36 y.o.	RE: 20/50 LE: 20/40 36 y.o.	−12.5(−2.0)0° −12.0(−3.0)/60°	Phakic IOL implanted at 36 y.o.	Normal discs Peripapillary atrophy (conus myopicus) Mild arteriolar narrowing Dark round atrophic lesion of the macula with indistinct borders Normal peripheral retina	Tritan defect	Static perimetry: Absolute central scotoma of 5° surrounded by a ring of reduced sensitivity OU	Generalized cone-rod dysfunction (scotopic responses 70% of normal amplitude and photopic responses 25% of normal amplitude)	Salt and pepper round macular lesion with hyperautofluorescent edges Normal autofluorescence in the peripheral retina	Dome-shaped macula Outer retinal layers (EZ, ONL) disappearance in the macula; normal aspect outside the macular lesion
IM-4476, M	Progressive visual acuity loss since childhood, Photophobia and rapid visual acuity loss since 42 y.o.	RE: 20/100 LE: 20/50 46 y.o.	−6.25(−3.0)/170° −6.0(−3.50)/35°	Normal	Normal discs Chorioretinal thinning between the macula and optic disc Yellowish atrophic round macular lesion Normal peripheral retina	Severe dyschromatopsia	V4e: 150° horizontal and 120° vertical II4e: 90° horizontal and 60° vertical I4e not perceived OU	Severe generalized cone system dysfunction with normal rod system function	Round foveal hyperautofluorescent lesion with irregular hyperautofluorescent edges	Foveal disappearance of outer retinal layers (EZ, ONL)
HD-2011304, M	Night vision disturbances since his forties Photophobia and rapid visual acuity loss since 45 y.o.	RE: 20/63 LE: 20/50 48 y.o.	−6.75(−3.50)/80° −9.50(−3.50)/110°	Normal	Normal disc Peripapillary atrophy (conus myopicus) Mild arteriolar narrowing surrounded by ovoid zone of macular discoloration Normal peripheral retina	Tritan defect	V4e: 100° horizontal and 90° vertical V4e central scotoma of 15°	Generalized cone-rod dysfunction (scotopic responses 50% of normal amplitude, photopic responses 30% of normal amplitude)	Foveal hyperautofluorescent spot surrounded by a round hypoautofluorescent area with hyperautofluorescent edges Macular lesion is continuous with the peripapillary atrophy	Perifoveal disappearance of outer retinal layers (EZ, ONL) Foveal sparing of EZ

Table 1. Contd.

Patient, Sex	Symptoms	BCVA at First Visit	Refraction	Anterior Segment	Fundus	Colour Vision	Visual Field	fERG	SWAF	SD-OCT
EB-163150, M	Progressive visual acuity loss from teens Photophobia since childhood, became disabling from thirties	RE: 20/80 LE: 20/80 70 y.o.	-6.0(-1.0)40° -7.0(-0.75)165°	Cortico-nuclear and posterior subcapsular cataract OU	Normal disc Peripapillary atrophy (conus myopicus) Mild arteriolar narrowing Round macular discoloration	Tritan defect	V4e: 140° horizontal and vertical V1e: central scotoma of 15° Humphrey 10-2: sparing of fixation point, absolute annular scotoma at 5° of eccentricity surrounded by a relative deficit	Severe cone system dysfunction with only residual photopic responses while scotopic responses were normal	Perifoveal hyperautofluorescent ring with indistinct edges	Perifoveal disappearance of outer retinal layers (EZ, ONL) Foveal sparing of EZ

BCVA—best corrected visual acuity, EZ—ellipsoid zone, ONL—outer nuclear layer, OU—both eyes, NA—Not applicable, SWAF—short wave fundus autofluorescence, SD-OCT—spectral domain optical coherence tomography, fERG—full-field electroretinography.

Table 2. In silico variant analysis.

Patient ID	Status	Genomic Position	DNA Variant	Protein Variant	Variant Type	GnomAD AF (NFE)	In Silico Prediction	ACMG Rules	ACMG Classification	Reference	
IA-CIC08269	Homozygous	76232616	c.1920G>A	p.(Trp640*)	Nonsense	0	CADD	36.0	PVS1 Very strong	Pathogenic	This study
									PM2 Moderate		
									PP3 Supporting		
									PP4 Supporting		
									PP5 Supporting		
XZ-358338	Compound Heterozygous	76147917	c.211C>T	p.(Arg71*)	Nonsense	0.00002	CADD	35.0	PVS1 Very strong	Pathogenic	Zampaglione 2020
									PM2 Moderate		
									PM3 Moderate		
									PP3 Supporting		
									PP4 Supporting		
76167836-76292188		c.585+2223_3326+5684del	c.585+2223_3326+5684del	p.(Pro196Gluifs*47)	Exons 8-28 deletion	0			PVS1 Very strong	Pathogenic	This study
									PM2 Moderate		
									PM3 Moderate		
									PP3 Supporting		
									PP4 Supporting		
PP5 Supporting											

Table 2. Cont.

Patient ID	Status	Genomic Position	DNA Variant	Protein Variant	Variant Type	GnomAD AF (NFE)	In Silico Prediction	ACMG Rules	ACMG Classification	Reference			
IM-4476	Compound Heterozygous	76213058_76365878	c.1487+1134_3741-2607delins15	p.(Ser497_Lys1247del)	Exons 18-30 deletion	0	Conservation (Grantham) CADD SIFT Polyphen2	PS3 Strong PM2 Moderate PP3 Supporting PP4 Supporting PP5 Supporting	Pathogenic	This study			
											56 (0–215)	PS3 Strong	Pathogenic
											27.6	PM2 Moderate	
											Deleterious (score: 0.02)	PP3 Supporting	
											Probably Damaging (1.000)	PP4 Supporting	
PP5 Supporting													
HD-2011304	Compound Heterozygous	76231034	c.1627G>A	p.(Glu543Lys)	Missense	0.0003	Conservation (Grantham) CADD SIFT Polyphen2	PM2 Moderate PM3 Moderate PP3 Supporting PP4 Supporting PP5 Supporting	Likely Pathogenic *	Sergouniotis 2014			
											101 (0–215)	PM2 Moderate	
											28.3	PM3 Moderate	
											Deleterious (score: 0)	PP3 Supporting	
											Probably Damaging (0.995)	PP4 Supporting	
HD-2011304	Compound Heterozygous	76231034	c.1627G>A	p.(Glu543Lys)	Missense	0.0003	Conservation (Grantham) CADD SIFT Polyphen2	PS3 Strong PM2 Moderate PP3 Supporting PP4 Supporting PP5 Supporting	Pathogenic	Sergouniotis 2014			
											56 (0–215)	PS3 Strong	
											27.6	PM2 Moderate	
											Deleterious (score: 0.02)	PP3 Supporting	
											Probably Damaging (1.000)	PP4 Supporting	
PP5 Supporting													

Table 2. Cont.

Patient ID	Status	Genomic Position	DNA Variant	Protein Variant	Variant Type	GnomAD AF (NFE)	In Silico Prediction	ACMG Rules	ACMG Classification	Reference	
EB-163150	Compound Heterozygous	76211456	c.1282-2A>G	p.(?)	Splicing	0.000009	CADD	PVS1 Very strong	Pathogenic	This study	
							SpliceSiteFinder	PM2 Moderate			
							MaxEnt	PP3 Supporting			
							SpliceAI	PP4 Supporting			
								Conservation (GrantHAM)	PM2 Moderate		
								CADD	PM3 Moderate		
								SIFT	PP3 Supporting	Likely Pathogenic*	This study
								Polyphen2	Possible Damaging (0.786)		

*Stand Alone VUS becoming Likely Pathogenic with a pathogenic variant in trans.

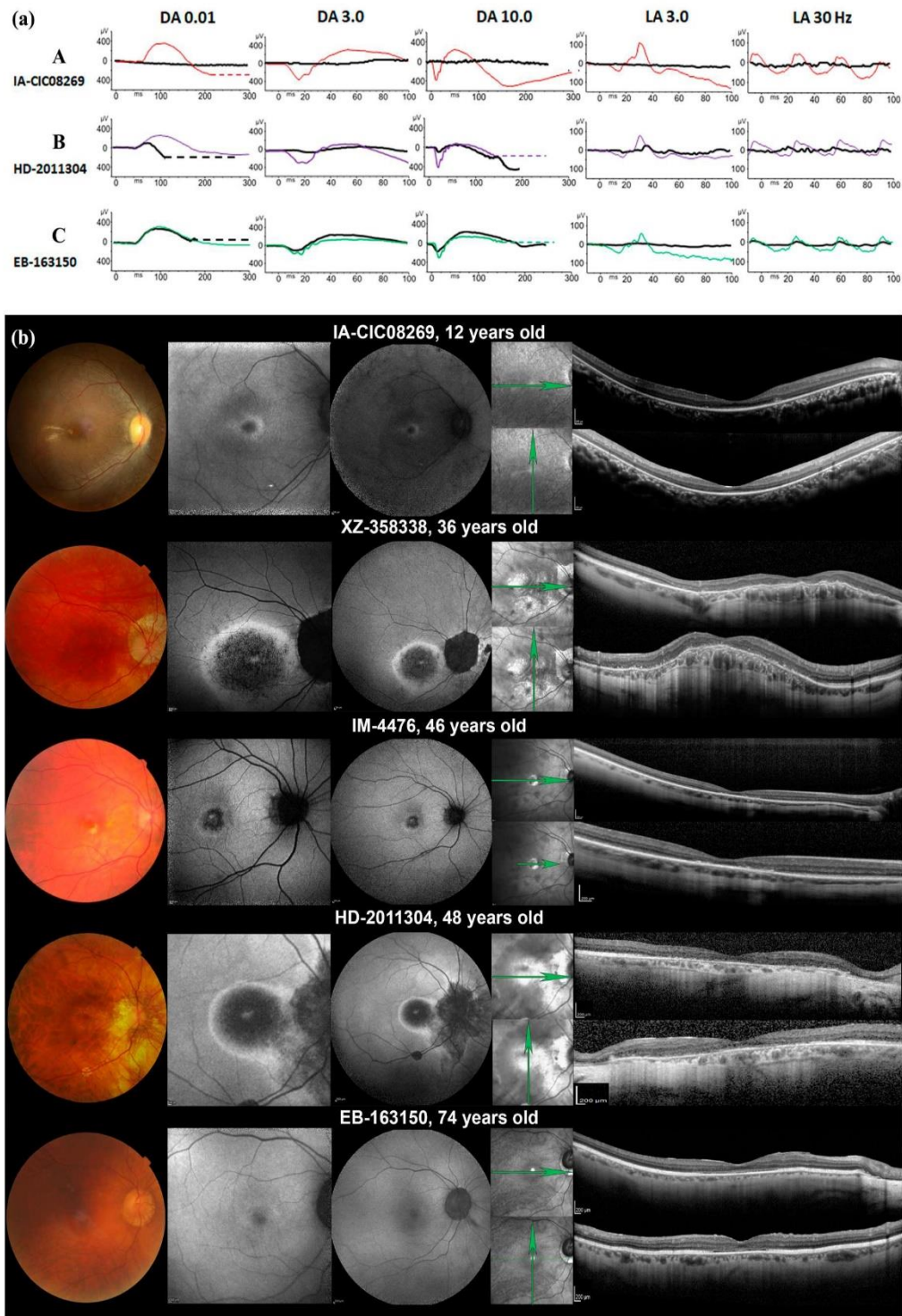


Figure 1. Full-field ISCEV-standard ERGs and Retinal imaging data. (a) In bold black, patients' fFERGs. In thin colour, age- and sex-matched controls. A. Early-onset severe retinal dystrophy. subject IA-CIC08269, 7 y.o. Undetectable dark- and light-adapted responses. B. Cone-rod dystrophy. subject HD-2011304, 48 y.o., mild reduction of dark-adapted responses (DA 0.01, DA 3.0), more pronounced at higher intensity flash (DA 10.0). Severe reduction of light-adapted responses and marked implicit time delay. C. Cone dystrophy. Subject EB-163150, 72 y.o. Normal dark-adapted responses to dim (DA 0.01)

and standard (DA 3.0) flash, small a-wave reduction to bright flash (DA 10.0). Residual light-adapted responses; (b) Only right eyes are shown. Columns (in order): fundus photography, SWAF 30°, SWAF 55°, IRR (the green arrows indicate the orientation of OCT scans), SD-OCT. Subject IA-CIC08269 presents with optic disc pallor, vascular attenuation, pigmentary changes of the fovea and outside the vascular arcades with yellowish band-like changes near the fovea. SWAF reveals a small perifoveal ring of increased autofluorescence. SD-OCT shows a preservation of the hyper reflective outer retinal bands at the fovea with outer nuclear layer thinning, some paramacular hyperreflective subretinal dots (better seen on the horizontal scan) with major thinning of the outer retina in the periphery. Subject XZ-358338 presents with some arteriolar narrowing, peripapillary chorioretinal atrophy and pigmentary changes in the macula. SWAF revealed a central area of loss of autofluorescence surrounded by a ring of increased autofluorescence leading to a bull's eye appearance. SD-OCT shows a dome-shaped macula with disorganized hyper reflective outer retinal bands and severe thinning of the ONL while the outer retina is preserved in the periphery. IM-4476 has normal optic disc and retinal vessels; a small foveal lesion surrounded by yellowish material. SWAF reveal a foveal loss of autofluorescence outlined by an irregular ring of increased autofluorescence. SD-OCT shows a global thinning of the ONL, disorganized outer retinal hyper-reflective bands and some hyper-reflective dots in the parafoveal region. Subject HD-2011304 has optic disc pallor, arteriolar narrowing, peripapillary and, perifoveolar chorioretinal atrophy. SWAF shows a central hyper autofluorescent spot surrounded by an area of autofluorescent loss outlined by a ring of increased autofluorescence. SD-OCT revealed foveal sparing surrounded by a loss of the outer retinal layers which reappear in the periphery. Subject EB-163150's fundus shows vascular narrowing and subtle foveal change. SWAF shows a subtle perifoveal ring of increased autofluorescence. SD-OCT shows a focal loss of the EZ and interdigitation zone at the fovea leading to a cavitation.

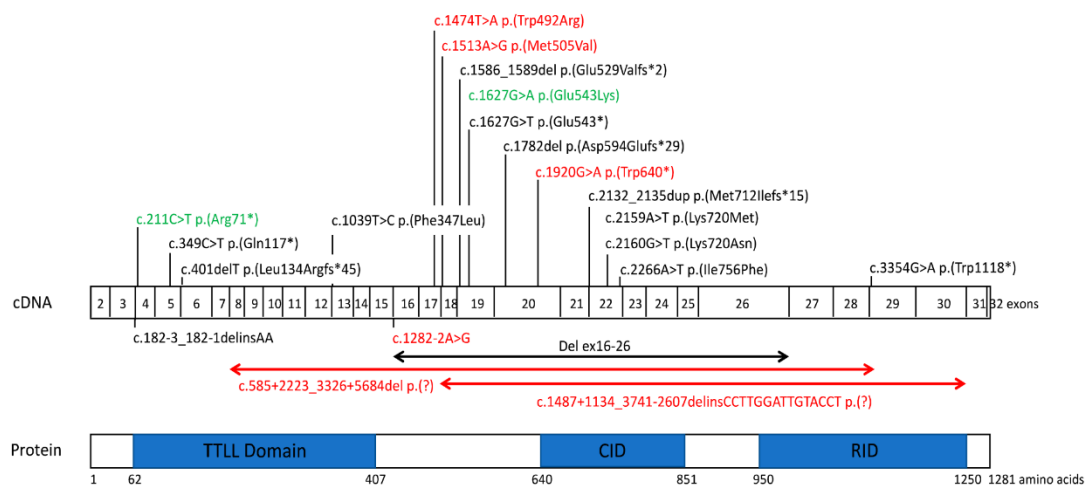


Figure 2. Localization of all reported and novel *TLL5* variants in cone and cone-rod dystrophies. Novel variations are in red, previously reported variants are in black and variants previously reported found in this study are in green. cDNA and protein (if known) nomenclatures are reported for each variant. *TLL5* is composed of 32 exons (depicted as boxes) and encodes 1281 amino acids. Protein domains, presented in blue boxes in the lower part, are as follows: TLL core domain (delineated from amino acid 62 to 407) has a role in side chain elongation activity and in initiating the side chain, and polyglutamylation activity requires addition sequences of 100–150 amino acids on either side of the core TTL domain for full activity; c-MTBD (cationic microtubule binding domain) (amino acids 378 to 488); CID (cofactor interaction domain) (amino acids 640 to 841); RID (receptor interaction domain) has an unknown function, a C-terminal extension, and is required for transcription factor activity.

Patient IA-CIC08269 harboured a presumably homozygous c.1920G>A p.(Trp640*) non-sense variant in *TLL5*, since no copy number variant was found. Three additional heterozygous variants were identified in *USH2A*: two missense variants, c.4586A>T p.(Lys1529Ile) and c.6800C>T p.(Pro2267Leu), and one splice variant, c.15297+3A>G p.(?). The p.(Lys1529Ile) variant [19] is considered to be of unknown significance according to ACMG criteria, whereas the not yet reported p.(Pro2267Leu) is classified as likely pathogenic. Loss of the splice donor site was predicted for the c.15297+3A>G variant (SpliceAI score: 0.65;

MaxEnt score: -42.1%). However, it was classified as a VUS in LOVD and in ClinVar. Unfortunately, cosegregation analysis could not be performed due to the lack of parental DNA samples.

We also identified two novel missense variants, c.1474T>A, p.(Trp492Arg) and c.1513A>G, p.(Met505Val), in exons 17 and 18, respectively, located in the region surrounded by the TLL and CID domains. These variants are rare: the first variant has not been reported, and the second is found with a 0.00005% frequency in the non-Finnish European population in gnomAD. The p.(Trp492Arg) variant is highly conserved (Table 2, Figure S2), the physicochemical distance between tryptophan and arginine is high, and the variant is predicted to be pathogenic by most of the predictive tools, with a CADD score of 28.3. The p.(Met505Val) is moderately conserved (Supplementary Figure S2), the physicochemical distance between methionine and valine is small, but the variant is predicted to be pathogenic by 12 of 19 prediction tools, and the CADD score is 23. Both missense variants were classified as variants of unknown significance according to ACMG. However, since each is in trans with a known pathogenic variant, the PM3 criteria could be applied, modifying the class to probably pathogenic. A novel splice variant, c.1282-2A>G p.(?), was identified, which affects the canonical splice site (SpliceAI score 0.85, MaxEnt and SpliceSiteFinder: -100%) and is extremely rare, since gnomAD reported only one case in the non-Finnish European population (Table 2).

2.3. CNV Identification and Breakpoint Characterization

Only one large intragenic deletion in *TLL5* has recently been reported [15] (Figure 2). Interestingly, we identified two additional deletions in this study and specified the breakpoints by whole genome sequencing (Supplementary Figure S3). The first one, c.585+2223_3326+5684del, p.(Pro196Glufs*47), encompassing exons 8–28, is an out-of-frame deletion, and therefore leads to a null allele. The second, c.1487+1134_3741-2607delins15, p.(Ser497_Lys1247del), removes exons 18–30, but maintains the reading frame.

To identify a possible mechanism, the breakpoints identified in patients XZ-358338 and IM-4476 were carefully evaluated by a bioinformatic analysis (Figure S4). For c.585+2223_3326+5684del, the search for repetitive elements revealed the presence of a LINE sequence (HALIME element, 282 base pair (bp) long) at the 5' end junction of the breakpoint, and the presence of one LTR retrotransposon at the 3' end junction (Gypsy, 51 bp). Several regions of microhomology from one to six bp were observed. For c.1487+1134_3741-2607delins15, microhomology sequences ranging from one to six bp were also detected. A 15-bp long insertion (CCTGGATTGTACCT) was observed at the breakpoint. The repetitive element search revealed the presence of an Alu sequence at the 5' end junction of the breakpoint (AluJb motif, 298 bp long), and a DNA/mariner element (Tigger16b, 174 bp long) at the 3' end junction. Oligo(G)_n, inverted and direct repeats were identified at the breakpoints. Despite the identification of microhomologies, repetitive elements, and non-B DNA conformations at the breakpoints, none of these elements could clearly explain the underlying mechanisms for these complex rearrangements and no recurrence shall be expected.

3. Discussion

The present study reports five patients with COD/CORD/EOSRD with mutations in *TLL5*. Six of ten alleles carried novel variants: two nonsense variants, two missense variants, one canonical splice site variant and two large deletions. All five patients were selected from three large French cohorts of IRD patients, among which 450 presented COD or CORD. *TLL5* variants account therefore for 1.1% of COD/CORD patients, which makes *TLL5* one of the rarest gene defect underlying cone disorders [5].

3.1. Phenotype Characteristics

In our series, four adult patients presented a relatively homogeneous disease course, with predominantly cone involvement (two COD and two CORD patients). Of note, three

of our patients had a tritan colour defect, reported in some COD/CORD pedigrees [20,21], progressing towards complete colour blindness, as in subject IM-4476. The stage of retinal degeneration and the perifoveal cone involvement [22] were suggested as the underlying mechanism of selective tritan defect in COD/CORD. These mechanisms are not linked to variants in opsin genes and could also be non-specific [23,24]. Patient EB-163150 had a milder course of retinal degeneration at the first examination (72 y.o.) compared to the three younger patients: only cone-driven ERG responses were altered, and SWAF and SD-OCT showed a milder alteration of outer retinal structures (Figure 1b). These data are in line with previously reported phenotypes [8,13,14].

In contrast, a peculiar clinical picture of early-onset severe retinal dystrophy (EOSRD) was observed in patient IA-CIC08269. EOSRD [25], also known as early-onset retinitis pigmentosa [26,27] or severe early childhood onset retinal dystrophy (SECORD) [28], is a retinal dystrophy usually manifesting before 5–6 years of age. EOSRD is genetically and phenotypically continuum of Leber congenital amaurosis, with patients presenting a better visual function due to more preserved photoreceptors. In addition, nystagmus and eye poking are not observed, and legal blindness is reached around the age of twenty [29]. This EOSRD phenotype in patient IA-CIC08269 might be due to other variants present in *USH2A*, which must be confirmed by cosegregation analysis. Sergouniotis and colleagues reported younger patients with predominant rod photoreceptor involvement [8], but the first clinical signs were more consistent with cone dysfunction (low BCVA and light sensitivity). Another atypical picture closer to a cone dysfunction syndrome, was described in a nine-year-old boy harbouring a homozygous splice site variant in *TLL5* [14]. The initial presentation suggested incomplete congenital stationary night blindness, but with no night blindness complaints, no peripheral vision loss and normal scotopic responses on ffERG. Interestingly, a patient with bilateral mixed hearing loss was also described by Sergouniotis et al. Patient IA-CIC08269 carried three *USH2A* variants, among which a variant of unknown significance, p.(Lys1529Ile), was previously reported in hearing loss [19]. However, no hearing defect on repeated audiometry was detected in our patient. *USH2A* gene defects lead to either syndromic or nonsyndromic IRD [30,31], and we hypothesized that the presence of both *TLL5* and *USH2A* variants might explain the more severe phenotype of IRD, consistent with EOSRD. Similar patients carrying gene defects in more than one IRD-associated gene have already been reported [32].

The EOSRD phenotype raised the question of rod involvement. *TLL5* variants have only been clearly associated with COD/CORD to date. However, some rare cases of retinitis pigmentosa (RP) presumably linked with *TLL5* have been reported in the literature [33,34]. However, no detailed clinical description and no segregation analysis data are available. On the other hand, RP is an umbrella term, and CORD might sometimes fall under this clinical description. The involvement of *TLL5* in RP cannot be ruled out if we consider the phenotypes associated with the connected gene *RPGR*, whose function in photoreceptor cilia requires *TLL5* glutamylation. Indeed, *Tll5*^{-/-} and *Rpgr*^{-/-} mice share common features (early cone involvement and overall long-term disease progression) because both phenotypes are due to a nonfunctional *RPGR*^{ORF15}. In humans, *RPGR*^{ORF15} gene defects are observed in both CORD and RCD patients [35–37]. Sun et al. suggested a selection bias for CORD involvement. However, among 3300 patients with IRD tested in our laboratories, except the EOSRD patient, only patients with a COD/CORD phenotype have been found in association with *TLL5* variants thus far. The reason for the initial rod sparing is not yet understood. Despite common molecular pathways between *TLL5* and the *RPGR* gene, *TLL5* variants may possibly lead to a milder disease than the *RPGR*^{ORF15} variants [12].

3.2. *TLL5* Variants and Structure-Function Correlation

All *TLL5* variants reported to date are located throughout the sequence, but two main hot spots have emerged (Figure 2): the 5' end of the TLL core and a zone surrounded by the TLL core and the cofactor interaction domain (CID), which are the two major functional domains [11,12]. Indeed, the binding of the basic domain of *RPGR*^{ORF15} with the CID

of *TLL5* allows glutamylation of the RPGR^{ORF15} Glu-Gly repeat region by *TLL5*. Most of the reported variants are frameshift, splice site or nonsense variations (10 out of 17 variants in HGMD; 59%) and can disrupt the glutamylase function. Among the novel variants reported in our study, three of them, c.211C>T, c.1920G>A and c.585+2223_3326+5684del, might lead to an absence of protein synthesis due to nonsense-mediated decay (NMD) or a shorter protein. In addition, two variants led to in-frame deletions: the large deletion c.1487+1134_3741-2607delins15 and the c.1282-2A>G splice site variant, which was predicted by all in silico tools to cause exon 16 skipping. For both variants, NMD is not expected, and a truncated and abnormal protein might be produced.

To date, only four missense variants associated with disease have been described in *TLL5*: p.(Glu543Lys) [8], p.(Ile756Phe) [13], and the novel p.(Trp492Arg) and p.(Met505Val). These might be hypomorphic variations with a milder effect. However, the course of the disease in two homozygous carriers for the p.(Glu543Lys) variant described by Sergouniotis et al. and Bedoni et al. seems to be similar to the other patients harbouring loss-of-function mutations [8,13]. A functional study by Sun et al. showed that the p.(Glu543Lys) variant, which preserves the CID domain, severely impairs but maintains trace glutamylation activity towards RPGR^{ORF15} and tubulin. This result supports rather a strong effect of this variant. We hypothesized that polyglutamylase function is impaired not only by a complete loss of function of the protein, but also by an abnormal protein conformation altering the *TLL* and CID domains, leading to reduced or lower levels of polyglutamylase activity [11,12].

Only one large deletion has been reported so far [15]. Large deletions represent 20% of the pathogenic *TLL5* alleles in our study and 10.8% of the total mutational load, considering all reported patients. This suggests that large rearrangements are common in *TLL5* and should be carefully examined. Indeed, the in-silico tool CENSOR (<https://www.girinst.org/censor/>) revealed the presence of a high *Alu* repeat content in the *TLL5* intronic regions. *Alu* repeats are common short interspersed nuclear elements throughout the genome leading to recurrent rearrangements through nonallelic homologous *Alu-Alu* recombination [38]. To decipher the mechanisms underlying the development of deletions, we investigated the local genomic architecture by searching for microhomology regions, repetitive elements, and sequences forming non-B DNA conformations that could all impair the replication process. This analysis identified repetitive elements in the regions surrounding the breakpoints SINE, LINE, LTR, and DNA elements, as previously reported [39], but none of them belonged to the same class, and only one *Alu* sequence was identified, ruling out the possibility of a nonallelic homologous recombination (NAHR) that concerns rearrangements between two repetitive elements of the same family. This could explain the absence of recurrence for the reported rearrangements. Furthermore, the presence of microhomology at breakpoint junctions, ranging from one to six base pairs (bp), and of scars characterized by the insertion of several random nucleotides (15 bp in patient IM-4476) lead us to propose nonhomologous end joining (NHEJ) or replication slippage models as the main mechanisms implicated in large structural rearrangements [40]. Therefore, large deletions should be investigated by standard testing of a patient presenting COD or CORD, especially when only a single nucleotide variant is identified in *TLL5* or in the case of a large region bearing homozygous single nucleotide variants suggestive of heterozygosity loss.

3.3. Genotype-Phenotype Correlations

Similar to other IRDs, phenotypic intersubject variability is not always explained by the underlying genotype. In our series, there was no evidence for a link between *TLL5* variant type and the severity of retinal degeneration. A less severe phenotype was observed in our oldest patient harbouring a splice site defect in *trans* with a likely pathogenic missense variant (EB-163150). As discussed above, loss-of-function defects in *TLL5* do not seem to be more severe than homozygous or compound heterozygous missense variants. For instance, in a similar study, a 53 y.o. man homozygous for p.(Glu543Lys), with adult-

onset cone dystrophy and rod preservation, had the same presentation as two younger patients (38 and 45 y.o.) carrying compound heterozygous truncating mutations [8].

Infertility is reported in the literature but not systematically shared by the patients. Male mouse models lacking the CID or RID domains display infertility and azoospermia, suggesting that patients with truncating mutations may have a higher probability of reduced fertility [9]. In our study, two adult patients out of four had no offspring (IM-4476 and HD-2011304). Although infertility in these patients was not proven, they both carried missense or in-frame deletions, leading to an abnormal conformation of the protein. These potential discrepancies between humans and the *Tll1*^{-/-} mouse model could be explained first by redundant activities among the TLL family members. Although different TLL isoforms are expressed in mice in a tissue-specific manner, all isoforms are highly expressed in the testis [41]. One can speculate that, in humans, other TLL proteins could intervene when TLL5 is defective. Second, the balance between glutamylase and deglutamylase enzymes [10] in the manner of enzymes encoded by the *AGBL5* gene [42] can modulate polyglutamate activity. However, further studies are required to investigate fertility in patients carrying *TLL5* pathogenic variants.

3.4. Future Directions

Due to the rarity of the disorder, international collaborative studies would be necessary to define the full spectrum of *TLL5*-related retinal disease and genotype-phenotype correlations. Middle-age onset and slow progression of retinal degeneration in most patients, combined with the availability of a murine model reproducing the human phenotype and the relatively suitable size of the gene, make *TLL5* a good target for gene therapy approaches.

Polyglutamylases are a large and ubiquitous class of enzymes, and one can expect gene defects in other members of this family to lead to human pathologies. Complementary whole exome and whole genome sequencing studies would be helpful to assess their implication in inherited diseases, not only in retinal degeneration, but also in neurodegenerative and/or fertility disorders.

4. Materials and Methods

4.1. Subject and Clinical Examination

Patients harbouring *TLL5* biallelic variants were retrospectively recruited from the following French institutions: Centre de référence des maladies rares neuro-rétiniennes (REFERET), Centre Hospitalier National d’Ophtalmologie des Quinze-Vingts, Paris (IA-CIC08269), National Center for Rare Genetic Retinal Dystrophies, Hôpital Guy de Chauliac, Montpellier (IM-4476), Fondation Ophtalmologique Adolphe de Rothschild, Paris (EB-163150), Centre de référence pour les affections rares en génétique ophtalmologiques, Hôpitaux Universitaires de Strasbourg, Strasbourg (HD-2011304) and Polyclinique Jules Verne, Nantes (XZ-358338). Informed consent was obtained from all patients and/or their parents when relevant and available. The study protocol adhered to the tenets of the Declaration of Helsinki and was approved by the local ethics committee (No. 2020-A02559-30; 25 November 2020).

Clinical data were retrospectively collected from medical records. These included sex, age at the time of diagnosis and examination, personal and familial history, visual complaints, best-corrected visual acuity (BCVA) assessed by the Early Treatment Diabetic Retinopathy Study (ETDRS) chart, refractive error, slit-lamp biomicroscopy, Lanthony D-15 panel, Goldmann kinetic visual fields (VFs), full-field electroretinogram (ffERG), spectral domain optical coherence tomography (SD-OCT), fundus photography, short wavelength autofluorescence (SWAF), and near-infrared reflectance (NIR) fundus imaging.

4.2. Genetic Analysis

Targeted NGS gene panel: Patients were tested by targeted NGS in three centers (gene panel details in Supplementary Table S1, and strategies are presented in Supplementary

Materials). The target regions comprised the coding exons and their flanking intronic regions. The strategy used for genotyping of subject IA-CIC08269 has been described previously [5,43]. Analysis of patient HD-2011304 was performed according to methods previously described [44].

All single nucleotide variations were confirmed by Sanger sequencing of the *TLL5* exons (OMIM 615860, NM_015072.4) (PCR-sequence conditions are available upon request). Segregation analysis was performed when family members' DNA samples were available.

Copy number variants (CNVs): CNVs were first detected by a quantitative analysis of the data obtained from the NGS pipeline and then confirmed by quantitative PCR (qPCR) using an ABI PRISM 7900 HT instrument (Applied Biosystems, Foster City, CA, USA). Whole genome sequencing (BGI Genomics, Hong Kong) of patients IM-4476 and XZ-358338 followed by targeted analysis of *TLL5* was also performed to delineate the breakpoints. The identification of repetitive elements and microhomology at deletion breakpoints is described in the Supplementary Materials.

Variant pathogenicity assessment: Variant pathogenicity was assessed through our in-house pipeline embedding commercially available bioinformatics software and using data available from public variant databases in accordance with the Guidelines of the American College of Medical Genetics and Genomics [18]. More details are provided in the Supplementary Materials.

Supplementary Materials: The following are available online at <https://www.mdpi.com/article/10.3390/ijms22126410/s1>, Figure S1: Pedigrees of families with *TLL5* variants, Figure S2: Conservation analysis of the novel missense variants on *TLL5*, Figure S3: Large multiexons deletions depicted by IGV screenshots, Figure S4: Multiple sequence alignment and schematic overview of breakpoint analysis, Table S1: List of genes tested.

Author Contributions: Conceptualization, C.-M.D., V.S., J.M., C.Z., H.D., X.Z., I.A., I.M. and E.B.-S.; investigation, V.S., O.G., J.M., C.Z., C.D.O., A.D., J.-L.B., B.B., C.A., V.P., E.L., S.M.-S., S.D.-D., J.-A.S., H.D., X.Z., I.A., I.M., E.B.-S. and C.-M.D.; data curation, C.-M.D., C.Z., J.M., O.G. and C.D.O.; writing—original draft preparation, C.-M.D. and V.S.; writing—review & editing, V.S., O.G., J.M., C.Z., C.D.O., A.D., J.-L.B., B.B., C.A., V.P., E.L., S.M.-S., S.D.-D., J.-A.S., H.D., X.Z., I.A., I.M., E.B.-S. and C.-M.D.; supervision, C.-M.D. All authors have read and agreed to the published version of the manuscript.

Funding: This research was funded by grants from Retina France (C.-M. Dhaenens); LabEx LifeSenses, IHU FORESIGHT, and Fondation Fighting Blindness grant [BR-GE-0619-0761-INSERM] (I. Audo, C. Zeitz). V. Smirnov was supported by RHU-Light 4 Deaf. The Strasbourg RP panel is supported by the French program PHRC I 2013 HUS N° 5724 (J. Muller, H. Dollfus).

Institutional Review Board Statement: The study was conducted according to the guidelines of the Declaration of Helsinki, and approved by the Institutional Review Board (No 2020-A02559-30; 25 November 2020).

Informed Consent Statement: Informed consent was obtained from all subjects involved in the study.

Data Availability Statement: All data are contained within the article or Supplementary Material.

Acknowledgments: We are grateful to C. Piriou and E. Gorecki (Lille University Hospital), A.S. Leuvre and E. Nourisson (Hôpitaux Universitaire de Strasbourg) for technical assistance. The authors are thankful to the patient and family members participating in the study and clinical staff from the Centre d'Investigation Clinique CIC1438 and the National reference center REFERET. DNA samples included in this study originate from NeuroSensCol, a biobank, part of the BioCollections network for research in neuroscience (PI: JA Sahel, coPI I Audo, partner with Centre Hospitalier National d'Ophthalmologie des Quinze-Vingts, INSERM and CNRS).

Conflicts of Interest: The authors declare no conflict of interest.

References

- Hamel, C.P. Cone Rod Dystrophies. *Orphanet J. Rare Dis.* **2007**, *2*, 7. [[CrossRef](#)] [[PubMed](#)]
- Michaelides, M.; Hardcastle, A.J.; Hunt, D.M.; Moore, A.T. Progressive Cone and Cone-Rod Dystrophies: Phenotypes and Underlying Molecular Genetic Basis. *Surv. Ophthalmol.* **2006**, *51*, 232–258. [[CrossRef](#)] [[PubMed](#)]
- Thiadens, A.A.H.J.; Phan, T.M.L.; Zekveld-Vroon, R.C.; Leroy, B.P.; van den Born, L.I.; Hoyng, C.B.; Klaver, C.C.W.; Writing Committee for the Cone Disorders Study Group Consortium; Roosing, S.; Pott, J.-W.R.; et al. Clinical Course, Genetic Etiology, and Visual Outcome in Cone and Cone-Rod Dystrophy. *Ophthalmology* **2012**, *119*, 819–826. [[CrossRef](#)] [[PubMed](#)]
- Michaelides, M.; Hunt, D.M.; Moore, A.T. The Cone Dysfunction Syndromes. *Br. J. Ophthalmol.* **2004**, *88*, 291–297. [[CrossRef](#)] [[PubMed](#)]
- Boulanger-Scemama, E.; El Shamieh, S.; Démontant, V.; Condroyer, C.; Antonio, A.; Michiels, C.; Boyard, F.; Saraiva, J.-P.; Letexier, M.; Souied, E.; et al. Next-Generation Sequencing Applied to a Large French Cone and Cone-Rod Dystrophy Cohort: Mutation Spectrum and New Genotype-Phenotype Correlation. *Orphanet J. Rare Dis.* **2015**, *10*, 85. [[CrossRef](#)] [[PubMed](#)]
- Gill, J.S.; Georgiou, M.; Kalitzeos, A.; Moore, A.T.; Michaelides, M. Progressive Cone and Cone-Rod Dystrophies: Clinical Features, Molecular Genetics and Prospects for Therapy. *Br. J. Ophthalmol.* **2019**. [[CrossRef](#)]
- Tsang, S.H.; Sharma, T. Progressive Cone Dystrophy and Cone-Rod Dystrophy (XL, AD, and AR). *Adv. Exp. Med. Biol.* **2018**, *1085*, 53–60. [[CrossRef](#)] [[PubMed](#)]
- Sergouniotis, P.I.; Chakarova, C.; Murphy, C.; Becker, M.; Lenassi, E.; Arno, G.; Lek, M.; MacArthur, D.G.; UCL-Exomes Consortium; Bhattacharya, S.S.; et al. Biallelic Variants in TLL5, Encoding a Tubulin Glutamylase, Cause Retinal Dystrophy. *Am. J. Hum. Genet.* **2014**, *94*, 760–769. [[CrossRef](#)] [[PubMed](#)]
- Lee, G.-S.; He, Y.; Dougherty, E.J.; Jimenez-Movilla, M.; Avella, M.; Grullon, S.; Sharlin, D.S.; Guo, C.; Blackford, J.A.; Awasthi, S.; et al. Disruption of Tll5/Stamp Gene (Tubulin Tyrosine Ligase-like Protein 5/SRC-1 and TIF2-Associated Modulatory Protein Gene) in Male Mice Causes Sperm Malformation and Infertility. *J. Biol. Chem.* **2013**, *288*, 15167–15180. [[CrossRef](#)]
- van Dijk, J.; Miro, J.; Strub, J.-M.; Lacroix, B.; van Dorsselaer, A.; Edde, B.; Janke, C. Polyglutamylation Is a Post-Translational Modification with a Broad Range of Substrates. *J. Biol. Chem.* **2008**, *283*, 3915–3922. [[CrossRef](#)]
- Mahalingan, K.K.; Keith Keenan, E.; Strickland, M.; Li, Y.; Liu, Y.; Ball, H.L.; Tanner, M.E.; Tjandra, N.; Roll-Mecak, A. Structural Basis for Polyglutamate Chain Initiation and Elongation by TLL Family Enzymes. *Nat. Struct. Mol. Biol.* **2020**, *27*, 802–813. [[CrossRef](#)] [[PubMed](#)]
- Sun, X.; Park, J.H.; Gumerson, J.; Wu, Z.; Swaroop, A.; Qian, H.; Roll-Mecak, A.; Li, T. Loss of RPGR Glutamylase Underlies the Pathogenic Mechanism of Retinal Dystrophy Caused by TLL5 Mutations. *Proc. Natl. Acad. Sci. USA* **2016**, *113*, E2925–E2934. [[CrossRef](#)] [[PubMed](#)]
- Bedoni, N.; Haer-Wigman, L.; Vaclavik, V.; Tran, V.H.; Farinelli, P.; Balzano, S.; Royer-Bertrand, B.; El-Asrag, M.E.; Bonny, O.; Ikonomidis, C.; et al. Mutations in the Polyglutamylase Gene *TLL5*, Expressed in Photoreceptor Cells and Spermatozoa, Are Associated with Cone-Rod Degeneration and Reduced Male Fertility. *Hum. Mol. Genet.* **2016**, dddw282. [[CrossRef](#)] [[PubMed](#)]
- Dias, M.d.S.; Hamel, C.P.; Meunier, I.; Varin, J.; Blanchard, S.; Boyard, F.; Sahel, J.-A.; Zeitz, C. Novel Splice-Site Mutation in TLL5 Causes Cone Dystrophy in a Consanguineous Family. *Mol. Vis.* **2017**, *23*, 131–139. [[PubMed](#)]
- Méjécase, C.; Kozak, I.; Moosajee, M. The Genetic Landscape of Inherited Eye Disorders in 74 Consecutive Families from the United Arab Emirates. *Am. J. Med. Genet. C Semin. Med. Genet.* **2020**, *184*, 762–772. [[CrossRef](#)]
- Patel, N.; Alkuraya, H.; Alzahrani, S.S.; Nowailaty, S.R.; Seidahmed, M.Z.; Alhemidan, A.; Ben-Omran, T.; Ghazi, N.G.; Al-Aqeel, A.; Al-Owain, M.; et al. Mutations in Known Disease Genes Account for the Majority of Autosomal Recessive Retinal Dystrophies. *Clin. Genet.* **2018**, *94*, 554–563. [[CrossRef](#)] [[PubMed](#)]
- Zampaglione, E.; Kinde, B.; Place, E.M.; Navarro-Gomez, D.; Maher, M.; Jamshidi, F.; Nassiri, S.; Mazzone, J.A.; Finn, C.; Schlegel, D.; et al. Copy-Number Variation Contributes 9% of Pathogenicity in the Inherited Retinal Degenerations. *Genet. Med. Off. J. Am. Coll. Med. Genet.* **2020**, *22*, 1079–1087. [[CrossRef](#)]
- Richards, S.; Aziz, N.; Bale, S.; Bick, D.; Das, S.; Gastier-Foster, J.; Grody, W.W.; Hegde, M.; Lyon, E.; Spector, E.; et al. Standards and Guidelines for the Interpretation of Sequence Variants: A Joint Consensus Recommendation of the American College of Medical Genetics and Genomics and the Association for Molecular Pathology. *Genet. Med. Off. J. Am. Coll. Med. Genet.* **2015**, *17*, 405–424. [[CrossRef](#)]
- Sloan-Heggen, C.M.; Bierer, A.O.; Shearer, A.E.; Kolbe, D.L.; Nishimura, C.J.; Frees, K.L.; Ephraim, S.S.; Shibata, S.B.; Booth, K.T.; Campbell, C.A.; et al. Comprehensive Genetic Testing in the Clinical Evaluation of 1119 Patients with Hearing Loss. *Hum. Genet.* **2016**, *135*, 441–450. [[CrossRef](#)]
- van Schooneveld, M.J.; Went, L.N.; Oosterhuis, J.A. Dominant Cone Dystrophy Starting with Blue Cone Involvement. *Br. J. Ophthalmol.* **1991**, *75*, 332–336. [[CrossRef](#)]
- Kohl, S.; Llavona, P.; Sauer, A.; Reuter, P.; Weisschuh, N.; Kempf, M.; Dehmelt, F.A.; Arrenberg, A.B.; Sliesoraityte, I.; Zrenner, E.; et al. A Duplication on Chromosome 16q12 Affecting the IRXB Gene Cluster Is Associated with Autosomal Dominant Cone Dystrophy with Early Tritanopic Color Vision Defect. *Hum. Mol. Genet.* **2021**. [[CrossRef](#)]
- Pinckers, A. Dominant Cone Dystrophy Starting with Blue Cone Involvement. *Br. J. Ophthalmol.* **1992**, *76*, 127. [[CrossRef](#)]
- Zrenner, E.; Nowicki, J.; Adamczyk, R. Cone Function and Cone Interaction in Hereditary Degenerations of the Central Retina. *Doc. Ophthalmol.* **1986**, *62*, 5–12. [[CrossRef](#)]
- Simunovic, M.P. Acquired Color Vision Deficiency. *Surv. Ophthalmol.* **2016**, *61*, 132–155. [[CrossRef](#)]

25. Kumaran, N.; Moore, A.T.; Weleber, R.G.; Michaelides, M. Leber Congenital Amaurosis/Early-Onset Severe Retinal Dystrophy: Clinical Features, Molecular Genetics and Therapeutic Interventions. *Br. J. Ophthalmol.* **2017**, *101*, 1147–1154. [[CrossRef](#)]
26. Foxman, S.G.; Heckenlively, J.R.; Bateman, J.B.; Wirtschafter, J.D. Classification of Congenital and Early Onset Retinitis Pigmentosa. *Arch. Ophthalmol. Chic. Ill. 1960* **1985**, *103*, 1502–1506. [[CrossRef](#)] [[PubMed](#)]
27. Lorenz, B.; Gyürüs, P.; Preising, M.; Bremser, D.; Gu, S.; Andrassi, M.; Gerth, C.; Gal, A. Early-Onset Severe Rod-Cone Dystrophy in Young Children with RPE65 Mutations. *Invest. Ophthalmol. Vis. Sci.* **2000**, *41*, 2735–2742. [[PubMed](#)]
28. Weleber, R.G.; Michaelides, M.; Trzuppek, K.M.; Stover, N.B.; Stone, E.M. The Phenotype of Severe Early Childhood Onset Retinal Dystrophy (SECORD) from Mutation of RPE65 and Differentiation from Leber Congenital Amaurosis. *Invest. Ophthalmol. Vis. Sci.* **2011**, *52*, 292–302. [[CrossRef](#)]
29. Kumaran, N.; Pennesi, M.E.; Yang, P.; Trzuppek, K.M.; Schlechter, C.; Moore, A.T.; Weleber, R.G.; Michaelides, M. Leber Congenital Amaurosis / Early-Onset Severe Retinal Dystrophy Overview. In *GeneReviews*[®]; Adam, M.P., Ardinger, H.H., Pagon, R.A., Wallace, S.E., Bean, L.J., Mirzaa, G., Amemiya, A., Eds.; University of Washington, Seattle: Seattle, WA, USA, 1993.
30. McGee, T.L.; Seyedahmadi, B.J.; Sweeney, M.O.; Dryja, T.P.; Berson, E.L. Novel Mutations in the Long Isoform of the USH2A Gene in Patients with Usher Syndrome Type II or Non-Syndromic Retinitis Pigmentosa. *J. Med. Genet.* **2010**, *47*, 499–506. [[CrossRef](#)] [[PubMed](#)]
31. Seyedahmadi, B.J.; Rivolta, C.; Keene, J.A.; Berson, E.L.; Dryja, T.P. Comprehensive Screening of the USH2A Gene in Usher Syndrome Type II and Non-Syndromic Recessive Retinitis Pigmentosa. *Exp. Eye Res.* **2004**, *79*, 167–173. [[CrossRef](#)]
32. Méjécase, C.; Hummel, A.; Mohand-Saïd, S.; Andrieu, C.; El Shamieh, S.; Antonio, A.; Condroyer, C.; Boyard, F.; Foussard, M.; Blanchard, S.; et al. Whole Exome Sequencing Resolves Complex Phenotype and Identifies CC2D2A Mutations Underlying Non-Syndromic Rod-Cone Dystrophy. *Clin. Genet.* **2019**, *95*, 329–333. [[CrossRef](#)] [[PubMed](#)]
33. Gao, F.-J.; Li, J.-K.; Chen, H.; Hu, F.-Y.; Zhang, S.-H.; Qi, Y.-H.; Xu, P.; Wang, D.-D.; Wang, L.-S.; Chang, Q.; et al. Genetic and Clinical Findings in a Large Cohort of Chinese Patients with Suspected Retinitis Pigmentosa. *Ophthalmology* **2019**, *126*, 1549–1556. [[CrossRef](#)]
34. Sharon, D.; Ben-Yosef, T.; Goldenberg-Cohen, N.; Pras, E.; Gradstein, L.; Soudry, S.; Mezer, E.; Zur, D.; Abbasi, A.H.; Zeitz, C.; et al. A Nationwide Genetic Analysis of Inherited Retinal Diseases in Israel as Assessed by the Israeli Inherited Retinal Disease Consortium (IIRDC). *Hum. Mutat.* **2020**, *41*, 140–149. [[CrossRef](#)] [[PubMed](#)]
35. Di Iorio, V.; Karali, M.; Melillo, P.; Testa, F.; Brunetti-Pierri, R.; Musacchia, F.; Condroyer, C.; Neidhardt, J.; Audo, I.; Zeitz, C.; et al. Spectrum of Disease Severity in Patients With X-Linked Retinitis Pigmentosa Due to RPGR Mutations. *Invest. Ophthalmol. Vis. Sci.* **2020**, *61*, 36. [[CrossRef](#)] [[PubMed](#)]
36. Hadalin, V.; Šuštar, M.; Volk, M.; Maver, A.; Sajovic, J.; Jarc-Vidmar, M.; Peterlin, B.; Hawlina, M.; Fakin, A. Cone Dystrophy Associated with a Novel Variant in the Terminal Codon of the RPGR-ORF15. *Genes* **2021**, *12*. [[CrossRef](#)] [[PubMed](#)]
37. Nguyen, X.-T.-A.; Talib, M.; van Schooneveld, M.J.; Brinks, J.; Ten Brink, J.; Florijn, R.J.; Wijnholds, J.; Verdijk, R.M.; Bergen, A.A.; Boon, C.J.F. RPGR-Associated Dystrophies: Clinical, Genetic, and Histopathological Features. *Int. J. Mol. Sci.* **2020**, *21*. [[CrossRef](#)] [[PubMed](#)]
38. Vissers, L.E.L.M.; Bhatt, S.S.; Janssen, I.M.; Xia, Z.; Lalani, S.R.; Pfundt, R.; Derwinska, K.; de Vries, B.B.A.; Gilissen, C.; Hoischen, A.; et al. Rare Pathogenic Microdeletions and Tandem Duplications Are Microhomology-Mediated and Stimulated by Local Genomic Architecture. *Hum. Mol. Genet.* **2009**, *18*, 3579–3593. [[CrossRef](#)] [[PubMed](#)]
39. Van Schil, K.; Naessens, S.; Van de Sompele, S.; Carron, M.; Aslanidis, A.; Van Cauwenbergh, C.; Mayer, A.K.; Van Heetvelde, M.; Bauwens, M.; Verdin, H.; et al. Correction: Mapping the Genomic Landscape of Inherited Retinal Disease Genes Prioritizes Genes Prone to Coding and Noncoding Copy-Number Variations. *Genet. Med. Off. J. Am. Coll. Med. Genet.* **2019**, *21*, 1998. [[CrossRef](#)]
40. Lieber, M.R. The Mechanism of Double-Strand DNA Break Repair by the Nonhomologous DNA End-Joining Pathway. *Annu. Rev. Biochem.* **2010**, *79*, 181–211. [[CrossRef](#)] [[PubMed](#)]
41. van Dijk, J.; Rogowski, K.; Miro, J.; Lacroix, B.; Eddé, B.; Janke, C. A Targeted Multienzyme Mechanism for Selective Microtubule Polyglutamylolation. *Mol. Cell* **2007**, *26*, 437–448. [[CrossRef](#)]
42. Astuti, G.D.N.; Arno, G.; Hull, S.; Pierrache, L.; Venselaar, H.; Carss, K.; Raymond, F.L.; Collin, R.W.J.; Faradz, S.M.H.; van den Born, L.I.; et al. Mutations in AGBL5, Encoding α -Tubulin Deglutamylase, Are Associated With Autosomal Recessive Retinitis Pigmentosa. *Invest. Ophthalmol. Vis. Sci.* **2016**, *57*, 6180–6187. [[CrossRef](#)] [[PubMed](#)]
43. Audo, I.; Bujakowska, K.M.; Léveillard, T.; Mohand-Saïd, S.; Lancelot, M.-E.; Germain, A.; Antonio, A.; Michiels, C.; Saraiva, J.-P.; Letexier, M.; et al. Development and Application of a Next-Generation-Sequencing (NGS) Approach to Detect Known and Novel Gene Defects Underlying Retinal Diseases. *Orphanet J. Rare Dis.* **2012**, *7*, 8. [[CrossRef](#)] [[PubMed](#)]
44. Geoffroy, V.; Stoetzel, C.; Scheidecker, S.; Schaefer, E.; Perrault, I.; Bär, S.; Kröll, A.; Delbarre, M.; Antin, M.; Leuvrey, A.-S.; et al. Whole-Genome Sequencing in Patients with Ciliopathies Uncovers a Novel Recurrent Tandem Duplication in IFT140. *Hum. Mutat.* **2018**, *39*, 983–992. [[CrossRef](#)] [[PubMed](#)]

3.5. Novel phenotype of congenital stationary night blindness associated with missense variants in *VSX2*

Our group is collaborating world-wide with many clinical centers and identified 10 genes underlying congenital stationary night blindness (CSNB). Exploring our cohort of unsolved cases with CSNB, we found three patients from two unrelated families harboring pathogenic variants in *VSX2*, which is a major gene important for early pan-ocular development and more particularly for bipolar cell fate and maintenance[174]. It was a collaborative work between Laboratory of Genetics in Ophthalmology (LGO), INSERM UMR1163, Institute of Genetic Diseases, Imagine and Paris University, Ophthalmology Department, Hôpital Universitaire Necker-Enfants Malades and our center.

The clinical phenotype of our CSNB patients was different than described earlier, including ciliary body hypoplasia with lens luxation and early cataracts. Also, from the electrophysiological point of view, we noted a peculiar full-field ERG appearance, suggestive of all-bipolar cell dysfunction, never described before. These clinical findings perfectly match observations on existing *Vsx2* knock-out animal models.

This work is published in *JAMA Ophthalmology*[175]. It was also presented as poster at ARVO 2022 meeting in Denver, USA and as an oral presentation at ISCEV 2022 meeting in Liverpool, UK.

Association of Missense Variants in *VSX2* With a Peculiar Form of Congenital Stationary Night Blindness Affecting All Bipolar Cells

Vasily M. Smirnov, MD; Matthieu P. Robert, MD, PhD; Christel Condroyer; Julien Navarro, MSc; Aline Antonio, BS; Jean-Michel Rozet, PhD; José-Alain Sahel, MD, PhD; Isabelle Perrault, PhD; Isabelle Audo, MD, PhD; Christina Zeitz, PhD

 Supplemental content

IMPORTANCE Congenital stationary night blindness (CSNB) is an inherited stationary retinal disorder that is clinically and genetically heterogeneous. To date, the genetic association between some cases with CSNB and an unusual complex clinical picture is unclear.

OBJECTIVE To describe an unreported CSNB phenotype and the associated gene defect in 3 patients from 2 unrelated families.

DESIGN, SETTING, AND PARTICIPANTS This retrospective case series was conducted in 2021 and 2022 at a national referral center for rare ocular diseases. Data for 3 patients from a cohort of 140 genetically unsolved CSNB cases were analyzed clinically and genetically.

EXPOSURES Complete ocular examination including full-field electroretinography and multimodal fundus imaging (spectral-domain optical coherence tomography, color, infrared reflectance, and short-wavelength autofluorescence photographs) were performed. The gene defect was identified by exome sequencing and confirmed by Sanger sequencing and co-segregation analysis in 1 family. Screening was performed for genetically unsolved CSNB cases for *VSX2* variants by direct Sanger sequencing.

MAIN OUTCOMES AND MEASURES Ocular and molecular biology findings.

RESULTS The series included 3 patients whose clinical investigations occurred at ages in the early 30s, younger than 12 years, and in the mid 40s. They had nystagmus, low stable visual acuity, and myopia from birth and experienced night blindness. Two older patients had bilateral lens luxation and underwent lens extraction. Full-field electroretinography revealed an electronegative Schubert-Bornschein appearance, combining characteristics of incomplete and complete CSNB, affecting the function of rod and cone ON- and OFF-bipolar cells. Exome sequencing and co-segregation analysis in a consanguineous family with 2 affected members identified a homozygous variant in *VSX2*. Subsequently, screening of the CSNB cohort identified another unrelated patient harboring a distinct *VSX2* variant.

CONCLUSIONS AND RELEVANCE This case series revealed a peculiar pan-bipolar cell retinopathy with lens luxation associated with variants in *VSX2*. Clinicians should be aware of this association and *VSX2* added to CSNB diagnostic gene panels.

JAMA Ophthalmol. doi:10.1001/jamaophthalmol.2022.4146
Published online October 20, 2022.

Author Affiliations: Author affiliations are listed at the end of this article.

Corresponding Authors: Christina Zeitz, PhD, Institut de la Vision, Department of Genetics, INSERM UMR S968, CNRS UMR 7210, Sorbonne University, 17 rue Moreau, 75012 Paris, France (christina.zeitz@inserm.fr); Isabelle Audo, MD, PhD, INSERM UMR S968, CNRS UMR 7210, Sorbonne University, Institut de la Vision, 17 rue Moreau, 75012 Paris, France (isabelle.audo@inserm.fr).

© 2022 American Medical Association. All rights reserved.

Downloaded From: <https://jamanetwork.com/> by a UNIVERSITE PIERRE ET MARIE CURIE (UPMC) User on 10/20/2022

E1

Congenital stationary night blindness (CSNB) with largely normal fundus appearance is a vast group of genetically and clinically heterogeneous congenital retinal disorders. The most common form manifests with infantile nystagmus, reduced visual acuity, variable degree of myopia, poor visual behavior in dim lighting, and/or photophobia.¹ The diagnosis is ascertained by full-field electroretinography (ffERG) displaying characteristic waveform changes.

Under dark adaptation (DA), the stimulation with a dim flash (DA 0.01 ERG, dark-adapted 0.01 cd/m²) generates a positive-going b-wave reflecting the rod ON-bipolar cell depolarization.² In the same dark-adapted conditions, the stimulations with brighter flashes (DA 3.0 ERG, DA 10.0 ERG) produce a negative a-wave, reflecting the hyperpolarization of photoreceptors, mainly dominated by rods in this adaptation state,^{3,4} followed by a positive b-wave, for which the ascending limb is dominated by ON-bipolar cell depolarization.⁵ Under light-adapted conditions, the stimulations with bright flashes (LA 3.0 ERG, light adapted 3.0 cd/m²) lead to a negative a-wave generated by the hyperpolarization of cones and then of OFF-bipolar cells. The second deflection is a positive b-wave, for which the ascending limb is dominated by cone ON-bipolar cell depolarization and descending limb by OFF-bipolar cell hyperpolarization.^{6,7} Long-duration stimulations allow the separation of responses generated by cone ON- and OFF-bipolar pathway.^{6,8}

Most of the patients with CSNB have a distinct Schubert-Bornschein electronegative waveform (b/a amplitude ratio <1) under dark-adapted conditions,⁹ in relation to a signaling defect from photoreceptors to adjacent bipolar cells. Two subtypes of Schubert-Bornschein CSNB can be distinguished on the basis of additional ffERG features: incomplete (icCSNB) and complete (cCSNB).¹⁰ In icCSNB, there is a preserved but reduced and delayed b-wave to the DA 0.01 ERG.¹⁰ Light-adapted responses are markedly reduced and delayed, reflecting a cone-to-cone ON- and OFF-bipolar cell transmission defect, which can be documented using long-duration stimulations.^{10,11} Patients have variable degrees of night blindness, strabismus, and nystagmus; a wide range of refractive errors¹²; and a normal fundus, apart from myopic changes. Photophobia may be the main concern for some patients who also experience difficulties in dimly lit environments. Pathogenic variants in *CACNA1F* (OMIM 300110)^{13,14} and *CABP4* (OMIM 608965)¹⁵ lead to icCSNB. Variants were also identified in *CACNA2D4* (OMIM 608171)¹⁶ in patients initially diagnosed with icCSNB but later associated with a cone dystrophy.¹⁷ Proteins encoded by these genes are localized at the presynaptic membrane of both rods and cones. They play a role in glutamate release into the synaptic cleft. Thus, icCSNB represents a photoreceptor to ON- and OFF-bipolar cell transmission defect.¹ Light sensitivity present in patients with icCSNB may be explained by the worse dysfunction in cone bipolar circuitry, unlike in other forms of CSNB.¹² In cCSNB, the b-wave is typically absent on the DA 0.01 ERG. The a-wave has typically a square shape with a sharply arising b-wave and a reduced b/a amplitude ratio at the LA 3.0 ERG,¹⁰ with absence of ON-bipolar responses but preserved OFF responses to long-duration stimulations.¹⁸ Patients with cCSNB present consis-

Key Points

Question What are the detailed clinical picture and underlying gene defect in patients with a peculiar form of congenital stationary night blindness (CSNB)?

Findings In this case series, we report on 3 patients from 2 families with CSNB, anterior segment abnormalities (ciliary body hypoplasia and lens luxation), and all-bipolar cell dysfunction. We identified 2 genetic variants in *VSX2*, a major gene important for ocular development and bipolar cell fate, in those families with CSNB.

Meaning This genetic defect of an inherited ocular disease has both functional and anatomical eye defects.

tently with high myopia, nystagmus, night blindness, and low visual acuity.¹² Variants in *NYX* (OMIM 300278),^{13,19} *GRM6* (OMIM 604096),^{20,21} *TRPM1* (OMIM 603576),²²⁻²⁴ *GPR179* (OMIM 614515),²⁵ and *LRIT3* (OMIM 615004)²⁶ lead to cCSNB. Genes listed above code for proteins localized mainly in the dendritic tips of the ON-bipolar cells. They are important for glutamate-induced signaling. Thus, cCSNB represents a photoreceptor to ON-bipolar cell transmission defect.¹

Other rare forms of CSNB with a different ERG and clinical phenotype have been associated with *SAG* (OMIM 181031), *GNAT1* (OMIM 139330), *RHO* (OMIM 180380), *PDE6B* (OMIM 180072), *GRK1* (OMIM 180381), and *SLC24A1* (OMIM 603617).¹ The goal of this study was to report an unusual CSNB phenotype and associated gene defects in 3 patients from 2 unrelated Turkish families.

Methods

Research procedures adhered to the tenets of the Declaration of Helsinki and were approved by the local ethics committee (CPP, Ile de France V, project 06693, N°EUDRACT 2006-A00347-44, December 11, 2006, and CPP, Ile de France II). Prior to testing, written informed consent was obtained from 2 adult participants and the parents of a participant who was younger than 18 years. No compensation or incentive was offered to patients to participate in the study. Relevant reporting guidelines were followed.

Clinical Studies

The cases were clinically investigated at the national reference center for rare ocular diseases REFERET of the Centre Hospitalier National d'Ophtalmologie (CHNO) des Quinze-Vingts as previously described.²⁷ Patient 2 was also assessed at the national reference center for rare ocular diseases OPHTARA of Necker-Enfants Malades Hospital as an infant (<6 months old).

Genetic Analysis

Blood samples from cases and all available family members were collected for genetic research, and genomic DNA was extracted as previously reported.²⁸ These DNA samples were collected within the NeuroSensCol DNA bank for research in neuroscience.

Direct Sanger sequencing was performed for patient 1 for all exons and exon-intron boundaries of the genes *CACNA1F*, *NYX*, *TRPM1*, *LRIT3*, *GRM6*, *GPR179*, *CABP4*, and *CACNA2D4* and for some other genes associated with inner retinal dysfunctions: *RIMS2*, *GNB3*, and *GNB5*. (The amplification and sequencing conditions can be obtained on request.)

Patient 2 was analyzed on a next-generation sequencing (NGS) molecular diagnostic panel, including CSNB- and pediatric retinal degeneration-associated genes (eTable 1 in the Supplement). Subsequently, exome sequencing was performed in the patient and both parents. Genomic DNA libraries were generated from DNA sheared with a Covaris S2 Ultrasonicator via SureSelectXT Library Prep Kit (Agilent). Regions of interest were captured with the SureSelect All Exon V5 kit (Agilent) and sequenced on an Illumina HiSeq2500 HT system (Illumina). Data analysis was performed with a homemade pipeline (POLYWEB)²⁹ created by the Imagine Institute Bioinformatics core facilities of Paris University. Considering that pathogenic variants are uncommon, we searched for recessive variants absent in the dbSNP, 1000 Genomes, EVS, ExAC, gnomAD, and all in-house databases and for variants with minor allele frequency up to 0.01. We searched in priority for homozygous consensus splice-site changes, nonsense variants, insertions, and deletions in coding regions. After this stringent filtering, variants in 4 candidate genes (*ITIH2*, *PRDM10*, *VSX2*, and *BCR*) were identified. All variants were classified using Human Genome Variation Society nomenclature,³⁰ and their pathogenicity was assessed in accordance with the American College of Medical Genetics and Genomics (ACMG) recommendations.³¹ Validation of putative pathogenic variants and a co-segregation study were performed by direct Sanger sequencing of exons of interest in all available family members.

In a second step, a cohort of 140 unsolved CSNB cases was screened for *VSX2* variants. One additional patient (patient 3) was identified. He previously had negative results on an NGS panel³² including all known-to-date CSNB-associated genes.

Results

Patients 1, 2, and 3 were clinically investigated at ages in the early 30s, younger than 12 years, and in the mid 40s, respectively. All 3 patients had infantile nystagmus, low visual acuity, myopia, and night blindness from birth, but the adult patients did not report changes in their symptoms or vision since childhood. Clinical data are summarized in the Table.

Their fERG recordings (Figure 1) under dark-adapted conditions showed no detectable responses to a dim 0.01 cd/m² flash (DA 0.01 ERG), a normal a-wave, but a severely reduced b-wave, leading to an electronegative waveform to bright flashes (DA 3.0 and DA 10.0 ERG). These alterations resembled ON-bipolar dysfunction in cCSNB. However, light-adapted responses to a 3 cd/m² single flash and to a 30 Hz, 3 cd/m² flicker (LA 3.0 ERG and LA 3.0 flicker) were reduced and delayed, unlike patients with cCSNB but resembling functional alterations in icCSNB.¹

The female patient 1 was referred to our clinic in her early 30s. Best-corrected visual acuity was 20/200 OU. Color vision was normal. Goldmann visual field was flattened in the superior part on all target sizes. Static visual field found a diffuse reduction of retinal sensitivity and reduction of foveal threshold. Both lenses were subluxated superiorly and showed cataract. Ophthalmoscopic evaluation revealed typical myopic changes, including oval tilted optic discs surrounded with peripapillary chorioretinal atrophy, thin retinas with increased visibility of choroidal vasculature, and narrowed retinal vessels (Figure 2A). Numerous glistening white crystals and atrophic chorioretinal patches were visible in the peripheral retina (Figure 2A). Infrared reflectance (eFigure 1B in the Supplement) and short-wavelength fundus autofluorescence (eFigure 1C in the Supplement) were unremarkable. Spectral-domain optical coherence tomography (SD-OCT) was not performed at the first visit. The patient underwent intracapsular cataract extraction without intraocular lens implantation. Best-corrected visual acuity improved to 20/63 OU.

The male patient 2, a nephew of patient 1, was referred to the clinic as a young child. Convergent squint and infantile nystagmus syndrome with an initial intermittent and transient up-beat component were present during infancy. Slitlamp examination results were unremarkable. Fundus examination revealed similar myopic changes as reported in the aunt (Figure 2B). In the peripheral retina, there was 360° white without pressure. Preserved outer retina and thinned inner retinal layers were shown on SD-OCT (Figure 2C). Multimodal retinal imaging was difficult due to nystagmus, with unremarkable infrared reflectance and short-wavelength fundus autofluorescence (eFigure 1E in the Supplement).

The male patient 3, from an unrelated family, was referred to the clinic when in his middle 40s. He had infantile nystagmus and poor vision since birth. In his early 40s, he underwent intracapsular lens extraction for bilateral subluxated cataract. Ultrasound biomicroscopy revealed hypoplastic ciliary body and posterior iris bowing (eFigure 2 in the Supplement). Ophthalmoscopic examination revealed triangular atrophic chorioretinal lesions inferior to the macula and white without pressure in the peripheral retina (Figure 3A). Atrophic chorioretinal lesions were hypoautofluorescent with hyperautofluorescent edges on short-wavelength fundus autofluorescence (Figure 3B) and were bright on infrared reflectance (Figure 3C) with outer retinal disruption on SD-OCT. Grade 3 foveal hypoplasia³³ as well as a thin epimacular membrane could be seen on SD-OCT (Figure 3D).

Genetic Assessment

Patients 1 and 2 were members of a family with North Turkish ancestry and were born from consanguineous unions (Figure 4A). Patient 3 was also of Turkish ancestry (Figure 4B). He did not report parental consanguinity.

Sanger sequencing and targeted NGS revealed the absence of disease-causing variants in patients 1 and 2, respectively. Exome sequencing performed in patient 2 and his parents revealed homozygous putative disease-causing variants in the genes *ITIH2* (OMIM 146640), *PRDM10* (OMIM 618319), *BCR* (OMIM 151410), and *VSX2* (OMIM 142993), consistent with

Table. Clinical Characteristics of Patients

Patient No., age at first assessment	BCVA, Snellen	Refraction	Axial length, mm	Color vision (15 hue Lanthony)	Visual field	ffERG	Anterior segment	Fundus	SW-FAF	OCT
Family with c.595C>T, p.(Arg199Cys)										
Patient 1, early 30s	20/200 OD, 20/200 OS; 20/63 OD, 20/63 OS after cataract surgery	-15.0 OD, -15.0 OS	28.76 OD, 28.23 OS	Normal	GP: superior flattening at all target sizes; SP: diffuse reduction of retinal sensitivity; MD: -6.6 dB OD, -10.2 dB OS; FT: 25 dB OU	DA 0.01: undetectable; DA 3.0, DA 10.0: electronegative Schubert-Bornschein configuration; LA 3.0, LA 3.0 flicker: severely	Superior lens subluxation OU; cataract OU; phaco- and iridodonesis	Oval pale tilted discs, peripapillary chorioretinal atrophy, vascular narrowing, increased visibility of choroidal vasculature, white glaustring crystals, atrophic patches, and retinal tears in peripheral retina	Normal	NA
Patient 2, <12 y	20/200 OU	-10.50 (-1.50) 17.5° OD; -8.75 (-1.50) 155° OS, cycloplegic	24.77 OD, 24.43 OS	NA	NA	DA 0.01: undetectable; DA 3.0, DA 10.0: electronegative Schubert-Bornschein configuration; LA 3.0, LA 3.0 flicker: reduced and delayed	Normal	Oval pale tilted discs, peripapillary chorioretinal atrophy, vascular narrowing, increased visibility of choroidal vasculature; white without pressure in peripheral retina	Normal	Preserved outer retina; thinned inner retinal layers
Family with c.698C>T, p.(Pro233Leu)										
Patient 3, mid 40s	20/50 OD, 20/100 OS	+2.0 OD, +3.50 (-0.50) 90° OS after cataract surgery; -2.75 (-3.0) 0° OD, -3.0 (-3.5) 25° OS before surgery	22.3 OD, 21.94 OS	NA	SP: diffuse reduction of retinal sensitivity	DA 0.01: undetectable; DA 3.0, DA 10.0: electronegative Schubert-Bornschein configuration; LA 3.0, LA 3.0 flicker: reduced	Pseudophakic OU; UBM: hypoplastic ciliary body; surgery for lens subluxation and cataracts in both eyes in early 40s	Normal discs, mild vascular narrowing, vessels crossing fovea, increased visibility of choroidal vasculature, triangular zone of chorioretinal atrophy, pointing macula inferiorly	Triangular hypoauto- fluorescent lesion with hyperauto- fluorescent edges	Grade 3 foveal hypoplasia; disappearance of outer reflective layers corresponding to atrophic fundus lesion

Abbreviations: BCVA, best-corrected visual acuity; DA, dark adapted; ffERG, full-field electroretinography; FT, foveal threshold; GP, Goldman perimetry; LA, light adapted; MD, mean deficit; NA, not available; OCT, optical coherence tomography; SP, automated static perimetry; SW-FAF, short-wavelength fundus autofluorescence; UBM, ultrasound biomicroscopy.

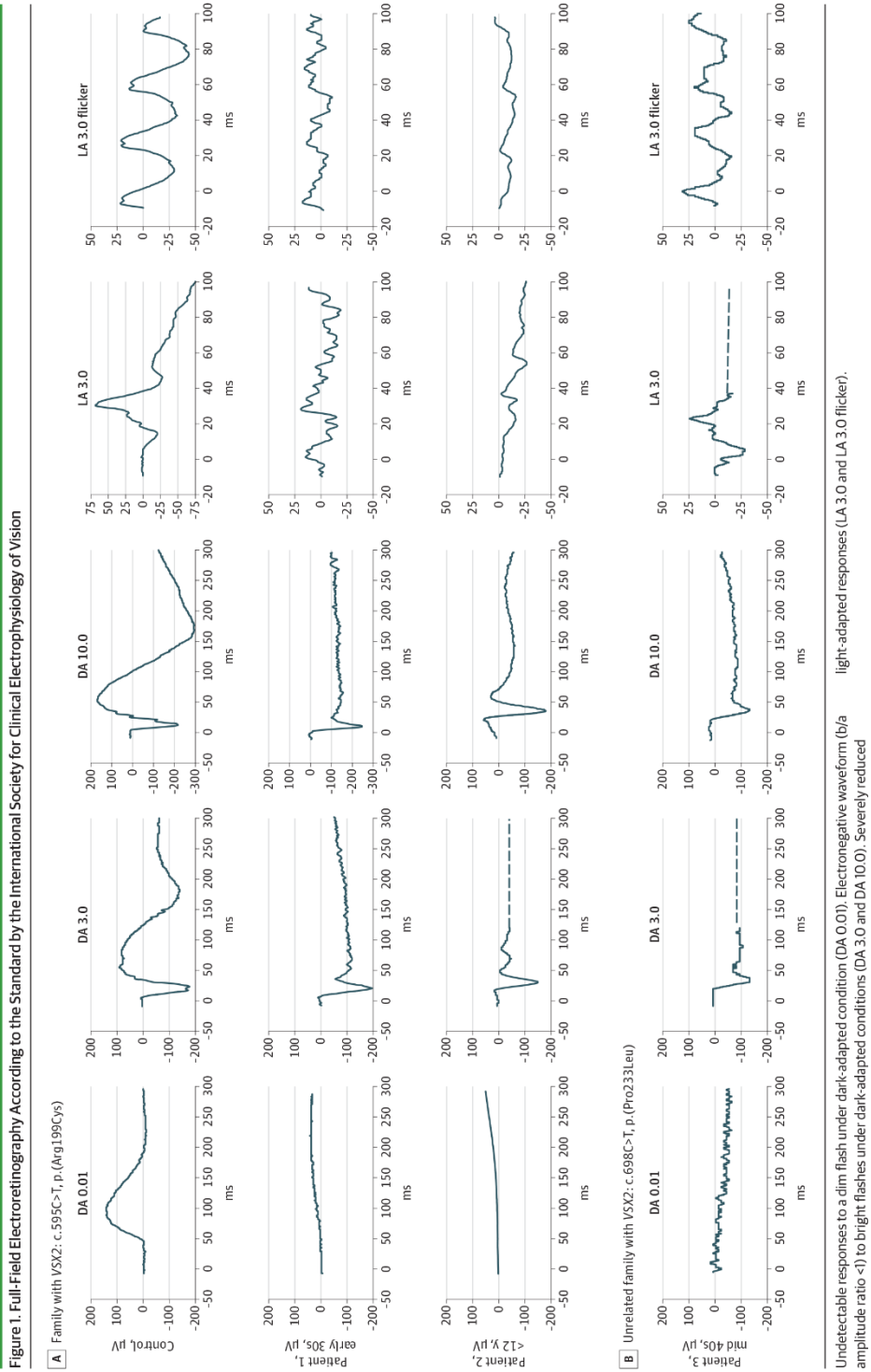
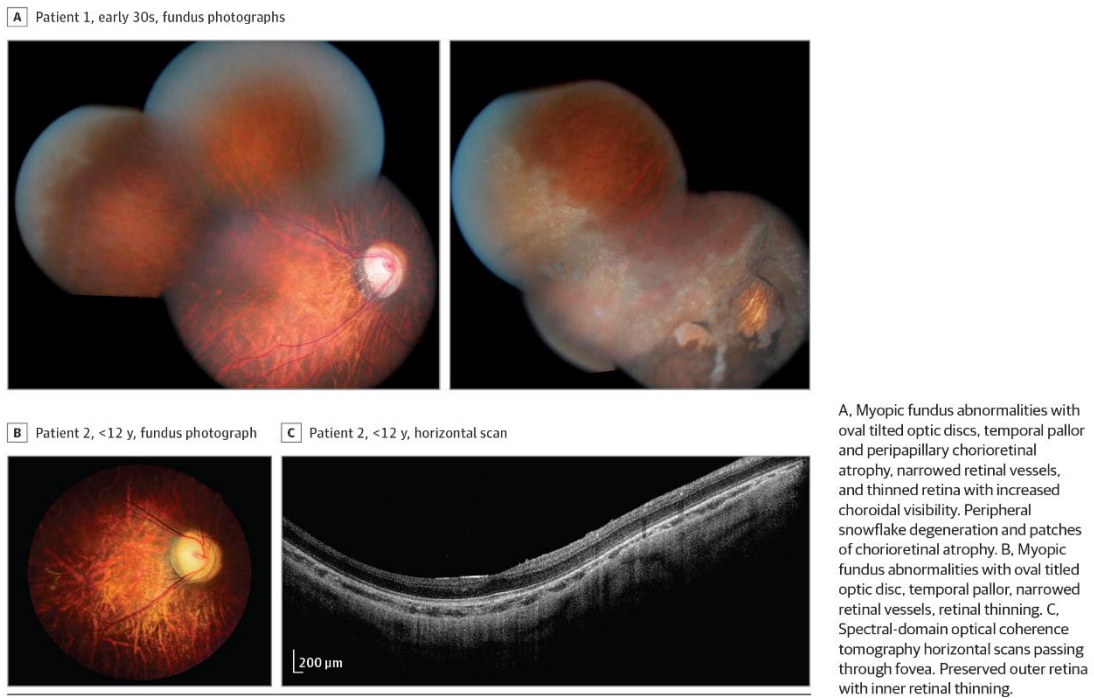


Figure 2. Retinal Findings in Patients 1 and 2 From the Same Family



autosomal-recessive inheritance (eTable 2 in the Supplement). However, only the missense variant in *VSX2* (NM_182894.3): c.595C>T, p.(Arg199Cys) co-segregated with the disease (Figure 4C). This variant is rare in population databases (minor allele frequency 8×10^{-6} in gnomAD; not present in the ExAC database) is predicted to be damaging by 25 of 40 prediction algorithms available at VarSome.³⁴ Thus, this variant is considered likely pathogenic by ACMG standards (with evidence classified as PM1, PM2, PP1-M, and PP3).³¹ *VSX2* Sanger sequencing in patient 3 revealed another missense homozygous variant: c.698C>T, p.(Pro233Leu) (Figure 4C). This variant is absent in population databases and predicted damaging by all the prediction algorithms available at VarSome.³⁴ It is considered a variant of unknown significance by ACMG standards (PM2, PML, PP3). Unfortunately, other members of the family were not available for co-segregation analyses.

Discussion

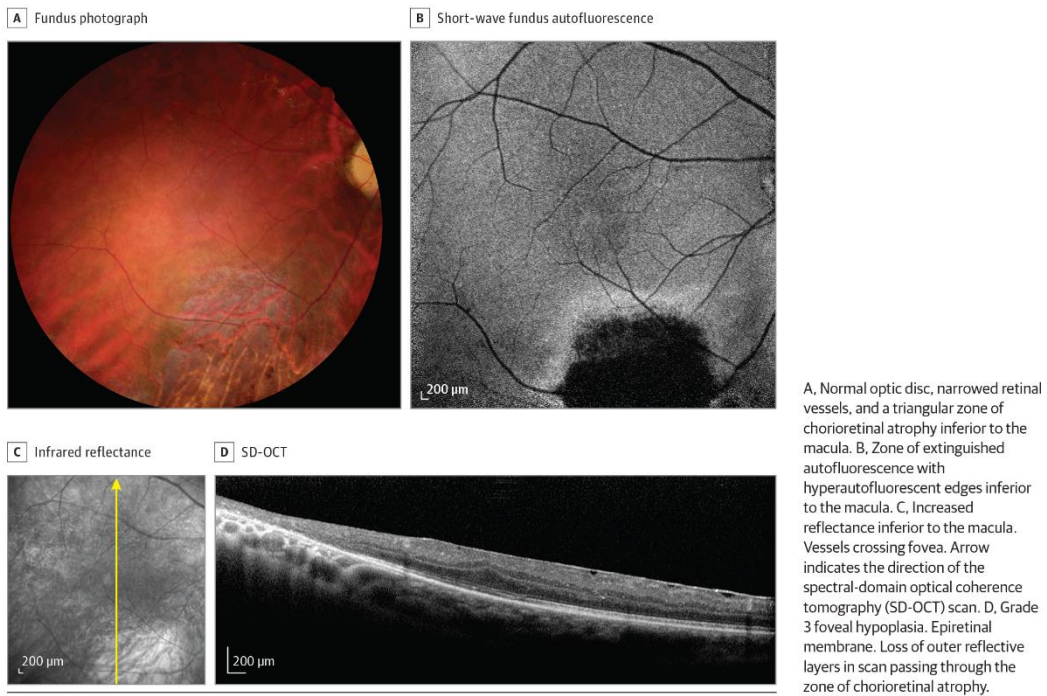
The clinical picture of the patients presented herein that included infantile nystagmus, low stable best-corrected visual acuity, and myopia was suggestive of CSNB. The upbeat component of nystagmus, present in patient 2, has also been reported as an early and transient feature of infantile nystagmus in CSNB.³⁵ Regarding functional alteration, the ffERG revealed an

electronegative dark-adapted response in keeping with a Schubert-Bornschein type of CSNB. However, both dark- and light-adapted response alterations were different than in cCSNB or icCSNB.¹⁰ On one hand, dark-adapted responses were in line with cCSNB with absent b-wave, and on the other hand, severely reduced light-adapted responses were suggestive for icCSNB. These ffERG alterations would reflect generalized both rod and cone post-phototransduction disorder. Because these patients had absent rod and cone ON- and OFF-bipolar cell responses, in contrast to cCSNB and icCSNB, we propose to call this finding a pan-bipolar cell dysfunction.

In general, *VSX2* (visual system homeobox 2, formerly described as *HOX10/CHX10*) recessive gene defects have been reported in association with isolated microphthalmia/anophthalmia (OMIM 610093),³⁶ microphthalmia with coloboma (OMIM 610092),³⁷ microphthalmia with cataracts, and iris abnormalities³⁸⁻⁴² (Figure 4). The adult patients presented lens subluxations and cataracts. None of the patients assessed in this study had microphthalmia. One report mentions lens ectopia without microphthalmia in a patient with a c.456-6C>G, r.(?) change in *VSX2*, but detailed data are lacking.⁴³

These patients presented a peculiar retinal dysfunction, between cCSNB and icCSNB, in keeping with generalized rod and cone post-phototransduction disorder. Only few data on retinal dysfunction in both heterozygous and homozygous pathogenic variants in *VSX2* are available^{44,45} as discussed in the eAppendix in the Supplement.

Figure 3. Retinal Findings in Patient 3 From an Unrelated Family

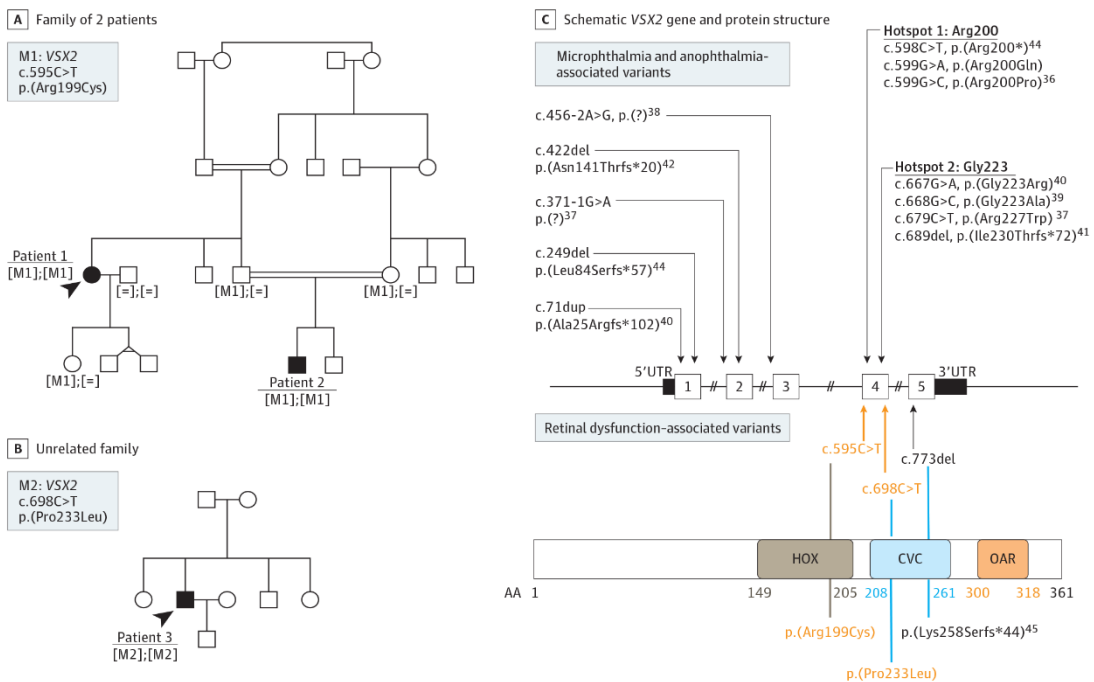


VSX2 is a 5-exon gene (Figure 4) located on chromosome 14q24.3⁴⁶ with a conserved sequence across vertebrates.³⁶ It is abundantly expressed in retinal progenitor cells during embryonic and fetal eye development.^{47,48} This abundant expression is transient: in adult vertebrate retina, the protein is found only in the nuclei of bipolar cells.^{36,47,49-51} According to available retinal gene expression databases, VSX2 is present in all types of bipolar cells, and thus it is considered as a pan-bipolar cell marker.⁵²⁻⁵⁵ VSX2 encodes a 361-amino-acid residue protein (Figure 4) with transcription factor activity. VSX2 is composed of several domains: residues 149 to 205 constitute the homeobox domain (HOX); residues 208 to 261, the CVC domain (standing for CHX10, VSX1 and CEH10); and residues 300 to 318, the OAR domain (OTP, aristaless, and RAX). HOX or homeodomain has a helix-turn-helix structure binding directly regulatory DNA sequences of target genes.⁵⁶ Disease-causing truncating or missense VSX2 variants were identified all over the gene (Figure 4). VSX2 presence defines the bipolar cell fate of retinal precursor cells.⁵⁷ Several retinal targets of VSX2 have been identified. VSX2 acts as a transcriptional repressor of *RHO*, cone opsin locus control region, and *SAG* (S-antigen visual arrestin), thus suppressing photoreceptor gene expression in bipolar cell precursors.^{58,59}

HOX is a common peptide found in transcription factors.⁶⁰ Within the HOX peptide, residue 50 and its surrounding amino acids are important for DNA binding.⁶¹ Residue 50

binds the DNA backbone, while the surrounding residues bind to neighbor DNA bases. These important residues would correspond to residue 200 and its surrounding amino acids in VSX2 that would explain the pathogenic mechanism associated with Arg200 missense variants leading to severe ocular malformations (microphthalmia and anophthalmia).^{36,62} Computational structure-based evaluation of the p.(Arg199Cys) variant predicts a modification of VSX2 binding to a neighbor base of targeted DNA sequence.⁶³ We hypothesize that Arg199 residue is probably less crucial for protein function as a regulator of ocular morphogenesis but is still required for correct bipolar cell differentiation and function. Indeed, in the 2 patients from 1 family, we are reporting that the p.(Arg199Cys) substitution leads to the CSNB phenotype without microphthalmia. The CVC domain and OAR domain, both less commonly found in the structure of transcription factors and found in proteins involved in neural tube and ocular development, are supposed to be involved in the specificity of DNA recognition, protein-protein interactions, and stability.⁶⁴⁻⁶⁶ The p.(Pro233Leu) variant found in patient 3 is in the CVC domain. The pathogenic variant described by Khan et al,⁴⁵ c.773delA, p.(Lys258Serfs*44), is also located in the CVC domain and leads to an ocular phenotype close to the phenotype of the patients presented herein. Missense variants in the CVC domain could change the pattern of gene interactions because of impairment of specific DNA-binding activity and

Figure 4. Pedigrees for the 2 Unrelated Families and the Schematic VSX2 Gene and Protein Structure



A, The c.595C>T variant in VSX2 co-segregated with disease in this consanguineous Turkish family. B, The c.698C>T variant was identified in 1 affected member; other family members were unavailable for co-segregation analyses. C, Microphthalmia- and anophthalmia-associated variants are listed above and retinal dysfunction associated variants below the schematic gene structure. In addition, the consequences on protein levels are depicted and the

schematic protein structure given. Variants identified by us are highlighted in orange. The different domains of VSX2 are indicated as follows: HOX, homeobox domain; CVC, CHX10, VSX1, and CEH10 domains; OAR, OTP, aristaless, and RAX domains. Amino acid residue positions of each domain are depicted in brown, light blue, and orange, respectively.

lead to severe ocular phenotypes in mice⁶⁷ and humans.³⁹⁻⁴¹ It is unclear why mutations in this region lead either to microphthalmia/anophthalmia or the CSNB-like phenotype. The 3-dimensional structures of different VSX2 mutations were similar (data not shown). Different variants may influence gene interactions differently, leading to the variability of the VSX2-associated phenotypes.

A naturally occurring mouse model carrying a nonsense variant in VSX2, p.Tyr176* (in the HOX domain), is known by the term *ocular retardation* phenotype (Or). Or mice are blind with microphthalmia, congenital cataracts, and an underdeveloped iris, retina, and optic nerve.⁶⁸⁻⁷⁰ They have abnormal retinal development with reduced retinal progenitor proliferations and a complete absence of bipolar cells.⁷⁰ Dependent on the genetic background of the mice, the ocular phenotype could be milder. In modified Or mice⁷¹ with only mild microphthalmia and better visual behavior, there was evidence of underdeveloped ciliary body.⁷¹ Lenses became cataractous by 6 months of age. The retina extended less in the periphery and did not reach the ciliary body root. Bipolar cells were present, but their number was severely reduced compared with wild-type mice. Bipolar

cell connections were abnormal: their dendrites extended into the outer nuclear layer, whereas the axons were not found in the inner plexiform layer. ERG recordings of modified Or mice showed an electronegative response to a bright flash (DA 5.0) in dark-adapted animals, resembling the fERG alteration of the patients presented herein. We hypothesize that the underdeveloped ciliary body might be a cause for lens subluxation. Peripheral retinal underdevelopment might be a cause of peripheral retinal alterations in our patients. The depletion of the bipolar cell population and abnormal bipolar cell wiring might be linked to a peculiar fERG waveform, which combines features of incomplete and complete CSNB. Future studies need to be performed to better understand the different phenotypes associated with VSX2 variants.

Limitations

This study is limited to only 2 families, making it difficult to determine the frequency or clinical relevance of this genetic defect. Functional in vitro or in vivo studies are needed to validate the pathogenic mechanism of the VSX2 variants leading to different eye phenotypes.

Conclusions

While only identified in 3 patients of 2 distinct families, the clinical phenotype of patients harboring missense variants in

VSX2 is in accordance with retinal VSX2 expression/localization data and resembles the phenotype reported in a Vsx2 knockout animal model. The peculiar pan-bipolar cell CSNB phenotype might be due to the global lack or dysfunction of bipolar cells.

ARTICLE INFORMATION

Accepted for Publication: August 23, 2022.

Published Online: October 20, 2022.
doi:10.1001/jamaophthalmol.2022.4146

Author Affiliations: Sorbonne Université, INSERM, CNRS, Institut de la Vision, Paris, France (Smirnov, Condroyer, Navarro, Antonio, Sahel, Audo, Zeitz); Université de Lille, Faculté de Médecine, Lille, France (Smirnov); Exploration de la Vision et Neuro-Ophthalmologie, CHU de Lille, Lille, France (Smirnov); Ophthalmology Department, Hôpital Universitaire Necker-Enfants Malades, Paris, France (Robert); Borelli Centre, UMR 9010, CNRS-SSA-ENS Paris Saclay-Paris University, Gif-sur-Yvette, France (Robert); Laboratory of Genetics in Ophthalmology (LGO), INSERM UMR 1163, Institute of Genetic Diseases, Imagine Institute, and Paris University, Paris, France (Rozet, Perrault); Centre Hospitalier National d'Ophthalmologie des Quinze-Vingts, Centre de Référence Maladies Rares REFERET and INSERM-DGOS CIC 1423, Paris, France (Sahel, Audo); Department of Ophthalmology, University of Pittsburgh School of Medicine, Pittsburgh, Pennsylvania (Sahel).

Author Contributions: Drs Audo and Zeitz had full access to all of the data in the study and take responsibility for the integrity of the data and the accuracy of the data analysis. Drs Perrault, Audo, and Zeitz contributed equally to the article. *Concept and design:* Smirnov, Robert, Rozet, Sahel, Audo, Zeitz.

Acquisition, analysis, or interpretation of data: Smirnov, Robert, Condroyer, Navarro, Antonio, Rozet, Perrault, Audo, Zeitz.

Drafting of the manuscript: Smirnov, Condroyer, Navarro, Zeitz.

Critical revision of the manuscript for important intellectual content: Smirnov, Robert, Antonio, Rozet, Sahel, Perrault, Audo, Zeitz.

Statistical analysis: Smirnov.

Obtained funding: Sahel, Audo, Zeitz.

Administrative, technical, or material support: Condroyer, Antonio, Sahel, Audo.

Supervision: Robert, Rozet, Audo, Zeitz.

Conflict of Interest Disclosures: Dr Sahel reported receiving grants from the National Institutes of Health (P30 EY08098) during the conduct of the study; grants from Research to Prevent Blindness outside the submitted work; and personal fees from Pixium Vision, GenSight Biologics, SparingVision, Prohese, Chronolife, Tilak Healthcare, VegaVect, Avista, Tenpoint, and SharpEye. Dr Audo reported being a consultant for 4DMT, Biogen, Novartis, ProQR, Roche, and SparingVision. No other disclosures were reported.

Funding/Support: Funding for this study was provided by the LABEX LIFESENSES project (ANR-10-LABX-65), supported by French state funds managed by the Agence Nationale de la Recherche within the Investissements d'Avenir program (ANR-11-IDEX-0004-0), and the Institut Hospitalo-Universitaire FOReSIGHT project (ANR-18-IAHU-0001), also supported by French

state funds managed by the Agence Nationale de la Recherche within the Investissements d'Avenir program. Funding was also received from RHU-Light4deaf (ANR-15-RHU-0001) and a Foundation Fighting Blindness center grant (C-CMM-0907-0428-INSERM04).

Role of the Funder/Sponsor: The funders had no role in the design and conduct of the study; collection, management, analysis, and interpretation of the data; preparation, review, or approval of the manuscript; and decision to submit the manuscript for publication.

Meeting Presentation: This work was presented at the International Society for Clinical Electrophysiology of Vision Symposium; August 4, 2022; Liverpool, United Kingdom.

Additional Contributions: We are thankful to all patients and family members who participated in this study. We are grateful to Katia Marazova, Institut de la Vision, for revising the manuscript. We thank the clinical staff from the different centers for collecting phenotypic data.

Additional Information: DNA samples from the Parisian group were obtained from the NeuroSensCol DNA bank, for research in neuroscience (principal investigator José-Alain Sahel, MD; co-principal investigator Isabelle Audo, MD, PhD; partnering with CHNO des Quinze-Vingts, INSERM, and CNRS, certified NFS96-900).

REFERENCES

- Zeitz C, Robson AG, Audo I. Congenital stationary night blindness: an analysis and update of genotype-phenotype correlations and pathogenic mechanisms. *Prog Retin Eye Res*. 2015;45:58-110. doi:10.1016/j.preteyeres.2014.09.001
- McCulloch DL, Marmor MF, Brigell MG, et al. ISCEV standard for full-field clinical electroretinography (2015 update). *Doc Ophthalmol*. 2015;130(1):1-12. doi:10.1007/s10633-014-9473-7
- Penn RD, Hagins WA. Signal transmission along retinal rods and the origin of the electroretinographic a-wave. *Nature*. 1969;223(5202):201-204. doi:10.1038/223201a0
- Baylor DA, Nunn BJ, Schnapf JL. The photocurrent, noise and spectral sensitivity of rods of the monkey *Macaca fascicularis*. *J Physiol*. 1984; 357:575-607. doi:10.1113/jphysiol.1984.sp015518
- Hood DC, Birch DG. Beta wave of the scotopic (rod) electroretinogram as a measure of the activity of human on-bipolar cells. *J Opt Soc Am A Opt Image Sci Vis*. 1996;13(3):623-633. doi:10.1364/JOSAA.13.000623
- Sieving PA, Murayama K, Naarendorp F. Push-pull model of the primate photopic electroretinogram: a role for hyperpolarizing neurons in shaping the b-wave. *Vis Neurosci*. 1994; 11(3):519-532. doi:10.1017/S0952523800002431
- Ueno S, Kondo M, Niwa Y, Terasaki H, Miyake Y. Luminance dependence of neural components that underlies the primate photopic electroretinogram. *Invest Ophthalmol Vis Sci*. 2004;45(3):1033-1040. doi:10.1167/iov.03-0657
- Audo I, Robson AG, Holder GE, Moore AT. The negative ERG: clinical phenotypes and disease mechanisms of inner retinal dysfunction. *Surv Ophthalmol*. 2008;53(1):16-40. doi:10.1016/j.survophthal.2007.10.010
- Schubert G, Bornschein H. Beitrag zur Analyse des menschlichen Elektroretinogramms [Analysis of the human electroretinogram]. *Ophthalmologica*. 1952;123(6):396-413. doi:10.1159/000301211
- Miyake Y, Yagasaki K, Horiguchi M, Kawase Y, Kanda T. Congenital stationary night blindness with negative electroretinogram: a new classification. *Arch Ophthalmol*. 1986;104(7):1013-1020. doi:10.1001/archophth.1986.01050190071042
- Langrová H, Gamer D, Friedburg C, Besch D, Zrenner E, Apfelstedt-Sylla E. Abnormalities of the long flash ERG in congenital stationary night blindness of the Schubert-Bornschein type. *Vision Res*. 2002;42(11):1475-1483. doi:10.1016/S0042-6989(02)00068-8
- Bijveld MMC, Florijn RJ, Bergen AAB, et al. Genotype and phenotype of IO1 Dutch patients with congenital stationary night blindness. *Ophthalmology*. 2013;120(10):2072-2081. doi:10.1016/j.ophtha.2013.03.002
- Bech-Hansen NT, Naylor MJ, Maybaum TA, et al. Loss-of-function mutations in a calcium-channel alpha1-subunit gene in Xp11.23 cause incomplete X-linked congenital stationary night blindness. *Nat Genet*. 1998;19(3):264-267. doi:10.1038/947
- Strom TM, Nyakatura G, Apfelstedt-Sylla E, et al. An L-type calcium-channel gene mutated in incomplete X-linked congenital stationary night blindness. *Nat Genet*. 1998;19(3):260-263. doi:10.1038/940
- Zeitz C, Kloeckener-Gruissem B, Forster U, et al. Mutations in CABP4, the gene encoding the Ca2+-binding protein 4, cause autosomal recessive night blindness. *Am J Hum Genet*. 2006;79(4):657-667. doi:10.1086/508067
- Wycisk KA, Budde B, Feil S, et al. Structural and functional abnormalities of retinal ribbon synapses due to *Cacna2d4* mutation. *Invest Ophthalmol Vis Sci*. 2006;47(8):3523-3530. doi:10.1167/iov.06-0271
- Wycisk KA, Zeitz C, Feil S, et al. Mutation in the auxiliary calcium-channel subunit *CACNA2D4* causes autosomal recessive cone dystrophy. *Am J Hum Genet*. 2006;79(5):973-977. doi:10.1086/508944
- Quigley M, Roy MS, Barsoum-Homsy M, Chevrette L, Jacob JL, Milot J. On- and off-responses in the photopic electroretinogram in complete-type congenital stationary night blindness. *Doc Ophthalmol*. 1996-1997;92(3):159-165. doi:10.1007/BF02583287
- Pusch CM, Zeitz C, Brandau O, et al. The complete form of X-linked congenital stationary night blindness is caused by mutations in a gene

encoding a leucine-rich repeat protein. *Nat Genet.* 2000;26(3):324-327. doi:10.1038/81627

20. Dryja TP, McGee TL, Berson EL, et al. Night blindness and abnormal cone electroretinogram ON responses in patients with mutations in the GRM6 gene encoding mGluR6. *Proc Natl Acad Sci U S A.* 2005;102(13):4884-4889. doi:10.1073/pnas.0501233102

21. Zeitz C, van Genderen M, Neidhardt J, et al. Mutations in GRM6 cause autosomal recessive congenital stationary night blindness with a distinctive scotopic 15-Hz flicker electroretinogram. *Invest Ophthalmol Vis Sci.* 2005;46(11):4328-4335. doi:10.1167/iov.05-0526

22. Li Z, Sergouniotis PI, Michaelides M, et al. Recessive mutations of the gene TRPM1 abrogate ON bipolar cell function and cause complete congenital stationary night blindness in humans. *Am J Hum Genet.* 2009;85(5):711-719. doi:10.1016/j.ajhg.2009.10.003

23. Audo I, Kohl S, Leroy BP, et al. TRPM1 is mutated in patients with autosomal-recessive complete congenital stationary night blindness. *Am J Hum Genet.* 2009;85(5):720-729. doi:10.1016/j.ajhg.2009.10.013

24. van Genderen MM, Bijveld MMC, Claassen YB, et al. Mutations in TRPM1 are a common cause of complete congenital stationary night blindness. *Am J Hum Genet.* 2009;85(5):730-736. doi:10.1016/j.ajhg.2009.10.012

25. Audo I, Bujakowska K, Orhan E, et al. Whole-exome sequencing identifies mutations in GPR179 leading to autosomal-recessive complete congenital stationary night blindness. *Am J Hum Genet.* 2012;90(2):321-330. doi:10.1016/j.ajhg.2011.12.007

26. Zeitz C, Jacobson SG, Hamel CP, et al; Congenital Stationary Night Blindness Consortium. Whole-exome sequencing identifies LRIT3 mutations as a cause of autosomal-recessive complete congenital stationary night blindness. *Am J Hum Genet.* 2013;92(1):67-75. doi:10.1016/j.ajhg.2012.10.023

27. Audo I, Friedrich A, Mohand-Saïd S, et al. An unusual retinal phenotype associated with a novel mutation in RHO. *Arch Ophthalmol.* 2010;128(8):1036-1045. doi:10.1001/archophthol.2010.162

28. Audo I, Lancelot ME, Mohand-Saïd S, et al. Novel C2orf71 mutations account for ~1% of cases in a large French arRP cohort. *Hum Mutat.* 2011;32(4):E2091-E2103. doi:10.1002/humu.21460

29. Gerber S, Alzayady IJ, Burglen L, et al. Recessive and dominant de novo ITPRI mutations cause Gillespie syndrome. *Am J Hum Genet.* 2016;98(5):971-980. doi:10.1016/j.ajhg.2016.03.004

30. Human Genome Variation Society. Updated March 1, 2021. <http://www.hgvs.org/>

31. Richards S, Aziz N, Bale S, et al; ACMG Laboratory Quality Assurance Committee. Standards and guidelines for the interpretation of sequence variants: a joint consensus recommendation of the American College of Medical Genetics and Genomics and the Association for Molecular Pathology. *Genet Med.* 2015;17(5):405-424. doi:10.1038/gim.2015.30

32. Audo I, Bujakowska KM, Léveillard T, et al. Development and application of a next-generation-sequencing (NGS) approach to detect known and novel gene defects underlying retinal diseases. *Orphanet J Rare Dis.* 2012;7:8. doi:10.1186/1750-1172-7-8

33. Thomas MG, Kumar A, Mohammad S, et al. Structural grading of foveal hypoplasia using spectral-domain optical coherence tomography a predictor of visual acuity? *Ophthalmology.* 2011;118(8):1653-1660. doi:10.1016/j.ophtha.2011.01.028

34. Kopanos C, Tsiolkas V, Kouris A, et al. VarSome: the human genomic variant search engine. *Bioinformatics.* 2019;35(11):1978-1980. doi:10.1093/bioinformatics/bty897

35. Simonsz HJ, Florijn RJ, van Minderhout HM, Bergen AA, Kamermans M. Nightblindness-associated transient tonic downgaze (NATTD) in infant boys with chin-up head posture. *Strabismus.* 2009;17(4):158-164. doi:10.3109/09273970903396893

36. Ferda Percin E, Ploder LA, Yu JJ, et al. Human microphthalmia associated with mutations in the retinal homeobox gene CHX10. *Nat Genet.* 2000;25(4):397-401. doi:10.1038/78071

37. Bar-Yosef U, Abuelalish I, Harel T, Hendlar N, Ofir R, Birk OS. CHX10 mutations cause non-syndromic microphthalmia/anophthalmia in Arab and Jewish kindreds. *Hum Genet.* 2004;115(4):302-309. doi:10.1007/s00439-004-1154-2

38. Burkitt Wright EM, Perveen R, Bowers N, et al. VSX2 in microphthalmia: a novel splice site mutation producing a severe microphthalmia phenotype. *Br J Ophthalmol.* 2010;94(3):386-388. doi:10.1136/bjo.2009.159996

39. Reis LM, Khan A, Kariminejad A, Ebadi F, Tyler RC, Semina EV. VSX2 mutations in autosomal recessive microphthalmia. *Mol Vis.* 2011;17:2527-2532.

40. Chassaing N, Causse A, Vigouroux A, et al. Molecular findings and clinical data in a cohort of 150 patients with anophthalmia/microphthalmia. *Clin Genet.* 2014;86(4):326-334. doi:10.1111/cge.12275

41. Monies D, Abouelhoda M, Assoum M, et al. Lessons learned from large-scale, first-tier clinical exome sequencing in a highly consanguineous population. *Am J Hum Genet.* 2019;104(6):1182-1201. doi:10.1016/j.ajhg.2019.04.011

42. Jakobsson C. Compound heterozygous VSX2 mutation causing bilateral anophthalmia in a consanguineous Egyptian family. *J Clin Exp Ophthalmol.* 2015;06(03). doi:10.4172/2155-9570.1000441

43. Maddirevula S, Kuwahara H, Ewida N, et al. Analysis of transcript-deleterious variants in Mendelian disorders: implications for RNA-based diagnostics. *Genome Biol.* 2020;21(1):145. doi:10.1186/s13059-020-02053-9

44. Iseri SU, Wyatt AW, Nürnberg G, et al. Use of genome-wide SNP homozygosity mapping in small pedigrees to identify new mutations in VSX2 causing recessive microphthalmia and a semidominant inner retinal dystrophy. *Hum Genet.* 2010;128(1):51-60. doi:10.1007/s00439-010-0823-6

45. Khan AO, Aldahmesh MA, Noor J, Salem A, Alkuraya FS. Lens subluxation and retinal dysfunction in a girl with homozygous VSX2 mutation. *Ophthalmic Genet.* 2015;36(1):8-13. doi:10.3109/13816810.2013.827217

46. De Chen J, Ploder L, Collins L, et al. Chromosomal sublocalization and cellular expression of the retinal homeobox gene HOX10 [abstract]. *Am J Hum Genet.* 1990;47(A102).

47. Liu IS, Chen JD, Ploder L, et al. Developmental expression of a novel murine homeobox gene (Chx10): evidence for roles in determination of the neuroretina and inner nuclear layer. *Neuron.* 1994;13(2):377-393. doi:10.1016/0896-6273(94)90354-9

48. Belecky-Adams T, Tomarev S, Li HS, et al. Pax-6, Prox 1, and Chx10 homeobox gene expression correlates with phenotypic fate of retinal precursor cells. *Invest Ophthalmol Vis Sci.* 1997;38(7):1293-1303.

49. Passini MA, Levine EM, Canger AK, Raymond PA, Schechter N. Vsx-1 and Vsx-2: differential expression of two paired-like homeobox genes during zebrafish and goldfish retinogenesis. *J Comp Neurol.* 1997;388(3):495-505. doi:10.1002/(SICI)1096-9861(19971124)388:3<495::AID-CNE11>3.0.CO;2-L

50. Chen CM, Cepko CL. Expression of Chx10 and Chx10-1 in the developing chicken retina. *Mech Dev.* 2000;90(2):293-297. doi:10.1016/S0925-4773(99)00251-8

51. Vitorino M, Jusuf PR, Maurus D, Kimura Y, Higashijima S, Harris WA. Vsx2 in the zebrafish retina: restricted lineages through derepression. *Neural Dev.* 2009;4:14. doi:10.1186/1749-8104-4-14

52. Shekhar K, Lapan SW, Whitney IE, et al. Comprehensive classification of retinal bipolar neurons by single-cell transcriptomics. *Cell.* 2016;166(5):1308-1323.e30. doi:10.1016/j.cell.2016.07.054

53. Uhlén M, Fagerberg L, Hallström BM, et al. Proteomics: tissue-based map of the human proteome. *Science.* 2015;347(6220):1260419. doi:10.1126/science.1260419

54. Siegert S, Cabuy E, Scherf BG, et al. Transcriptional code and disease map for adult retinal cell types. *Nat Neurosci.* 2012;15(3):487-495.S1-2. doi:10.1038/nn.3032

55. Clark BS, Stein-O'Brien GL, Shiao F, et al. Single-cell RNA-seq analysis of retinal development identifies NFI factors as regulating mitotic exit and late-born cell specification. *Neuron.* 2019;102(6):1111-1126.e5. doi:10.1016/j.neuron.2019.04.010

56. Scott MP, Tamkun JW, Hartzell GW III. The structure and function of the homeodomain. *Biochim Biophys Acta.* 1989;989(1):25-48. doi:10.1016/S0167-4838(00)00120-5

57. Livne-Bar I, Pacal M, Cheung MC, et al. Chx10 is required to block photoreceptor differentiation but is dispensable for progenitor proliferation in the postnatal retina. *Proc Natl Acad Sci U S A.* 2006;103(13):4988-4993. doi:10.1073/pnas.0600083103

58. Dorval KM, Bobechko BP, Fujieda H, Chen S, Zack DJ, Bremner R. CHX10 targets a subset of photoreceptor genes. *J Biol Chem.* 2006;281(2):744-751. doi:10.1074/jbc.M509470200

59. West ER, Cepko CL. Development and diversification of bipolar interneurons in the mammalian retina. *Dev Biol.* 2022;481:30-42. doi:10.1016/j.ydbio.2021.09.005

60. Bürglin TR, Affolter M. Homeodomain proteins: an update. *Chromosoma.* 2016;125(3):497-521. doi:10.1007/s00412-015-0543-8

61. Wilson DS, Guenther B, Desplan C, Kuriyan J. High resolution crystal structure of a paired (Pax) class cooperative homeodomain dimer on DNA. *Cell.* 1995;82(5):709-719. doi:10.1016/0092-8674(95)90468-9

- 62.** Faiyaz-Ul-Haque M, Zaidi SHE, Al-Mureikhi MS, Peltekova I, Tsui LC, Teebi AS. Mutations in the CHX10 gene in non-syndromic microphthalmia/anophthalmia patients from Qatar. *Clin Genet*. 2007;72(2):164-166. doi:10.1111/j.1399-0004.2007.00846.x
- 63.** Barrera LA, Vedenko A, Kurland JV, et al. Survey of variation in human transcription factors reveals prevalent DNA binding changes. *Science*. 2016;351(6280):1450-1454. doi:10.1126/science.aad2257
- 64.** Ohtoshi A, Justice MJ, Behringer RR. Isolation and characterization of Vsxl, a novel mouse CVC paired-like homeobox gene expressed during embryogenesis and in the retina. *Biochem Biophys Res Commun*. 2001;286(1):133-140. doi:10.1006/bbrc.2001.5372
- 65.** Knauer SK, Carra G, Stauber RH. Nuclear export is evolutionarily conserved in CVC paired-like homeobox proteins and influences protein stability, transcriptional activation, and extracellular secretion. *Mol Cell Biol*. 2005;25(7):2573-2582. doi:10.1128/MCB.25.7.2573-2582.2005
- 66.** Furukawa T, Kozak CA, Cepko CL. *rax*, a novel paired-type homeobox gene, shows expression in the anterior neural fold and developing retina. *Proc Natl Acad Sci U S A*. 1997;94(7):3088-3093. doi:10.1073/pnas.94.7.3088
- 67.** Zou C, Levine EM. Vsx2 controls eye organogenesis and retinal progenitor identity via homeodomain and non-homeodomain residues required for high affinity DNA binding. *PLoS Genet*. 2012;8(9):e1002924. doi:10.1371/journal.pgen.1002924
- 68.** Truslove GM. A gene causing ocular retardation in the mouse. *J Embryol Exp Morphol*. 1962;10:652-660. doi:10.1242/dev.10.4.652
- 69.** Robb RM, Silver J, Sullivan RT. Ocular retardation (or) in the mouse. *Invest Ophthalmol Vis Sci*. 1978;17(5):468-473.
- 70.** Burmeister M, Novak J, Liang MY, et al. Ocular retardation mouse caused by Chx10 homeobox null allele: impaired retinal progenitor proliferation and bipolar cell differentiation. *Nat Genet*. 1996;12(4):376-384. doi:10.1038/ng0496-376
- 71.** Bone-Larson C, Basu S, Radel JD, et al. Partial rescue of the ocular retardation phenotype by genetic modifiers. *J Neurobiol*. 2000;42(2):232-247. doi:10.1002/(SICI)1097-4695(20000205)42:2<232::AID-NEU7>3.0.CO;2-4

4. Novel gene defect identification and characterization in F4752 with North Carolina Macular Dystrophy

WGS was applied to F4752 (Fig.25) with North Carolina Macular Dystrophy (NCMD, MIM# 136550) (GENMED project, investigated at the Centre National de Recherche en Génomique Humaine (CNRGH), Institut de Biologie François Jacob, CEA, Université Paris Saclay, Evry, France).

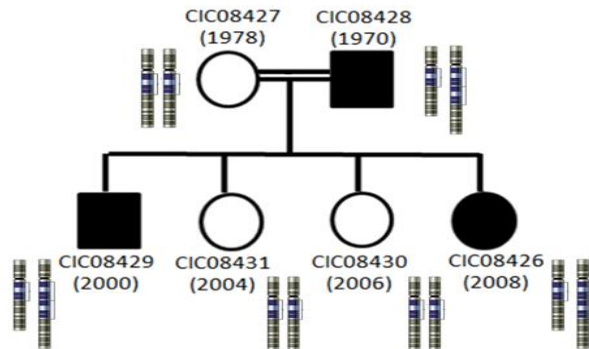


Figure 25. Pedigree of F4752 with North Carolina Macular Dystrophy

First, in collaboration with the bioinformatic engineer from our team, Julien Navarro, we analyzed the WGS data for known IRD genes and there were no variants found to co-segregate with the disease. Subsequently, we analyzed three known loci of NCMD (MCDR1 locus, involving *PRDM13* and *CCNC* and three point variants V1-3; MCDR3 in 5p15-p13, between *IRX1* and *ADAMTS16*). The MCDR1 locus was additionally explored by qPCR and Sanger sequencing. This revealed no known or novel variants in these studied regions. Then filtering was open to all ultra-rare variants found by WGS.

Subsequently, we found a novel heterozygous 1.57 Mb duplication which co-segregated with the disease in this family. The duplicated sequence included 15 genes (Gene Distiller: <http://www.genedistiller.org/> and Genome Browser: <https://genome.ucsc.edu/>), among them 4 pseudo-genes and 4 genes coding for miRNA. This region lacks known genes associated with IRD.

We used 3 of 15 genes to validate the duplication by qPCR (Fig.26). The junctions were amplified by PCR and sequenced. The duplicated sequence was unchanged (i.e. insertions/deletions of supplementary nucleotides on the boundaries and inversion of duplicated fragments were absent).

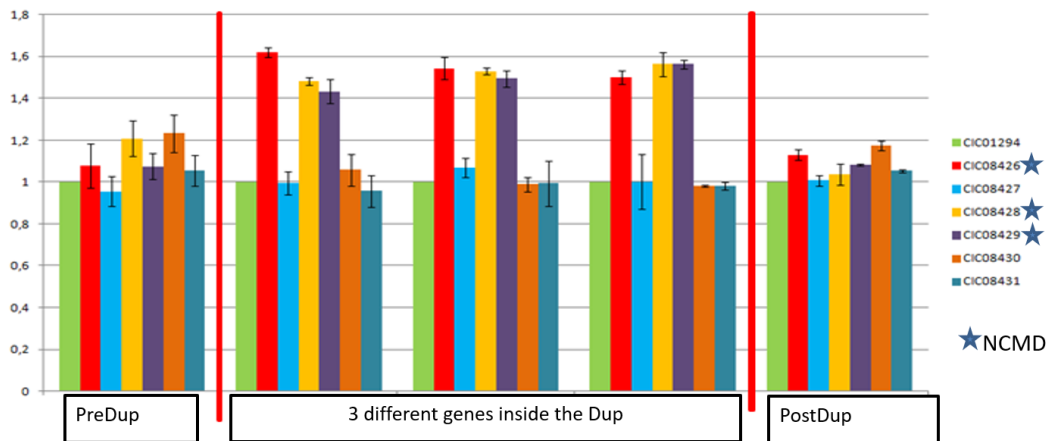


Figure 26. qPCR on chosen 3 of 12 genes inside and 2 chosen genes outside the duplication. All patients affected by NCMD (highlighted with a star) harbour this duplication in heterozygous state.

Querying the human, mouse and human retinal organoid transcriptomic databases, the best expression predictions were obtained for a gene we subsequently called *AZDINE7*: it was predicted to be expressed in mouse and human retina and more specifically in rod and cone photoreceptors, bipolar and amacrine cells (Fig.27).

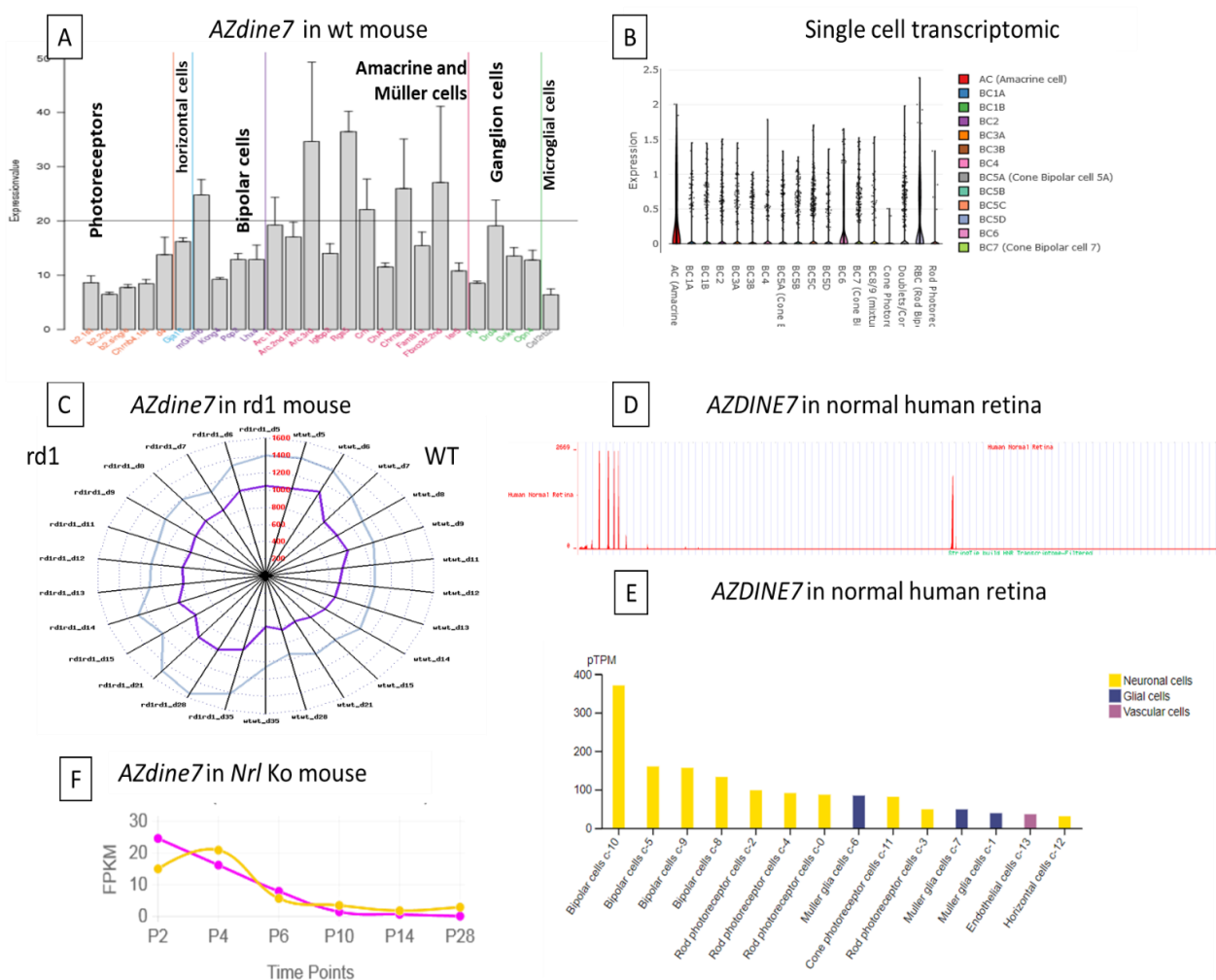


Figure 27. Predictions for retinal expression of *AZDINE7*. A. Roska database (<http://www.fmi.ch/roska.data/>). *Azidine7* is predicted to be expressed in the inner retinal layers

(bipolar, amacrine and Müller cells). B. Single bipolar cell enriched transcriptomic database (Single Cell Portal (broadinstitute.org)). The highest levels of transcription are observed in amacrine and various types of bipolar cells. C. In-house rd1 mouse retina transcriptome database. The relative levels of transcription of *AZdine7* are increasing over time in an age dependent rod-photoreceptor degenerative mouse model, suggesting an enriched inner retinal expression. D. Human Normal Retinal Transcriptome database (<https://oculargenomics.meei.harvard.edu/retinal-transcriptome/>). High levels of *AZDINE7* expression are present in the human retina. E. Single-cell transcriptomic data in normal human retina (<https://www.proteinatlas.org/>) are suggestive of expression in inner retinal layers, photoreceptors and in Müller glia. F. RetSeq Nrl mouse database (<https://retseq.nei.nih.gov/retseqvis.jsp>). The relative levels of transcription of *AZdine7* are decreasing over time in rod-photoreceptor degenerative mouse model (in yellow), suggesting retinal expression (in pink – expression in wt mice).

AZDINE7 encodes a known modulator of the cell cycle, a part of ubiquitin-ligase complex which triggers proteasome degradation of cell cycle check-point proteins, finally down-regulating cell proliferation. Its localization is mainly nuclear.

RNA *in situ* hybridization on mouse retina sections revealed *AZdine7* transcript in nuclei of all retinal layers, with a slightly stronger staining in the INL, where the nuclei of bipolar and amacrine cells are located. These findings are in accordance with the transcriptome datasets (Fig.28).

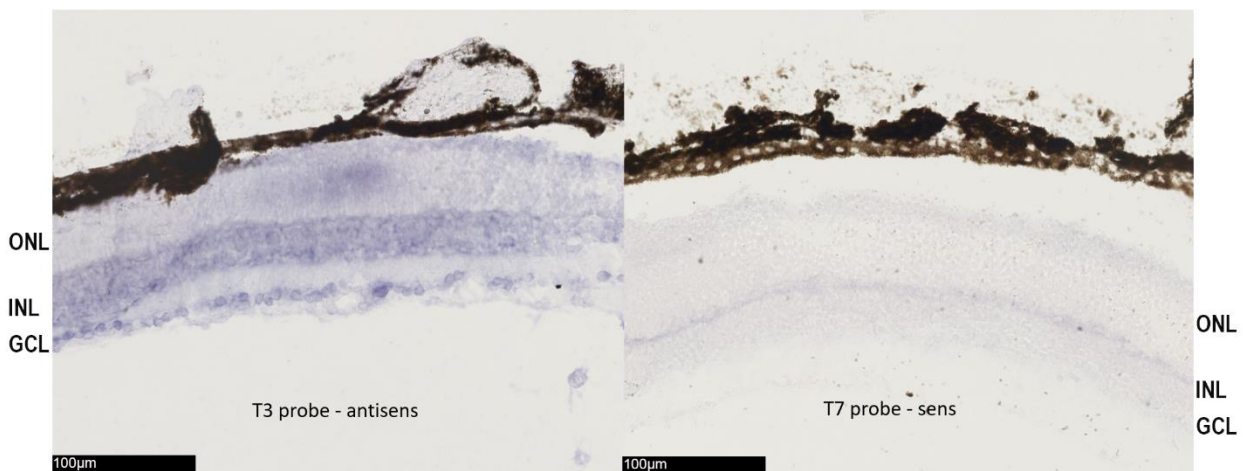


Figure 28. *In situ* RNA hybridization with *AZdine7* exon 9_10 probes. Intense staining at the level of INL and GCL with antisense probe, suggestive of *AZdine7* mRNA presence. Light microscopy, x20. Scale bar: 100µm.

Immuno histofluorescence studies with a commercially available anti-*AZDINE7* antibody on mouse retina sections revealed an intense staining in the INL and the external limiting membrane (ELM). Co-localization studies with antibodies directed towards specific retinal cell markers (anti-SOX9 and anti-Glutamine synthetase) showed that *AZIDINE7* co-localized mostly with Müller cells (both cell bodies and expansions (Figs.29 and 30)).

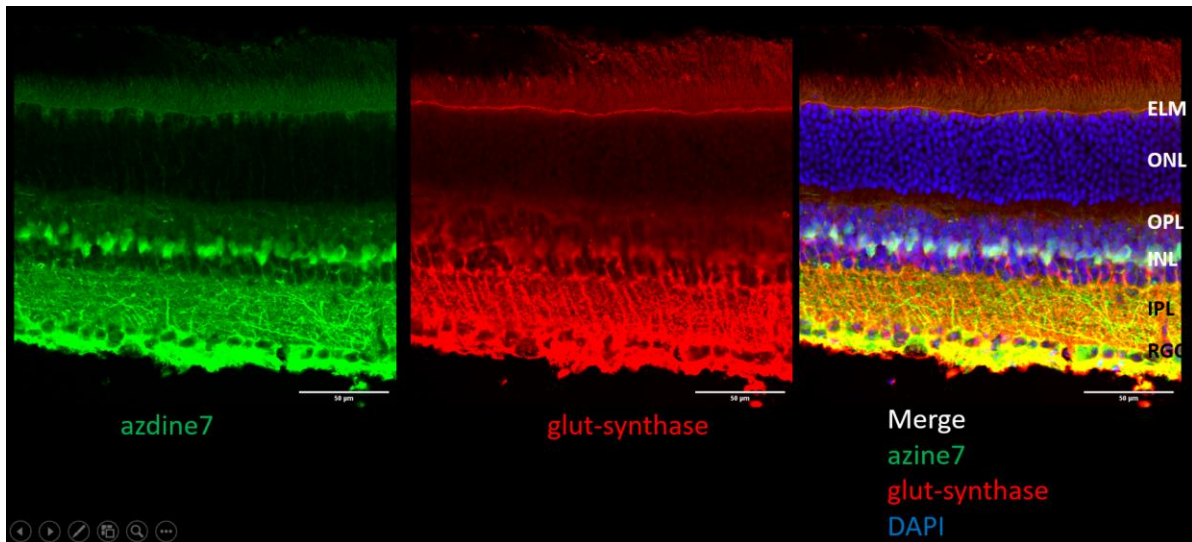


Figure 29. Immuno-histo-fluorescence on mouse retina. Co-staining with anti-AZdine7 and anti-glutamine-synthetase. Confocal microscopy, 3-images stack, x40.

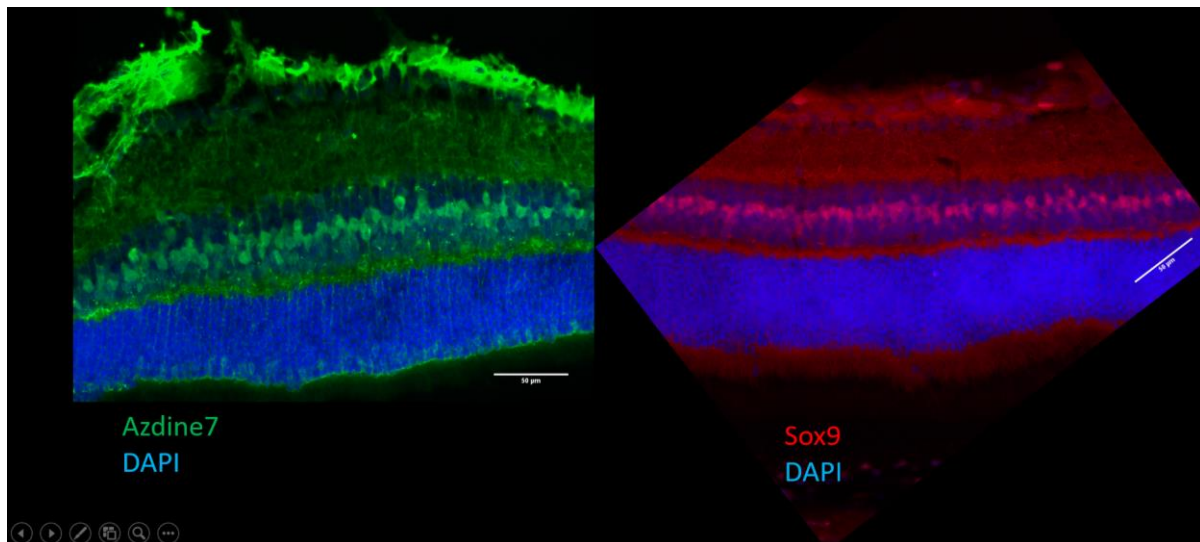


Figure 30. Immuno histofluorescence on mouse retina. Staining with anti-AZdine7 and anti-Sox9. Due to the nature of the antibodies (same host), only separate staining could be done. Nevertheless, the images are suggestive of Muller cell staining with both antibodies. Fluorescent epimicroscopy, x40.

Immuno histofluorescence studies with the same commercially available anti-AZDINE7 antibody used above but now on human retina sections were different. All retinal layers were stained with a perinuclear localization of the signal (Fig.31).

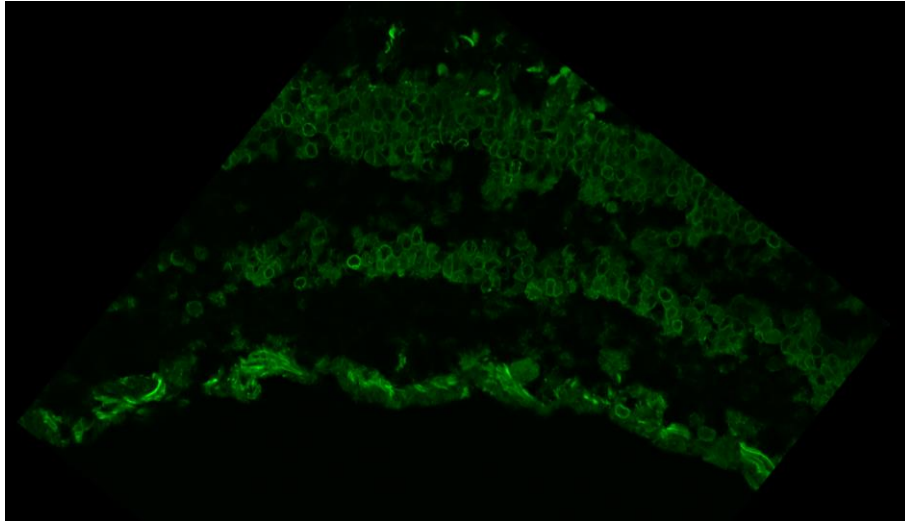


Figure 31. Immuno-histo-fluorescence on human retina. Anti-AZdine 7 staining in all nucleated layers, perinuclear. Confocal microscopy, 3-images stack, x63.

Further functional studies (RNA extraction from lymphocytes with subsequent rtqPCR; fibroblast culture; induced pluripotent cell production and differentiation into retinal organoids) need to be performed to validate this novel candidate gene.

Discussion and perspectives.

1. Deep phenotyping, phenotype-genotype correlations and natural history studies

Exact and in-depth description of IRD symptoms and clinical manifestations provide a basis for their correct molecular diagnosis. The vast majority of IRD are rare diseases and their phenotypic spectrum is yet to be reported. Specific traits on functional retinal studies, fundus examination and retinal imaging will allow the clinician to class the IRD into a big nosological group and sometimes even to pinpoint a specific gene defect, if the phenotype is highly specific and recognizable ((e.g. pathognomonic ERG[176]).

One of the goals of IRD studies is this precise phenotyping allowing to distill those specific and recognizable traits of retinal degenerations in order to guide the genotyping. In many cases, molecular diagnosis could be obtained by inexpensive direct Sanger sequencing of suspected candidate gene.

Phenotype-genotype correlations are helpful in deciphering of mechanisms involved in the pathogenesis of IRD, dependent on the type of variants, their localization in the DNA sequence, their influence on splicing and transcription. Moreover, knowledge of the spectrum of IRD is useful for prognosis and for research of systemic non ocular manifestations. In my thesis, I described 15 cases of exclusive ocular involvement in a gene previously linked with systemic severe neuro-degenerative disease, neuronal ceroid lipofuscinosis[161]. The presence of isolated ocular involvement in multisystemic disorder-linked genes is a challenging question, raising some ethical concerns. How far should we clinically explore our patients? Should we announce the possibility of a second-organ involvement or should we wait and see for clinical signs, as there is usually no specific therapy to prevent the degeneration? These questions would need to be addressed by further studies of patient experience and acceptance in genetic counselling[177,178].

Major advances in the study of IRDs have placed efforts to develop treatments for these blinding conditions at the forefront of the emerging field of precision medicine. Natural history studies in IRD are highly relevant, as they provide the basis for therapeutic approaches and allow indirect comparison intervention/sham in diseases with very low incidence. In addition, the choice and constitution of the correct control group is an issue. It could also guide the choice for meaningful outcome measures in therapeutic trials[179]. They are also important in order to know the rate of progression in a given IRD, that can help in planning of visual aids and occupational therapy in visually challenged patients.

2. Identification of gene defects in IRD

Since the discovery of the first retinal disease gene[180], more than 300 different genes and loci mutated in patients with IRD have been characterized or mapped.

There is an unmet need for ascertaining the genetic cause of IRD, as the participation in emerging clinical trials are usually gene-dependent, whether or not interventions are gene-specific[181]. Several therapies that are and will be developed in the next years are gene-, or even mutation-specific[182,183], emphasizing the importance for patients to receive a molecular diagnosis.

To increase the chance to identify disease-causing variants in a candidate gene, a clear phenotypic description and information about other family members are essential. Indeed, this can

help to identify gene defects in complex phenotypes, as in our patient with *RBP4*-linked fundus albipunctatus[170].

Classically, positional cloning as determined by linkage analysis has been used effectively, though this generally requires the availability of large families or a large set of families in which the same locus is involved. Linkage studies were also performed using microarrays that test single nucleotide variants (SNVs) spread across the genome. The search for IRD-associated variants in genes encoding proteins with known functions (candidate gene approach) in the retina has been very successful as well[107].

High throughput sequencing, using targeted NGS panels, WES and WGS, rapidly became the most promising approaches to identify novel and known gene defects associated with IRD, correlate genotype-phenotype, resolve complex traits and lead to a better understanding of retinal physiology and physiopathology.

Targeted NGS panels allow to genetically solve about 60-80% of IRD patients, depending on the “entry phenotype” and the number of genes included in the panel[110,184–187]. The targeted IRD panel developed at the Institut de la Vision[110] in its current version (Tab.5) allows the identification of causative variants in 75% of RCD cases, as it is shown in the present work.

The current IRD targeted NGS panel used in Institut de la Vision was conceived for the analysis of all types of IRD. As RCD is the most frequent form of IRD[64] and at the same time IRD usually lacking specific clinical traits to guess the causative gene defect, the vast majority of patients explored in this study were affected with non-syndromic RCD (87,2% of samples). I did not report on the other forms of IRD analyzed on our NGS panel (ACL, COD/CORD, MD, syndromic forms of IRD) as there was only a limited number of cases, not representative of IRD-department recruitment.

Genetic landscape in solved cases of RCD is in line with data reported in other Western Europe IRD studies. In AD RCD cases, variants in splicing factor genes (namely *PRPF3*, *PRPF4*, *PRPF6*, *PRPF8*, *PRPF31* and *SNRNP200*) were the most frequent (nearly 25% of AD RP cases), as reported in Belgium[188], British[189] and Chinese[190] cohorts. “Top 5” genes in AD RP in our practice are *RHO*, *RP1*, *PRPH2*, *PRPF31* and *PRPF8*. In AR RCD cases, “top 5” are *USH2A* (23% in our cohort), *EYS* (11%) followed by *PDE6B* and *PDE6A*, then *CRB1*. *USH2A* and *EYS* are the most frequent genes linked with AR RCD worldwide[184,185,191,192].

In cases unsolved by targeted NGS (25% in this study), WES and WGS increase the chance to identify the causative gene defect. When possible, the optimal configuration would be to perform WES/WGS on trio: the two unaffected parents and their affected child in AR IRD, two affected and one unaffected sibling in AD IRD. Larger families with multiple affected members can also provide more genetic data to analyze and to filter stringently and thus improve the identification of novel gene defects.

A previous PhD student, Cécile Méjécase, analyzed WES data from 43 unrelated families and found a gene defect in 7 of them. She pointed a candidate gene for 7 additional families. The strategy of analysis was implemented by re-alignment to hg19 and variant calling and annotation using the up-to-date databases through a bioinformatic pipeline developed in collaboration with the bioinformatic engineer from our team, Julien Navarro. In this stringent filtering, we added the coverage of a larger splice site region (+/- 25 nucleotides to the exon-intron junction), where variants may have been overlooked in our previous filtering. It enabled me to find a non-canonical splice site variant in *TULPI* (c.1496-6C>A) in one family. Non-canonical splice site and deep

intronic variants are a frequent cause of missed gene defects in IRD[193]. I found hypomorphic variants in genes usually linked with multiorgan disorders: *HGSNAT* and *IDUA* in two additional families. These findings reinforce the presence of the large clinical spectrum and extreme phenotypic variability of IRD. Biologists interpreting wide-genome sequencing data should be aware of this possibility and ought not to rule out genes linked with systemic multiorgan disorders, as the retinal involvement could be an inconstant part of it, as for example in mucopolysaccharidoses[151–153]. Pangenomic studies produce a wide range of unsolicited findings, i.e. predispositions for diseases that exceed the diagnostic question. Genetic counselling in such cases should be made with caution, personalized and context-dependent[178] with repeated clinical work-up. However, ethical questions remains regarding the disclosure of genetic information.

3. Candidate genes and novel mechanisms in inherited retinal disorder field

The candidate gene approach (i.e., the search for IRD-associated variants in genes encoding proteins with known functions in the retina) has been very successful. In the era of –omics (genomics, transcriptomics, proteomics, metabolomics, interactomics), multiple databases are freely accessible and provide efficient information to have a body of evidence to corroborate candidate genes. Our conventional strategy is based on deep phenotyping, stringent filtering, pathogenic mechanism predictions, tissue expression, known or predicted protein domains, localization, function and disease modelling.

To identify “the” disease causing variant among thousands of variants, stringent filtering is applied considering the mode of inheritance, the frequency of identified variants in the general population and sub-populations, pathogenic predictions based on conservation and chemical properties of the variants. In addition, different databases are queried to check if a candidate is expressed in the eye (<https://www.proteinatlas.org/>), in human retina (<https://oculargenomics.meei.harvard.edu/retinal-transcriptome/>), in photoreceptors[121,135] and in different retinal cell subtypes[118,134]. Other transcriptomic databases/open datasets exist based on single cell RNA sequencing in mouse retina[137] (https://portals.broadinstitute.org/single_cell/study/retinal-bipolar-neurondrop-seq) or in retinal organoids derived from human embryonic pluripotent stem cells[194], which can also be informative. In the later, it is possible to follow retinal expression over the course of differentiation of retinal organoids in specific retinal cells.

Several bioinformatics tools exist to pinpoint to different protein domains and functions, to the subcellular protein localization, proteome and interactomes analyses (ExpASY: <https://www.expasy.org/>; STRING database: <https://string-db.org/>)[195]. This “database” approach was used in my work to identify candidate gene in a family with North Carolina Macular Dystrophy (cf. Results, paragraph 4).

The bioinformatic evidence must be corroborated experimentally. The challenging part here is to use the best model. Human retina is obviously the best option to perform expression studies and immunolocalization or western blot experiments, but this tissue is also the most difficult to obtain. Mouse tissues are more accessible and often represent a good alternative due to ortholog genes and proteins, showing 80% identity with human tissues[196]. However, care should be taken in inferring results from mouse retinal expression experiments to human pathology. Indeed, in our candidate for NCMD (*AZINE7*), intense immunostaining of Müller cells was obtained in mouse retina. Indeed, in human retina the staining was perinuclear and ubiquitous, more consistent with

in-situ hybridization experiments. The same unspecific and misleading mouse Müller cell staining had been previously observed when *GPR179* was first described and studied by our team[112,140].

If the protein is secreted into body fluids, western blot offers a good way of identifying the functional consequence of a gene defect. Using this technique, we showed that a nonsense variant in *RBP4* led to the absence of protein from a blood sample of a patient with a fundus albipunctatus-like phenotype, showing no variant in the usual associated genes (i.e. *RDH5* and *RLBP1*). In this case, deciphering the molecular mechanism gave way to a possible treatment strategy[170].

The disease-mechanism(s) linked to identified variants in the affected tissue must also be examined. Due to difficulties obtaining the affected retinal tissues, there is a need to develop relevant models to functionally characterize newly identified defects. Mammalian cell lines can be used to overexpress the wild-type or the mutated form of the protein and subcellular localization can be studied: mislocalization of the mutated form can be observed and may explain the retinal phenotype[140]. For splice site variants, different approaches can be applied. When the gene of interest is expressed in blood cells and/or skin fibroblasts, RT-PCR experiments can be performed from these sample to confirm the predicted splice effect of the splice site variant. Alternatively, mini-gene approaches can be performed in a cellular model and may reveal altered splicing[193]. If the expression profile of a given gene is retina only, retinal organoids obtained from induced pluripotent cells may be used to perform transcriptomic studies and immunostaining of candidate proteins and/or proteomic analyses. Disease-modelling using retinal organoids is a powerful approach to mimic the phenotype observed in patients[197], but has its inherent limitations (it is an expensive, laborious and long process: approximately nine months needed to obtain photoreceptors[198]).

Animal models may also be helpful in studying pathogenic mechanisms of retinal degeneration. Several animal mutant models are naturally occurring. On the other hand, animals can be genetically modified, by introducing the mutation (knock in), or by completely or partially knocking down its expression (knock out or down respectively)[199]. Comparing phenotypes of existing animal models with a known gene defect and subsequent screening of the respective candidate gene enabled the identification of many genes associated with IRD. In this respect, we reported a peculiar CSNB phenotype of patients harboring *VSX2* variants and ocular findings in *attenuated Or* mouse[200] (cf. Results, paragraph 3.5). Animal models have also some limitations, in particular due to the different retinal organization in mammalian species. Mouse models are less suited to study macular degeneration and COD/CORD modelling, as there is no macula and fewer cones in mouse retinas. Mongolian gerbil could be a good candidate in these disorders, as the retinal organization is closer to human[201]. Primate modeling is potentially a best choice but is expensive and subject to multiple legal restrictions.

4. Novel strategies in inherited retinal disorder gene defect identification

Known genes. The identification of gene defects by targeted NGS panel reached probably the highest level of resolution currently, ranging between 60 and 80%[184,185,191,202,203], which is also their limit of variant detection. In our team, we applied a sequential approach to identify disease-causing variants. After screening for *RPGR-ORF15* defects by direct Sanger sequencing, we perform NGS covering exons and flanking intronic regions from 123 to 351 genes

known to be associated with IRD. The resolution rate is 75%, as shown in this study. However, 25% of patients remain unsolved.

The next step of our approach is WES/WGS in informative families. A previous PhD student, Cécile Méjécase, showed that WES applied to unsolved families gave 16% uplift in diagnostic yield. WGS can improve it up to 30%[204].

Where do the remaining gene defects reside? This missing inheritance may be explained by novel gene defects, by overlooked copy number variations or complex structural variants, by variants in intronic or regulatory regions or represent synonymous variants with unexpected functional consequences[193,205]. Several emerging strategies could be helpful to increase the level of gene defect identification:

- Novel algorithms for bioinformatic analysis of raw sequencing data, enabling better identification of structural variants[206–208]. In this respect, we found 2 novel multiexon deletions in *TLL5* in patients with COD/CORD and analyzed the possible mechanisms leading to the deletion [173]. This option could be applied to all sequencing data, including old samples. It is important to “return” and reanalyze data of unsolved cases with novel tools. We reanalyzed unsolved WES cases and solved three additional families.
- Long-read sequencing strategies (e.g. nanopore sequencing[209]), with the potential to unravel complex structural variants through a more accurate sequence alignment [210,211];
- Hi-C, a high-throughput genomic and epigenomic technique allowing the capture of chromatin three-dimensional conformation may deliver data on complex epigenetic interactions. This strategy was recently able to resolve the presume pathogenic mechanism underlying RP17 [108] and contributed to the emerging notion of enhanceropathies[212].

Novel genes. After a “boom” of IRD-associated genes discovery in the 1990s – beginning of the 2000s, we are currently assisting at a general slowdown in novel gene identification. Major genes involved in retinal structure and function have already been reported and we are now reaching a plateau (Fig.32).

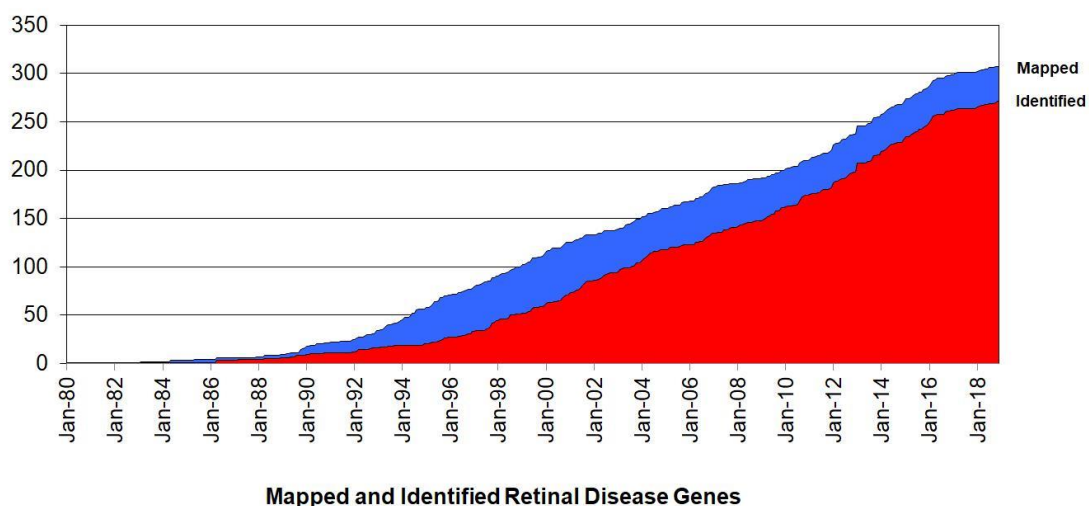


Figure 32. Annual rate of gene identification in IRD since 1980. There is a general slowdown since 2016. Adapted from RetNet (<https://sph.uth.edu/retnet/sum-dis.htm#A-genes>)

The strategies of novel gene identification in IRD are impeded by the small number of families which could be gathered to provide evidence for the pathogenicity of novel candidates. Recent discoveries usually report small pedigrees with a limited number of cases[213,214]. We faced the same issue reporting *VSX2* implication in CSNB with only 3 patients from 2 distinct families. International collaborative initiatives may be important in this instance. To facilitate the identification of additional cases with a variant in rarely mutated genes, for instance, the European retinal disease consortium (ERDC, <https://www.erd.c.info> /) or GeneMatcher (<https://genematcher.org/>) regularly publish the list of candidate genes and provide the possibility to contact researchers/clinicians.

There is also currently a general enthusiasm in the scientific and medical community working with IRD around gene therapy. Recent advances in biotechnology allowed the development of Luxturna®[215] for the treatment of *RPE65*-associated IRD and Lumevox®[216] for Leber Hereditary Optic Neuropathy. Multiple promising new drugs are under phase 2/3 trials. This topic is beyond the scope of this thesis but it outlines the importance of improving our current knowledge of IRD genetic to provide a better/faster access for IRD patients to treatment innovation.

In conclusion, high throughput sequencing technologies (targeted NGS, WES, WGS), remains an unfailing and endless source to identify novel gene defects associated with IRD, open the way to deepen genotype-phenotype correlations in IRD cohorts and to resolve complex traits. Ultimately, it will lead to a better understanding of retinal physiology and physiopathology and pave the way for exciting bench-to-bedside research.

References.

1. Duke-Elder S, Wybar K. System of ophthalmology Vol.2 The anatomy of the visual system ; by Sir Stewart Duke-Elder and Kenneth C. Wybar. Vol.2 The anatomy of the visual system ; by Sir Stewart Duke-Elder and Kenneth C. Wybar. London; St. Louis: Kimpton : Mosby; 1961.
2. Hubel DH. Eye, brain, and vision. New ed. New York s.l: Distributed by W.H. Freeman; 1995. 242 p. (Scientific American Library series).
3. Rodieck RW. The first steps in seeing. Sunderland, Mass: Sinauer Associates; 1998. 562 p.
4. Khanna H. Photoreceptor Sensory Cilium: Traversing the Ciliary Gate. *Cells*. 2015 Oct 15;4(4):674–86.
5. Bujakowska KM, Liu Q, Pierce EA. Photoreceptor Cilia and Retinal Ciliopathies. *Cold Spring Harb Perspect Biol*. 2017 Oct 3;9(10):a028274.
6. Beavo J, Francis SH, Houslay MD. Cyclic nucleotide phosphodiesterases in health and disease. Boca Raton: CRC Press/Taylor & Francis; 2007.
7. Sahly I, Dufour E, Schietroma C, Michel V, Bahloul A, Perfettini I, Pepermans E, Estivalet A, Carette D, Aghaie A, Ebermann I, Lelli A, Iribarne M, Hardelin JP, Weil D, Sahel JA, El-Amraoui A, Petit C. Localization of Usher 1 proteins to the photoreceptor calyceal processes, which are absent from mice. *J Cell Biol*. 2012 Oct 15;199(2):381–99.
8. Hoon M, Okawa H, Santana LD, Wong ROL. Functional Architecture of the Retina: Development and Disease. *Prog Retin Eye Res*. 2014 Sep;42:44–84.
9. Molday RS, Moritz OL. Photoreceptors at a glance. *J Cell Sci*. 2015 Nov 15;128(22):4039–45.
10. Delmaghani S, El-Amraoui A. The genetic and phenotypic landscapes of Usher syndrome: from disease mechanisms to a new classification. *Hum Genet*. 2022 Apr 1;141(3):709–35.
11. Osterberg G. Topography of the layer of rods and cones in the human retina.
12. Hanazono G, Tsunoda K, Kazato Y, Suzuki W, Tanifuji M. Functional Topography of Rod and Cone Photoreceptors in Macaque Retina Determined by Retinal Densitometry. *Investigative Ophthalmology & Visual Science*. 2012 May 14;53(6):2796–803.
13. Wikler KC, Rakic P. Distribution of photoreceptor subtypes in the retina of diurnal and nocturnal primates. *J Neurosci*. 1990 Oct;10(10):3390–401.
14. Tachibanaki S, Shimauchi-Matsukawa Y, Arinobu D, Kawamura S. Molecular mechanisms characterizing cone photoresponses. *Photochem Photobiol*. 2007 Feb;83(1):19–26.
15. Kawamura S, Tachibanaki S. Rod and cone photoreceptors: molecular basis of the difference in their physiology. *Comp Biochem Physiol A Mol Integr Physiol*. 2008 Aug;150(4):369–77.
16. Salesse C. [Physiology of the visual retinal signal: From phototransduction to the visual cycle]. *J Fr Ophtalmol*. 2017 Mar;40(3):239–50.
17. Kolb H, Linberg KA, Fisher SK. Neurons of the human retina: a Golgi study. *J Comp Neurol*. 1992 Apr 8;318(2):147–87.

18. Dowling JE, Werblin FS. Organization of retina of the mudpuppy, *Necturus maculosus*. I. Synaptic structure. *J Neurophysiol*. 1969 May;32(3):315–38.
19. Werblin FS, Dowling JE. Organization of the retina of the mudpuppy, *Necturus maculosus*. II. Intracellular recording. *J Neurophysiol*. 1969 May;32(3):339–55.
20. Wässle H. Parallel processing in the mammalian retina. *Nat Rev Neurosci*. 2004 Oct;5(10):747–57.
21. Reichenbach A, Bringmann A. New functions of Müller cells: New Functions of Müller Cells. *Glia*. 2013 May;61(5):651–78.
22. Sparrow JR, Hicks D, Hamel CP. The retinal pigment epithelium in health and disease. *Curr Mol Med*. 2010 Dec;10(9):802–23.
23. Palczewski K. G protein-coupled receptor rhodopsin. *Annu Rev Biochem*. 2006;75:743–67.
24. Kukura P, McCamant DW, Yoon S, Wandschneider DB, Mathies RA. Structural observation of the primary isomerization in vision with femtosecond-stimulated Raman. *Science*. 2005 Nov 11;310(5750):1006–9.
25. Emeis D, Kühn H, Reichert J, Hofmann KP. Complex formation between metarhodopsin II and GTP-binding protein in bovine photoreceptor membranes leads to a shift of the photoproduct equilibrium. *FEBS Lett*. 1982 Jun 21;143(1):29–34.
26. Heck M, Hofmann KP. Maximal rate and nucleotide dependence of rhodopsin-catalyzed transducin activation: initial rate analysis based on a double displacement mechanism. *J Biol Chem*. 2001 Mar 30;276(13):10000–9.
27. Mou H, Grazio HJ, Cook TA, Beavo JA, Cote RH. cGMP binding to noncatalytic sites on mammalian rod photoreceptor phosphodiesterase is regulated by binding of its gamma and delta subunits. *J Biol Chem*. 1999 Jun 25;274(26):18813–20.
28. Arshavsky VY, Wensel TG. Timing is everything: GTPase regulation in phototransduction. *Invest Ophthalmol Vis Sci*. 2013 Nov 21;54(12):7725–33.
29. Méjécase C, Laurent-Coriat C, Mayer C, Poch O, Mohand-Saïd S, Prévot C, Antonio A, Boyard F, Condroyer C, Michiels C, Blanchard S, Letexier M, Saraiva JP, Sahel JA, Audo I, Zeitz C. Identification of a Novel Homozygous Nonsense Mutation Confirms the Implication of GNAT1 in Rod-Cone Dystrophy. *PLoS One*. 2016;11(12):e0168271.
30. Kim HM, Joo K, Han J, Woo SJ. Clinical and Genetic Characteristics of Korean Congenital Stationary Night Blindness Patients. *Genes (Basel)*. 2021 May 21;12(6):789.
31. Millo T, Rivera A, Obolensky A, Marks-Ohana D, Xu M, Li Y, Wilhelm E, Gopalakrishnan P, Gross M, Rosin B, Hanany M, Webster A, Tracewska AM, Koenekoop RK, Chen R, Arno G, Schueler-Furman O, Roosing S, Banin E, Sharon D. Identification of autosomal recessive novel genes and retinal phenotypes in members of the solute carrier (SLC) superfamily. *Genet Med*. 2022 Apr 29;S1098-3600(22)00715-8.
32. Thirkill CE, FitzGerald P, Sergott RC, Roth AM, Tyler NK, Keltner JL. Cancer-Associated Retinopathy (CAR Syndrome) with Antibodies Reacting with Retinal, Optic-Nerve, and Cancer Cells. *N Engl J Med*. 1989 Dec 7;321(23):1589–94.

33. Thirkill CE, Tait RC, Tyler NK, Roth AM, Keltner JL. The cancer-associated retinopathy antigen is a recoverin-like protein. *Invest Ophthalmol Vis Sci*. 1992 Sep;33(10):2768–72.
34. Mizener JB, Kimura AE, Adamus G, Thirkill CE, Goeken JA, Kardon RH. Autoimmune Retinopathy in the Absence of Cancer. *American Journal of Ophthalmology*. 1997 May 1;123(5):607–18.
35. Keltner JL, Thirkill CE. Cancer-associated retinopathy vs recoverin-associated retinopathy. *Am J Ophthalmol*. 1998 Aug;126(2):296–302.
36. Lamb TD. Photoreceptor physiology and evolution: cellular and molecular basis of rod and cone phototransduction. *The Journal of Physiology [Internet]*. [cited 2022 Jun 4];n/a(n/a). Available from: <https://onlinelibrary.wiley.com/doi/abs/10.1113/JP282058>
37. Zhang X, Wensel TG, Kraft TW. GTPase regulators and photoresponses in cones of the eastern chipmunk. *J Neurosci*. 2003 Feb 15;23(4):1287–97.
38. Shao Z, Tumber A, Maynes J, Tavares E, Kannu P, Heon E, Vincent A. Unique retinal signaling defect in GNB5-related disease. *Doc Ophthalmol*. 2019 Nov 12;
39. Zeitz C, Robson AG, Audo I. Congenital stationary night blindness: An analysis and update of genotype–phenotype correlations and pathogenic mechanisms. *Progress in Retinal and Eye Research*. 2015 Mar;45:58–110.
40. Pircher B, Pircher T, Feigenspan A. Ionotropic glutamate receptors in the retina – a bioinformatical meta-analysis [Internet]. *Neuroscience*; 2021 Nov [cited 2022 Jun 4]. Available from: <http://biorxiv.org/lookup/doi/10.1101/2021.11.27.470202>
41. Wycisk KA, Budde B, Feil S, Skosyrski S, Buzzi F, Neidhardt J, Glaus E, Nürnberg P, Ruether K, Berger W. Structural and functional abnormalities of retinal ribbon synapses due to *Cacna2d4* mutation. *Invest Ophthalmol Vis Sci*. 2006 Aug;47(8):3523–30.
42. R BA, G A, K C, K S, Cj P, At M, M M, Fl R, Ar W, Ge H. Mutations in *CACNA2D4* Cause Distinctive Retinal Dysfunction in Humans. *Ophthalmology [Internet]*. 2016 Mar [cited 2022 Jun 7];123(3). Available from: <https://pubmed.ncbi.nlm.nih.gov/26560832/>
43. Wang Y, Liu X, Quan X, Qin X, Zhou Y, Liu Z, Chao Z, Jia C, Qin H, Zhang H. Pigment epithelium-derived factor and its role in microvascular-related diseases. *Biochimie*. 2022 Jun 1;S0300-9084(22)00160-2.
44. Quazi F, Lenevich S, Molday RS. *ABCA4* is an N-retinylidene-phosphatidylethanolamine and phosphatidylethanolamine importer. *Nat Commun*. 2012 Jun 26;3(1):925.
45. Rattner A, Smallwood PM, Nathans J. Identification and characterization of all-trans-retinol dehydrogenase from photoreceptor outer segments, the visual cycle enzyme that reduces all-trans-retinal to all-trans-retinol. *J Biol Chem*. 2000 Apr 14;275(15):11034–43.
46. Zeng S, Zhang T, Madigan MC, Fernando N, Aggio-Bruce R, Zhou F, Pierce M, Chen Y, Huang L, Natoli R, Gillies MC, Zhu L. Interphotoreceptor Retinoid-Binding Protein (IRBP) in Retinal Health and Disease. *Frontiers in Cellular Neuroscience [Internet]*. 2020 [cited 2022 Jun 10];14. Available from: <https://www.frontiersin.org/article/10.3389/fncel.2020.577935>

47. Haeseleer F, Jang GF, Imanishi Y, Driessen CAGG, Matsumura M, Nelson PS, Palczewski K. Dual-substrate specificity short chain retinol dehydrogenases from the vertebrate retina. *J Biol Chem.* 2002 Nov 22;277(47):45537–46.
48. Hamel CP, Tsilou E, Pfeffer BA, Hooks JJ, Detrick B, Redmond TM. Molecular cloning and expression of RPE65, a novel retinal pigment epithelium-specific microsomal protein that is post-transcriptionally regulated in vitro. *J Biol Chem.* 1993 Jul 25;268(21):15751–7.
49. Monaco HL, Rizzi M, Coda A. Structure of a complex of two plasma proteins: transthyretin and retinol-binding protein. *Science.* 1995 May 19;268(5213):1039–41.
50. Kawaguchi R, Yu J, Honda J, Hu J, Whitelegge J, Ping P, Wiita P, Bok D, Sun H. A Membrane Receptor for Retinol Binding Protein Mediates Cellular Uptake of Vitamin A. *Science.* 2007 Feb 9;315(5813):820–5.
51. During A, Doraiswamy S, Harrison EH. Xanthophylls are preferentially taken up compared with β -carotene by retinal cells via a SRBI-dependent mechanism. *J Lipid Res.* 2008 Aug;49(8):1715–24.
52. Lewandowski D, Sander CL, Tworak A, Gao F, Xu Q, Skowronska-Krawczyk D. Dynamic lipid turnover in photoreceptors and retinal pigment epithelium throughout life. *Prog Retin Eye Res.* 2021 Dec 29;101037.
53. Arditi A, Cagenello R. On the statistical reliability of letter-chart visual acuity measurements. *Investigative Ophthalmology & Visual Science.* 1993 Jan 1;34(1):120–9.
54. Grzybowski A. Harry Moss Traquair (1875-1954), Scottish ophthalmologist and perimetrist. *Acta Ophthalmol.* 2009 Jun;87(4):455–9.
55. Choplin NT, Edwards RP. *Visual fields.* Thorofare, NJ: Slack Incorporated; 1998. 255 p. (The basic bookshelf for eyecare professionals).
56. McCulloch DL, Marmor MF, Brigell MG, Hamilton R, Holder GE, Tzekov R, Bach M. ISCEV Standard for full-field clinical electroretinography (2015 update). *Doc Ophthalmol.* 2015 Feb;130(1):1–12.
57. Heckenlively JR, Arden GB, editors. *Principles and practice of clinical electrophysiology of vision.* 2nd ed. Cambridge, Mass: MIT Press; 2006. 977 p.
58. Yung M, Klufas MA, Sarraf D. Clinical applications of fundus autofluorescence in retinal disease. *International Journal of Retina and Vitreous.* 2016 Apr 8;2(1):12.
59. Keilhauer CN, Delori FC. Near-Infrared Autofluorescence Imaging of the Fundus: Visualization of Ocular Melanin. *Investigative Ophthalmology & Visual Science.* 2006 Aug 1;47(8):3556–64.
60. Elsner AE, Burns SA, Weiter JJ, Delori FC. Infrared imaging of sub-retinal structures in the human ocular fundus. *Vision Res.* 1996 Jan;36(1):191–205.
61. Puech B, Kostubiec B, Hache JC, François P. [Epidemiology and prevalence of hereditary retinal dystrophies in the Northern France]. *J Fr Ophtalmol.* 1991;14(3):153–64.
62. Krumpaszky HG, Lüdtke R, Mickler A, Klauss V, Selbmann HK. Blindness incidence in Germany. A population-based study from Württemberg-Hohenzollern. *Ophthalmologica.* 1999;213(3):176–82.

63. Bourne RRA, Stevens GA, White RA, Smith JL, Flaxman SR, Price H, Jonas JB, Keeffe J, Leasher J, Naidoo K, Pesudovs K, Resnikoff S, Taylor HR, Vision Loss Expert Group. Causes of vision loss worldwide, 1990-2010: a systematic analysis. *Lancet Glob Health*. 2013 Dec;1(6):e339-349.
64. Verbakel SK, van Huet RAC, Boon CJF, den Hollander AI, Collin RWJ, Klaver CCW, Hoyng CB, Roepman R, Klevering BJ. Non-syndromic retinitis pigmentosa. *Progress in Retinal and Eye Research*. 2018 Sep 1;66:157–86.
65. Aboshiha J, Dubis AM, Carroll J, Hardcastle AJ, Michaelides M. The cone dysfunction syndromes. *Br J Ophthalmol*. 2016 Jan;100(1):115–21.
66. Gottlob I, Reinecke RD. Eye and head movements in patients with achromatopsia. *Graefes Arch Clin Exp Ophthalmol*. 1994 Jul;232(7):392–401.
67. Hirji N, Aboshiha J, Georgiou M, Bainbridge J, Michaelides M. Achromatopsia: clinical features, molecular genetics, animal models and therapeutic options. *Ophthalmic Genet*. 2018 Apr;39(2):149–57.
68. Tsang SH, Sharma T. Blue Cone Monochromatism. *Adv Exp Med Biol*. 2018;1085:65–6.
69. Schubert G, Bornschein H. Beitrag zur Analyse des menschlichen Elektroretinogramms. *OPH*. 1952;123(6):396–413.
70. Miyake Y, Yagasaki K, Horiguchi M, Kawase Y, Kanda T. Congenital stationary night blindness with negative electroretinogram. A new classification. *Arch Ophthalmol*. 1986 Jul;104(7):1013–20.
71. Riggs LA. Electroretinography in cases of night blindness. *Am J Ophthalmol*. 1954 Jul;38(1:2):70–8.
72. Hartong DT, Berson EL, Dryja TP. Retinitis pigmentosa. *The Lancet*. 2006 Nov;368(9549):1795–809.
73. Keats BJ, Corey DP. The usher syndromes. *Am J Med Genet*. 1999 Sep 24;89(3):158–66.
74. Hamel CP. Cone rod dystrophies. *Orphanet J Rare Dis*. 2007 Dec;2(1):7.
75. Boulanger-Scemama E, El Shamieh S, Démontant V, Condroyer C, Antonio A, Michiels C, Boyard F, Saraiva JP, Letexier M, Souied E, Mohand-Saïd S, Sahel JA, Zeitz C, Audo I. Next-generation sequencing applied to a large French cone and cone-rod dystrophy cohort: mutation spectrum and new genotype-phenotype correlation. *Orphanet J Rare Dis*. 2015 Dec;10(1):85.
76. Gill JS, Georgiou M, Kalitzeos A, Moore AT, Michaelides M. Progressive cone and cone-rod dystrophies: clinical features, molecular genetics and prospects for therapy. *Br J Ophthalmol*. 2019 May;103(5):711–20.
77. Tsang SH, Sharma T. Progressive Cone Dystrophy and Cone-Rod Dystrophy (XL, AD, and AR). In: Tsang SH, Sharma T, editors. *Atlas of Inherited Retinal Diseases* [Internet]. Cham: Springer International Publishing; 2018 [cited 2021 Mar 29]. p. 53–60. (Advances in Experimental Medicine and Biology; vol. 1085). Available from: http://link.springer.com/10.1007/978-3-319-95046-4_12
78. Tsang SH, Sharma T. Best Vitelliform Macular Dystrophy. *Adv Exp Med Biol*. 2018;1085:157–8.

79. Georgiou M, Kane T, Tanna P, Bouzia Z, Singh N, Kalitzeos A, Strauss RW, Fujinami K, Michaelides M. Prospective Cohort Study of Childhood-Onset Stargardt Disease: Fundus Autofluorescence Imaging, Progression, Comparison with Adult-Onset Disease, and Disease Symmetry. *Am J Ophthalmol*. 2020;211:159–75.
80. Mitchell P, Liew G, Gopinath B, Wong TY. Age-related macular degeneration. *Lancet*. 2018 Sep 29;392(10153):1147–59.
81. Warwick A, Lotery A. Genetics and genetic testing for age-related macular degeneration. *Eye (Lond)*. 2018 May;32(5):849–57.
82. Tanna P, Strauss RW, Fujinami K, Michaelides M. Stargardt disease: clinical features, molecular genetics, animal models and therapeutic options. *Br J Ophthalmol*. 2017 Jan;101(1):25–30.
83. Pinckers A. Patterned dystrophies of the retinal pigment epithelium. A review. *Ophthalmic Paediatr Genet*. 1988 Jul;9(2):77–114.
84. Meredith S, Snead M. Hereditary Vitreoretinopathies. In: Dartt DA, editor. *Encyclopedia of the Eye* [Internet]. Oxford: Academic Press; 2010 [cited 2022 Jun 22]. p. 233–43. Available from: <https://www.sciencedirect.com/science/article/pii/B9780123742032002682>
85. Ayuso C, Millan JM. Retinitis pigmentosa and allied conditions today: a paradigm of translational research. *Genome Med*. 2010 May 27;2(5):34.
86. Boughman JA, Vernon M, Shaver KA. Usher syndrome: definition and estimate of prevalence from two high-risk populations. *J Chronic Dis*. 1983;36(8):595–603.
87. Weil D, Blanchard S, Kaplan J, Guilford P, Gibson F, Walsh J, Mburu P, Varela A, Leveilliers J, Weston MD. Defective myosin VIIA gene responsible for Usher syndrome type 1B. *Nature*. 1995 Mar 2;374(6517):60–1.
88. Bonnet C, El-Amraoui A. Usher syndrome (sensorineural deafness and retinitis pigmentosa): pathogenesis, molecular diagnosis and therapeutic approaches. *Curr Opin Neurol*. 2012 Feb;25(1):42–9.
89. Ávila-Fernández A, Cantalapiedra D, Aller E, Vallespín E, Aguirre-Lambán J, Blanco-Kelly F, Corton M, Riveiro-Álvarez R, Allikmets R, Trujillo-Tiebas MJ, Millán JM, Cremers FPM, Ayuso C. Mutation analysis of 272 Spanish families affected by autosomal recessive retinitis pigmentosa using a genotyping microarray. *Mol Vis*. 2010 Dec 3;16:2550–8.
90. McGee TL, Seyedahmadi BJ, Sweeney MO, Dryja TP, Berson EL. Novel mutations in the long isoform of the USH2A gene in patients with Usher syndrome type II or non-syndromic retinitis pigmentosa. *J Med Genet*. 2010 Jul;47(7):499–506.
91. Nuutila A. Dystrophia retinae pigmentosa--dysacusis syndrome (DRD): a study of the Usher- or Hallgren syndrome. *J Genet Hum*. 1970 May;18(1):57–88.
92. Gorlin RJ, Tilsner TJ, Feinstein S, Duvall AJ. Usher's syndrome type III. *Arch Otolaryngol*. 1979 Jun;105(6):353–4.
93. Adato A, Vreugde S, Joensuu T, Avidan N, Hamalainen R, Belenkiy O, Olender T, Bonne-Tamir B, Ben-Asher E, Espinos C, Millán JM, Lehesjoki AE, Flannery JG, Avraham KB, Pietrokovski S, Sankila EM, Beckmann JS, Lancet D. USH3A transcripts encode clarin-1, a four-transmembrane-domain

protein with a possible role in sensory synapses. *European Journal of Human Genetics*. 2002 Jun;10(6):339–50.

94. Forsyth R, Gunay-Aygun M. Bardet-Biedl Syndrome Overview. In: Adam MP, Everman DB, Mirzaa GM, Pagon RA, Wallace SE, Bean LJ, Gripp KW, Amemiya A, editors. *GeneReviews*[®] [Internet]. Seattle (WA): University of Washington, Seattle; 1993 [cited 2022 Sep 19]. Available from: <http://www.ncbi.nlm.nih.gov/books/NBK1363/>
95. Stokman M, Lilien M, Knoers N. Nephronophthisis. In: Adam MP, Everman DB, Mirzaa GM, Pagon RA, Wallace SE, Bean LJ, Gripp KW, Amemiya A, editors. *GeneReviews*[®] [Internet]. Seattle (WA): University of Washington, Seattle; 1993 [cited 2022 Sep 19]. Available from: <http://www.ncbi.nlm.nih.gov/books/NBK368475/>
96. Yahalom C, Volovelsky O, Macarov M, Altalishi A, Alswaiti Y, Schneider N, Hanany M, Khan MI, Cremers FPM, Anteby I, Banin E, Sharon D, Khateb S. SENIOR-LØKEN SYNDROME: A Case Series and Review of the Renoretinal Phenotype and Advances of Molecular Diagnosis. *Retina*. 2021 Oct 1;41(10):2179–87.
97. Oberklaid F, Danks DM, Mayne V, Campbell P. Asphyxiating thoracic dysplasia. Clinical, radiological, and pathological information on 10 patients. *Arch Dis Child*. 1977 Oct;52(10):758–65.
98. Ku CA, Hull S, Arno G, Vincent A, Carss K, Kayton R, Weeks D, Anderson GW, Geraets R, Parker C, Pearce DA, Michaelides M, MacLaren RE, Robson AG, Holder GE, Heon E, Raymond FL, Moore AT, Webster AR, Pennesi ME. Detailed Clinical Phenotype and Molecular Genetic Findings in CLN3-Associated Isolated Retinal Degeneration. *JAMA Ophthalmol*. 2017 01;135(7):749–60.
99. Roosing S, van den Born LI, Sangermano R, Banfi S, Koenekoop RK, Zonneveld-Vrieling MN, Klaver CCW, van Lith-Verhoeven JJC, Cremers FPM, den Hollander AI, Hoyng CB. Mutations in MFSD8, encoding a lysosomal membrane protein, are associated with nonsyndromic autosomal recessive macular dystrophy. *Ophthalmology*. 2015 Jan;122(1):170–9.
100. Mechaussier S, Perrault I, Dollfus H, Bloch-Zupan A, Loundon N, Jonard L, Marlin S. Heimler Syndrome. *Adv Exp Med Biol*. 2020;1299:81–7.
101. Kim YJ, Abe Y, Kim YJ, Fujiki Y, Kim JW. Identification of a Homozygous PEX26 Mutation in a Heimler Syndrome Patient. *Genes (Basel)*. 2021 Apr 26;12(5):646.
102. Krebs JE, Goldstein ES, Kilpatrick ST. *Lewin's genes XII*. Burlington, MA: Jones & Bartlett Learning; 2018. 837 p.
103. Chinnery PF. Mitochondrial Disorders Overview. In: Adam MP, Ardinger HH, Pagon RA, Wallace SE, Bean LJ, Stephens K, Amemiya A, editors. *GeneReviews*[®] [Internet]. Seattle (WA): University of Washington, Seattle; 1993 [cited 2020 Aug 28]. Available from: <http://www.ncbi.nlm.nih.gov/books/NBK1224/>
104. Morton NE. Sequential tests for the detection of linkage. *Am J Hum Genet*. 1955 Sep;7(3):277–318.
105. Sanger F, Nicklen S, Coulson AR. DNA sequencing with chain-terminating inhibitors. *Proc Natl Acad Sci U S A*. 1977 Dec;74(12):5463–7.

106. Mullis K, Faloona F, Scharf S, Saiki R, Horn G, Erlich H. Specific enzymatic amplification of DNA in vitro: the polymerase chain reaction. *Cold Spring Harb Symp Quant Biol.* 1986;51 Pt 1:263–73.
107. Broadgate S, Yu J, Downes SM, Halford S. Unravelling the genetics of inherited retinal dystrophies: Past, present and future. *Prog Retin Eye Res.* 2017 Jul;59:53–96.
108. de Bruijn SE, Fiorentino A, Ottaviani D, Fanucchi S, Melo US, Corral-Serrano JC, Mulders T, Georgiou M, Rivolta C, Pontikos N, Arno G, Roberts L, Greenberg J, Albert S, Gilissen C, Aben M, Rebello G, Mead S, Raymond FL, Corominas J, Smith CEL, Kremer H, Downes S, Black GC, Webster AR, Inglehearn CF, van den Born LI, Koenekoop RK, Michaelides M, Ramesar RS, Hoyng CB, Mundlos S, Mhlanga MM, Cremers FPM, Cheetham ME, Roosing S, Hardcastle AJ. Structural Variants Create New Topological-Associated Domains and Ectopic Retinal Enhancer-Gene Contact in Dominant Retinitis Pigmentosa. *Am J Hum Genet.* 2020 Nov 5;107(5):802–14.
109. Dryja TP. Human genetics. Deficiencies in sight with the candidate gene approach. *Nature.* 1990 Oct 18;347(6294):614.
110. Audo I, Bujakowska KM, Léveillard T, Mohand-Saïd S, Lancelot ME, Germain A, Antonio A, Michiels C, Saraiva JP, Letexier M, Sahel JA, Bhattacharya SS, Zeitz C. Development and application of a next-generation-sequencing (NGS) approach to detect known and novel gene defects underlying retinal diseases. *Orphanet J Rare Dis.* 2012 Jan 25;7:8.
111. Audo I, Bujakowska K, Orhan E, El Shamieh S, Sennlaub F, Guillonneau X, Antonio A, Michiels C, Lancelot ME, Letexier M, Saraiva JP, Nguyen H, Luu TD, Léveillard T, Poch O, Dollfus H, Paques M, Goureau O, Mohand-Saïd S, Bhattacharya SS, Sahel JA, Zeitz C. The familial dementia gene revisited: a missense mutation revealed by whole-exome sequencing identifies ITM2B as a candidate gene underlying a novel autosomal dominant retinal dystrophy in a large family. *Hum Mol Genet.* 2014 Jan 15;23(2):491–501.
112. Audo I, Bujakowska K, Orhan E, Poloschek CM, Defoort-Dhellemmes S, Drumare I, Kohl S, Luu TD, Lecompte O, Zrenner E, Lancelot ME, Antonio A, Germain A, Michiels C, Audier C, Letexier M, Saraiva JP, Leroy BP, Munier FL, Mohand-Saïd S, Lorenz B, Friedburg C, Preising M, Kellner U, Renner AB, Moskova-Doumanova V, Berger W, Wissinger B, Hamel CP, Schorderet DF, De Baere E, Sharon D, Banin E, Jacobson SG, Bonneau D, Zanlonghi X, Le Meur G, Casteels I, Koenekoop R, Long VW, Meire F, Prescott K, de Ravel T, Simmons I, Nguyen H, Dollfus H, Poch O, Léveillard T, Nguyen-Ba-Charvet K, Sahel JA, Bhattacharya SS, Zeitz C. Whole-exome sequencing identifies mutations in GPR179 leading to autosomal-recessive complete congenital stationary night blindness. *Am J Hum Genet.* 2012 Feb 10;90(2):321–30.
113. Bamshad MJ, Ng SB, Bigham AW, Tabor HK, Emond MJ, Nickerson DA, Shendure J. Exome sequencing as a tool for Mendelian disease gene discovery. *Nat Rev Genet.* 2011 Sep 27;12(11):745–55.
114. Susgun S, Kasan K, Yucesan E. Gene Hunting Approaches through the Combination of Linkage Analysis with Whole-Exome Sequencing in Mendelian Diseases: From Darwin to the Present Day. *Public Health Genomics.* 2021;24(5–6):207–17.
115. Watson CM, Dean P, Camm N, Bates J, Carr IM, Gardiner CA, Bonthron DT. Long-read nanopore sequencing resolves a TMEM231 gene conversion event causing Meckel-Gruber syndrome. *Hum Mutat.* 2020 Feb;41(2):525–31.
116. Ascari G, Rendtorff ND, De Bruyne M, De Zaeytijd J, Van Lint M, Bauwens M, Van Heetvelde M, Arno G, Jacob J, Creytens D, Van Dorpe J, Van Laethem T, Rosseel T, De Pooter T, De Rijk P, De

Coster W, Menten B, Rey AD, Strazisar M, Bertelsen M, Tranebjaerg L, De Baere E. Long-Read Sequencing to Unravel Complex Structural Variants of CEP78 Leading to Cone-Rod Dystrophy and Hearing Loss. *Front Cell Dev Biol.* 2021;9:664317.

117. Kurosaki T, Maquat LE. Nonsense-mediated mRNA decay in humans at a glance. *J Cell Sci.* 2016 Feb 1;129(3):461–7.
118. Siegert S, Cabuy E, Scherf BG, Kohler H, Panda S, Le YZ, Fehling HJ, Gaidatzis D, Stadler MB, Roska B. Transcriptional code and disease map for adult retinal cell types. *Nat Neurosci.* 2012 Jan 22;15(3):487–95, S1-2.
119. Farkas MH, Au ED, Sousa ME, Pierce EA. RNA-Seq: Improving Our Understanding of Retinal Biology and Disease. *Cold Spring Harb Perspect Med.* 2015 Feb 26;5(9):a017152.
120. Uhlén M, Fagerberg L, Hallström BM, Lindskog C, Oksvold P, Mardinoglu A, Sivertsson Å, Kampf C, Sjöstedt E, Asplund A, Olsson I, Edlund K, Lundberg E, Navani S, Szigartyo CAK, Odeberg J, Djureinovic D, Takanen JO, Hober S, Alm T, Edqvist PH, Berling H, Tegel H, Mulder J, Rockberg J, Nilsson P, Schwenk JM, Hamsten M, von Feilitzen K, Forsberg M, Persson L, Johansson F, Zwahlen M, von Heijne G, Nielsen J, Pontén F. Tissue-based map of the human proteome. *Science.* 2015 Jan 23;347(6220):1260419.
121. Kim JW, Yang HJ, Brooks MJ, Zelinger L, Karakulah G, Gotoh N, Boleda A, Gieser L, Giuste F, Whitaker DT, Walton A, Villasmil R, Barb JJ, Munson PJ, Kaya KD, Chaitankar V, Cogliati T, Swaroop A. NRL-Regulated Transcriptome Dynamics of Developing Rod Photoreceptors. *Cell Rep.* 2016 Nov 22;17(9):2460–73.
122. Foltz LP, Clegg DO. Patient-derived induced pluripotent stem cells for modelling genetic retinal dystrophies. *Prog Retin Eye Res.* 2019 Jan;68:54–66.
123. Gonorazky HD, Naumenko S, Ramani AK, Nelakuditi V, Mashouri P, Wang P, Kao D, Ohri K, Vithithiyapaskaran S, Tarnopolsky MA, Mathews KD, Moore SA, Osorio AN, Villanova D, Kemaladewi DU, Cohn RD, Brudno M, Dowling JJ. Expanding the Boundaries of RNA Sequencing as a Diagnostic Tool for Rare Mendelian Disease. *Am J Hum Genet.* 2019 Mar 7;104(3):466–83.
124. Audo I, Sahel JA, Mohand-Saïd S, Lancelot ME, Antonio A, Moskova-Doumanova V, Nandrot EF, Doumanov J, Barragan I, Antinolo G, Bhattacharya SS, Zeitz C. EYS is a major gene for rod-cone dystrophies in France. *Hum Mutat.* 2010 May;31(5):E1406-1435.
125. Sharon D, Bruns GA, McGee TL, Sandberg MA, Berson EL, Dryja TP. X-linked retinitis pigmentosa: mutation spectrum of the RPGR and RP2 genes and correlation with visual function. *Invest Ophthalmol Vis Sci.* 2000 Aug;41(9):2712–21.
126. Breuer DK, Yashar BM, Filippova E, Hiriyanina S, Lyons RH, Mears AJ, Asaye B, Acar C, Vervoort R, Wright AF, Musarella MA, Wheeler P, MacDonald I, Iannaccone A, Birch D, Hoffman DR, Fishman GA, Heckenlively JR, Jacobson SG, Sieving PA, Swaroop A. A comprehensive mutation analysis of RP2 and RPGR in a North American cohort of families with X-linked retinitis pigmentosa. *Am J Hum Genet.* 2002 Jun;70(6):1545–54.
127. Shu X, Black GC, Rice JM, Hart-Holden N, Jones A, O’Grady A, Ramsden S, Wright AF. RPGR mutation analysis and disease: an update. *Hum Mutat.* 2007 Apr;28(4):322–8.
128. Branham K, Othman M, Brumm M, Karoukis AJ, Atmaca-Sonmez P, Yashar BM, Schwartz SB, Stover NB, Trzupek K, Wheaton D, Jennings B, Ciccarelli ML, Jayasundera KT, Lewis RA, Birch D,

Bennett J, Sieving PA, Andreasson S, Duncan JL, Fishman GA, Iannaccone A, Weleber RG, Jacobson SG, Heckenlively JR, Swaroop A. Mutations in *RPGR* and *RP2* Account for 15% of Males with Simplex Retinal Degenerative Disease. *Invest Ophthalmol Vis Sci*. 2012 Dec 13;53(13):8232.

129. Audo I, Lancelot M, Mohand-Saïd S, Antonio A, Germain A, Sahel J, Bhattacharya SS, Zeitz C. Novel *C2orf71* mutations account for ~1% of cases in a large French arRP cohort. *Hum Mutat* [Internet]. 2011 Apr [cited 2020 Oct 13];32(4). Available from: <https://onlinelibrary.wiley.com/doi/abs/10.1002/humu.21460>
130. Jaganathan K, Panagiotopoulou SK, McRae JF, Darbandi SF, Knowles D, Li YI, Kosmicki JA, Arbelaez J, Cui W, Schwartz GB, Chow ED, Kanterakis E, Gao H, Kia A, Batzoglou S, Sanders SJ, Farh KKH. Predicting Splicing from Primary Sequence with Deep Learning. *Cell*. 2019 Jan 24;176(3):535-548.e24.
131. Richards S, Aziz N, Bale S, Bick D, Das S, Gastier-Foster J, Grody WW, Hegde M, Lyon E, Spector E, Voelkerding K, Rehm HL. Standards and Guidelines for the Interpretation of Sequence Variants: A Joint Consensus Recommendation of the American College of Medical Genetics and Genomics and the Association for Molecular Pathology. *Genet Med*. 2015 May;17(5):405–24.
132. Brandt T, Sack LM, Arjona D, Tan D, Mei H, Cui H, Gao H, Bean LJH, Ankala A, Del Gaudio D, Knight Johnson A, Vincent LM, Reavey C, Lai A, Richard G, Meck JM. Adapting ACMG/AMP sequence variant classification guidelines for single-gene copy number variants. *Genet Med*. 2020 Feb;22(2):336–44.
133. El Shamieh S, Neuillé M, Terray A, Orhan E, Condroyer C, Démontant V, Michiels C, Antonio A, Boyard F, Lancelot ME, Letexier M, Saraiva JP, Léveillard T, Mohand-Saïd S, Goureau O, Sahel JA, Zeitz C, Audo I. Whole-Exome Sequencing Identifies KIZ as a Ciliary Gene Associated with Autosomal-Recessive Rod-Cone Dystrophy. *The American Journal of Human Genetics*. 2014 Apr;94(4):625–33.
134. Siegert S, Scherf BG, Del Punta K, Didkovsky N, Heintz N, Roska B. Genetic address book for retinal cell types. *Nat Neurosci*. 2009 Sep;12(9):1197–204.
135. Kalathur R, Gagniere N, Berthommier G, Poidevin L, Raffelsberger W, Ripp R, Léveillard T, Poch O. RETINOBASE: a web database, data mining and analysis platform for gene expression data on retina. *BMC Genomics*. 2008;9(1):208.
136. Farkas MH, Grant GR, White JA, Sousa ME, Consugar MB, Pierce EA. Transcriptome analyses of the human retina identify unprecedented transcript diversity and 3.5 Mb of novel transcribed sequence via significant alternative splicing and novel genes. *BMC Genomics*. 2013;14(1):486.
137. Shekhar K, Lapan SW, Whitney IE, Tran NM, Macosko EZ, Kowalczyk M, Adiconis X, Levin JZ, Nemesh J, Goldman M, McCarroll SA, Cepko CL, Regev A, Sanes JR. Comprehensive Classification of Retinal Bipolar Neurons by Single-Cell Transcriptomics. *Cell*. 2016 Aug 25;166(5):1308-1323.e30.
138. Fahey ME, Bennett MJ, Mahon C, Jäger S, Pache L, Kumar D, Shapiro A, Rao K, Chanda SK, Craik CS, Frankel AD, Krogan NJ. GPS-Prot: A web-based visualization platform for integrating host-pathogen interaction data. *BMC Bioinformatics*. 2011;12(1):298.
139. Szklarczyk D, Gable AL, Lyon D, Junge A, Wyder S, Huerta-Cepas J, Simonovic M, Doncheva NT, Morris JH, Bork P, Jensen LJ, Mering C von. STRING v11: protein-protein association networks

with increased coverage, supporting functional discovery in genome-wide experimental datasets. *Nucleic Acids Res.* 2019 08;47(D1):D607–13.

140. Orhan E, Prézeau L, El Shamieh S, Bujakowska KM, Michiels C, Zagar Y, Vol C, Bhattacharya SS, Sahel JA, Sennlaub F, Audo I, Zeitz C. Further insights into GPR179: expression, localization, and associated pathogenic mechanisms leading to complete congenital stationary night blindness. *Invest Ophthalmol Vis Sci.* 2013 Dec 9;54(13):8041–50.
141. Bader I, Brandau O, Achatz H, Apfelstedt-Sylla E, Hergersberg M, Lorenz B, Wissinger B, Wittwer B, Rudolph G, Meindl A, Meitinger T. X-linked Retinitis Pigmentosa: *RPGR* Mutations in Most Families with Definite X Linkage and Clustering of Mutations in a Short Sequence Stretch of Exon ORF15. *Invest Ophthalmol Vis Sci.* 2003 Apr 1;44(4):1458.
142. de Bruijn SE, Fiorentino A, Ottaviani D, Fanucchi S, Melo US, Corral-Serrano JC, Mulders T, Georgiou M, Rivolta C, Pontikos N, Arno G, Roberts L, Greenberg J, Albert S, Gilissen C, Aben M, Rebello G, Mead S, Raymond FL, Corominas J, Smith CEL, Kremer H, Downes S, Black GC, Webster AR, Inglehearn CF, van den Born LI, Koenekoop RK, Michaelides M, Ramesar RS, Hoyng CB, Mundlos S, Mhlanga MM, Cremers FPM, Cheetham ME, Roosing S, Hardcastle AJ. Structural Variants Create New Topological-Associated Domains and Ectopic Retinal Enhancer-Gene Contact in Dominant Retinitis Pigmentosa. *Am J Hum Genet.* 2020 Nov 5;107(5):802–14.
143. Kohl S, Llavona P, Sauer A, Reuter P, Weisschuh N, Kempf M, Dehmelt FA, Arrenberg AB, Sliesoraityte I, Zrenner E, van Schooneveld MJ, Rudolph G, Kühlewein L, Wissinger B. A duplication on chromosome 16q12 affecting the *IRXB* gene cluster is associated with autosomal dominant cone dystrophy with early tritanopic color vision defect. *Human Molecular Genetics* [Internet]. 2021 Apr 22 [cited 2021 Jun 5];(ddab117). Available from: <https://doi.org/10.1093/hmg/ddab117>
144. Gu S, Lennon A, Li Y, Lorenz B, Fossarello M, North M, Gal A, Wright A. Tubby-like protein-1 mutations in autosomal recessive retinitis pigmentosa. *The Lancet.* 1998 Apr 11;351(9109):1103–4.
145. Jespersgaard C, Fang M, Bertelsen M, Dang X, Jensen H, Chen Y, Bech N, Dai L, Rosenberg T, Zhang J, Møller LB, Tümer Z, Brøndum-Nielsen K, Grønsvov K. Molecular genetic analysis using targeted NGS analysis of 677 individuals with retinal dystrophy. *Sci Rep.* 2019 Feb 4;9(1):1219.
146. Weisschuh N, Mayer AK, Strom TM, Kohl S, Glöckle N, Schubach M, Andreasson S, Bernd A, Birch DG, Hamel CP, Heckenlively JR, Jacobson SG, Kamme C, Kellner U, Kunstmann E, Maffei P, Reiff CM, Rohrschneider K, Rosenberg T, Rudolph G, Vámos R, Varsányi B, Weleber RG, Wissinger B. Mutation Detection in Patients with Retinal Dystrophies Using Targeted Next Generation Sequencing. *PLoS One.* 2016;11(1):e0145951.
147. Hagstrom SA, North MA, Nishina PL, Berson EL, Dryja TP. Recessive mutations in the gene encoding the tubby-like protein *TULP1* in patients with retinitis pigmentosa. *Nat Genet.* 1998 Feb;18(2):174–6.
148. Bernardis I, Chiesi L, Tenedini E, Artuso L, Percesepe A, Artusi V, Simone ML, Manfredini R, Camparini M, Rinaldi C, Ciardella A, Graziano C, Balducci N, Tranchina A, Cavallini GM, Pietrangelo A, Marigo V, Tagliafico E. Unravelling the Complexity of Inherited Retinal Dystrophies Molecular Testing: Added Value of Targeted Next-Generation Sequencing. *Biomed Res Int.* 2016;2016:6341870.

149. Clarke LA, Scott HS. Two novel mutations causing mucopolysaccharidosis type I detected by single strand conformational analysis of the alpha-L-iduronidase gene. *Hum Mol Genet.* 1993 Aug;2(8):1311–2.
150. Bertola F, Filocamo M, Casati G, Mort M, Rosano C, Tylki-Szymanska A, Tüysüz B, Gabrielli O, Grossi S, Scarpa M, Parenti G, Antuzzi D, Dalmau J, Di Rocco M, Dionisi Vici C, Okur I, Rosell J, Rovelli A, Furlan F, Rigoldi M, Biondi A, Cooper DN, Parini R. IDUA mutational profiling of a cohort of 102 European patients with mucopolysaccharidosis type I: identification and characterization of 35 novel α -L-iduronidase (IDUA) alleles. *Hum Mutat.* 2011 Jun;32(6):E2189-2210.
151. Ashworth JL, Biswas S, Wraith E, Lloyd IC. Mucopolysaccharidoses and the eye. *Surv Ophthalmol.* 2006 Feb;51(1):1–17.
152. Del Longo A, Piozzi E, Schweizer F. Ocular features in mucopolysaccharidosis: diagnosis and treatment. *Ital J Pediatr.* 2018 Nov 16;44(Suppl 2):125.
153. Suppiej A, Rampazzo A, Cappellari A, Traverso A, Tormene AP, Pinello L, Scarpa M. The role of visual electrophysiology in mucopolysaccharidoses. *J Child Neurol.* 2013 Oct;28(10):1203–9.
154. Hřebíček M, Mrázová L, Seyrantepe V, Durand S, Roslin NM, Nosková L, Hartmannová H, Ivánek R, Cízková A, Poupětová H, Sikora J, Urinová J, Stranecký V, Zeman J, Lepage P, Roquis D, Verner A, Ausseil J, Beesley CE, Maire I, Poorthuis BJHM, van de Kamp J, van Diggelen OP, Wevers RA, Hudson TJ, Fujiwara TM, Majewski J, Morgan K, Kmoch S, Pshezhetsky AV. Mutations in TMEM76* cause mucopolysaccharidosis IIIC (Sanfilippo C syndrome). *Am J Hum Genet.* 2006 Nov;79(5):807–19.
155. Comander J, Weigel-DiFranco C, Maher M, Place E, Wan A, Harper S, Sandberg MA, Navarro-Gomez D, Pierce EA. The Genetic Basis of Pericentral Retinitis Pigmentosa-A Form of Mild Retinitis Pigmentosa. *Genes (Basel).* 2017 Oct 5;8(10):E256.
156. Van Cauwenbergh C, Van Schil K, Cannoodt R, Bauwens M, Van Laethem T, De Jaegere S, Steyaert W, Sante T, Menten B, Leroy BP, Coppieters F, De Baere E. arrEYE: a customized platform for high-resolution copy number analysis of coding and noncoding regions of known and candidate retinal dystrophy genes and retinal noncoding RNAs. *Genet Med.* 2017 Apr;19(4):457–66.
157. Non-syndromic retinitis pigmentosa due to mutations in the mucopolysaccharidosis type IIIC gene, heparan-alpha-glucosaminide N-acetyltransferase (HGSNAT) - PubMed [Internet]. [cited 2021 Aug 26]. Available from: <https://pubmed-ncbi-nlm-nih-gov.ressources-electroniques.univ-lille.fr/25859010/>
158. Lerner TJ, Boustany RMN, Anderson JW, D'Arigo KL, Schlumpf K, Buckler AJ, Gusella JF, Haines JL. Isolation of a novel gene underlying batten disease, CLN3. *Cell.* 1995 Sep;82(6):949–57.
159. Mole SE, Williams RE. Neuronal Ceroid-Lipofuscinoses. In: Adam MP, Ardinger HH, Pagon RA, Wallace SE, Bean LJ, Stephens K, Amemiya A, editors. *GeneReviews*® [Internet]. Seattle (WA): University of Washington, Seattle; 1993 [cited 2019 Nov 24]. Available from: <http://www.ncbi.nlm.nih.gov/books/NBK1428/>
160. Wang F, Wang H, Tuan HF, Nguyen DH, Sun V, Keser V, Bowne SJ, Sullivan LS, Luo H, Zhao L, Wang X, Zaneveld JE, Salvo JS, Siddiqui S, Mao L, Wheaton DK, Birch DG, Branham KE, Heckenlively JR, Wen C, Flagg K, Ferreyra H, Pei J, Khan A, Ren H, Wang K, Lopez I, Qamar R, Zenteno JC, Ayala-Ramirez R, Beatriz-Buentello-Volante, Fu Q, Simpson DA, Li Y, Sui R, Silvestri G, Daiger SP, Koenekoop RK, Zhang K, Chen R. Next generation sequencing-based molecular diagnosis of

retinitis pigmentosa: identification of a novel genotype-phenotype correlation and clinical refinements. *Hum Genet.* 2014 Mar;133(3):331–45.

161. Smirnov VM, Nassisi M, Solis Hernandez C, Méjécasse C, El Shamieh S, Condroyer C, Antonio A, Meunier I, Andrieu C, Defoort-Dhellemmes S, Mohand-Said S, Sahel JA, Audo I, Zeitz C. Retinal Phenotype of Patients With Isolated Retinal Degeneration Due to CLN3 Pathogenic Variants in a French Retinitis Pigmentosa Cohort. *JAMA Ophthalmol.* 2021 Jan 28;
162. Traboulsi EI. Hereditary Systemic Diseases Can Have a Predominant Ocular Phenotype, but They Are Still Systemic Diseases. *JAMA Ophthalmol.* 2021 Mar 1;139(3):291–2.
163. Masten MC, Augustine EF, Mink JW. Challenges of Phenotype-Genotype Correlations in Rare Diseases. *JAMA Ophthalmol.* 2021 Dec 1;139(12):1323.
164. Smirnov VM, Zeitz C, Audo I. Challenges of Phenotype-Genotype Correlations in Rare Diseases-Reply. *JAMA Ophthalmol.* 2021 Dec 1;139(12):1323–4.
165. Leroy BP, Hogg CR, Rath PR, McBain V, Kestelyn P, Bird AC, Holder GE. Clinical features & retinal function in patients with adult Refsum syndrome. *Adv Exp Med Biol.* 2003;544:57–8.
166. Rüether K, Baldwin E, Casteels M, Feher MD, Horn M, Kuranoff S, Leroy BP, Wanders RJ, Wierzbicki AS. Adult Refsum Disease: A Form of Tapetoretinal Dystrophy Accessible to Therapy. *Survey of Ophthalmology.* 2010 Nov;55(6):531–8.
167. Chinnery PF. Mitochondrial Disorders Overview. In: Adam MP, Ardinger HH, Pagon RA, Wallace SE, Bean LJ, Stephens K, Amemiya A, editors. *GeneReviews*® [Internet]. Seattle (WA): University of Washington, Seattle; 1993 [cited 2020 Aug 28]. Available from: <http://www.ncbi.nlm.nih.gov/books/NBK1224/>
168. Thompson DA, Gal A. Genetic defects in vitamin A metabolism of the retinal pigment epithelium. *Dev Ophthalmol.* 2003;37:141–54.
169. Thompson B, Katsanis N, Apostolopoulos N, Thompson DC, Nebert DW, Vasiliou V. Genetics and functions of the retinoic acid pathway, with special emphasis on the eye. *Hum Genomics.* 2019 03;13(1):61.
170. Smirnov VM, Wilmet B, Nassisi M, Condroyer C, Antonio A, Andrieu C, Devisme C, Sancho S, Sahel JA, Zeitz C, Audo I. Large Benefit from Simple Things: High-Dose Vitamin A Improves RBP4-Related Retinal Dystrophy. *International Journal of Molecular Sciences.* 2022 Jan;23(12):6590.
171. Bonnet C, Riahi Z, Chantot-Bastaraud S, Smagghe L, Letexier M, Marcaillou C, Lefèvre GM, Hardelin JP, El-Amraoui A, Singh-Estivalet A, Mohand-Said S, Kohl S, Kurtenbach A, Sliesoraityte I, Zobor D, Gherbi S, Testa F, Simonelli F, Banfi S, Fakin A, Glavač D, Jarc-Vidmar M, Zupan A, Battelino S, Martorell Sampol L, Claveria MA, Catala Mora J, Dad S, Møller LB, Rodriguez Jorge J, Hawlina M, Auricchio A, Sahel JA, Marlin S, Zrenner E, Audo I, Petit C. An innovative strategy for the molecular diagnosis of Usher syndrome identifies causal biallelic mutations in 93% of European patients. *Eur J Hum Genet.* 2016;24(12):1730–8.
172. Smirnov VM, Nassisi M, Mohand-Said S, Bonnet C, Audo I, Devisme C, Dib T, Zeitz C, Loundon N, Marlin S, Petit C, Bodaghi B, Sahel JA, Audo I. Retinal Phenotype of Patients with CLRN1-Associated Usher 3A Syndrome in French Light4Deaf Cohort. *Invest Ophthalmol Vis Sci.* 2022 Apr 1;63(4):25.

173. Smirnov V, Grunewald O, Muller J, Zeitz C, Obermaier CD, Devos A, Pelletier V, Bocquet B, Andrieu C, Bacquet JL, Lebredonchel E, Mohand-Saïd S, Defoort-Dhellemmes S, Sahel JA, Dollfus H, Zanlonghi X, Audo I, Meunier I, Boulanger-Scemama E, Dhaenens CM. Novel TLL5 Variants Associated with Cone-Rod Dystrophy and Early-Onset Severe Retinal Dystrophy. *International Journal of Molecular Sciences*. 2021 Jan;22(12):6410.
174. Zou C, Levine EM. Vsx2 controls eye organogenesis and retinal progenitor identity via homeodomain and non-homeodomain residues required for high affinity DNA binding. *PLoS Genet*. 2012 Sep;8(9):e1002924.
175. Smirnov VM, Robert MP, Condroyer C, Navarro J, Antonio A, Rozet JM, Sahel JA, Perrault I, Audo I, Zeitz C. Association of Missense Variants in VSX2 With a Peculiar Form of Congenital Stationary Night Blindness Affecting All Bipolar Cells. *JAMA Ophthalmol*. 2022 Oct 20;
176. Vincent A, Robson AG, Holder GE. Pathognomonic (diagnostic) ERGs. A review and update. *Retina (Philadelphia, Pa)*. 2013 Jan;33(1):5–12.
177. Saelaert M, Mertes H, Moerenhout T, De Baere E, Devisch I. Ethical values supporting the disclosure of incidental and secondary findings in clinical genomic testing: a qualitative study. *BMC Med Ethics*. 2020 Jan 30;21(1):9.
178. Saelaert M, Mertes H, Moerenhout T, Van Cauwenbergh C, Leroy BP, Devisch I, De Baere E. A qualitative study among patients with an inherited retinal disease on the meaning of genomic unsolicited findings. *Sci Rep*. 2021 Aug 4;11:15834.
179. Thompson DA, Iannaccone A, Ali RR, Arshavsky VY, Audo I, Bainbridge JWB, Besirli CG, Birch DG, Branham KE, Cideciyan AV, Daiger SP, Dalkara D, Duncan JL, Fahim AT, Flannery JG, Gattegna R, Heckenlively JR, Heon E, Jayasundera KT, Khan NW, Klassen H, Leroy BP, Molday RS, Musch DC, Pennesi ME, Petersen-Jones SM, Pierce EA, Rao RC, Reh TA, Sahel JA, Sharon D, Sieving PA, Strettoi E, Yang P, Zacks DN, Monaciano Consortium. Advancing Clinical Trials for Inherited Retinal Diseases: Recommendations from the Second Monaciano Symposium. *Transl Vis Sci Technol*. 2020 Jun;9(7):2.
180. Mitchell GA, Brody LC, Looney J, Steel G, Suchanek M, Dowling C, Der Kaloustian V, Kaiser-Kupfer M, Valle D. An initiator codon mutation in ornithine-delta-aminotransferase causing gyrate atrophy of the choroid and retina. *J Clin Invest*. 1988 Feb;81(2):630–3.
181. Black GC, Sergouniotis P, Sodi A, Leroy BP, Van Cauwenbergh C, Liskova P, Grønskov K, Klett A, Kohl S, Taurina G, Sukys M, Haer-Wigman L, Nowomiejska K, Marques JP, Leroux D, Cremers FPM, De Baere E, Dollfus H, ERN-EYE study group. The need for widely available genomic testing in rare eye diseases: an ERN-EYE position statement. *Orphanet J Rare Dis*. 2021 Mar 20;16(1):142.
182. Russell SR, Drack AV, Cideciyan AV, Jacobson SG, Leroy BP, Van Cauwenbergh C, Ho AC, Dumitrescu AV, Han IC, Martin M, Pfeifer WL, Sohn EH, Walshire J, Garafalo AV, Krishnan AK, Powers CA, Sumaroka A, Roman AJ, Vanhosebrouck E, Jones E, Nerinckx F, De Zaeytijd J, Collin RWJ, Hoyng C, Adamson P, Cheetham ME, Schwartz MR, den Hollander W, Asmus F, Platenburg G, Rodman D, Girach A. Intravitreal antisense oligonucleotide sepirofen in Leber congenital amaurosis type 10: a phase 1b/2 trial. *Nat Med*. 2022 May;28(5):1014–21.
183. Dulla K, Slijkerman R, van Diepen HC, Albert S, Dona M, Beumer W, Turunen JJ, Chan HL, Schulkens IA, Vorthoren L, den Besten C, Buil L, Schmidt I, Miao J, Venselaar H, Zang J, Neuhaus SCF, Peters T, Broekman S, Pennings R, Kremer H, Platenburg G, Adamson P, de Vrieze E, van Wijk

E. Antisense oligonucleotide-based treatment of retinitis pigmentosa caused by USH2A exon 13 mutations. *Mol Ther.* 2021 Aug 4;29(8):2441–55.

184. Weisschuh N, Obermaier CD, Battke F, Bernd A, Kuehlewein L, Nasser F, Zobor D, Zrenner E, Weber E, Wissinger B, Biskup S, Stingl K, Kohl S. Genetic architecture of inherited retinal degeneration in Germany: A large cohort study from a single diagnostic center over a 9-year period. *Hum Mutat.* 2020 Sep;41(9):1514–27.
185. Jespersgaard C, Fang M, Bertelsen M, Dang X, Jensen H, Chen Y, Bech N, Dai L, Rosenberg T, Zhang J, Møller LB, Tümer Z, Brøndum-Nielsen K, Grønsvkov K. Molecular genetic analysis using targeted NGS analysis of 677 individuals with retinal dystrophy. *Sci Rep.* 2019 Feb 4;9(1):1219.
186. Shah M, Shanks M, Packham E, Williams J, Haysmoore J, MacLaren RE, Németh AH, Clouston P, Downes SM. Next generation sequencing using phenotype-based panels for genetic testing in inherited retinal diseases. *Ophthalmic Genet.* 2020 Aug;41(4):331–7.
187. Tracewska AM, Kocyła-Karczarewicz B, Rafalska A, Murawska J, Jakubaszko-Jabłńska J, Rydzanicz M, Stawiński P, Ciara E, Lipska-Ziętkiewicz BS, Khan MI, Cremers FPM, Płoski R, Chrzanowska KH. Non-syndromic inherited retinal diseases in Poland: Genes, mutations, and phenotypes. *Mol Vis.* 2021;27:457–65.
188. Van Cauwenbergh C, Coppieters F, Roels D, De Jaegere S, Flipts H, De Zaeytijd J, Walraedt S, Claes C, Franssen E, Van Camp G, Depasse F, Casteels I, de Ravel T, Leroy BP, De Baere E. Mutations in Splicing Factor Genes Are a Major Cause of Autosomal Dominant Retinitis Pigmentosa in Belgian Families. *PLoS One.* 2017;12(1):e0170038.
189. Pontikos N, Arno G, Jurkute N, Schiff E, Ba-Abbad R, Malka S, Gimenez A, Georgiou M, Wright G, Armengol M, Knight H, Katz M, Moosajee M, Yu-Wai-Man P, Moore AT, Michaelides M, Webster AR, Mahroo OA. Genetic Basis of Inherited Retinal Disease in a Molecularly Characterized Cohort of More Than 3000 Families from the United Kingdom. *Ophthalmology.* 2020 Oct;127(10):1384–94.
190. Wang J, Xiao X, Li S, Jiang H, Sun W, Wang P, Zhang Q. Landscape of pathogenic variants in six pre-mRNA processing factor genes for retinitis pigmentosa based on large in-house data sets and database comparisons. *Acta Ophthalmol.* 2022 Feb 9;
191. Perea-Romero I, Gordo G, Iancu IF, Del Pozo-Valero M, Almoguera B, Blanco-Kelly F, Carreño E, Jimenez-Rolando B, Lopez-Rodriguez R, Lorda-Sanchez I, Martin-Merida I, Pérez de Ayala L, Riveiro-Alvarez R, Rodriguez-Pinilla E, Tahsin-Swafiri S, Trujillo-Tiebas MJ, ESRETNET Study Group, ERDC Study Group, Associated Clinical Study Group, Garcia-Sandoval B, Minguez P, Avila-Fernandez A, Corton M, Ayuso C. Genetic landscape of 6089 inherited retinal dystrophies affected cases in Spain and their therapeutic and extended epidemiological implications. *Sci Rep.* 2021 Jan 15;11(1):1526.
192. Kamenarova K, Mihova K, Veleva N, Mermeklieva E, Mihaylova B, Dimitrova G, Oscar A, Shandurkov I, Cherninkova S, Kaneva R. Panel-based next-generation sequencing identifies novel mutations in Bulgarian patients with inherited retinal dystrophies. *Mol Genet Genomic Med.* 2022 Aug;10(8):e1997.
193. Zeitz C, Michiels C, Neullé M, Friedburg C, Condroyer C, Boyard F, Antonio A, Bouzidi N, Milicevic D, Veaux R, Tourville A, Zoumba A, Seneina I, Foussard M, Andrieu C, N Preising M, Blanchard S, Saraiva JP, Mesrob L, Le Floch E, Jubin C, Meyer V, Blanché H, Boland A, Deleuze JF, Sharon D, Drumare I, Defoort-Dhellemmes S, De Baere E, Leroy BP, Zanlonghi X, Casteels I, de Ravel TJ,

- Balikova I, Koenekoop RK, Laffargue F, McLean R, Gottlob I, Bonneau D, Schorderet DF, L Munier F, McKibbin M, Prescott K, Pelletier V, Dollfus H, Perdomo-Trujillo Y, Faure C, Reiff C, Wissinger B, Meunier I, Kohl S, Banin E, Zrenner E, Jurklics B, Lorenz B, Sahel JA, Audo I. Where are the missing gene defects in inherited retinal disorders? Intronic and synonymous variants contribute at least to 4% of CACNA1F-mediated inherited retinal disorders. *Hum Mutat.* 2019 Jun;40(6):765–87.
194. Collin J, Queen R, Zerti D, Dorgau B, Hussain R, Coxhead J, Cockell S, Lako M. Deconstructing Retinal Organoids: Single Cell RNA-Seq Reveals the Cellular Components of Human Pluripotent Stem Cell-Derived Retina. *Stem Cells.* 2019 May;37(5):593–8.
 195. von Mering C, Jensen LJ, Snel B, Hooper SD, Krupp M, Foglierini M, Jouffre N, Huynen MA, Bork P. STRING: known and predicted protein-protein associations, integrated and transferred across organisms. *Nucleic Acids Res.* 2005 Jan 1;33(Database issue):D433-437.
 196. Gharib WH, Robinson-Rechavi M. When orthologs diverge between human and mouse. *Brief Bioinform.* 2011 Sep;12(5):436–41.
 197. Goureau O, Reichman S, Orioux G. [Retinal organoids as a new tool for understanding and treating retinal diseases]. *Med Sci (Paris).* 2020 Jul;36(6–7):626–32.
 198. Reichman S, Goureau O. Production of Retinal Cells from Confluent Human iPS Cells. In: Turksen K, Nagy A, editors. *Induced Pluripotent Stem (iPS) Cells* [Internet]. New York, NY: Springer New York; 2014 [cited 2022 Aug 15]. p. 339–51. (Methods in Molecular Biology; vol. 1357). Available from: http://link.springer.com/10.1007/7651_2014_143
 199. Neullé M, El Shamieh S, Orhan E, Michiels C, Antonio A, Lancelot ME, Condroyer C, Bujakowska K, Poch O, Sahel JA, Audo I, Zeitz C. *Lit3* Deficient Mouse (*nob6*): A Novel Model of Complete Congenital Stationary Night Blindness (*cCSNB*). Neuhaus SCF, editor. *PLoS ONE.* 2014 Mar 5;9(3):e90342.
 200. Bone-Larson C, Basu S, Radel JD, Liang M, Perozek T, Kapousta-Bruneau N, Green DG, Burmeister M, Hankin MH. Partial rescue of the ocular retardation phenotype by genetic modifiers. *J Neurobiol.* 2000 Feb 5;42(2):232–47.
 201. Govardovskii VI, Röhlich P, Szél A, Khokhlova TV. Cones in the retina of the Mongolian gerbil, *Meriones unguiculatus*: an immunocytochemical and electrophysiological study. *Vision Res.* 1992 Jan;32(1):19–27.
 202. Carrigan M, Duignan E, Malone CPG, Stephenson K, Saad T, McDermott C, Green A, Keegan D, Humphries P, Kenna PF, Farrar GJ. Panel-Based Population Next-Generation Sequencing for Inherited Retinal Degenerations. *Sci Rep.* 2016 Sep 14;6:33248.
 203. Eisenberger T, Neuhaus C, Khan AO, Decker C, Preising MN, Friedburg C, Bieg A, Gliem M, Charbel Issa P, Holz FG, Baig SM, Hellenbroich Y, Galvez A, Platzer K, Wollnik B, Laddach N, Ghaffari SR, Rafati M, Botzenhart E, Tinschert S, Börger D, Bohring A, Schreml J, Körtge-Jung S, Schell-Apacik C, Bakur K, Al-Aama JY, Neuhann T, Herkenrath P, Nürnberg G, Nürnberg P, Davis JS, Gal A, Bergmann C, Lorenz B, Bolz HJ. Increasing the yield in targeted next-generation sequencing by implicating CNV analysis, non-coding exons and the overall variant load: the example of retinal dystrophies. *PLoS One.* 2013;8(11):e78496.
 204. Ellingford JM, Barton S, Bhaskar S, Williams SG, Sergouniotis PI, O’Sullivan J, Lamb JA, Perveen R, Hall G, Newman WG, Bishop PN, Roberts SA, Leach R, Tearle R, Bayliss S, Ramsden SC, Nemeth AH, Black GCM. Whole Genome Sequencing Increases Molecular Diagnostic Yield Compared with

Current Diagnostic Testing for Inherited Retinal Disease. *Ophthalmology*. 2016 May;123(5):1143–50.

205. Bauwens M, Garanto A, Sangermano R, Naessens S, Weisschuh N, De Zaeytijd J, Khan M, Sadler F, Balikova I, Van Cauwenbergh C, Rosseel T, Bauwens J, De Leeneer K, De Jaegere S, Van Laethem T, De Vries M, Carss K, Arno G, Fakin A, Webster AR, de Ravel de l'Argentièrè TJL, Sznajer Y, Vuylsteke M, Kohl S, Wissinger B, Cherry T, Collin RWJ, Cremers FPM, Leroy BP, De Baere E. ABCA4-associated disease as a model for missing heritability in autosomal recessive disorders: novel noncoding splice, cis-regulatory, structural, and recurrent hypomorphic variants. *Genet Med*. 2019 Aug;21(8):1761–71.
206. Wei L, Dugas M, Sandmann S. SimFFPE and FilterFFPE: improving structural variant calling in FFPE samples. *Gigascience*. 2021 Sep 22;10(9):giab065.
207. Chen X, Schulz-Trieglaff O, Shaw R, Barnes B, Schlesinger F, Källberg M, Cox AJ, Kruglyak S, Saunders CT. Manta: rapid detection of structural variants and indels for germline and cancer sequencing applications. *Bioinformatics*. 2016 Apr 15;32(8):1220–2.
208. McHale P, Quinlan AR. trfermikit: a tool to discover VNTR-associated deletions. *Bioinformatics*. 2021 Dec 2;btab805.
209. Rhee M, Burns MA. Nanopore sequencing technology: research trends and applications. *Trends Biotechnol*. 2006 Dec;24(12):580–6.
210. Long-Read Sequencing Allows Increased Detection of De Novo Mutations. *Am J Med Genet A*. 2022 Sep;188(9):2523–4.
211. Ascari G, Rendtorff ND, De Bruyne M, De Zaeytijd J, Van Lint M, Bauwens M, Van Heetvelde M, Arno G, Jacob J, Creytens D, Van Dorpe J, Van Laethem T, Rosseel T, De Pooter T, De Rijk P, De Coster W, Menten B, Rey AD, Strazisar M, Bertelsen M, Tranebjaerg L, De Baere E. Long-Read Sequencing to Unravel Complex Structural Variants of CEP78 Leading to Cone-Rod Dystrophy and Hearing Loss. *Front Cell Dev Biol*. 2021;9:664317.
212. Claringbould A, Zaugg JB. Enhancers in disease: molecular basis and emerging treatment strategies. *Trends in Molecular Medicine*. 2021 Nov 1;27(11):1060–73.
213. Williams LB, Javed A, Sabri A, Morgan DJ, Huff CD, Grigg JR, Heng XT, Khng AJ, Hollink IHIM, Morrison MA, Owen LA, Anderson K, Kinard K, Greenlees R, Novacic D, Nida Sen H, Zein WM, Rodgers GM, Vitale AT, Haider NB, Hillmer AM, Ng PC, Shankaracharya null, Cheng A, Zheng L, Gillies MC, van Slegtenhorst M, van Hagen PM, Missotten TOAR, Farley GL, Polo M, Malatack J, Curtin J, Martin F, Arbuckle S, Alexander SI, Chircop M, Davila S, Digre KB, Jamieson RV, DeAngelis MM. ALPK1 missense pathogenic variant in five families leads to ROSAH syndrome, an ocular multisystem autosomal dominant disorder. *Genet Med*. 2019 Sep;21(9):2103–15.
214. Cogné B, Latypova X, Senaratne LDS, Martin L, Koboldt DC, Kellaris G, Fievet L, Le Meur G, Caldari D, Debray D, Nizon M, Frengen E, Bowne SJ, 99 Lives Consortium, Cadena EL, Daiger SP, Bujakowska KM, Pierce EA, Gorin M, Katsanis N, Bézieau S, Petersen-Jones SM, Occelli LM, Lyons LA, Legeai-Mallet L, Sullivan LS, Davis EE, Isidor B. Mutations in the Kinesin-2 Motor KIF3B Cause an Autosomal-Dominant Ciliopathy. *Am J Hum Genet*. 2020 Jun 4;106(6):893–904.
215. Russell S, Bennett J, Wellman JA, Chung DC, Yu ZF, Tillman A, Wittes J, Pappas J, Elci O, McCague S, Cross D, Marshall KA, Walshire J, Kehoe TL, Reichert H, Davis M, Raffini L, George LA, Hudson FP, Dingfield L, Zhu X, Haller JA, Sohn EH, Mahajan VB, Pfeifer W, Weckmann M, Johnson C,

Gewaily D, Drack A, Stone E, Wachtel K, Simonelli F, Leroy BP, Wright JF, High KA, Maguire AM. Efficacy and safety of voretigene neparvovec (AAV2-hRPE65v2) in patients with RPE65-mediated inherited retinal dystrophy: a randomised, controlled, open-label, phase 3 trial. *Lancet*. 2017 Aug 26;390(10097):849–60.

216. Biousse V, Newman NJ, Yu-Wai-Man P, Carelli V, Moster ML, Vignal-Clermont C, Klopstock T, Sadun AA, Sergott RC, Hage R, Esposti S, La Morgia C, Priglinger C, Karanja R, Blouin L, Tiel M, Sahel JA, LHON Study Group. Long-Term Follow-Up After Unilateral Intravitreal Gene Therapy for Leber Hereditary Optic Neuropathy: The RESTORE Study. *J Neuroophthalmol*. 2021 Sep 1;41(3):309–15.

Abstract

Inherited retinal degenerations (IRD) are a clinically and genetically heterogeneous group of stationary and progressive diseases, affecting vision. These diseases affect approximately 4.5 million people worldwide. The goal of this thesis was to identify known and novel gene defects associated with IRD in a cohort of patients followed at the national reference center for rare ocular diseases of the Centre Hospitalier National d'Ophtalmologie des Quinze-Vingts through targeted next generation sequencing (NGS), whole exome sequencing (WES) and whole genome sequencing (WGS) analyses, with subsequent functional studies to better understand the associated disease mechanisms. Specific genotype-phenotype correlations in IRD patients were performed. A cohort of 768 index cases have been analyzed on targeted NGS panel including 351 known and candidate genes of IRD. Isolated rod-cone dystrophy (RCD) was a major phenotype in the studied cohort (n=670, 87%). We genetically solved 75% of patients. The major genes underlying RCD in our cohort were *USH2A*, *RPI* and *EYS* accounting for 12, 6.7 and 6.5% cases respectively. WES identified disease causing variants in *TULP1*, *HGSNAT*, *IDUA*. WGS identified a novel duplication co-segregating with the phenotype of North Carolina Macular Dystrophy. We reported known and novel phenotype-genotype correlations in patients harboring known and novel *TLL5* gene defects; in fifteen patients with isolated RCD harboring biallelic variants in *CLN3*, a gene previously linked with syndromic neurodegenerative disorder and an unusual retinal phenotype amenable to oral retinol treatment in a patient harboring novel *RBP4* variant. In addition, the retinal phenotype was reported in four patients with Usher 3 syndrome linked with *CLRN1* variants. Additionally, we reported a novel complex phenotype of congenital stationary night blindness with anterior segment abnormalities and identified underlying gene defect in *VSX2* in three patients from two unrelated families. The identification of novel gene defects and further functional analyzes will provide a better understanding of the physiology of the retina and deliver the basis for novel therapeutic approaches.

Keywords: inherited retinal dystrophies, high throughput sequencing, candidate genes, phenotype-genotype correlations.

Résumé.

Les dystrophies rétiniennes héréditaires (DRH) sont un groupe cliniquement et génétiquement hétérogène de maladies qui détériorent la vision. Environ 4.5 millions de personnes sont atteintes dans le monde entier. Le but de cette thèse était de déterminer les défauts géniques (connus et nouveaux) chez les patients atteints de DRH, suivis dans le Centre Hospitalier National d'Ophtalmologie des Quinze-Vingts en utilisant les technologies de séquençage de nouvelle génération (NGS), de séquençage d'exome (WES) et de séquençage de génome (WGS). Les études fonctionnelles ont été entreprises pour déchiffrer les mécanismes pathologiques associés aux variations génétiques. Les corrélations phénotype-génotype ont été réalisées. Une cohorte de 768 cas-index a été analysée sur le panel NGS comportant 351 gènes (connus et candidats) associés aux DRH. La Dystrophie rétinienne bâtonnet-cône (DBC) isolée était un phénotype prédominant dans la cohorte (n=670, 87%). Nous avons pu trouver les variants causaux chez 75% de patients. Les gènes majeurs impliqués dans DRH étaient *USH2A*, *RPI* et *EYS* qui comptaient pour 12, 6.7 et 6.5% de cas respectivement. Par la technique de WES nous avons identifié les variants pathogènes dans les gènes *TULP1*, *HGSNAT* et *IDUA*. En utilisant la technique de WGS, nous avons identifié une nouvelle duplication qui ségrégeait avec le phénotype dans une famille atteinte de Dystrophie Maculaire de Caroline du Nord. Nous avons rapporté les corrélations génotype-phénotype : chez les patients porteurs de variants connus et nouveaux dans le gène *TLL5* ; dans le groupe de 15 patients atteints de DBC non-syndromique, porteurs de variants bialléliques dans le gène *CLN3* (gène surtout connu pour une maladie neuro-dégénérative syndromique) ; enfin, nous avons étudié un phénotype rétinien atypique, sensible au traitement par rétinol chez un patient porteur d'un nouveau variant de *RBP4*. De même, nous avons rapporté le phénotype rétinien de 4 patients atteints du syndrome de Usher de type 3, lié aux variants pathogènes dans le gène *CLRN1*. Enfin, nous avons décrit un nouveau phénotype complexe d'héméralopie essentielle associée aux défauts dans le gène *VSX2* dans deux familles non reliées. Identification de nouveaux défauts géniques et les analyses fonctionnelles subséquentes permettent de mieux comprendre la physiologie de la rétine et constituent une base pour des développements thérapeutiques ultérieurs.

Mots clés : dystrophies rétiniennes héréditaires, séquençage haut débit, gènes-candidats, corrélations phénotype-génotype